Junction remodeling under mechanical forces

Xinyi Yang

UNIVERSITÉ DE STRASBOURG

ÉCOLE DOCTORALE DES SCIENCES DE LA VIE ET DE LA SANTÉ

Laboratoire de Biologie du Développement - UMR7622 - IBPS - UPMC

Biologie du développement et cellules souches - UMR7104 - IGBMC- Université de Strasbourg

THÈSE présentée par :

Xinyi YANG

soutenue le : **25 Septembre 2017**

pour obtenir le grade de : **Docteur de l'université de Strasbourg**

Discipline/ Spécialité : Biologie du développement

Remodelage des jonctions sous stress mécanique

THÈSE dirigée par :

Dr. LABOUESSE Michel Directeur de Recherche, Université de Strasbourg

RAPPORTEURS :

Dr. PLASTINO Julie Directeur de Recherche, Institut Curie
Dr. MICHAUX Grégoire Directeur de Recherche, Université de Rennes 1

AUTRES MEMBRES DU JURY :

Dr. VERMOT Julien Directeur de Recherche, Université de Strasbourg
Dr. CASTERN Janke Directeur de Recherche, Institut Curie

“Nobody ever figures out what life is all about, and it doesn't matter. Explore the world.”

Richard P. Feynman

Acknowledgements

First of all, I would like to deeply thank my Ph.D. supervisor, Dr. **Michel Labouesse**, for his excellent mentorship and guidance during my research. Throughout my Ph.D., you provided constant encouragement, sound advice, liberty to think and execute experiments and useful tips about scientific writing and presentation. You helped me to push my project into the right direction. In spite of your very tight schedule, you were always available for me whenever I faced difficulties. You inspired me when I was confused and encouraged me to be autonomous not only for my study but also for my future long-term plans. For all of these, I am profoundly grateful.

Then, I would like to acknowledge to the wonderful colleagues with whom I have worked. **Nicola** and **Loïc**, you built up the incredible SPIM microscope from nothing and also developed the whole user-friendly operating system. Without your help, this project will not be so exciting. **Teresa**, your excellent help in difficult image analysis for calcium sensor and the single molecule imaging would always be acknowledged. You are always with your warm smiles and saved me from tearing up in front of MATLAB. **Julien**, thank you for providing the point tracking Fiji plugins, from where I get used to all the complex analysis processes. **Shashi** and **Thanh**, the two most intelligent Asians in the lab. You guys helped me in so many ways in these years, from lab to office, from microscopy to worm-injections and so on. You guys are my inspirations and role models. And I am happy to share the stacks, mostly Shashi's, and the laughter with you. Thank you, **François**, for all the supports for improving my coding skills and trained me for single molecule microscope to approach better imaging. I admire your beautiful British-accent English, even though you are a French and we all love your FOOD-CHAIN concept.

I would also like to express my gratitude to the members of the lab and François lab: **Saurabh**, we started academic career together, and now we are going to finish together in few days. We had a nice time together with everybody in Strasbourg and

Paris too. Thank you, **Flora**, **Alicia** and **Loan**, for all the nice conversations about science and life, which is used to happen in the kitchen. **Vlad**, thank you for your valuable suggestions for the imaging. **Camille** and **Serena**, the two beautiful French girls, I would always cherish the moments with you, especially during my French contest.

I would also like to thank my master internship supervisor Dr. **Carsten Janke**, who supported me greatly in my first year in France and from whom I learnt how to be organized. I also thank all the wonderful colleagues with whom I shared my early lab days, especially when I was in IGBMC, Strasbourg: **Sophie, Christelle, Gabi, Sarah, David, Ccile, Vincent, Marie, Steve, Arnold, Marc, Pascale, Yves, Marcel, Coralie, Yannick** from EMBO and **Stephan Grill** from MPI-CBG.

In the end, I would like to show my appreciation to my dear friends who have always been here for me. **Cecilia**, you have ever been so nice since the day we met. You always care for me, supporting me in my most difficult days. You are like my big sister and thank you for the unconditional love. **Maria**, thank you for always supporting me. No matter what happened, you always take my side and being so understanding and caring. I spent a lot of joyful time in your apartment. I also thank other significant people, who had been there for me my difficult times.

Finally, I deeply thank my **Mom** and **Dad** for their unconditional support and love and always standing next to me whenever I need despite the long geographical distance.

Abbreviations

AJM-1	Apical junction molecule-1
A/P	Anterior/Posterior
ABD	actin binding domain
C. elegans	*Caenorhabditis elegans*
CeHD	*C. elegans* hemidesmosome
CFB	Circumferential actin bundle
DLG-1	(Drosophila) Discs-Large (homologue)-1
D/V	Dorsal/Ventral
ECM	Extracellular Matrix
EGF	Epidermal Growth Factor
FGF	Fibroblast Grouth Factor
FO	Fibrous Organelles
IF	intermediate filament
L1-L4	larval stage of *C. elegans* development
MLC	Myosin essential light chain
MHC	Myosin essential heavy chain
MT	microtubule
Pat	Paralyzed arrest at two-fold
PCP	Planar Cell Polarity
POI	Points Of Interest
RLC	regulatory light chain (of non-muscle myosin-II)
RNAi	RNA interference
ROI	Region Of Interest
sgRNA	small guide RNA
SPIM	Single Plane Illustrating Microscopy
TIRF	Total Internal Reflection Fluorescence microscope
NTD	Neural Tube Defect

Table of Contents

Part I

Introduction

Preface

Epithelia form layers of cells to coat the exterior surface of organs or to line up the internal surface of organs. They separate different environments and regulate chemical substance exchanges. During embryonic development, epithelial cells undergo a dramatic change to drive morphogenetic processes. They can change their shapes, increase their numbers, rearrange their positions or lose their cell integrities. Mechanical forces, generated by actomyosin and transmitted by adhesive junctions, drive most of these changes. Thus, understanding how mechanical forces remodel epithelia and their adhesive junctional complexes, as well as how they contribute to large-scale tissue shape change are essential to understand embryonic morphogenesis in development.

The introduction of this thesis will be presented in three chapters. The first chapter introduces epithelia and the changes they go through in morphogenesis at a general level. The second part takes a closer look at the cellular and molecular level at the generation and transmission of forces in epithelia, mainly in our model system *C. elegans*, together with the valuable lessons we learn from other model animals. The third chapter introduces the adherens junction and the establishment of planar polarity during morphogenesis.

Chapter 1

Epithelia in morphogenesis

1.1 General characterization of epithelial cells

One of the biggest organs of human body, the skin, is formed by epithelia. They support the structures of organs and protect the body from the outside pathogens. Epithelia form various layers of cells to coat the exterior surface of organs or to line body cavity and ducts. In developing embryos and the gut, sheets of epithelial cells are organized in a monolayer; while in the skin, they are arranged in multilayers [1]. Biologically, epithelia separate the interior from the exterior environment as a total barrier or control the substance exchange cross the plasma membrane as a regulated barrier.

This section describes the classification and the embryonic origin of epithelia, as well as their usual locations and their primary functions.

1.1.1 Classification of epithelia

Closely adjoined epithelia form the epithelial tissues. In general, epithelial tissues can be classified according to their shape, their organizations, and their functions.

Based on the shape of epithelial cells, they can be subdivided into three groups: squamous, cuboidal and columnar (Figure 1.1(a)). Squamous epithelium has cells that have a bigger width than their height, with a flat and scale like shape. Cuboidal epithelium has cells that have the approximately same width and height, with a cube shape. Columnar epithelium has cells that have a bigger height than their width, with a column shape [2].

Based on the organization of their layers, epithelia can be subdivided into the simple, stratified, and pseudostratified epithelium.

The simple epithelium is formed by one single layer of epithelial cells. They are in direct connection to the basement membrane that separates them from the connective tissue. Based on their shapes, simple epithelium can be further classified into three sub-groups: simple-squamous epithelium, simple cuboidal epithelium, and

simple columnar epithelium.

The stratified epithelium is formed by multiple layers of epithelial cells. They are therefore more durable than simple epithelia and found more easily in the body parts that withstand higher mechanical and chemical insults to protect the underlying tissues without exposing the sub-epithelial layers [2]. Based on their shapes, stratified epithelium can also be subdivided into three groups: stratified-squamous epithelium, stratified-cuboidal epithelium, and stratified-columnar epithelium.

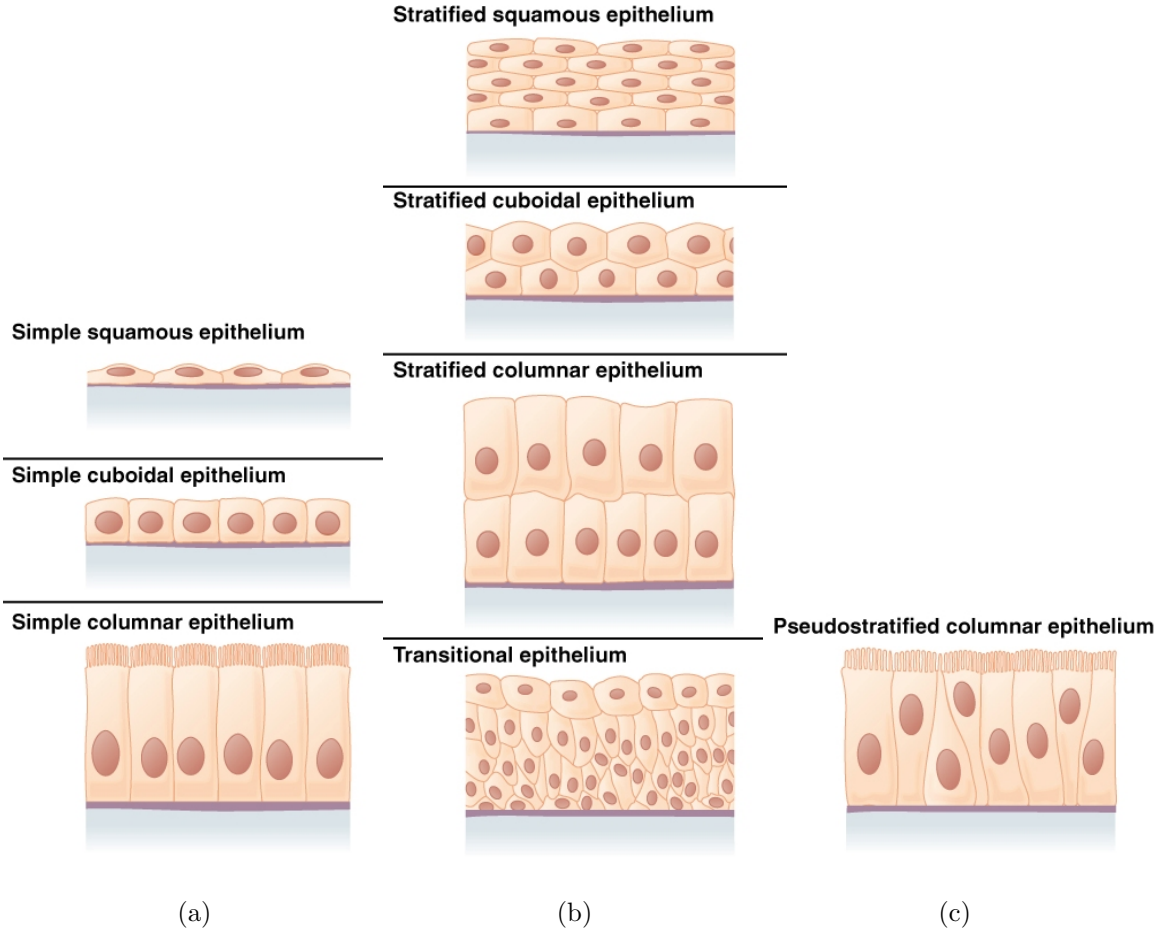

Figure 1.1: Classification of epithelia. (a) Simple epithelium, (b) Stratified and transitional epithelium, (c) Pseudostratified epithelium. Figure derived from [3].

The pseudostratified epithelium has simple columnar epithelial cells that seem to be arranged into several layers. These cells each has a nucleus that appears at different heights, giving a misleading impression that there are many layers of cells when viewed at a cross section. The transitional epithelium is a particular form of epithelium whose cells can adapt themselves to different conditions of tissue tension and change their shapes from squamous to cuboidal. The cells from the outer layer tend to be large and round, and the inner cells tend to be flat. This special structure allows the tissue to stretch and even expand under the tension without breakage. It

is often found in bladder, parts of uterus and urethra [2].

1.1.2 Location of epithelia

Epithelia lay on both the outside of the body and organs and the inside of cavities and ducts. The location of different epithelium is mainly based on their different biological functions. Their locations and functions can decide the shape and the organization of the epithelium. For example, in ducts and secretion portions of glands, there is mainly simple epithelium, which functions to secret and to absorb. In air sacs of lung heart and vessels, there is mainly simple squamous epithelium, to allow the materials to pass by filtration and diffusion. In skin, mouth, vagina, and ducts of some glands, there is mainly stratified epithelium to protect body or organ from mechanical and chemical damage.

1.1.3 Functions of epithelia

The primary functions of epithelia can be divided into four categories: a) Protection, b) Secretion and absorption, c) Forming a secretory duct, d) Providing sensation. Based on their functions, epithelia can be subdivided into covering and lining epithelium and glandular epithelium [2].

The covering and lining epithelium serves as a total barrier to prevent the invasion of outside pathogens, mechanical and chemical damages and dehydration. It allows the exchange of materials, such as the simple cuboidal epithelium in the kidney tubules. It can also sense the extracellular environment by, for example, smelling, hearing, and touching.

The main function of the glandular epithelium is to secrete. One or a group of highly specialized epithelial cells can form a gland from the enfolding and the subsequent growth within the underlying connective tissues. The glandular epithelium produces a secretion and then releases it to the external or the internal environment by an excretory duct or release it into vascular system as hormone.

1.1.4 The origin of epithelia

After gastrulation, the previously hollow ball of cells becomes multilayered. There are the ectoderm, outer germ layer of the embryo; the endoderm, the inner germ layer of the embryo; and the mesoderm, cells lying between the two layers. Epithelial tissues are derived from all three parts.

One important type of epithelial tissues derived from ectoderm is the epidermis, which is the outer part of the integumentary system. The lining of mouth, anus, nostrils and sweat glands are also derived from ectoderm. The epithelial tissues that are derived from the endoderm line the ducts and tracts in the gastrointestinal system, respiration system, endocrine glands, as well as the auditory system and urinary system.

Though most of the epithelial tissues are formed by endoderm and ectoderm, two

exceptions are derived from mesoderm. They are the collecting duct-lining cells of the kidney and the mesothelium cells, the body cavities-lining cells such as peritoneum and pleura.

1.2 The structure of epithelium

As the epithelial tissues consist of one or several layers of cells, they have almost no intercellular spaces and are interconnected tightly through junctions. Also, epithelial tissues are usually anchored to the underlying tissues by an extracellular fibrous basement membrane, which also separates epithelia from the underlying connective tissue.

Also, to fulfill the primary function of shielding the underlying tissues, the lining cells are reinforced and fiber-bearing. The roughness of lining cells is derived from the cytoskeleton, which is mainly composed of intermediate filaments.

In the following subsections, the three most important structures of epithelial cells will be discussed at a global level. The cellular and molecular details involved in this thesis will be discussed in the following chapters.

1.2.1 Basement membrane

The basement membrane is a thin and fibrous tissue that separates the epithelia and the underlying connective tissues. Basement membranes are usually secreted by the lining epithelial cells that rest on it. It not only anchors the cells onto it but also serves as a permeability barrier that controls the exchange of substances.

Though thin, the basement membrane is still composed of two layers, the basal lamina and the underlying reticular connective tissue (Figure 1.2). The most distinctive and crucial layer is the basal lamina, to which the epithelial cells anchor. It looks like a dense layer and is a network of fibrils, made of type IV collagen and other proteins such as laminin and proteoglycans. Basal lamina connects to epithelial cells by fine bridging filaments. Integral membrane proteins link the cytoskeleton filaments of the cells to the bridging filaments. Also, the basal lamina is bound to the reticular connective tissue with collagen VII anchoring fibrils and fibrillin microfibrils. The underlying reticular connective tissue also contains fibrillary protein, but not very distinctive from the underlying interstitial tissues.

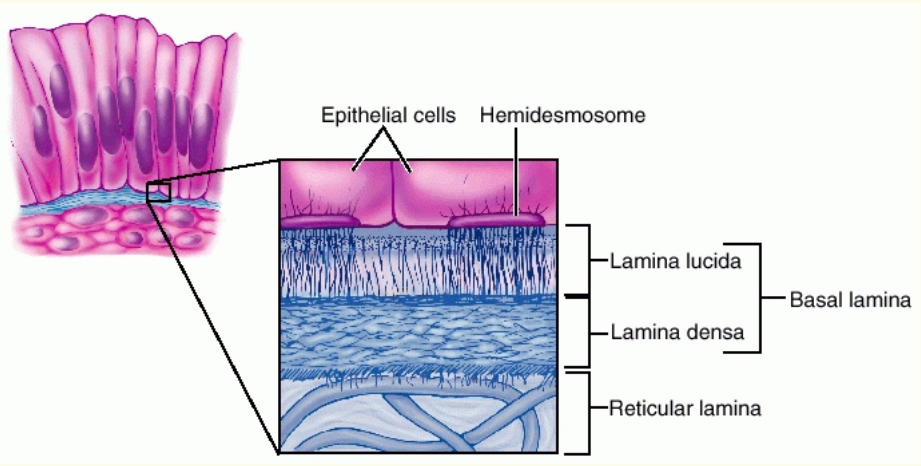

Figure 1.2: Structure of epithelial basement membrane. Derived from *Medical-dictionary*.

1.2.2 Junctions

Epithelial cells are tightly connected to form a sheet. This tight connection is achieved through specialized junctions. They interconnect the membrane of adjoining cells, or between a cell and the extracellular matrix. They also build up the paracellular barrier and control the paracellular transport. In epithelia, junctions can be mainly divided into five different types, tight junctions, adherens junctions, desmosomes, hemidesmosomes, and gap junctions. At the apical pole of some epithelial cells, different types of junctions can even combine to form junction complexes.

Tight junctions

Tight junctions are the least complicated junction type: they are composed of a pair of integral transmembrane proteins that are fused on the outer plasma membrane and join them. Tight junctions lie at the apical pole of cells and form a belt to encircle them. The intercellular space where tight junction happens is very narrow and filled with this dense junction material. Therefore, the passage of substances between epithelial cells is impossible because the intercellular space is sealed [4]. Also, tight junctions help to maintain the integrity as they keep the apical membrane domain to have a different composition by limiting the lateral movements of integral membrane proteins [3, 5].

Adherens junctions

Adherens junctions are fibrous proteins in the intercellular spaces, which are connected to the end of actin microfilaments of the both adjoining epithelial cells. Like the tight junctions, adherens junctions also form a belt to encircle the apical pole

of epithelial cells (Figure 1.3). Through the net of adherens junctions and microfilaments, the components of adjoining epithelial cytoskeleton are effectively interconnected. This allows the tensile forces to be transmitted and spread among epithelial cells, which in turn affects the roughness of epithelial tissue. The cellular and molecular basis of this are going to be discussed in the next chapter. In addition, some supportive fibers are also anchored to the adherens junction web [6]. The detailed composition, biological functions, as well as the remodeling during morphogenesis of adherens junctions, will be discussed in chapter three, as adherens junctions are the main study objective in this thesis.

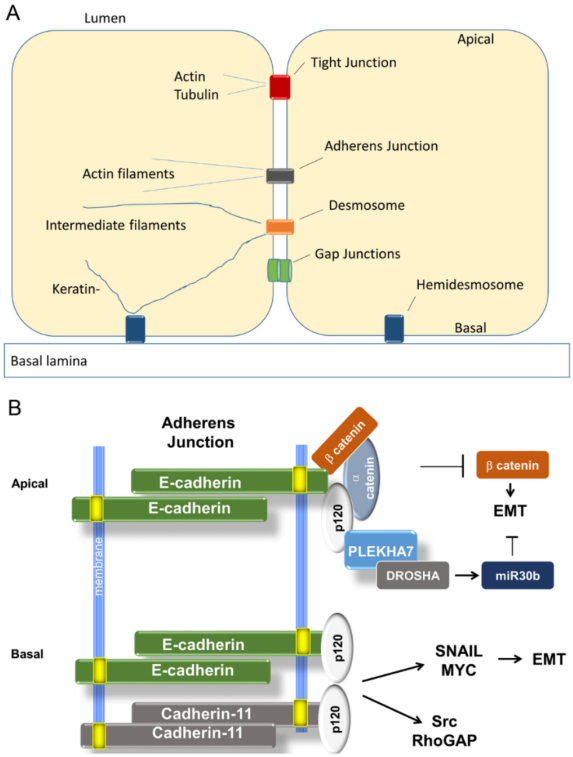

Figure 1.3: Epithelial junctions. (A) Scheme of cell-cell and cell-matrix attachments. (B) Scheme of apical and basal adherens junctions. From [7].

Desmosome

Like adherens junctions, desmosome attached to cytoskeleton intermediate filaments and allow the transmission of tensile forces between epithelial cells. The difference between these two types of junctions is that desmosome does not form a continuous belt, but circular patches. They are also located more basally compared to adherens junctions: they are distributed over the lateral membranes, with an up limit of adherens junctions. Also, the intercellular space at the desmosome is wider due to the receding of the cell membrane sections. Compared to adherens junctions, the attachment plaque is better developed [8].

Hemidesmosomes

Under the electron microscope, hemidesmosomes (HDs) has a similar structure as desmosome. However, while desmosome links two epithelial cells together, hemidesmosomes link the cell to the extracellular matrix. Noticeable, different from other types of junctions, hemidesmosomes are asymmetric as they connect the basal face of the cell to the basal lamina. Hemidesmosomes comprise two rivet-like plaques. Like adherens junctions, they also anchor to intermediate filaments of epithelial cells [8]. The plaques and the anchoring fibrils and filaments are collectively called HD-stable adhesion complex. The HD-stable adhesion complex forms a continuous link between the epithelia and the underlying basement membrane zone [8, 9]. Therefore, hemidesmosome can transmit the forces between them, like the adherens junctions. The details of hemidesmosome structure and function and the tension transmission will be discussed in chapter three.

Gap junction

Unlike all other types of junctions, gap junctions connect the cytoplasm of two neighboring cells directly. As implied in its name, a gap junction allows the direct pass of various molecules, ions, and electrical impulses between two cells. One gap junction comprises two connexions, also called hemichannels, to form a homo-dimer in the intercellular space. The homo-dimer of connexions can undergo a conformational change between close and open in different conditions and thus functions as a regulating gate between cells. Gap junctions are found in many tissues, especially in neurons and nerves, where they are called an electrical synapse [10, 11].

1.2.3 Cytoskeleton

The cytoskeleton is present in all type of cells in the body. It organizes cells in space and helps cells to interact mechanically with each other and with the environment. It is a complex network in a remarkable system of filaments that extend throughout the cytoplasm, from the plasma membrane to the nucleus [12]. The structure, function, and dynamics of cytoskeleton can vary. They depend on the behavior of three families of filaments: intermediate filaments, actin filaments, and microtubules. Here we take a general look on these three cytoskeleton filaments and will discuss the contribution of the cytoskeleton during morphogenesis in the next chapter.

Intermediate filaments

Unlike actin and tubulin, intermediate filaments (IFs) do not present in all eukaryotic cells, but only in some metazoans. In the most exposed epithelia, such as the skin, and the cells undertaking mechanical stress, IFs are chemically modified and fill the cell in a massive amount. This implies that IFs endure mechanical tension and impart them to tissues [12, 13].

The construction of IFs eventually reaches a rope-like filament of an average diameter of 10nm. Two monomers pair with each other to form a dimer, which lines up side by side with another one to form a tetramer. Furthermore, eight tetramers associate laterally in a helical array. The soluble subunit of IFs is dimer and tetramer (Figure 1.4) [14].

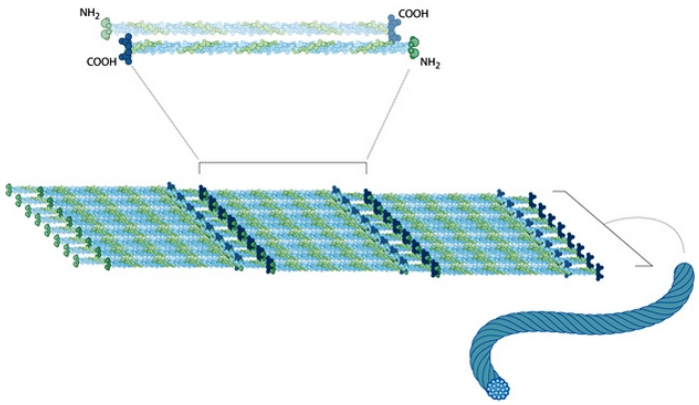

Figure 1.4: The structure of intermediate filaments. Up, tetramer made of four monomers. Middle, eight tetramers aligned with other eight tetramers in a staggered array. Lower right, an inter intermediate filament. From *Microtubules and Filaments, Nature education.*

The functions of IFs include anchoring the organelles and the nuclear envelope and organizing the internal structure of epithelial cells. Also, IFs function in maintaining the cell shape by bearing the mechanical tensions [8, 13]. Also, as mentioned in the last part of the junction, IFs participate in the cell-cell desmosomes and cell-matrix hemidesmosomes. Therefore, they also play a role in the tension transmission between epithelial cells.

Actin and myosin

The actin skeleton conducts a broad range of functions in epithelial cells. Although the monomers of actin assemble the helical rope-like filaments, these filaments are modified by and interact with other proteins to carry essential cellular functions [15]. In epithelial cells, actin forms contractile structures with myosin motor proteins to form cross-links and to slide relative to one another. As epithelial cells do not need to generate a high amount of contractile tension as the muscle cells, they only contain a small amount of actomyosin II bundles. The regulation of these contractile bundles activity is through the phosphorylation of myosin (Figure 1.5). One important function of these contractile bundles is to provide mechanical support for cells. Actomyosin bundles can assemble into cortical stress fibers to connect epithelial cells to adjoining cells or extracellular matrix through adherens junctions [15]. Also, actomyosin can generate forces inside epithelial cells for their remodeling, as well as the regulation of cell adhesion and migration during morphogenesis.

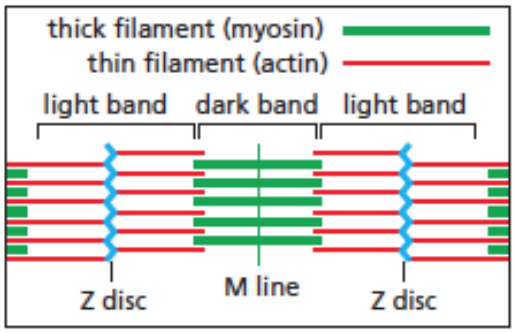

Figure 1.5: Schematic diagram of a single sarcomere. Figure derived from *Molecular biology of the cell*.

Microtubules

Compared to two other cytoskeleton filaments, microtubules (MTs) are more complex and more dynamics. The subunits of MTs are tubulins, which are heterodimers formed by two closely related globular proteins: α- and β- tubulins. Assembly of tubulins forms hollow, helical tubes of microtubules, which can be as long as 50 micrometers [16, 17]. The dynamics instability that microtubules undergo is profoundly influenced by the binding and hydrolysis of GTP. The dynamics and organization of MTs are also modulated by the polymer-stabilizing/destabilizing drugs and MT-binding proteins [17, 18]. A major function of MTs is to enable motor proteins to transport cargos within the cells. Two families of MT-based motors, kinesins, and dyneins move along microtubules to transport vesicles and even organelles during interphase. Our lab has recently discovered that MTs also contribute to the process of embryonic morphogenesis as transport machinery [19]. Details will be discussed in chapter two.

1.3 Overview of epithelial morphogenesis

Morphogenesis is a biological process, which, interpreted from its Greek meaning, causes the organism to form shape. A major goal of developmental biology is to understand how this process is accomplished with an exquisite degree of reproducibility and precision. Morphogenesis is often driven by the complex morphogenetic movements of epithelial tissues. A profound study of epithelial cell dynamics will promote our understanding of how these cell-level deformations facilitate the large-scale tissue rearrangements.

In the following subsection, several cell-based morphogenetic rearrange models will be summarized, and the chemical and mechanical principles that determine the tissue patterning will be discussed. At least, tension generation and transmission, which is a crucial player during morphogenesis process, will be analyzed.

1.3.1 Common morphogenetic movements of epithelia

The morphogenesis process is often driven by the epithelial cell growth or conformational change. They may lose or gain their integrity, reshape themselves, rearrange their locations and form tubes. The morphogenetic movements can be divided into three categories by different levels: a.) Individual cell changes at the cellular level, b.) Epithelial sheet movement, c.) Fusion and separation of sheets at a multi-sheet scale.

Individual cell changes

At the cellular level, epithelial cells go through conformational changes mainly due to the mechanical forces exerted by cortical tension, membrane-bound components and the extrinsic forces from surrounding tissues.

Apical constriction of epithelium is one of the driving forces for the change of cell shape (Figure 1.6). Due to the symmetrical constriction of actomyosin, the apical side of epithelial cells contracts resulting in cells taking on a wedged shape [20].

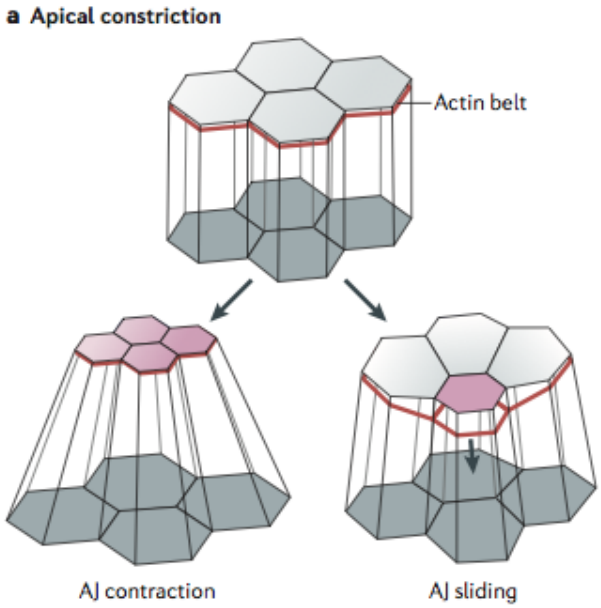

Figure 1.6: Scheme of apical constriction. Figure from [20].

Also, muscles activity can contribute to the reshaping of epithelial cells. During *C. elegans* late elongation, muscles that lie beneath the ventral and dorsal epidermis of the embryo promote the shape change of epithelial cells to drive the embryonic elongation. However, the mechanism of muscle-promoted embryo elongation is not completely understood. In this thesis, we discover another impact of muscle activity in epithelial cell reshape, and the details will be presented in the results part.

Epithelia movements at epithelial-sheet level

With the coordination of reshaping of cells, the epithelial sheets, therefore, undergo the complex movements including folding, invagination, tube forming, sheet extending and relative position changing. These precise shaping and organizing of epithelial cells shapes result in characterized shapes of different organs.

Folding happens in response to the radial tension on the epithelial sheet from a sudden increase intraocular pressure [21]. The formation of folds is similar to the formation of wrinkles when pulling a wrap of plastic from the two ends. Unlike the folding, which is a passive response to the extrinsic tension, invagination is often a result of intrinsic epithelial cell shape change. Apical constrictions that happen in one or several neighboring epithelial cells enfold this part of epithelial sheets. The most and first studied case of invagination is the gastrulation. Besides, neural tube formation also requires the apical constriction and the junction enrichment of myosin II [4]. The sheet extension can be a result of the unidirectional change in epithelial cell shape, which involves the apical constriction and apicobasal elongation. At last, epithelial cells can go through the relative position rearrangements such as rotation and intercalation. Intercalation happens under the impact of junction remodeling: during the extension of *Drosophila* embryo germband, the vertical junctions shorten, and the horizontal junctions lengthen. In this way, without cell migration, the inner arrangement of the epithelial sheet is achieved.

During the formation of organs, one or more epithelial sheet movements can happen and coordinate with each other to fulfill the morphogenetic process of embryonic development.

Fusion and separation of sheets at a multi-sheet scale

Even though most of the well-studied epithelial morphogenetic movement happen within a single layer of the epithelial sheet, there are instances where epithelial sheets separate from each other or fuse together. Intriguingly, separation and fusion of epithelial sheets are often observed together. During neurulation, the neural furrow separates from the overlying ectoderm after its formation and then fuses into a tube [22].

Individual cell shape change leads to the epithelial sheet movements. Likewise, epithelial sheets movements lead to the changes of epithelial cells at a multi-sheets scale. During the fusion of endodermal vesicles to ectoderm, a head-to-tail intercalation triggers the fusion event and results in a region of alternate epithelial cells having opposite apical-basal polarity [23].

In summary, epithelial cells achieve complex morphogenetic movements during development, with a coordination of single cell shape change; epithelial sheet movements and the multi-sheet fusion and separation. The mechanisms involved in these complex processes are not fully understood. Yet, the large amount of data that we acquired from the embryonic development process allows us to generate careful interpretations and refine our current understanding of epithelial morphogenesis. In

chapter two, we will discuss how the cell-level process can facilitate these large-scale tissue rearrangements at a cellular and molecular level.

1.3.2 Driving forces generations and transmissions

The morphogenetic changes of epithelia, including the size, shape, and position changing as we discussed in the last part, as well as their number and gene expression, are mainly controlled and regulated by mechanical forces. These forces can either be generated from the contractility of intracellular actomyosin networks, or extrinsic forces transmitted from the underlying tissues. After the generation of the forces within each cell, the coordination and the integration of the forces among cells produce the rearrangement of tissue. During this process, the long-range transmission of tension and cell mechanosensing play crucial orchestrating roles.

Tension generation and transmission at cell-level

In epithelial cells, non-muscle Myosin II is the common force generator that drives the cells to go through the morphogenetic process [24]. Myosin II interacts with the cytoskeleton molecules, frequently with actin fibers to form the actin-myosin networks. The regulation of myosin II activity generates the intracellular flow of actin and myosin in single cell-level process. There are three main aspects of actin-myosin-generated forces and their transmission need to be considered during morphogenesis.

The first aspect is that how the dynamics and direction of actin-myosin flows affect force generation in cells at the spatial and temporal range. For example, the mesoderm invagination during *Drosophila* gastrulation is driven by pulsatile and centripetal actin-myosin flows [25]. At the beginning of this process, myosin molecules enrich at the apical cortex of mesodermal cell. The apical actin-myosin increase their intensity in a ratchet model and move from the side toward the center of cell apex. However, for cell intercalation, the actin-myosin flows show a pulsatile but in an anisotropic manner, accumulating at the dorsal-ventral junctions, to trigger the endocytosis of junctional component to shorten them to vertices [25]. Actomyosin flows can also be non-pulsatile, as observed in the yolk cell gastrulation of zebrafish embryos [26]. These flows occur at the surface of yolk cells and pull towards the enveloping cell layer. With a circumferential contraction of the actomyosin cable, the continuous flows pull the enveloping cell layer spreading over the yolk cell.

The second aspect to consider is how actin-myosin flows can be effectively coupled to adherens junctions to transmit the forces to the other parts of the tissue. During the cell intercalation, since the accumulation of actomyosin triggers the shortening of junctions, the coupling between actomyosin network and junction component is crucial to this process. The coupling and/or the orientation of actomyosin require the activity of α-catenin and E-cadherin [27]. The shortening of junction decreases the distance between two vertices of one dorsal/ventral junction and pull two non-neighboring epithelial cells together, to rearrange their relative positions of epithelia. The endocytosis and recycling of these junctional components that determine their

turnover rate at the cytoplasm membrane and the binding/unbinding of actomyosin network to junctions control the force transduction among cells [28].

The third aspect is how the stabilization of cell shape change due to the pulsatile contraction of actomyosin network can be achieved during this process. During the germband extension of *Drosophila* cells, the pulsatile pattern of actin-myosin flows is associated with an accumulation of myosin II at adherens junctions and the increased cortical tension [29]. As a consequence, cells stabilize the decrease of apical area and recruit more myosin molecules for the next pulse to an incremental decrease in the apical area [29].

Regulation of actomyosin flows and tension transmission

As we discussed, there are three main aspects of force generation and transmission. Illustrating how these factors are controlled and coupled will be essential to understand how actomyosin functions during morphogenesis. Although the whole picture of actomyosin flow regulation is not completely drawn yet, several directions have been clarified [30]. a) Since the main motor myosin is normally connected to the cytoskeleton, the amplitude of actomyosin flows depends on the mechanical properties of the network and its coupling to the links. However, the specific upstream regulators are not yet identified. b) Inside the network, the composition and the activation of actin, myosin and their linkers, and also the turnover rate of these components can decide the mechanical property of the network and thus become crucial too. c) Also, within the anisotropic flows, the direction of these flows will be regulated for cortical tensions. d) The stability of junctional complex and the binding/unbinding of actomyosin networks will control the force transduction among cells.

1.3.3 Principles determining tissue patterning

The analysis of actomyosin dynamics and its regulations promote the understanding of the local generation and cell-cell transmission of mechanical forces. However, to better pattern the shape change of tissues, forces and tensions have to be integrated at a tissue-scale. A different situation of tissue reshape can be concluded within five major principles [30].

a) The integration of local and extrinsic forces. For example, during the mesodermal invagination, the centripetal apical constrictions at the apex of cells reduce the apical cellular area. Yet there is a higher tension along to anterior-posterior direction. Thus, the cellular apical area reduction is associated with the preferential constriction along the dorsal-ventral direction. During the germband extension of *Drosophila* embryos, extrinsic forces along the anterior-posterior direction associated with the actomyosin contractions that shorten the dorsal-ventral junctions to promote the elongation of germband along the anterior/posterior direction [27].

b) The coordination of gene expression. In *Drosophila* epithelial cells, Fat and Ds genes are found to control the polarized distribution of Myosin Dachs [31, 32, 33]. Fat excludes myosin from the cortex to regulate Hippo signaling, while Ds defines the lines

of myosin polarized distribution. Also, a study on Wnt/Fz-PCP signaling pathway shows that Celsr1, the Wnt/Fz-PCP component is polarized localized at the apical junctions at the dorsal-ventral axis to accumulate Rho-kinase, to activate myosin II at the apex of epithelial cells for the coordinated apical constrictions. The studies of these two pathways demonstrate how the gene expression pathways control the subcellular distribution of myosin II and further regulation the intracellular tension generation [31, 34, 35].

c) Force feedback on adhesion. Direct mechanotransduction between cells or cell and extracellular matrix has been shown to be critical for tissue patterning. In *C. elegans*, the hemidesmosomes connecting muscles and the basal side of the epidermis have been shown to be necessary for embryo elongation [36]. Extrinsic forces from muscle activities promote intermediate filaments re-organization through a p21-activated kinase-signaling cascade. Also, during the germband extension of *Drosophila*, cortical tension induced by myosin contraction further recruit more myosin II at the dorsal-ventral junction, to form supracellular MyoII cables. These MyoII cables trigger the intercalation of epithelial cells during germband extension [37, 38].

d) Forces coupling with tissues dynamics and signaling. Evidence has shown that the tissue-scale cell rearrangement mediated by tension can, in turn, regulate the global tissue planar polarity and patterning. A recent study has shown that the localization of Wnt/Fz-PCP proteins is a result of an initial polarization and subsequence rearrangement of the wing cells [39, 40]. Similar feedbacks have been observed in plants [41, 42]. Although the specific players and precise mechanisms involved in these feedbacks are to be discovered, the influence from local-tissue rearrangement on global tissue conformational changes starts to be unraveled.

e) Force regulation on differentiation and proliferation. The tension that affects the tissue rearrangement can influence the cell fate on a longer temporal scale. Cooperation of different factors plays together in this regulation [43].

The intracellular-generated forces play a crucial role in tissue rearrangement has become a widely accepted idea. How they interact with other processes such as the gene expression and extrinsic forces are not fully understood yet. One important step forward would be to apply a computational method to mimic and interpret forces from tissues deformation.

1.4 Conclusions

Epithelial cells are one of the most important cell types in organ and body. The reshape and rearrangement of epithelial cells at the cell-scale and the tissue-scale drive the process of morphogenesis. Cellular components such as the cytoskeleton and the adhesion complex can trigger and regulate the morphogenetic process by generating intercellular forces and transmitting them among cells. Thorough studies of the mechanisms by which tissue perturbing is regulated will provide a better and more profound understanding of development.

Chapter 2

Epithelia remodeling during *C. elegans* elongation

The elongation of *C. elegans* embryo takes place after ventral enclosure. The whole elongation process takes around 250 minutes. During elongation, the embryo increases its length along the anterior/posterior axis by four times and decreases its circumference by three times [44]. Like other morphogenesis processes, the elongation of *C. elegans* embryos is largely driven by the morphogenesis of epidermis. However, unlike in *Drosophila* and zebrafish embryonic development, there is neither cell division, cell intercalation nor cell migration [45]. Only epidermis shape changes drive the whole process of *C. elegans* elongation. Laser killing experiments have shown that the integrity of the epithelial sheet is crucial for the elongation process [46, 47]. There are two driving forces for elongation: the actomyosin contractility throughout the whole elongation process and the muscle activity beneath the epidermis that starts after the 2-fold stage (Figure 2.1).

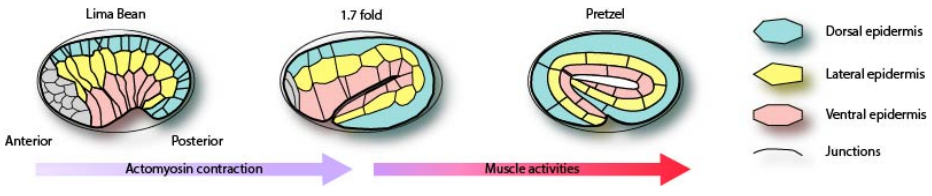

Figure 2.1: Embryo elongation process from Lima Bean to three-fold. More details see text.

This chapter will introduce several common epithelial activities that drive morphogenesis at a cellular and molecular level. Also, this chapter will summarize the knowledge on the actomyosin-induced tension in *C. elegans* epidermis, compared with

other well-studied systems, and how muscle activity induces embryo elongation, as well as the contribution from other cellular players.

2.1 Overview of morphogenesis process driven by epithelia

Morphogenesis is the process during which organism develops into its shape. Different cell activities direct this process in different situations. This part will give an overview of the common types of morphogenetic processes.

2.1.1 Cell division

During development, cell division profoundly affects the growth and organization of tissues. The rate, location and orientation of the division events can decide the rearrangement of tissue differentially [48, 49, 50]. Although in some situations, cells division seems to contribute to tissue growth and rearrangement by providing the raw materials, studies in chicken and plants showed that cell divisions could drive the morphogenesis of tissue directly by themselves or by triggering other cell rearrangements.

Formative cells division determining plant morphogenesis

One of the important roles during morphogenesis that cell division takes is to orient tissue growth and to help to decide the tissue shape. By precisely regulating the location of mitotic spindles and the rotation of cell division planes, they contribute to dictating multicellular morphogenesis [51, 52].

In the most common model plant, *Arabidopsis thaliana*, zygote first undergoes the asymmetric division to produce a basal cell and an apical cell [53, 54]. While the basal part of the zygote increases cell number at basal-apical direction through a series of anticlinal divisions, the apical cell follows a choreographic cell division program. During apical cell divisions, the division plane changes its orientation in every round of cell division, to establish the apical embryonic domain that contains cells of different shape and positions [52, 55] (Figure 2.2). Losing the rotation of cell division plane will lead to different embryonic defects and even lethality [56, 57, 58, 59].

The molecular modulations of this process for plants have been identified in recent years. One of the plant-specific molecules is auxin [60, 61, 62, 63, 64]. Auxin is responsible for several downstream transcriptional factors, including MONOPTERS (MP/ARF5) and its repressor BODENLOS (BDL/IAA12) [56, 65]. In a loss-of-function *mp* mutant, the orientation of dividing plane is disrupted. The same phenomenon is observed in the gain-of-function mutant of its repressor BDL. In both mutants, the formation of the primary root meristem is disrupted, resulting in a rootless phenotype of seedlings [66, 67, 68].

POLTERGEIST (POL) and POLTERGEIST-LIKE1 (PLL1) are other two molecular factors that are required for the dividing plane orientation and the cell division execution. The *pol/pll1* double mutant shows a loss of asymmetry during cell division, leading to defects in root meristem organization [69, 70, 71].

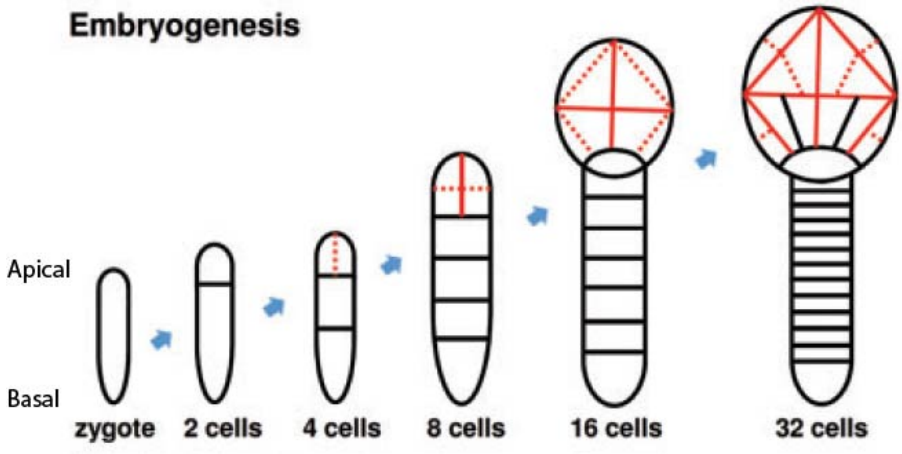

Figure 2.2: Two different types of cell division that shape the embryo during early embryogenesis of *Arabidopsis thaliana*. Red dashed lines indicate the rotations of cell division planes. Figure adapted from [48].

Cell divisions drive intercalation in chick development

Cell division can not only decide the direction of tissue development; it can also trigger other forms of cell morphogenesis and therefore promote tissue reorganization[72]. During gastrulation in chick, cell intercalation mainly induces the process of tissue rearrangement [73, 74, 75]. However, cell divisions induce intercalation initially, through an interplay between the actomyosin network of the dividing cell and the cortical actomyosin of its neighboring cells, which enables junction remodeling [49].

Experimental data have indicated that cell divisions promote cell intercalation: the neighboring cells intercalate between the daughter cells and the daughter cells themselves intercalate between the neighboring cells (Figure 2.3A). When cell division is inhibited under the exposure of aphidicolin, epithelial cells converged toward the primitive peak rather than display asymmetric rotations as normal [49]. This suggests that cell divisions affect the rearrangement of tissue by impacting spatial patterning.

During the cell division-induced intercalation, junctions went through remodeling and new junctions formed. Importantly, the inhibition of cell division stabilized junctions. When tissue exhibited a division-induced rearrangement, myosin and actin do not accumulate basolaterally in epithelial cells. This makes it possible for them to form new contact when dividing cells rounds up, contract and split from each other. The upregulation of cortical actomyosin accumulation in epiblast by the treatment

of jasplakinolide or calyculin A, or by RhoA in the neighboring cells is responsible for the functional relevance of actin and myosin (Figure 2.3B). This accumulation of actin and myosin impairs the formation of new junctions after division. When this accumulation of actomyosin is not activated, cell division-induced intercalation becomes possible to drive the tissue rearrangement [49].

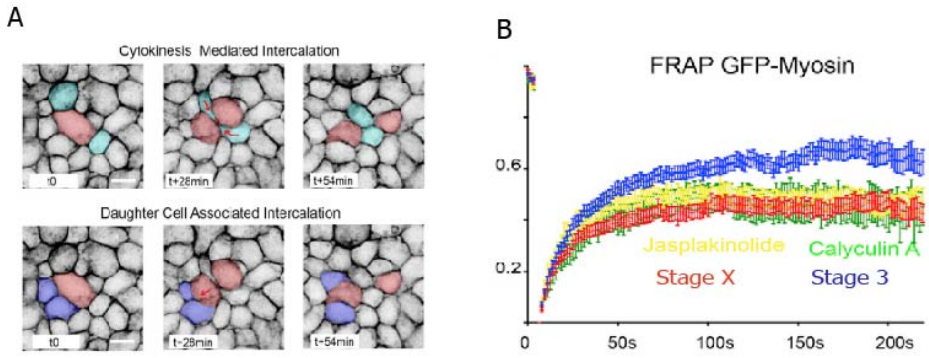

Figure 2.3: (A) Cell intercalation rises after cell division at stage 3. The first panel shows the intercalation in between daughter cells. The second panel shows a daughter cell intercalates in between its neighboring cells. Dividing cells in red. Neighboring cells in blue or purple. (B) FRAP experiment showed that Calyculin A and Jasplakinolide induced myosin accumulation at basolateral side of the neighboring cell next to a dividing cell. Figures adapted from [49].

2.1.2 Cell migration

Cell migration is a complex and widespread process during morphogenesis. Single cell migration allows cells to re-position themselves in the tissue. The coordinated and cooperative migration of a group of cells is referred to collective cell migration [76]. It is a hallmark of tissue remodeling events [76]. Cells specified at one region migrate extensively until they reach their target. Cell migration does not only happen during morphogenesis process but also underlies wound repair and cancer invasion [76].

Three important questions have been asked on the migration of cells during morphogenesis: 1) How do cells become motile and then detach from their original location? 2) What is the guide for cell migration? 3) How do cells recognize their target location and stop migration? Around these three questions, cell migration has been studied in many model systems, vertebrates and invertebrates.

The contribution of protrusions to motility of cells

During oogenesis of *Drosophila*, border cells form a collective motile cluster of six or ten cells [77, 78, 79]. In the leading cells of this cluster, the Rac-dependent actin-rich protrusions are generated [80, 81], initiating the cell migration through direct E-cadherin-mediated cell-cell contact and coordinating with the multicellular rear retraction mediated by myosin II [82, 83, 84]. The initiation of the border cell migration

in this cluster is under the control of two classes of ligands: the epidermal growth factor (EGF) and the platelet-derived growth factor and vascular endothelia growth factor-related factor 1 and 2 (PVF1 and PVF2) [85]. The following migrating cells depend on EGF alone [86] (Figure 2.4).

Also in *Drosophila*, the single cell forms dynamic cytoskeletal protrusions, including pseudopodia and filopodia to migrate toward the fibroblast growth factor FGF during tracheal branching [87, 88]. After the tip cell emerges in an FGF environment, the expression of the Notch ligand Delta in tipping cells increases, in turn suppressing actin dynamics in the following stalk cells [89, 90]. These two examples explain the motility generation and the migration guidance.

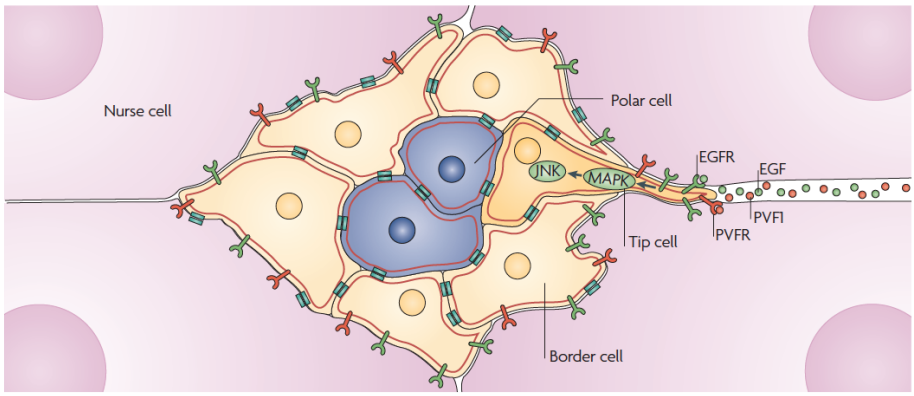

Figure 2.4: Polarized induction and guidance in border cell migration. Details see text. Figure from [76].

Signaling regulated migration

During the formation of Zebrafish lateral line, more than 100 cells form a cohesive cohort and migrate along the flank of the embryo to assemble into the mechanosensing organ [91]. A Sdf1-Cxcr4 chemokine-signaling axis regulates the polarization, restriction and the termination of the process of collective cell migration [92]. Though expressed universally in this cellular cohort, Cxcr4 is only activated in the cells at the leading tips to direct the cell strand polarity of the entire tissue [93]. While the whole groups of cells are moving, Fgf10 expresses central spot to induce the radial epithelialization and the apical constriction in the following cells to form the tissue progenitor [94, 95]. Finally, a Sdf1 receptor, Cxcr7, which expresses in the trailing edge of the cell group, decelerates and arrests the migration by sequestering Sdf1 and thereby suppressing the activity of Cxcr4 in the leading cells [96, 97, 98] (Figure 2.5).

The ventral enclosure of *C. elegans*

Cell migration also happens during the morphogenesis of *C. elegans*, the model system of this thesis. During ventral enclosure, the ventral epidermal cells that are initially located at the two sides of embryo migrate toward the ventral midline to zip

in the underlying cells beneath an epithelial monolayer. Like in the other system, the migration of the ventral epidermis is polarized, determined as leading cells and following cells. The ventral enclosure process happens in two steps. In the first phase, the two pairs of leading cells generate large protrusions to migrate towards the ventral midline. After the epidermal cells in each group meet each other, they form new junctional connections at the ventral midline. In the second step, the following cells become wedge shaped and extend to the ventral midline, zipping up the cell pocket at the ventral midline, and forming new junctional connections too. Laser ablation experiments have shown that both the anterior (leading) and the posterior (following) epidermis are required for the ventral enclosure.

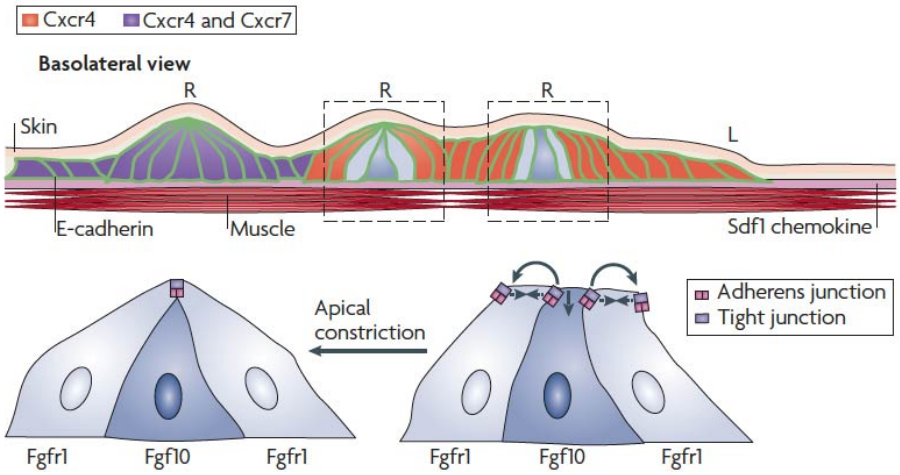

Figure 2.5: The lateral line primordium migration. Figure from [76].

The formation of the protrusion in epidermal cells replies on the dynamics of actin (Figure 2.6). The small GTPase CED-10/Rac-1 affects actin dynamics through its downstream effectors WAVE/SCAR (suppressor of the cAMP receptor) and ARP2/3 complexes. Mutations in these two complexes lead to a great decrease of actin dynamics at the leading edge of the epidermis, and less formation of smaller protrusions [99, 100, 101, 102]. The correct accumulation of CED-10/Rac-1 is guided by three proteins VAB-1, SAX-3, and UNC-40 that express in both epidermis and neuroblast [99]. UNC-34/VASP binds to the proline-rich domain of WAVE/SCAR protein to enhance actin dynamics [103]. Another protein that contributes to actin branching is the downstream factor of Cdc-42, WSP-1/WASP. It can promote the nucleation of F-actin in the epidermis [101, 104, 105].

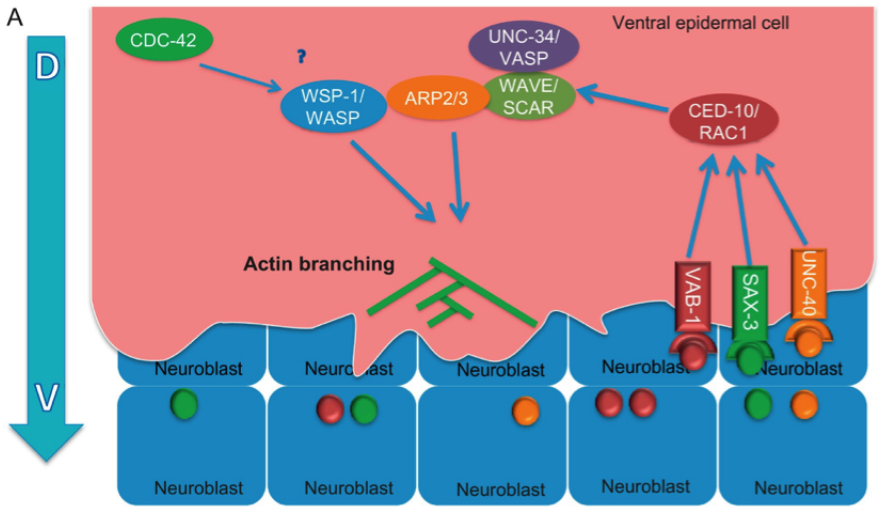

Figure 2.6: Signaling pathway promoting the branching of F-actin in the epidermis during *C. elegans* ventral enclosure. D, dorsal. V, ventral. Figure from [106].

2.1.3 Cell invagination

Epithelial cells invagination is a fundamental module to study infold of cells during morphogenesis. As we mentioned in the first chapter, invagination can be involved in many structure formation during tissue rearrangement including gastrulation and neural tube formation and primordial eye formation. Constrictions of actomyosin at the apical apex of epithelial cells reducing the apical area of epithelium is the key driver and initiator of this process. However, following cell shape changes are crucial for the whole process too. Invagination is well studied during the gastrulation of *Drosophila*.

Epithelial cell shape changes during gastrulation

Gastrulation profoundly impacts the shape changes in two different epithelia: the mesoderm epithelial cells that go through a fast shape change and finish inside to form the mesodermal tube, and the ectoderm epithelial cells that rearrange accordingly to this furrow formation [107, 108].

At the beginning of gastrulation, the most ventral part of the mesoderm, comprising of 8 to 10 cells, called ventral mesoderm, reduces their apical area because of the apical constriction due to the contractility of actomyosin enriched at the apex of the cell. As the apical area of ventral mesoderm keeps reducing, the lateral mesectoderm, the two bands of epithelial cells around ventral mesoderm, stretches to the middle of the embryo, resulting in a flattening bottom of the embryo. At the same time, the ventral mesodermal cells start to elongate along the apical/basal axis of the embryo. When the elongation of mesoderm reaches a certain level, the ventral mesoderm starts

to shorten along the apical/basal axis and to lengthen at their basal side. The combination of cell shape change in the ventral and lateral mesoderm causes the buckling of the embryo and initiates the furrow formation. After the furrow formation, the ventral mesoderm keeps shortening, and the lateral mesoderm starts to shorten along the apical/basal axis, to close the furrow. The process of invagination will reach its end when the ectoderm cells next to lateral mesoderm at each side of the furrow come to contact with each other (Figure 2.7) [107, 108, 109, 110, 111, 112, 113].

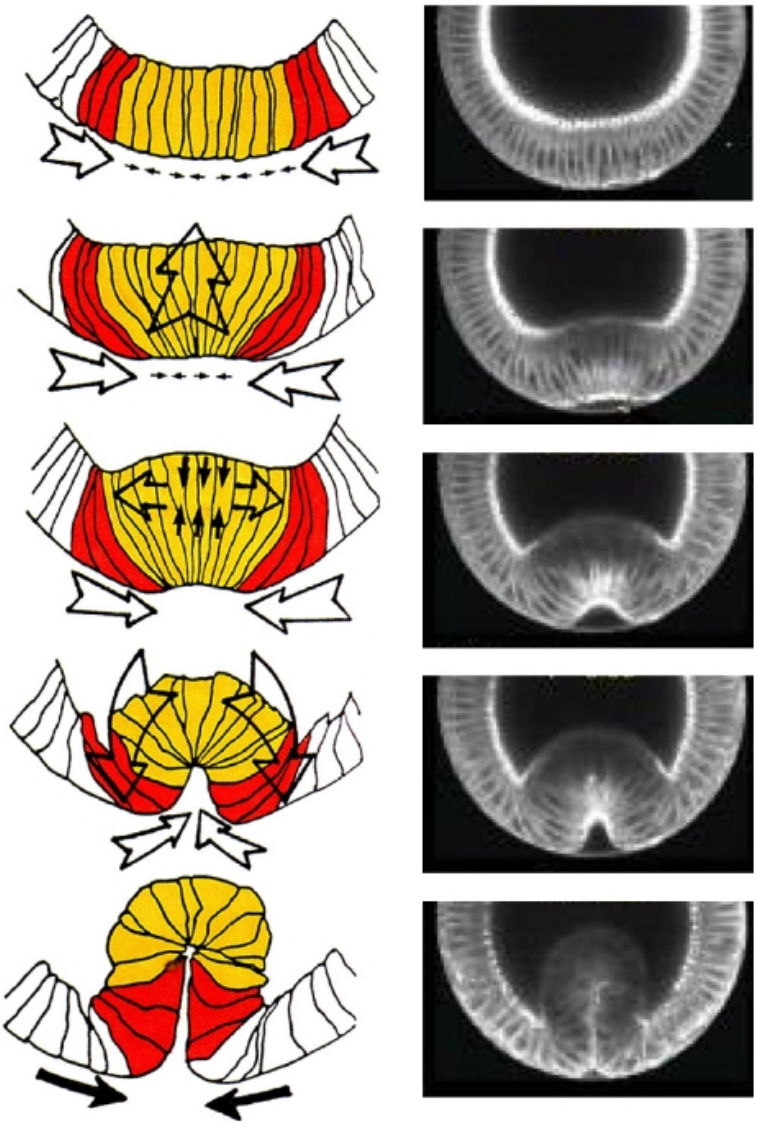

Figure 2.7: Cell rearrangement during *Drosophila* invagination. Left panel, scheme showing invagination. Yellow cells indicate to mesodermal; red cells indicate to ectodermal, from [112]. Right panel, invagination under the light microscope, from [113].

The shape remodeling of the ectoderm happens after the shape changes of the mesoderm. Recent research divides the shape change of ectoderm into two phases. During the first phase, invagination initiates, and the furrow starts to form. However, there is no lateral cell displacement of the ectoderm. Meanwhile, the apical area of mesoderm reduces due to the apical constriction and then starts to recover during the furrow formation. However, during the second phase, when the furrow depth becomes deeper, the lateral displacement of the ectoderm starts to increase correspondingly (Figure 2.8A) [109].

Recent research also reports the interaction between the mesoderm and the ectoderm during furrow formation. Even though the lateral displacement of the ectoderm occurs synchronously with the furrow deepening process, immobilization experiment demonstrates that it may not be the driving force of furrow deepening [109]. When the right-lateral ectoderm is fixed to the overlying vitelline membrane, the newly formed furrow no longer locates in the central ventral part of the embryo, but leans to the right, implying the reshape of mesodermal cells is the driving forces for furrow formation (Figure 2.8B).

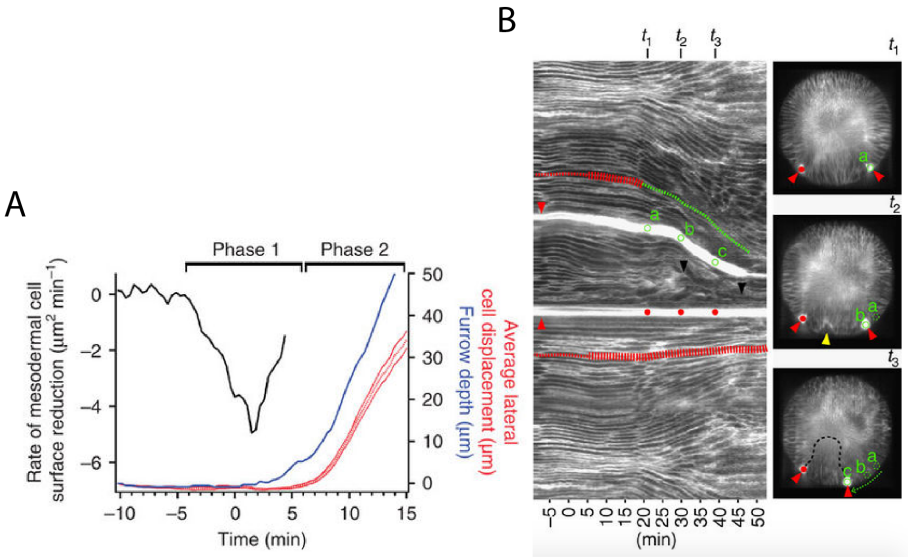

Figure 2.8: (A) Different behavior of mesodermal and ectodermal cells during invagination. (B) Mesoderm internalization and ectoderm movement. Red line in the lower left panel, fixed ectoderm, indicated as the red dot in the right panel. Green line in the upper left panel, the track of moving ectoderm, indicated as green dots in the right panel. Figure adapted from [109].

Molecular pathways involved in gastrulation of *Drosophila*

Besides being regulated by myosin activation during apical constriction, gastrulation can be regulated by other molecular pathways. They can be summarized at three different levels [114].

The first level is the developmental signals, which decide the dorsal/ventral axis of the embryo [115, 116]. During oogenesis, a protein cascade is triggered to establish the axis. Two transcription factors, Twist and Snail, determine the boundary of mesoderm and help to internalize the furrow during invagination [117].

The second level is the cell surface signals, which are controlled by developmental signals. Two G-proteins coupled receptors (GPCR); mist [118] and smog [119] are activated in the mesoderm [120].

The third level is the conserved intracellular Rho1 pathway, the most important pathway to regulate the activity of myosin II, which induces the formation of the actin network, thus, initiates the apical constriction. This pathway is regulated by the second level signals, mist, and smog [119, 121].

2.1.4 Cell intercalation

Cell intercalation is a very conserved step during morphogenesis. It leads to a direct exchange of neighboring cells, without changing the total number of cells [122]. Cell intercalation can occur in both early embryonic development, such as during the gastrulation and the later stage of organization when the tissue requires an extended morphogenesis [122]. Depending on the direction of intercalation, there are two types of intercalation: mediolateral intercalation, during which the cells exchange positions with their neighbors within one epithelial plane and the radial intercalation, during which cells exchange their places throughout a multilayer tissue to form a single layer of epithelial cells [122].

Depending on the tissue type, cell intercalation can either rely on the remodeling of apical junctions of epithelial cells, or on the basolateral protrusions of the mesodermal cells [122]. These two cases are well studied during the germband extension of *Drosophila* and dorsal intercalation of *C. elegans*, respectively. But radial intercalation is more context-dependent and requires non-autonomous signals.

Germband extension of *Drosophila*

The germband extension of *Drosophila* is a typical example of the apical epithelial cell intercalation. During germband extension, the tissue shortens along the dorsal/ventral axis and elongates along the anterior/posterior direction (Figure 2.9 A) [123, 124]. This tissue remodeling requires the shrink of junctions followed by a formation of new contact between the intercalating epithelial cells [37, 38, 123, 124, 125, 126]. The remodeling can either go through a so-called T1 transition or the formation of a high-order structure known as rosettes (Figure 2.9 B) [127]. Two research articles from Thomas Lecuit lab demonstrate that the non-muscle myosin II activity is the driving force for both the junction shrinking and junction formation and elongation during cell intercalation in *Drosophila* germband extension.

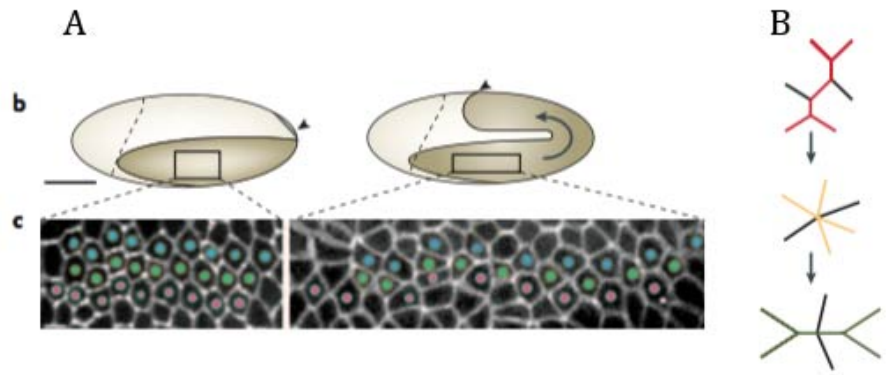

Figure 2.9: (A) Germband extension and cell intercalation in *Drosophila* embryo. Colored cells show the rearrangement. (B) T1 transition and rosette formation during intercalation. Figures adapted from [127].

During the first phase of T1 transition and rosette formation, only the junctions along the dorsal-ventral direction between the neighboring cells shorten. This polarized junction remodeling is under control of myosin II. The activation of myosin II and formin Diaphanous promote the AP2 and clathrin coated endocytosis of E-cadherin. Therefore, junctions connecting neighboring cells are shortened. The activities of myosin II and Diaphanous are regulated by guanine exchange factor RhoGEF2, which is enriched in the intercalation region and polarized distributed along the dorsal/ventral axis (Figure 2.10 A) [28].

During the second phase of T1 transition and the deformation of the rosette, new connections form between the intercalating cells. This process is largely driven by the local and the tissue-scale mechanical forces. Medial myosin II pulses drive the growth of a new junction in this process by pulling at the two vertices of the newly formed junction. Moreover, this polarized tissue extension is coupled with invagination. A tissue-scale pulling force from the invagination posterior midgut acts as the extrinsic tension source for the germband extension by orienting the direction of junction growth and thus, the direction of germband extension. These results suggest the importance of interactions between different tissue remodeling patterns during morphogenesis (Figure 2.10 B) [128].

Dorsal intercalation of *C. elegans*

Aside from the apical epithelial cells intercalation, basal epithelial cells also go through intercalation process during morphogenesis. One of the well-studied cases is the cell intercalation of *C. elegans*. In such basal intercalation, cell mobility comes from the activity of protrusion [45, 129]. During the formation of dorsal midline, the two rows of dorsal cells first form a wedged shape, with their medial tips pointing to the mid dorsal line. Then the dorsal epithelial cells interdigitate between their contralateral neighbors, elongating until they meet the other side of the embryo [45, 130]. During this process, the nuclei of dorsal epithelial cells migrate contralaterally too. However,

the nuclei migration is not necessary for intercalation [131] (Figure 2.11).

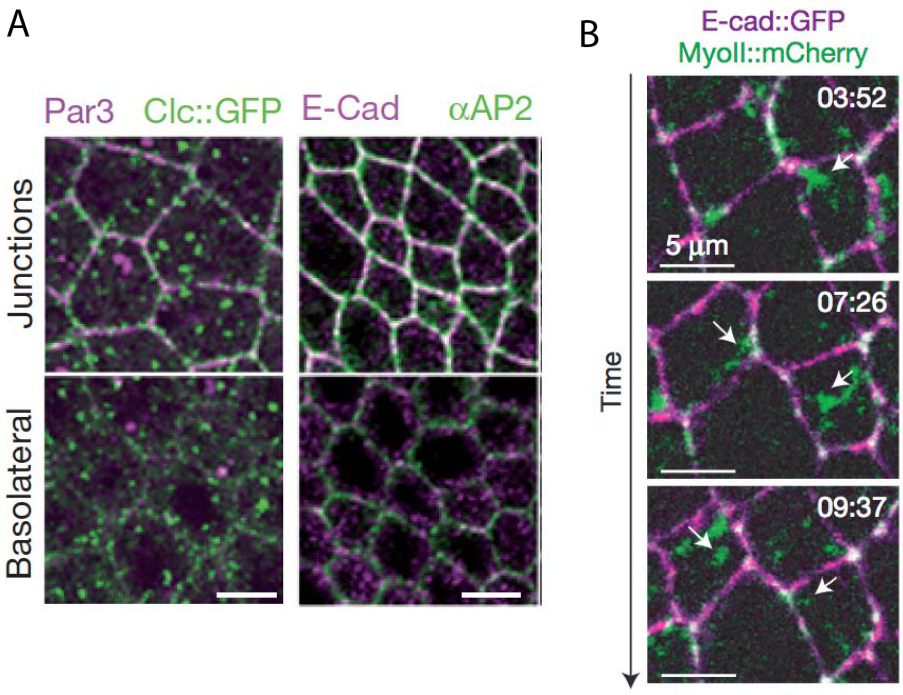

Figure 2.10: (A) Polarized distribution of the endocytic machinery at adherens junctions. (B) MyoII clusters promote the extension of new junctions by pulling on the vertices of the new junction. Figures adapted from [28] and [128].

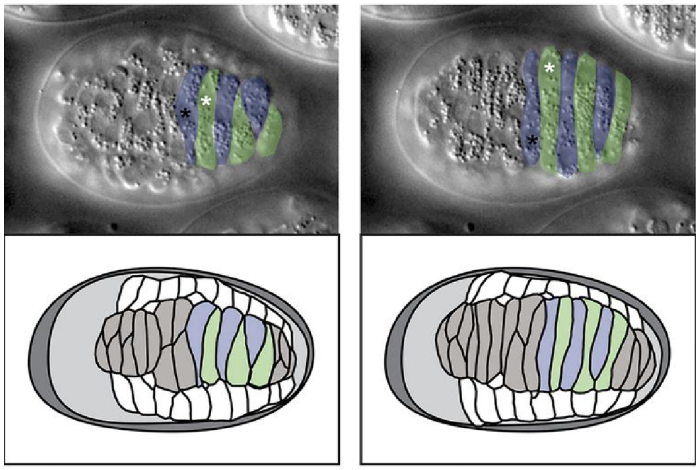

Figure 2.11: Dorsal intercalation of *C. elegans* embryo. Figure adapted from [132].

During intercalation, dorsal epidermal cells extend basolateral protrusions that are just beneath the apical junctions [45, 133]. Actin microfilaments and microtubules

are shown to be necessary for the dynamics of these protrusions. Activation of actin nucleating ARP2/3 complex through WAVE/SCAR protein in the RAC signaling pathway is required for intercalation, but the detailed mechanisms are not clear yet [134]. Laser killing experiment shows that the existence of neighboring cells is not required for intercalation [45, 133], suggesting that the initiation of intercalation is an autonomous process.

Radial intercalation during morphogenesis

Unlike the tissue reshaping within one single plane during medial intercalation, radial intercalation involves cells going through the thickness of the tissue [122]. Therefore, radial intercalation drives the tissue thinning process and the formation of concomitant epiboly during gastrulation [122]. Radial intercalation was first observed in the animal cap ectoderm of the *X. laevis* embryo [135]. In this case, animal cap ectoderm spreads to form a monolayer of cells, requiring the interactions between integrin and fibronectin [135, 136]. Radial intercalation is observed in the zebrafish epiboly [137]. Zebrafish epiboly formation depends on the intercalation of deep cells beneath the enveloping layer [137]. Cell adhesion molecules EpCAM and E-cadherin are required in this process [137, 138]. On one hand, the strong attachment of E-cadherin to the cytoskeleton allows the efficient cell intercalation [137, 138]. On the other hand, the epidermal growth factor pathway regulated E-cadherin endocytosis is required for intercalation [139].

2.1.5 Cell shape change

One intriguing re-patterning of tissue is due to the shape change of the epidermis and only due to the cell shape change. Without any cell division, migration or intercalation, stable coordinated shape changes in epidermal cells result in the corresponding shape change of the tissue. Depending on the direction of tissue shape change, there are two types of morphogenetic cell shape changes. The first type is that the cell surface changes equally in the apical and the basal side, resulting in an isotropic expansion or contraction of the epithelial sheet, such as in the unified flattening or columnization of epithelia. The second type is that the epithelial cells change their shapes along only one axis, resulting in an anisotropic shape change, like invagination as discussed in the previous part [140].

C. elegans embryonic elongation

C. elegans elongation is one typical example of anisotropic epithelial sheet extension by cell shape changes. During this three-hours process, the elongation of the embryos is driven by the lengthening of hypodermal cells along the anterior/posterior direction. Meanwhile, the cells become narrower circumferentially.

As the junction remodeling during *C. elegans* elongation is the main goal of my thesis, this morphogenetic process will be described in the following session, so will the cellular and molecular mechanisms behind this process.

2.2 Overview of *C. elegans* elongation

Before *C. elegans* embryo starts to elongate, it goes through the dorsal intercalation and the ventral enclosure. Immediately after ventral enclosure, embryos start to elongate, converting from a lima-bean shaped embryo into an elongated worm shape. Within three hours, the embryos elongate along the anterior/posterior axis by four times and reduce their circumference to one-third [47]. The rapid elongation speed and the transparency of the egg make *C. elegans* an ideal model animal to study epithelial morphogenesis.

The elongation process of *C. elegans* can be divided into two phases: the early elongation and the late elongation, depending on the activation of muscle activity. The next part will briefly describe the two phases.

2.2.1 Early elongation

Early elongation refers to the period between lima bean and 2-fold stages when the muscles become active. During early elongation, the epidermis starts to go through shape change, as can be most easily observed in the lateral epidermis: they shorten themselves along the dorsal/ventral (D/V) direction and lengthen themselves along the anterior/posterior (A/P) direction. However, the perimeter of these lateral epidermal cells stays the same during early elongation (Vuong and Labouesse, unpublished data).

Genetic and pharmacological studies have shown that actomyosin contractions are crucial for elongation since the beginning of this process [47, 130, 141, 142]. Treatment with actin polymerization inhibitor cytochalasin D blocks the early elongation [47]. Also, microtubules are proven to be important for elongation too. When treated with microtubule inhibitor nocodazole, embryos present a disorganized elongation [47].

2.2.2 Late elongation

When *C. elegans* embryos reach 1.7-fold to 1.8-fold, muscles that locate beneath the dorsal and ventral epidermis start to become active, with contractions and extensions, driving the embryos to move.

During late elongation, muscle activity plays a more crucial role in embryonic elongation. The actomyosin contractility still exists but is thought to become less important for elongation [143]. Analysis from muscle defective mutants showed that complete loss of muscle function leads to failure of elongation beyond 2-folds. These mutants are also called the Pat mutant, paralyzed arrest at two-fold [130]. Though Pat mutants maintain a normal elongation rate during early elongation as wild-type embryos, they are completely paralyzed and stop at 2-fold, suggesting the muscle activity is crucial for late elongation process.

2.3 Actomyosin contractions and early elongation

As introduced before, the contraction of actomyosin provides one crucial driving force throughout the entire morphogenetic process, mainly during the early elongation. Unlike the actomyosin constriction during invagination that reduces the apical area of the cell, actomyosin contract circumferentially to narrow the epidermis and to squeeze the embryo to elongate radially to increase their length along the A/P direction by an increase of in hydrostatic pressure [106, 144].

The active contractions of actomyosin are generated in the lateral epidermal cells and transmitted to the dorsal and ventral epidermis through junction complex. A Rho-kinase pathway regulates the activation of actomyosin in the lateral epidermis and the dorsal/ventral epidermis.

2.3.1 Actomyosin

Non-muscle Myosin II

Myosin II is the ATP-dependent motor using actin as a substrate involved in muscle contractions and a wild range of cell movements. It comprises two heavy chains, two regulatory light chains and two essential light chains [144, 145]. In *C. elegans*, the two heavy chains are named *nmy-1* and *nmy-2*; the regulatory light chain is named *mlc-4* and the essential light chain is named *mlc-5* [146] [147]. The N-terminal of heavy chain contains a globular domain that interacts with actin and ATP, required for the motility of the motor protein. The C-terminal of heavy chain contains an α-helical coiled-coil domain that interacts with another heavy chain to dimerize and form myosin filaments (Figure 2.12 A). The essential light chains and regulatory light chains are small proteins that contain two Ca^{2+}-bind EF-Hand domains that interact with the neck region of the heavy chain. The neck region is thought to amplify the movements resulting from the conformation changes due to the ATP-binding and ADP-binding [148, 149].

The mechanical mobility of myosin is a result of the globular domain conformational change: whether it is bound to ATP or ADP and whether it binds to actin filaments. ATP bound myosin binds to actin. Then the hydrolysis of ATP releases the phosphate and causes the conformational change of the globular domain. Therefore, the heavy chain displaces from actin. After, the replacement of ADP by ATP restores the initial conformation of a globular domain, leading to the re-interaction of myosin and actin [149]. Myosin starts to walk on actin filaments through the bindings and the re-bindings. Yet before the conformation change happens, one myosin molecule has low mobility [150]. Two myosin molecules often form a polymer through the long tails of heavy chains. The polymers further form highly motile bipolar filaments to attach and to pull the antiparallel actin filaments (Figure 2.12 C) [151].

The association of these myosin and actin molecules is referred as actomyosin network. Actomyosin network generates most of the tension that is responsible for

epithelial morphogenetic change during development. The mechanical property of actomyosin network depends on the activity of myosin, the structure of the network and the presence of actin linkers [152, 153, 154].

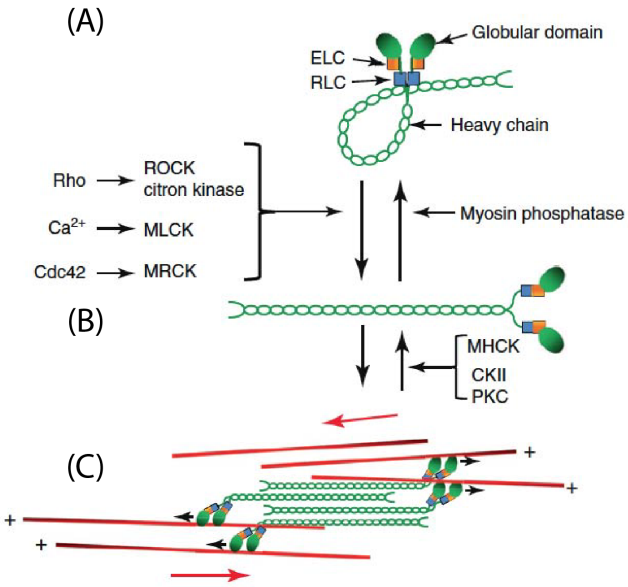

Figure 2.12: Myosin II structure (A), activation (B) and actomyosin network (C). Figures adapted from [155].

Regulation of myosin II activity in the epidermis

The activation of myosin largely depends on the phosphorylation of two highly conserved residues within the regulatory light chain. Inactive myosin before phosphorylation presents a folding hexamer conformation that does not bind to actin. The phosphorylation releases the hexamer conformation of myosin and allows it to bind to actin. Different kinases involve in the activation of myosin in different contexts. In epidermis, the phosphorylation of myosin is mainly controlled by Rho kinase. Activation of myosin also increases the stability of myosin filaments. The inactivation of myosin II is mediated by phosphatase (Figure 2.12 B) [155].

Actomyosin network

Since myosin can form bipolar filaments to pull on the actins to generate intercellular tension, the structure of actin in this network is as crucial for force generation as the activation of myosin. The structure of actin can be either un-branched or branched. In the un-branched actin network, myosin-dependent actin filament rearranges in an antiparallel array, leading to a high contractility. In the branched actin network, the rearrangement of actin is limited, and the contractility of this type of network is low [25, 156, 157].

It has been reported in recent years that during tissue morphogenesis, actomyosin

network can drive the tissue shape change. In *C. elegans* zygote, a gradient in actomyosin contractility drives a large-scale cortical tension in the viscous cortex to generate an anisotropic cortical flow to ensure the efficient polarization of the *C. elegans* zygote [158]. This cortical flow, in turn, aligns actin filaments to form a furrow [159]. During *Drosophila* germband extension, the stability and pulsatility of actomyosin network are governed by phosphorylation-dephosphorylation cycles of the regulatory light chain and the advection as a result of the contraction of the F-actin networks [160].

2.3.2 Actomyosin contraction and cell shape change

During early elongation, actin filaments are organized in the dorsal and ventral epidermis in circumferential bundles. But in the lateral epidermis, actin filaments are shorter, thinner and less oriented in a disorganized pattern [47, 144, 147]. The mechanism controlling the circumferential organization of actin filament bundles in the dorsal and ventral epidermis is unclear yet. The tension that squeezes the embryo radially to elongate is generated in the lateral epidermis. However, the actomyosin activity is regulated in both dorsoventral cells and lateral epidermis, but in different directions (Figure . 2.13)

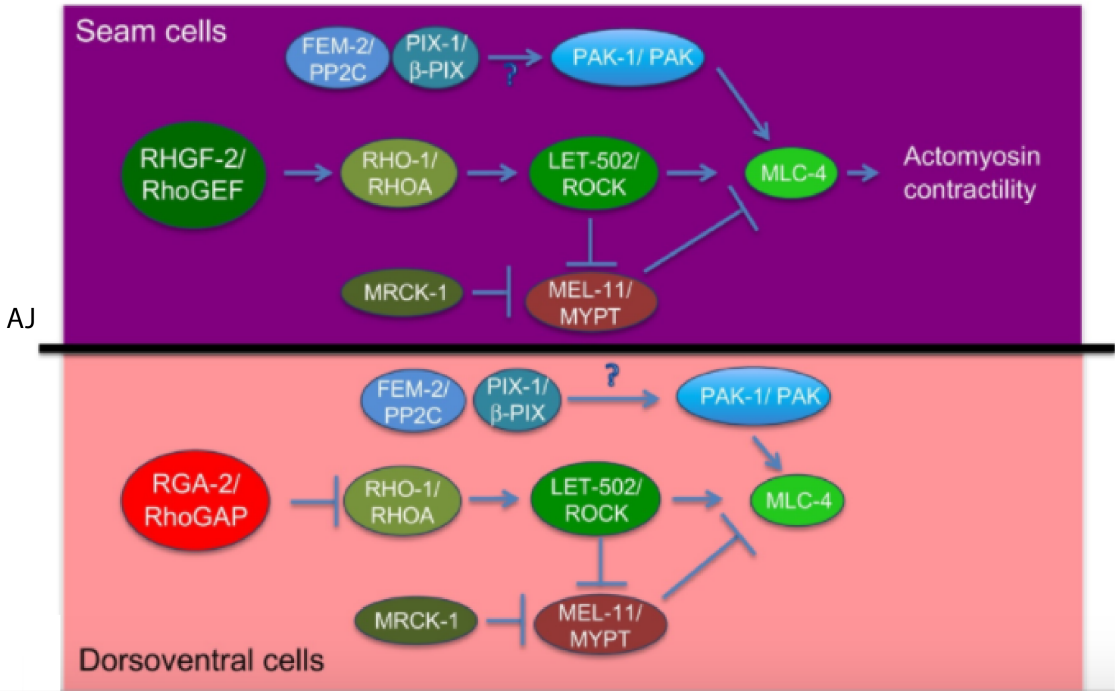

Figure 2.13: Molecular pathways of actomyosin activation in the dorsal and ventral epidermis. AJ, adherens junction. Details see text. Figure from [106].

The activation of myosin pathway in epidermis

During *C. elegans* embryo elongation, myosin II is activated by the phosphorylation of the regulatory light chain, MLC-4 by the LET-502/Rho-binding kinase and is deactivated by the MEL-11/Myosin binding subunit of myosin phosphatase [147, 161, 162]. LET-502 is the effector of the Rho GTPase RHO-1. Rho-1 can be activated by the *C. elegans* Rho Guanine Nucleotide Exchange Factor (RhoGEF) RHGF-2 and deactivated by the Rho-GTPase-activating Protein RGA-2 [143, 163]. Mutations that affect the up-regulators of myosin contractility, such as RHGF-2/RhoGEF, LET-502/ROCK, MLC-4 and the heavy chains of myosin result in the hypoelongation that is embryos arrest earlier than or at 2-fold [147, 161, 163, 164, 165]. On the contrary, mutations that block the down-regulators of myosin activation such as mel-11 or rga-2, cause embryos to burst and increase tension on junctions during elongation due to an abnormal increased hydrostatic pressure [143, 161].

Though the activation of actomyosin is mainly through the regulation of LET-502/Rho kinase, two additional kinase pathways contribute to myosin II activity in the epidermis. The first one is the p21-activated kinase PAK-1, which is downstream of phosphatase FEM-2/PP2C and the CDC-42/RAC-specific GEF PIX-1/β-PIX [147, 166, 167]. How did PAK-1 activated by the upstream players is still unknown yet. The second one is the Cdc42-activated kinase MRCK-1, which inhibits the activity of MEL-11 [147].

The active generation and the passive response in epidermis

Genetic and molecular studies have suggested that the actomyosin induced mechanical forces are actively generated in the lateral epidermis and the dorsal and ventral epidermis remain passive to respond to these forces during elongation [106]. The different behaviors of myosin in lateral and dorsal/ventral cells lay in three aspects. The first is that the activity of regulatory light chain is mainly required in lateral epidermis rather than the dorsal and ventral epidermis [147]. The second is that the essential light chain of myosin MLC-5 and the heavy chain, NMY-1 are enriched in lateral epidermis rather than the dorsal or the ventral epidermis [147, 164, 165]. The third evidence comes from the signaling pathway rescue experiment, which demonstrates that the up-regulator of LET-502/Rho kinase pathway, RHGF-2/RhoGAP acts specifically in lateral epidermis, whereas the down-regulators of MCL-4 RGA-2/RhoGAP is required only in dorsal and ventral epidermis [143, 163]. In these ways, the myosin regulatory pathway is under control, to specify the myosin contractility in the lateral and the dorsal/ventral epidermis.

Epidermis remodeling during early elongation

During early elongation, the epidermis shortens along the dorsal/ventral direction and elongation along the anterior/posterior direction. Along with this cell shape change, apical junctions undergo remodeling too. During the germband extension of *Drosophila*, as we discussed in the previous part, the polarized distribution of myosin

II with higher accumulation at the junctions is responsible for the junction remodeling, both shortening and the formation and elongation of new junctions [28, 128, 168]. This planar polarity-dependent junction remodeling is also observed in *Xenopus* mesoderm [168]. However, the planar polarized distribution and the flows of myosin II are not observed in *C. elegans* embryo elongation.A recent study of our lab showed that during early elongation, the coordination between the anisotropic Myosin-II-dependent force within the lateral epidermis and the anisotropic stiffness within the fiber-reinforced dorsoventral epidermis mainly contributes to early embryo elongation [144].

2.3.3 Effect of actomyosin activity on a tissue-scale

To better understand how epithelia remodel during early elongation, it is necessary to explore the effect of actomyosin at the tissue-scale.

The tension transmission and converge through junction/supracellular actomyosin network

While contractile forces are generated in the lateral epidermis, they are transmitted into the dorsal and ventral epidermis via the linkage between actin filament bundles (CFBs) and adherens junction. The catenin-cadherin complex plays a crucial role in force transmission [142]. In catenin-cadherin core and associated proteins mutants, the embryos fail to elongate or elongate abnormally due to the detachment of CFBs from adherens junctions. In *hmp-1* and *hmp-2* mutants, embryos form a weird bulge after ventral enclosure when they attempt to elongate. Compared to wild type embryos, CFBs in HMP mutant visibly detach from adherens junctions [142]. One of the associated catenin-cadherin complex proteins VAB-9 functions in linking junctions and CFBs together. *vab-9* mutants have perturbed CFB organization at adherens junctions, which result in abnormalities in body-shape and elongation [169].

Disruptions in adherens junctions also harm the elongation process. JAC-1/p120 is another associated catenin-cadherin complex protein. In a weak mutant of *hmp-1*, JAC-1/p120 modulates the junction of catenin-cadherin complex for embryo elongation and affects the normal elongation process [170]. Junction basal boundary defining protein LET-413 also contributes to elongation. *let-413* mutants form improper junctions and are blocked during elongation [171].

During the formation of ventral furrow in *Drosophila*, recent research has reported that under the regulation of radial polarized distributed ROCK and the downstream activation of myosin II, apical constriction induces tissue folding. Moreover, actin filaments network also presents a radial polarization: the pointed ends are enriched in the center of the cell and the barbed ends around the periphery of the cell, oriented to junctions [172]. This observation suggests that centrally located myosin binds to and pulls the actin filaments network toward the central through junctions for force transmission.

The intracellular contraction and the entire embryo elongation

The elongation of the whole embryo is a typical example of polarized growth along a preferred direction. It can either be a result of anisotropic forces, that is, higher forces in one direction, or a result of an anisotropic response to an isotropic force. As in the first case, an obvious example comes from the *Drosophila* germband extension. It is a result of the polarized distribution of actomyosin network and the anisotropic forces it generates [124]. While in the early elongation of *C. elegans*, the oriented growth of a plant is a more similar case. In plants, the turgor pressure generated by the osmosis across semipermeable cell membrane plays the part of elongation driving force [173]. Meanwhile, the circumferentially aligned micro-fibrils in plants restrict the radial expansion and result in the longitudinal growth [147]. Likewise, though the alignment of actomyosin is less oriented in the lateral epidermis, it is more organized into long and parallel bundles in the dorsal and ventral cells. This alignment of actomyosin in the dorsal and ventral epidermis can function as micro-fibrils to restrain the radial expansion of embryo during early elongation [106]. Moreover, as we discussed before, the actomyosin activity is inhibited in the dorsal and ventral epidermis, suggesting that these epidermal cells are more likely to create a passive response to the hydrostatic pressure that is generated in the lateral epidermis. When actin bundles are disrupted in the dorsal and ventral cells in *zoo-1/zo-1* and *vab-9/claudin* homologues mutants, embryos deform and fail to complete elongation process [169, 174]. Likewise, when the actin bundles detach from junctions in the dorsal and ventral cell, the embryo displays bulges and fails to elongate [47].

2.4 Muscle contraction and late elongation

When embryos reach 1.7-fold, the muscles beneath dorsoventral epidermal cells start to contract, indicating the beginning of late elongation. Although laser-killing experiments demonstrate that the epidermis shape changes drive the process of elongation, muscle activities are required additionally for embryo elongation. The muscle defective mutant, which lacks the body-muscle-specific myosin heavy chain *myo-3*, arrest at the 2-fold stage and cannot complete the elongation process [175].

To accomplish the late elongation, *C. elegans* embryo must coordinate the morphogenesis of two adjacent tissues. The body muscle beneath the dorsal and ventral epidermal cells separated by the basement membrane and the hemidesmosomes that link the epithelial cells and basement membrane for tension transmission.

2.4.1 Muscle

As found in most of the animals, muscles exist in the simple invertebrate *C. elegans*. Muscles fibers consist of myofibrils that primarily contain actin filaments and myosin. Muscle fibers either generate contractions and extensions that may change the length or/and the shape of themselves or maintain their shapes against extrinsic tensions. During *C. elegans* embryo development, muscle activity can be observed by using the

fluorescent-marked muscle proteins in the light microscope.

C. elegans muscle structure

In *C. elegans* body, there are four rows of body-wall muscles, two of which are underneath the dorsal epidermis and the other two are under the ventral epidermis. Muscle cells in each longitudinal quadrant are separated from epidermal cells by a basal lamina. They are also laterally against the neighboring cells (Figure 2.14).

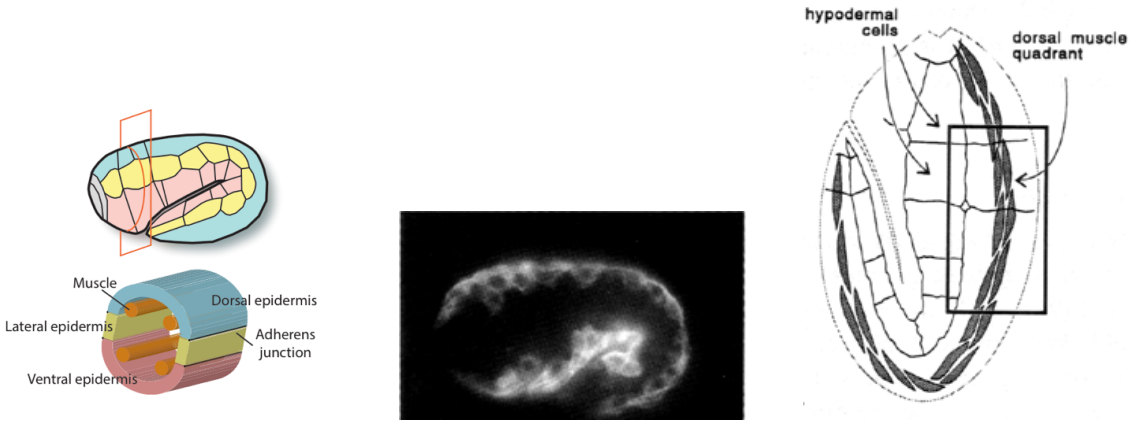

(a) (b) (c)

Figure 2.14: *C. elegans* muscles. (a) Scheme of the embryo section, (b) Ca^{2+} sensor-marked muscle cells, (c) Scheme of embryo hypodermal and muscle cells. Panel (c) adapted from *C. elegans II. 2nd edition.*

The muscle-muscle adhesion plaques link the neighboring cells together. Two muscle-hypodermal structures, the dense bodies and the M-lines, connect the actin filaments and myosin filaments, respectively, to epidermis through the muscle plasma membrane and then the basal lamina to transmit the contractile forces out from muscle cells [176]. Muscle membranes connect to the cuticle through epidermis via cell basement membrane junction called fibrous organelle (FO) [177]. Also, like vertebrate animal muscles, *C. elegans* muscles cells contain a greater amount of mitochondria than other body cells for energy supply.

Muscle activities and embryo elongation

Muscle activities are irreplaceable in the late elongation process. Different mutants with Pat phenotype fail to finish elongation process even though the actomyosin network functions properly during the whole elongation process. Loss-of-function in muscle structural protein, basement membrane component or integrin subunits will all lead to the failure of elongation. For example, mutants lacking the body-muscle-specific myosin heavy chain *myo-3* [175], or the calcium channel subunit EGL-19 have defects in muscle contraction [178]. These mutants suggest that muscle contraction

itself is crucial for elongation process. Another common Pat mutant is *unc-112*. This gene encodes a pleckstrin homology domain-containing protein in the dense-body [179]. Knockdown of *unc-112* will lead to a detachment of dense-body from the muscle membrane [179].

2.4.2 *C. elegans* hemidesmosome (CeHD)

Fibrous organelle is an essential structure to transmit mechanical muscle tension through the epidermis to the cuticle exoskeleton. It mediates the connection between muscles and the dorsal and ventral epidermis [177, 180]. FOs comprise two facing hemidesmosome-like structures in the epidermis, thus referred as CeHD (*C. elegans* hemidesmosome) [181]. Under the microscope, two electron densities can be observed on the apical and basal membranes of the dorsal and ventral epidermis [177, 181]. The core protein of CeHD is VAB-10A, a plakin homologous to vertebrate plectin and BPAG1e, which anchors intermediate filaments to the apical and basal membranes of the dorsal and ventral epidermis.

Intermediate filaments are the central component of CeHD [182]. It comprises IFB-1/IFA-3 and IFB-1/IFA-3 [182, 183] and interacts with *C. elegans* specific transmembrane adhesion molecules, LET-805/myotactin on the basal membrane [184] and MUA and MUP-4 on the apical membrane [185, 186].

2.4.3 Mechanotransduction

The transmission of muscle contraction requires hemidesmosome-like junction connecting epidermal cells and the cuticle exoskeleton. Defects in integrin subunits, which connects ECM and muscles, will also lead to the failure of elongation. Mutations in fibrous organelle protein LET-805/myotactin result in a 2-fold, non-paralyzed arrest [187]. Another mutant reveals the connection between muscle contractions and epidermis morphogenesis is MUP-4. Transmembrane protein MUP-4 can couple the muscle contractions to the cuticle. Loss-of-function in MUP-4 leads to variable defects in the morphogenetic process of the epidermis [188], suggesting the role CeHD and the intermediate filaments play during epidermal cell morphogenesis.

A successful mechanotransduction requires the right connection between the actin and myosin filaments to the muscle membrane and the connection between the muscle membranes to epidermal cells.

C. elegans dense bodies and M-lines

Attachments that are responsible for transmitting the actomyosin contractile movements to the muscle cell membrane are the dense body and the M-line. Dense body and M-line are both finger like structures in adult worms that extend from the muscle cell membrane (Figure 2.15). They reach into the cytoplasm to recognize and attachment to the actomyosin filaments. In embryo muscle cells, they are dot-like structures that link to the less-organized actin and myosin filaments [176].

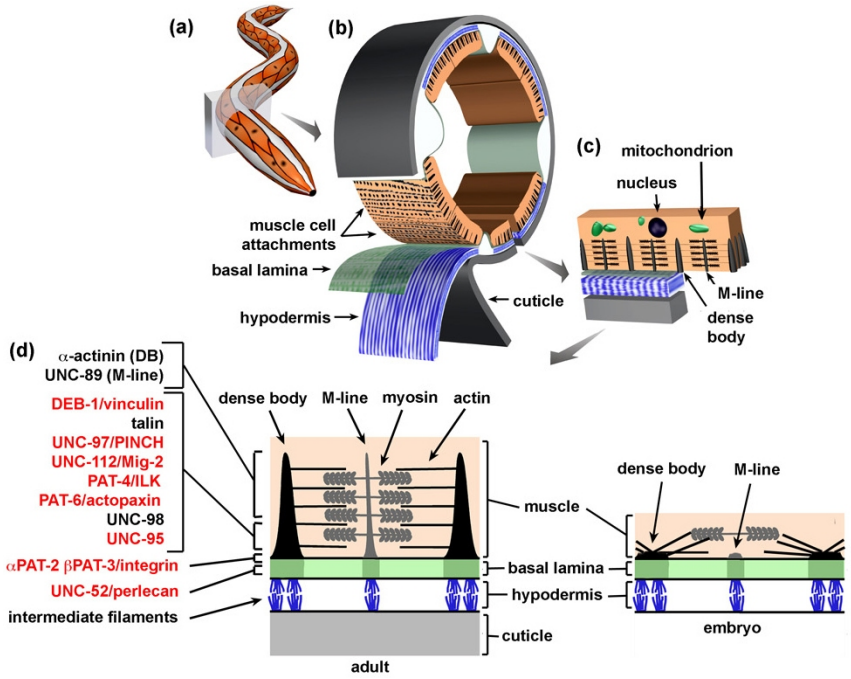

Figure 2.15: Scheme of the dense body and the M-line in muscles. From *Wormbook.*

One important protein of muscle attachments is the extracellular matrix (ECM) receptor PAT-2/PAT-3 integrin [189]. PAT-2/PAT-3 is concentrated at the dense bodies and the M-lines to transmit the mechanical tensions generated in muscle cells to the basal lamina. It is also enriched in the muscle-muscle attachment plaques, allowing the contractile force to be transmitted between muscles as well [177].

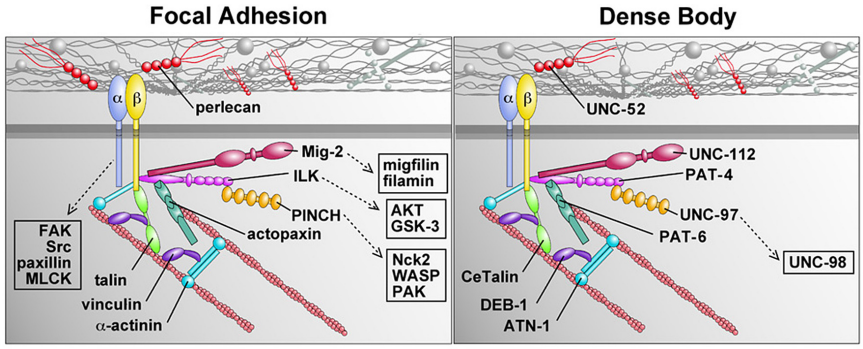

Figure 2.16: Left, vertebrate focal adhesions. Right, *C. elegans* dense bodies. Figure from *Wormbook.*

To form the linkage between myosin filaments and muscle cell membrane, cytoskeletal adaptors, such as DEB-1/vinculin, ATN-1/α-actinin, talin, and PAT-6/actopaxin, complete the linkage between the cytoplasmic domain of integrin and actin filaments in the cytoplasm tip of the dense-body [176, 177, 179, 190, 191, 192, 193]. The M-line that attach to actin filaments contains almost the same membrane-proximal adaptors,

except vinculin and α-actinin, but contains the M-line specific protein UNC-89 [194]. At the membrane site of the dense body, UNC-112/MIG-2, PAT-3/β-integrin, PAT-6/actopaxin, and PAT-4/integrin-linked kinase forms a ternary complex, stabilizing this muscle cell attachment site [176, 179, 190, 191, 192, 193] (Figure 2.16).

Dense body and M-line are considered to be analogous and homologous, given the similar protein composition and function. They present an interval alignment in *C. elegans* muscle cells to fulfill their attaching function.

2.4.4 Muscle contraction and epidermis remodeling

CeHD maturation through a tension induced pathway

Muscle contraction is the crucial driving force for epidermis remodeling during late elongation. Yet the mechanisms for this is not entirely understood. Our lab has recently discovered one important aspect explaining how muscle re-shape epidermis by stimulating the reorganization of CeHD through a mechanotransduction pathway. Muscle contractions recruit the G-protein-receptor kinase interactor (GIT-1), leading to the association of its partner PIX-1 and the Rac GTPase CED-10. The activation of this signaling cascade results in the activation of p21-activated kinase PAK-1, which phosphorylates the intermediate filaments in CeHD. After phosphorylation, intermediate filaments undergo reorganization and stabilize the structure of CeHD. The conformational change of CeHD, from puncta to parallel circumferentially organized stripes, assures a stronger connection between muscles and the epidermis and a more efficient tension transduction organelle [36] (Figure 2.17).

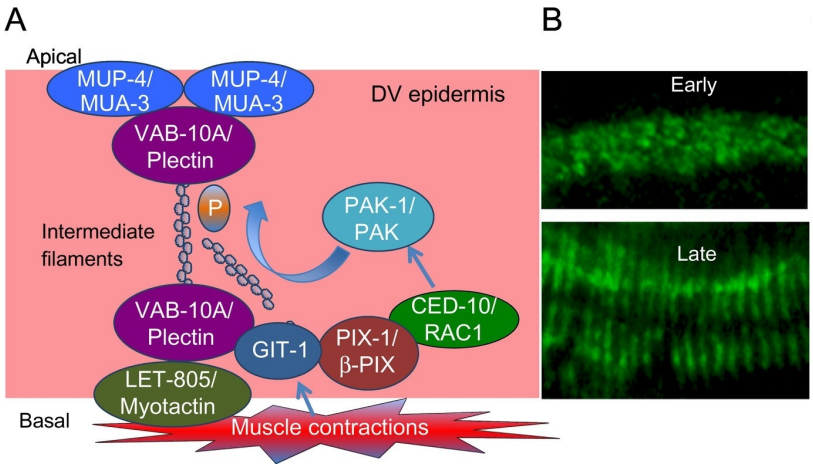

Figure 2.17: Remodeling of CeHD promoted by muscle contractions. (A) GIT-1 signaling cascade in the dorsal and ventral epidermis. (B) CeHD organization before and after muscle contraction. Figure from [106].

Other possible impacts on epidermis from muscle contractions

After the maturation of CeHD, mechanical forces from muscle contractions can be transmitted to epidermal cells. However, it is possible that muscle contractions contribute to epidermis remodeling in other aspects since the mutations in the mechanotransductive cascade do not present a severe elongation phenotype as in Pat mutant.

One possibility is that muscle contractions trigger the shortening of actin bundles in the dorsal and ventral epidermis since the diameter of embryos decreases in total by three-fold during the entire elongation process. Another possibility is that through the mechanosensitive pathway, the expression of certain genes is up-regulated or down-regulated due to muscle activity. Also, as studied in this thesis, muscle activity may promote the lengthening of adherens junctions along the anterior/posterior direction. Since the muscles are oriented beneath dorsal and ventral epidermal cells, their contractions force epidermal cells to compress along the anterior/posterior direction. How the compression of hypodermal cells leads to the lengthening of junctions in *C. elegans* embryonic development is to be answered in the thesis.

2.5 Other cellular players contributing to elongation

Besides the most two important and dominating driving forces we discussed in the previous part. Other players also contribute to the successful elongation.

2.5.1 Spectrin network and the growth of the embryo

Spectrin plays a major role in maintaining the cytoskeleton structure and the cellular integrity. In cells, spectrin forms tetramers and associates with short actin to form a hexagonal mesh. In red blood cells, this submembranous meshwork maintains the cell shape. During development, spectrin has also been shown to play a role in morphogenesis and the formation of neurons.

Actin-spectrin network in cells

In cells, spectrin has been reported to form the apical submembrane network with actin and other associated molecules. This membrane-associated skeleton has been observed in neuron cells and during the development process and has been found in both invertebrate and vertebrate animals [195, 196, 197].

In rat, the spectrin tetramer consisted of α- and β-spectrin has been detected to form a meshwork with plectin, surrounding the actin cuffs of the tubulobular complex at the apical membrane of Sertoli cell [198]. During *Drosophila* mid-oogenesis, the repolarization process requires β-spectrin in follicle cell. Similar to in mammalian cells, the loss of β-spectrin leads to the inhibition of Hippo signaling pathway in follicle cells. This is due to the fact that the mutation in β-spectrin affects the basal

actin network structure, disrupting the planar polarized organization of actin bundles and leading to the formation of actin patches at the base of epithelial cells. Mutated β-spectrin also affects the actin dynamics, resulting in the failure of the assembly of parallel actin bundles [196].

Intriguingly, the spectrin network has been reported to contribute to mechanotransduction in osteocytes. Osteocytes are the most important mechanosensor in bones. Through the cytoplasm of osteocytes, spectrin organizes into a porous network and forms a dense layer through a linkage with F-actin beneath the apical membrane. This dense layer of actin/spectrin is pivotal to maintain the elasticity and the cortex stiffness of osteocytes. Disruption of this meshwork leads to an obvious softening of cells, loss of secretion and cell-cell connection. This result demonstrates that spectrin/actin mesh work is a global structural support in the mechanotransduction process [197].

Spectrins in *C. elegans* morphogenesis

In *C. elegans*, there are three spectrins, the α-spectrin/SPC-1, the β-spectrin/UNC70 and the β_H-spectrin/SMA-1. All these three spectrin proteins have been shown to be essential for morphogenesis and/or muscular and neuron formation.

Mutations in α-spectrin cause a failure to complete the entire embryonic elongation and death of the larvae just after they hatch. Light microscpoe imaging shows that these α-spectrin mutants have defects to organize the structure of actin cytoskeleton property in the dorsal and ventral epidermis, which leads to an unsuccessful elongation. Besides, during the late elongation, the mutation in α-spectrin seems to affect the proper differentiation of body wall muscles, as the myofilaments of muscles in the mutants are oriented abnormally from the longitudinal anterior/posterior direction of the embryo. What is more, the muscle cells do not present a normal muscle cell shape [199].

Research showed that α-spectrin localizes beneath the cytoplasmic membrane during embryonic development in almost all cells. This location requires the help of β-spectrin. In turn, β-spectrin also required α-spectrin to localize to the cell membrane [199]. Knock-down experiment shows that when β-spectrin is depleted, larvae cannot survive beyond the L1 stage and present an uncoordinated coiling, which severely harm the mobility of the larvae. The β-spectrin gene is named UNC-70 [200]. The defects of moving ability in *unc-70* larva are due to the progressive disorganization of myofilaments and the discontinuities in the dense bodies. In body wall muscles, a reduction or loss of the sarcoplasmic reticulum is also observed [200, 201]. Though *unc-70* larvae are lethal at a young stage, the embryos complete the development process and hatch, which means the β-spectrin is not indispensable for embryogenesis. Intriguingly, β-spectrin has also been shown to be important for neuron formation. Depletion of β-spectrin in early larvae leads to multiple defects in nerve system. Abnormally enlarged neuronal bodies, apparent vacuolation in amphid neurons, abnormal axon outgrowth and ectopic displacement of neuronal bodies can be observed in these larvae. *unc-70* mutants lose the ability to develop sensory neurons

under stress in moving larvae. Atomic force spectroscopy experiments on isolated neurons showed that the β-spectrin is held under continuous tension, to transmit the pre-stress to touch receptor neurons [200, 201].

Mutations in β_H-spectrin lead to smaller larvae with big round heads, which gives the gene name SMA-1. *sma-1* mutant requires the same time for embryogenesis, but elongates at a lower rate, resulting in a shorter larva. β_H-spectrin has first been identified in *Drosophila*. In *Drosophila*, β_H-spectrin is enriched in the apical cytoplasm membrane of the epithelial cells. In *C. elegans*, SMA-1 also associated in the apical membrane of lateral epidermis when these cells are rapidly elongating. The organization of SMA-1 at the apical membrane requires the presence of α-spectrin, suggesting that α- and β_H-spectrin form an apical enriched spectrin-based membrane skeleton. In severe *sma-1* mutants, actin partially disassociates from the apical cytoskeleton network in the dorsal and ventral epidermis, affecting elongation. Researches show that SMA-1 is responsible for the linkage between actin and apical membrane through its N-terminus. In SMA-1 dislocated mutants, actin organization is disrupted in the lateral epidermis, leading to cell shape defects [44, 202]. SMA-1 has also been reported to function in the surrounding musculature of the pharynx. In *sma-1* mutations, pharynx gland graduately becomes abnormal overtime due to the defects in the pharyngeal muscles [203].

2.5.2 Microtubule network contribution

In *C. elegans* embryos, microtubules are oriented circumferentially and often present a great intensity. Therefore, they are traditionally considered to provide a passive response to help elongation in the dorsal and ventral epidermis [47, 204]. However, recent researches have indicated that microtubules are more likely to function as a transport key structure to favor the morphogenesis process.

During *Drosophila* morphogenesis, MTs regulate the embryonic development by regulating the polymerization of actin and the activation of myosin II. Depolymerization of MTs leads to the loss of apical F-actin and thus the inhibition of apical constriction [205]. At the beginning of *X. laevis* gastrulation, MTs are also required for the apical constriction [206]. MTs are organized as a parallel array in the hinge point cell during *X. laevis* neural tube enclosure. The MT nucleator γ-tubulin is redistributed apically in hinge point cells. This apical redistribution of γ-tubulin is promoted by the actin binding protein Shroom3, coupled with the activation of myosin II before apical constriction happens [207].

Recent data from our lab have shown that during *C. elegans* embryogenesis, MTs promote elongation process in parallel to the actomyosin activation pathway LET502/ROCK [19]. MTs are shown to be essential for elongation in a LET-502/ROCK partially impaired background. MTs promote the transport of E-cadherin to adherens junction. Double mutants in MTs regulator NOCA-1 and LET-502/ROCK reduce the mobile fraction of E-cadherin. Frap experiment shows that the E-cadherin dynamics is impaired in LET502/ROCK mutant and MTs severing background, suggesting the role of LET502/ROCK in MT-dependent junction transportation pathway in *C.*

elegans elongation [19].

2.5.3 Cuticle contribution to elongation

Besides the intracellular players, the mechanical forces can originate from the extracellular matrices (ECM) that bound the epithelial cells both apically and basally. The role of basal ECM has been intensively investigated, but not the apical ECM [208]. Recent studies have discovered the mechanisms through which the apical ECM contributes to morphogenesis.

During the formation of *Drosophila* wings, the apical ECM shapes the appendages by defining the global force pattern. The apical ECM protein Dumpy localizes the anchorage of appendages to epithelial cells after its shape arises from the apical constriction tension. Mutations in dumpy will lead to multiple shape changes in wings, such as dumpy and truncated wings [209]. During the formation of the tracheal tube, the apical ECM couples with the apical membrane as a viscoelastic material. A computational model reveals the mechanical interaction between the apical ECM elasticity and the growth of apical membrane, suggesting the apical ECM defining the morphogenetic pattern of tube growth [210]. In *Drosophila* epidermis, apical ECM has also been shown to be responsible for the local interaction between the membrane and the extracellular matrix through zona pellucida domain proteins during the development of denticles, an apical bristle-like structure [211].

ECM has also been shown to be important during *C. elegans* epithelial cells shape changes. On the apical membrane of some tubular epithelial cells, including the excretory ducts and excretory pores, ECM contributes to the cell-cell junction and modulates the junction dynamics. Mutations in ECM structure-maintaining proteins lead to ruptures in epithelial junctions when duct and pores excrete and the remodeling of cell-matrix interactions [212].

A recent research from our lab shows that the apical ECM plays an important role during embryonic morphogenesis too. It helps to preserve the integrity of embryos and distribute tension throughout the embryo during elongation. Two zona pellucida domain proteins NOAH-1 and NOAH-2 preserve the embryonic integrity together with p21-activated kinase via maintaining and relaying the actomyosin contractile tension before muscle contraction. Also during late elongation, these ECM proteins are essential for muscle-epidermis anchorage and the input of muscle contraction transduction to epithelia [213].

2.6 Conclusion

During morphogenesis, epithelial behaviors determine the direction of embryo development. Many cellular remodeling patterns and molecular pathways behind the patterns are studied. Yet there are some points left not fully understand. *C. elegans* embryo development provides a perfect model to study the morphogenesis process. The two main driving forces for embryonic elongation are already well understood.

Moreover, recent work from our lab and other labs discover the contribution from different organelles such as the cytoskeleton and the cell-membrane connection. During the study of *C. elegans* embryo and other model systems, one important aspect during worm morphogenesis still remains mysterious: the polarized junction remodeling and the establishment of planar polarity.

Therefore, these two heroes in this thesis, the adherens junction and the planar cell polarity, are going to be introduced in next chapter, explaining the background of them and presenting the latest related updates.

Chapter 3

Polarized lengthening of apical junction

3.1 *C. elegans* epithelial adherens junctions

3.1.1 Basic components of *C. elegans* apical junctions

The main structure of *C. elegans* adherens junction looks like its counterpart in *Drosophila* and vertebrate cells [214]. The cellular and genetic analysis identified two distinct junction complexes that present different molecular structures and convey different functions (Figure 3.1). Under the transmission electron microscopy, a single electron dense junction structure can be observed.

The cadherin-catenin complex

The cadherin-catenin complex (CCC) comprises E-cadherin/HMR-1, α-catenin/HMP-2, β-catenin/HMP-1 and p120 catenin/JAC-1 [142, 169, 170]. The CCC is the most apical junction complex in *C. elegans* adherens junction [215, 216]. The transmembrane protein HMR-1 forms homologous dimers in the extracellular domain to connect two neighboring cells. The intracellular domain of HMR-1 binds to HMP-2 that further binds to HMP-1, which further links to F-actin. In this way, the anchorage between adherens junction and actomyosin network is primarily established. Two *C. elegans* specific proteins in adherens junction are VAB-9/BCMP1, a distant claudin superfamily member, and ZO-1/ZOO-1, a homologue of MAGuK protein [169, 174].

The DLG-1/AJM-1 complex

The second complex that locates basal to the CCC is the DLG-1/AJM-1 complex (DAC). This complex consists of two membrane-associated proteins, DLG-1, the homologue of *Drosophila* Disk Large protein, and AJM-1, a nematode specific coiled-coil protein [215, 216, 217, 218]. The localizations of DLG-1 and AJM-1 at membrane depend on the presence of each other [215, 216, 219]. How DLG-1/AJM-1 complex anchors to the membrane is still unknown. One possibility is that CLC-1 or CLC-2, the claudin homologues fulfill this role. However, the depletion of these proteins does not lead to apparent connective defects [220].

Other junctional proteins

One potential new junction protein is the MAGuK homologue, MAGI-1 [219, 221]. It has been reported to anchor the membrane via the transmembrane L1-CaM homologue SAX-7. It has also been reported to interact with Afadin homologue AFD-1. Although the location of MAGI-1 is under debate now, it is believed that MAGI-1 functions in separating the CCC and DAC in a potential SAX-7/MAGI-1/ADF-1 complex.

3.1.2 The assembly of adherens junction and the establishment of cellular polarity

When new cell contacts happen during a development process, such as during cell division, cell migration, and cell intercalation, new junctions have to be assembled to ensure the proper stable connection between cells. Except in these circumstances, new junctions will form when non-polarized epithelial cells differentiate to be polarized since the apical junction assembly can establish the apicobasal cellular polarity.

When the apical junctions are assembled in epithelial cells, they segregate the distinct membrane domains. The apical side of epithelial cells form the luminal surface and the basal side connect to the tissue beneath or the basement membrane. Losing the proper assembly of junctions will result in the loss of specialized regions of the membrane and lead to potential tumorigenesis [222].

Molecules determining junction components recruitment

In *Drosophila*, the interaction between the apical complexes and basal complexes has been shown to be critical for establishing the epithelial polarity. But this process is modulated in a slightly different mechanism in *C. elegans*.

Initially, the components of CeAJ distribute along the lateral membrane of epithelial cells, and then they re-distribute from their original positions to their final apical positions. Three proteins that seem to be important for this re-distribution of CeAJ components are PAR-3, PAR-6, and PCK-3. In *par-6* deficient embryos, CeAJ fails to form mature junctions and stays fragmented at the lateral side of epithelia

[223]. How PAR-6 affects junction maturation is unknown in *C. elegans* embryos. In *Drosophila*, however, PAR-6 has been shown to control the trafficking of junction components together with the small GTPase Cdc42 [224, 225].

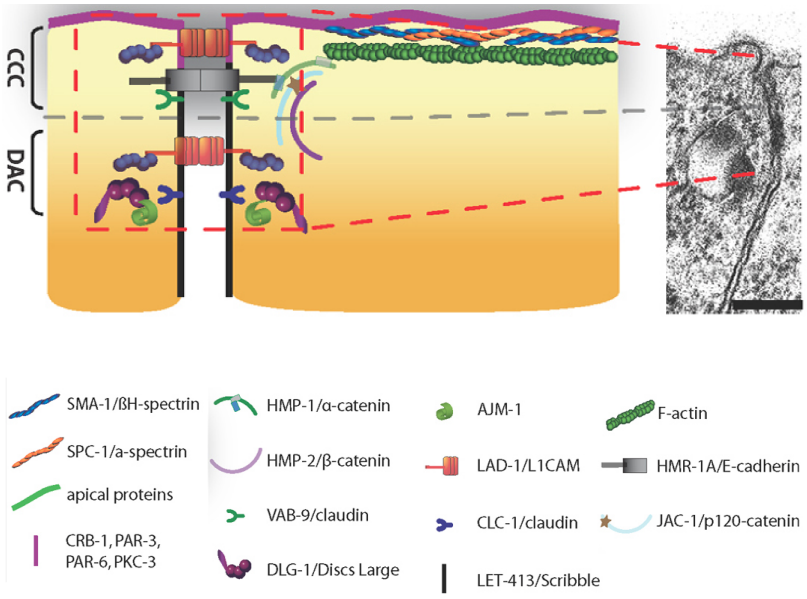

Figure 3.1: Left, Scheme of *C. elegans* apical junction components. Right, *C. elegans* apical junction under electron microscopy. Figure adapted from *Wormbook*.

In the intestine, PAR-3 controls the migration of junction components to the midline and the assembly to define the lumen. Like in epithelial cells, junctional proteins also form puncta and migrate to the midline progressively before they eventually form junction [226, 227]. In *par-3* mutants, the cadherin-catenin complex, together with PAR-6 and PCK-3 fail to gather at the apical side of the membrane and thus fail the polarization [227].

Basal position determining for CeAJ

Defining the basal position of CeAJ is an essential step for correct junction assembly. In *Drosophila*, the basal proteins Scribble and Disc-Large interact with apical complexes to determine the basal position of adherens junctions. However, in *C. elegans* epidermis, DAC is not essential to determine the basal position of CeAJ. In *C. elegans*, the homologue of Scribble, LET-413, a basolateral protein defines the basal position of CeAJ at a discrete subapical position (Figure 3.2) [171, 216].

In *let-413* mutant, CeAJs remain lateral but present a discontinuous and largely extended format, further basally distributed along the lateral membrane, suggesting a failure in reaching their sub-apical positions [215, 216]. The similarity between N-terminal leucine-rich repeat of LET-413 and Ras-interacting protein SUR-8 suggests that LET-413 may control the lateral polarity through a small GTPase-like way [228]. Interestingly, the *let-413/dlg-1* pathway has been reported to be affected by the

IP3/Ca^{2+} signaling, indicating that the junction basal position determining process can be calcium-sensitive [229]. Non-muscle myosin II has been reported to interact with ITR-1, an inositol triphosphate receptor increasing the intracellular Ca^{2+} level in cells [230], which is required for cell migration during ventral enclosure [231]. These observations bring up an intriguing possibility that non-muscle myosin II may also be involved in junction lateral recruitment.

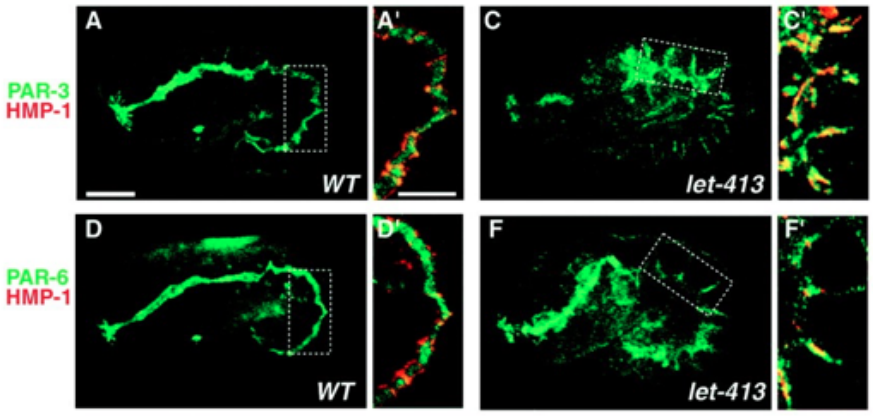

Figure 3.2: *let-413* mutant loses the basolateral position of PAR-3 and PAR-6 in the intestine and presents a disrupted junction architecture of junction. Figure adapted from [216].

3.1.3 Cellular functions of apical junctions

In vertebrate animals and *Drosophila*, the adherens junction is responsible for cell-cell connection and microfilaments anchorage. The tight junction in vertebrates and septate junction in *Drosophila* are responsible for paracellular gate function. Both of these two types of junction help to maintain the cell polarity and function as a signal platform. As will be discussed below, however, adherens junction ensures all three functions together in *C. elegans* epithelial cells. In general, the CCC and DAC are together responsible for cell-cell adhesion; CCC is responsible for adhesion in newly formed contacts and intracellular actin anchoring whereas DAC is responsible for the paracellular gate function.

Cell-cell adhesion

The two most important complexes of CeAJ, cadherin-catenin complex and DLG-1/AJM-1 complex are likely to maintain the cell-cell adhesion through a cooperative way. In the mutants that lose both complexes together, embryos present severe adhesion defects in both epidermal and intestinal cells (Figure 3.3) [169, 219].

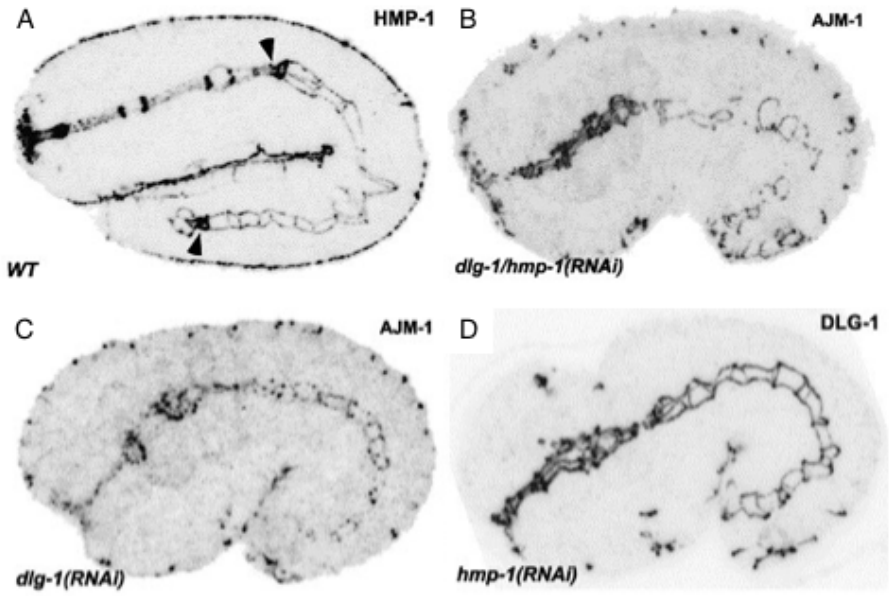

Figure 3.3: Defectives of the intestinal and epidermal junctions in cadherin-catenin complex and DLG-1/AJM-1 complex impaired embryos. Figure adapted from [219].

In mutants where only CCC is inactivated, cell-cell adhesion will be affected, but only in restrained situations. For example, the mutated E-cadherin or the loss of α-catenin or β-catenin prevents the assembly of new junctions between two migrating cells when they meet at the midline during ventral enclosure process [142, 232]. However, these mutations do not affect the cell-cell adhesion in other epidermal and intestine cells where adherens junctions are already formed (Figure 3.4).

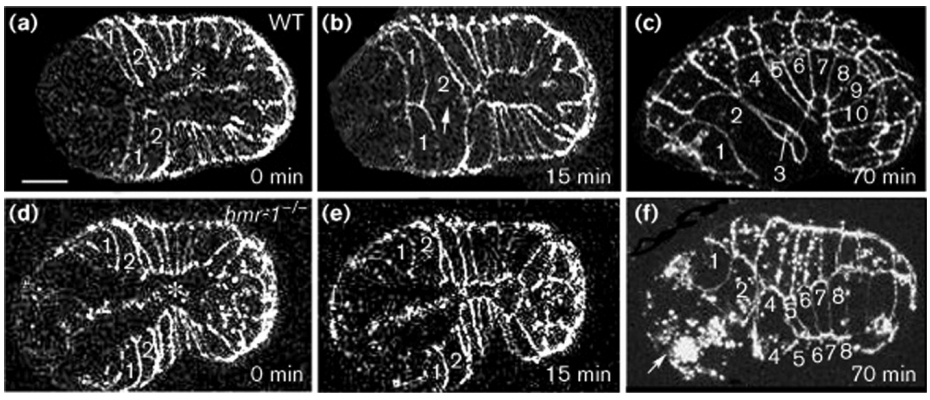

Figure 3.4: Failure in junction formation of two rows of epidermis at the midline during ventral enclosure in *hmr-1* knockout embryos (d-f). Normal junction formation at midline during ventral enclosure in wild-type embryo (a-c). Figure from [232].

The loss of DLG-1/AJM-1 complex does not lead to the defects in cell-cell adhesion, but the absence of the electron-dense region between epidermis in DLG-1

deficient embryos or bubble-like separations between epidermis in AJM-1 deficient embryos [215, 216]. When expressing the dominant negative form of LAD-1/SAX-7, the homologue of DAC component, transgenic animals present morphogenesis germline defects in early embryogenesis [233], due to cell-cell adhesion defects between oocytes (Figure 3.5). Null mutation of LAD-1/SAX-7 leads to lethality during embryogenesis, which can be totally rescued by expressing LAD-1/SAX-7 in either epidermis or muscle cells, indicating that tissue-specific expression of LAD-1/SAX-7 in either of these two tissues is efficient for morphogenesis [234].

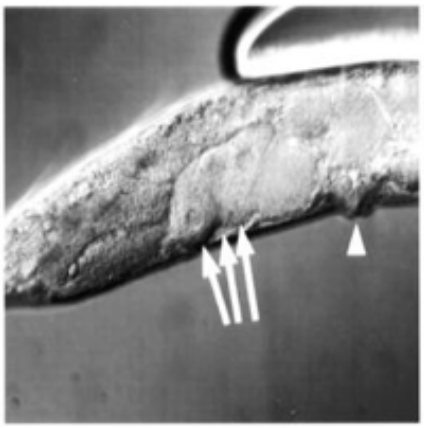

Figure 3.5: Germline morphogenesis defects in *sax-7* mutant. Figure from [233].

Actin anchoring

As introduced previously, the cadherin-catenin complex anchors to actin bundles. The linkage between the CCC and cytoskeleton actin bundles is essential for embryo elongation. Mutants that lose HMP-1/α-catenin or HMP-2/β-catenin present a detachment of actin bundles from adherens junction and fail to elongate (Figure 3.6 upper panel) [142]). This phenomenon proves that the proper anchoring of actin bundle to adherens junction is necessary for embryo elongation. Inhibition of actin polymerization leads to the failure of elongation as well [47]. Furthermore, the actin-anchoring ability of cadherin-catenin complex can be modulated by JAC-1/p120 catenin. Loss of JAC-1/p120 catenin in weak *hmp-1* mutant will enhance the elongation defects due to the further disruption of actin anchoring (Figure 3.6 lower panel) [170].

Except for HMP-1 and HMP-2, which directly link actin bundles to adherens junctions, some other proteins have been reported to modulate the interaction between actin bundles and CeAJ, such as SPC-1/α-spectrin, SMA-1/β-spectrin and one of the cadherin-catenin complex component, VAB-9/Claudin. In mutants of these proteins, actin often forms thicker bundles. These thicker actin bundles fail to align properly or attach to the junction (Figure 3.7) [169, 199].

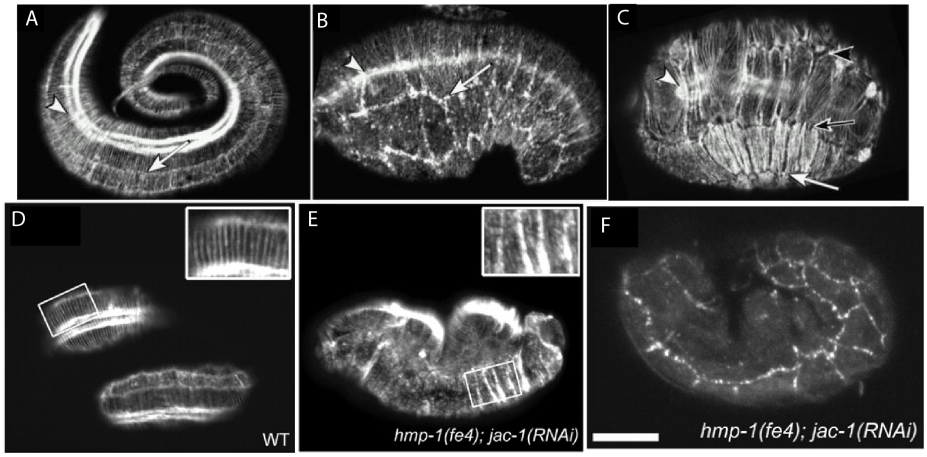

Figure 3.6: Upper panel, actin bundles fail to attach to the apical junction in *hmp-1* (B) and *hmp-2* (C) mutant. Lower panel, Loss of JAC-1/p12 catenin in a weak *hmp-1* mutant leads to actin anchoring defects and elongation failure. Figure adapted from [142] and [170].

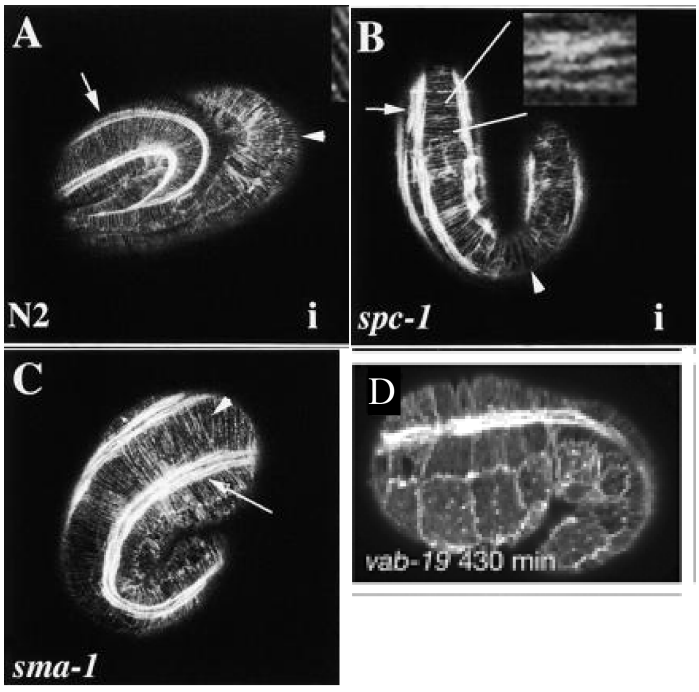

Figure 3.7: Actin anchoring defects in *spc-1*, *sma-1* and *vab-19* mutants. Figure adapted from [169] and [199].

Likewise, these thicker actin bundles can also be found in fibrous organelle components VAB-10 and VAB-19 mutants (Figure 3.8) [235].

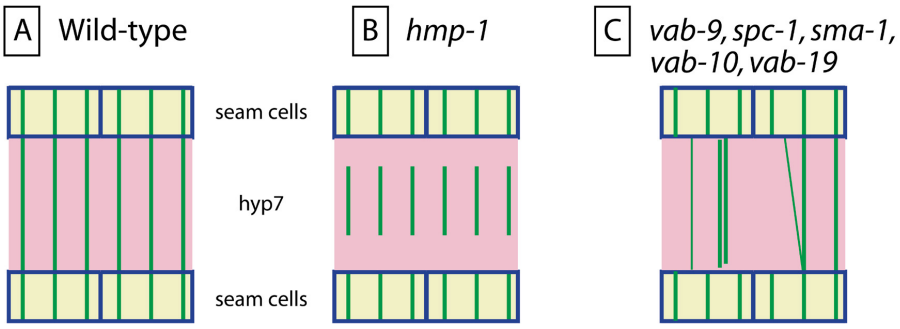

Figure 3.8: (A). Actin bundles anchoring to the junction in wild-type *C. elegans* epidermis. (B). In *hmp-1* or *hmp-2* mutants, actin bundles fail to attach to the CeAJ. (C). Disorganized actin filaments fail to anchor to junction properly in several mutants. Figure adapted from *Wormbook*.

Paracellular gate function

Septate junction and tight junction, in *Drosophila* and vertebrate animals, respectively, work as a barrier to regulate diffusion through the intracellular space. In *C. elegans*, however, it is the DAC that seems to function for this propose. DAC component DLG-1 is the homologue of the septate junction component Discs Large in *Drosophila*. In *ajm-1* or *dlg-1* null mutants, vacuoles are present in the epidermis [215]. Besides, the possible DAC component Claudins, CLC-1 and CLC-2 have been shown to involve in the barrier function [220]. Knockdown of CLC-1 by RNAi results in a severe defect in the barrier function in digestive tube. CLC-2 expresses in the lateral epidermis and also involves in the barrier function. In *clc-2* defective mutants, epidermal cells become weaker against TRITC-dextran [220].

3.2 Junction remodeling during morphogenesis

During morphogenesis, junctions have to undergo remodeling due to different morphogenesis events. Some old junctions have to shorten or even be disassembled during cell fusion, intercalation or cell re-shape. In other cases, such as cell division, cell migration or cell shape change, junctions will lengthen and new junctions sometimes will assemble when new cell contacts form.

3.2.1 Junction shortening and disassembly

Junction shortening and disassembly are often observed during cell intercalation and cell fusion, respectively. But the mechanisms that control and modulate these two processes are different.

Junction disassembly during cell fusion

Multiple cell fusion is a natural yet important part of *C. elegans* development. Cell fusion can happen during fertilization, during which the membrane of sperm and oocytes fuse together. During morphogenesis, dorsal epithelial cells fuse to form the hypodermal syncytia (multinucleate cell). During larval development, part of the lateral epidermal cells, as well as part of the ventral epidermal cells fuse to form more syncytium (Figure 3.9) [45, 236]. This process has been studied thoroughly by the confocal and transmission electron microscopy.

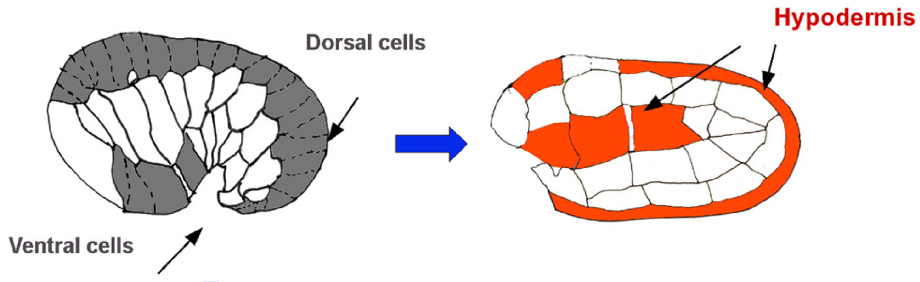

Figure 3.9: Dorsal fusion of *C. elegans* embryo. Figure from *Wormbook*.

To study the membrane fusion and theboundary change between cells, apical junction markers are used for monitoring, using the MH27 monoclonal antibody against AJM-1. 3D reconstruction reveales that after dorsal migration of epidermis, cell fusion starts with the anterior dorsal epidermis and then the posterior ones. In this way, the fusion of hypodermis is not totally invariant (Figure 3.10 upper panel) [236, 237]. This sequence in the dorsal epidermis is conversed to that during the vulva formation [237], which we are not going to discuss in detail here.

The Multiphoton laser scanning microscopy observation suggested that a pore-forming process that happens within apical or in a very close range of junction is the key step of cell fusion. Fusion appears when the pore forms at the apical side of the cell within or close to junctions. This pore will expand along the membrane in a basal wave to enlarge itself (Figure 3.10, lower panel, left) [238]. As the pore on the lateral membrane keeps enlarging, the final elimination of the lateral membrane will occur in about 30 min after the beginning of fusion [239]. Apparently, the fusion pore expansion is accompanied by the migration of apical junction components to the basal side of the cell (Figure 3.10, lower panel middle and right). However, the disappearance of this migrated basal junction will start in about 10 minutes after the initiation of membrane fusion [239]. Even though the disassembly of junction occurs during the dorsal epidermis fusion, it is not necessary for all the fusion events. Myoepithelial cells fuse to form syncytia in the pharynx with the apical junctions remaining at the apical side [240].

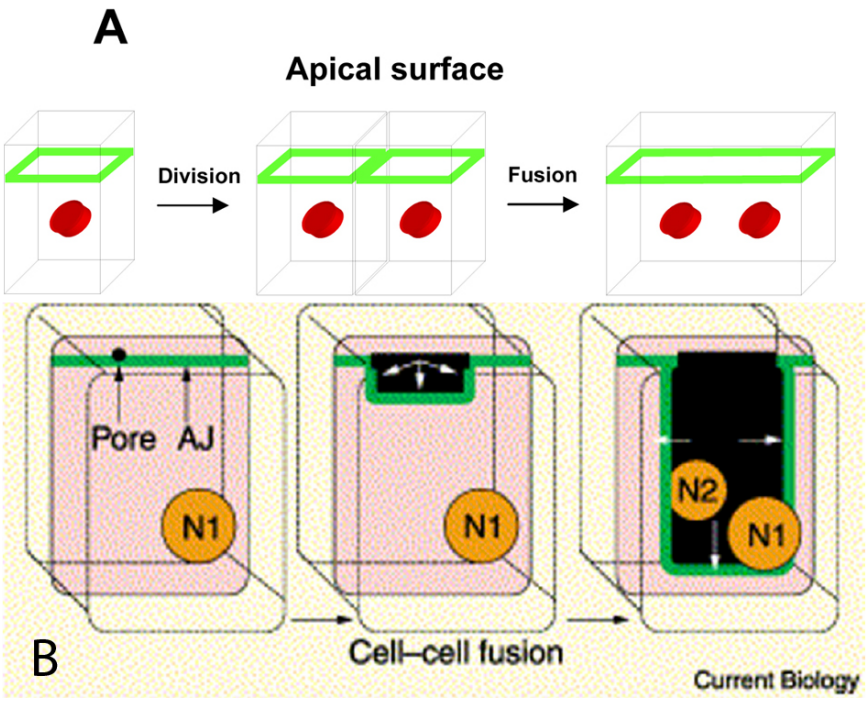

Figure 3.10: Scheme of cell fusion process. Upper panel, a simplified model of the fusion process. Green belt, apical junction. Red spots, nuclei. Lower panel. Left, the formation of the fusion pore on the apical junction. Middle, enlargement of the fusion pore. Right. Fusion pore expands to the basal side of epithelial cells. Figures adapted from *Wormbook*.

The detailed mechanism for junction disassembly during the enlargement of fusion pore is not clear yet. Cellular and genetic biology studies have shown that *eff-1* activity is necessary and efficient for both the initiation and the expansion of the fusion pores [241]. It also accomplishes the fusion events in both epithelial and myoepithelial cells, similar to the fusogen of Influenza virus [242, 243, 244, 245, 246, 247, 248]. *eff-1* mutation blocks cell fusion at early steps [241]. And the ectopic expression of EFF-1 leads to macro fusion, resulting in the disassembly of junction within one hour of expression [240].

Junction removal during cell extrusion

Another example of junction removal during morphogenesis is cell extrusion. Together with cell death, cell extrusion ensures that the tissue can stay in a stable final adult size by balancing the tissue expansion from cell division. One common yet striking example is the mammalian gut, in which progenitors keep dividing in the crypt, pushing the older cells to migrate to microvilli and to reach their tips, where cells get extruded from epithelia. Extrusion also happens during development such as in the fins of zebrafish [249] or the notum of *Drosophila* [250]. Due to the tissue growth or cell moving, build-up tissue compression triggers the nonapoptotic cell extrusion [251].

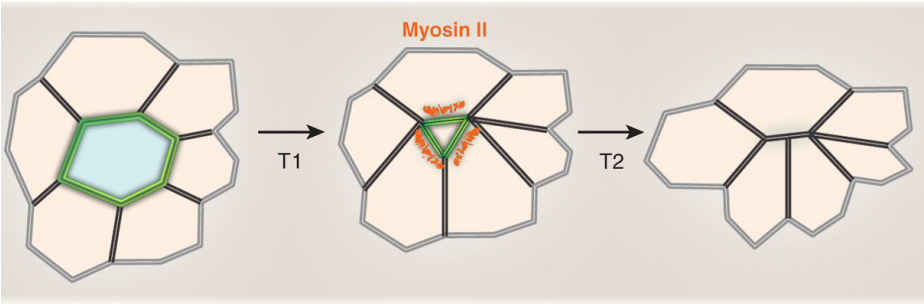

Figure 3.11: Junction disassembly during cell extrusion. Left, T1 swaps. Middle, actomyosin supracellular ring contracting around the extruding cell. Right, extruding cell removed and junction disassembled. Figure adapted from [251].

During cell extrusion, an average of six junctions will be removed once a whole cell leaves the tissue plane [251]. The junction removal happens in two main steps. In the first stage, two to three junctions will be pushed away by local cell intercalation, called T1 swaps [251] (Figure 3.11). In the second step, after the first remove of junctions, an actomyosin supracellular ring appears in the surrounding cells, contracting around the extruding cell to remove the remaining junctions and to complete the process of extrusion [251] (Figure 3.11). This second step is called T2 process, which is also reported during wound healing and apoptotic cell extrusion [252].

In the case of cell extrusion, both the non-local tissue pressure and the local neighboring compression force the junction removal.

Endocytosis and subsequent recycling of junctional proteins under mechanical forces

Although the junction disassembly mechanism is not very clear in *C. elegans* dorsal epidermis fusion, research from *Drosophila* cell intercalation during germband extension has revealed a possible mechanism for junction shortening.

Cell intercalation allows cells to re-position and possibly elongate tissues or organisms, such as in the mouse visceral endoderm [253], in the chicken neural tube [254] and *Xenopus* [255], as well as during *Drosophila* germband extension [37, 124]. In some cases, such as in *Drosophila* pupal wing development, external constraints from hinge contraction control the junction remodeling and cell re-arrangement [39]. In other development situations, local tension generated by the planar polarized distributed actomyosin cables provides the mechanical forces for the junction remodeling and the cell intercalation. One Rho-kinase involved pathway has been delineated in *Drosophila* and chicken embryos. After receiving the up-stream polarity signals from the surface receptors, RhoGEFs transmit the signals through Rho1 GTPase and ROCK to non-muscle myosin-II, resulting in a planar-polarized recruitment and activation of the regulatory light chain of myison-II (Figure 3.12) [28, 37, 124, 254, 256, 257]. In chicken, this signaling pathway is activated by a planar cell polarity pathway in chicken, called Celsr2, which is the ortholog of *Drosophila* Fmi [254].

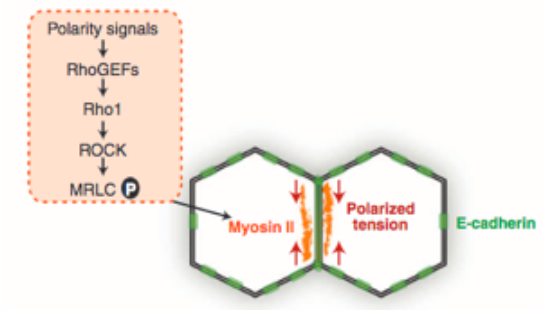

Figure 3.12: RhoGEFs signaling pathway to planar-polarized recruit and activate non-muscle myosin-II to exert polarized tension on the junction. Figure from [251].

Studies from Lecuit lab demonstrated that the shortening and the disassembly of apical junctions during morphogenesis could be modulated through a mechanical pathway. The planar polarized remodeling of the apical junction and tissue extension in the early *Drosophila* embryos is under control of the polarized distributed non-muscle myosin II. Through the endocytosis of the junction component E-cadherin, junctions along the dorsal/ventral direction undergo a disassembly process [28].

As discussed in the previous part, planar polarized junctions undergo remodeling when the cells exchange neighbors. During the remodeling, vertical junctions shrink and horizontal junctions elongate [37, 124]. Planar polarized distributed myosin-II generates an anisotropic flow from the medial apical region to drive the shortening of vertical junctions (Figure 3.13) [258].

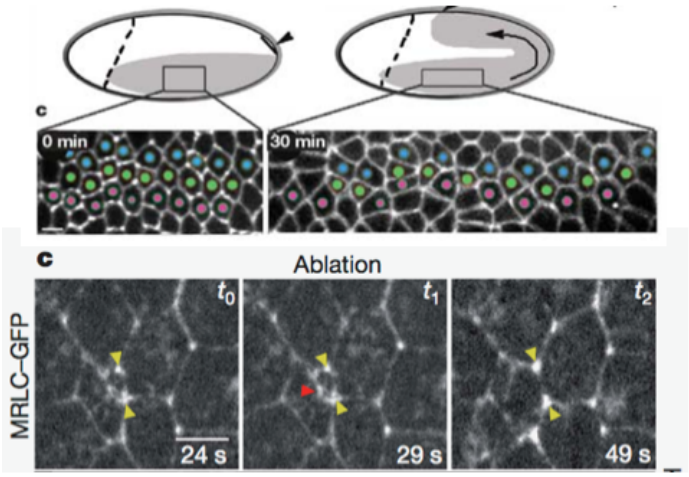

Figure 3.13: Non-muscle myosin-II exerting tension on the dorsal/ventral junction. Upper panel, Scheme of cell intercalation during *Drosophila* germband extension. Lower panel, laser ablation results showing the recoil of junction vertices under tension. Yellow arrow heads, junction vertices. Figures adapted from [124] and [258].

Through a clathrin- and dynamin-mediated endocytosis, vertical junctions shrink along the dorsal-ventral direction. Inhibition of E-cadherin will lead to defects in intercalation. This crucial E-cad endocytosis is modulated through the AP2 regulation and an E-cadherin induced clathrin coat recruitment. This modulation requires formin Diaphanous and non-muscle myosin-II, whose activities are regulated by the guanine exchange factor RhoGEF2. Interestingly, RhoGEF2 is polarized distributed in the germband along the dorsal-ventral axis and absent in non-intercalating regions of the embryo. These results demonstrated that planar polarized mechanical forces can be one molecular key for junction disassembly during morphogenesis [28].

3.2.2 Junction assembly and lengthening

Likewise, during morphogenesis, junctions undergo lengthening and new contact formation too. Research in other model systems such as chicken and *Drosophila* have provided us both the molecular and the mechanical view of junction lengthening and formation. During junction remodeling, it is important for junctions to resist the tensions, and to maintain a stable structure.

New junction formation during cell division

The most obvious event, during which new contacts form, is the cell division. What enables the formation of new junctions between two daughter cells is the most fundamental question since the daughter cells have to maintain the integrity of epithelial tissue and the barrier functions within it. The following question is what the link between junction formation and cell cleavage is [251]. In most cases of cell division, daughter cells maintain the adhesion during and immediately after cell division. Instead of scattering, daughter cells gather together and tend to form a cohesive clone, such as in early zebrafish [259] and *Drosophila* [260].

In general, partitioning of the dividing cell starts from the basal side of the cell and progresses to the apical side. A cytokinetic ring will anchor to the apical adherens junction to assist the formation of new junctions after cell cleavage. During the cell division in *Drosophila* embryos, the cytokinesis ring deforms the existing junction to a point. E-cadherin complexes in the cleavage furrow disengage at this point and lead to the separation of the dividing cell and its neighbors [261, 262]. In this way, a new membrane forms between the two daughter cells due to the folding of the separated pre-existing membrane, which, like other cytoplasm membranes, restores E-cadherin and other junction components and therefore maintains the adhesion between the new cells. In *Drosophila* embryos, non-autonomous actomyosin tension is required for the lengthening of the new membrane by forcing the annealing of the space between two daughter cells [261, 262]. Besides the pulling forces from the constraining cytokinesis ring, tension from the neighboring cells also pull the membrane orthogonally to separate the pre-existing membrane (Figure 3.14) [261, 263].

However, local biochemical regulations may also contribute to the disengagement of E-cadherin. For example, in the pupal epithelial cells, Arp2/3-dependent actin

polymerization stabilizes and maintains the newly formed intracellular surface [262]. Loss of this actin polymerization causes a strong delay and an ultimate failure in junction formation or results in shorter and much less stable junctions that lead to improper cell intercalation.

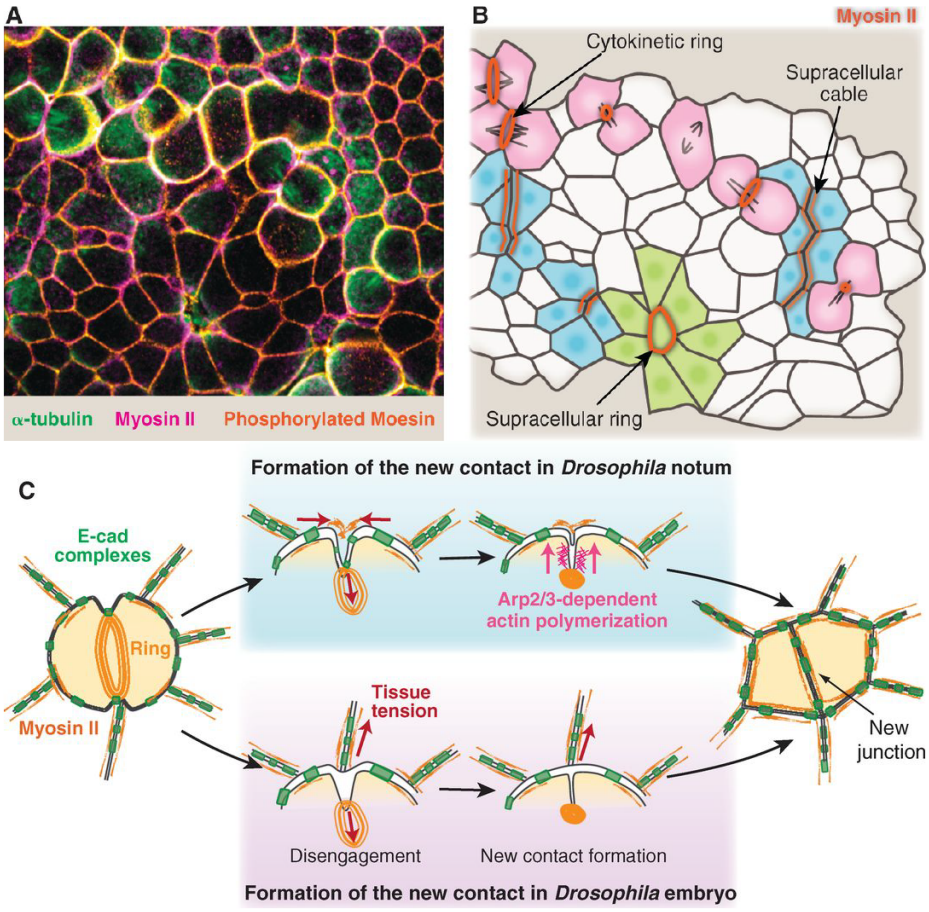

Figure 3.14: (A) Cytokinetic ring after cell division. (B) Scheme of cytokinetic ring. (C) Two situations of new junction formation under the help of E-cad complexes. Details see text. Figure adapted from [251].

Junction dynamics and actin cytoskeleton modulation

Besides cell division, cell migration such as *C. elegans* ventral enclosure and cell intercalation are morphogenesis events where new contacts will form. Researches have demonstrated that the dynamic flows of junction components largely depend on the proper interaction between them and actin network at the connecting points. During *C. elegans* ventral enclosure, as discussed before, cadherin-catenin complexes are recruited at the actin-enriched protrusion to form new contacts at the midline of the embryo (Figure 3.15) [232]. Apparently, when the cadherin-catenin complexes are missing maternally or zygotically, new junctions cannot be established even after

the successful migration [142]. In fact, actin dynamics largely dictate the formation of new junctions during morphogenesis. Blocking actin polymerization by depleting UNC-34/Enabled will enhance the junction defects in α-catenin/HMP-1 mutants during ventral sealing since the actin binding activity is greatly reduced [264, 265]. Even before the formation of adheres junction, F-actin delimits E-cadherins cluster to form nano-scale building blocks in the cytoplasmic membrane to prepare for junction formation [266].

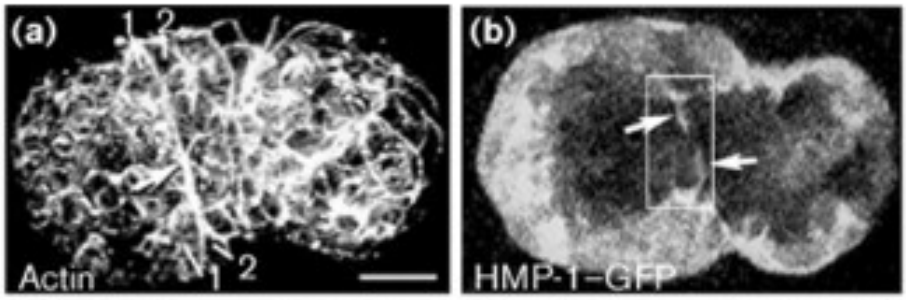

Figure 3.15: (a) Actin-enriched protrusion during *C. elegans* ventral enclosure. (b) cadherin-catenin complexes enriched at the midline of the embryo to form new contact. Figure from [232].

This actin-dynamics-modulated junction formation is also observed in *Drosophila* and mammalian cells. For example, cytoskeleton adaptor protein Girdin, which helps to stabilize the actin network, mediates the interaction between cadherin-catenin complexes and actin. Loss of Girdin impairs the association between E-cadherin, α-catenin and β-catenin and the actin cytoskeleton [267]. Also, the apical polarity protein Crumbs has been shown to position F-actin to the marginal zone and adherens junctions [268]. In mammalian cells, E-cadherin cluster lifetime and mobility will greatly expand when coupled to F-actin through α-catenin [269]. By contrast, a Hippo pathway effector Yes-associated protein (YAP) has been shown to affect the normal adherens junction assembly. It upregulates the expression of nonmuscle myosin-II to promote the actin network contractility and therefore antagonizes the assembly of the cadherin-catenin complex [270].

One possible explanation for how the actin dynamics regulatory machinery cooperate with adherens junction assembly is that actin polymerization proteins and complexes such as Arp2/3, formin, and VASP/Mena are located at adherens junction. Apr2/3 may be recruited to junctions by vinculin [271] or bound to p120-catenin and ZO-1 through cortactin [272]. Another clue is that nucleation-promoting factors such as WASP and WAVE that active Apr2/3 are associated with adherens junctions through p120-catenin as well [273]. Likewise, formin and VASP/Mena will be recruited to adherens junction by different adaptors [274, 275, 276]. Specific recruitment of the actin polymerization machinery enhances the possibility of interactions between adherens junctions and actin networks.

Another important contributor during actin-dynamics modulation for junction

assembly is the Rho GTPase. Actin nucleation-promoting factors need to be activated by the GTPase. Two factors to activate GTPase, Tiam1, and Ect2, are recruited at adherens junctions [277, 278, 279] and two other factors, ARHGEF12 and ARHGEF16, are located in cadhesome proteomics (Figure 3.16) [280].

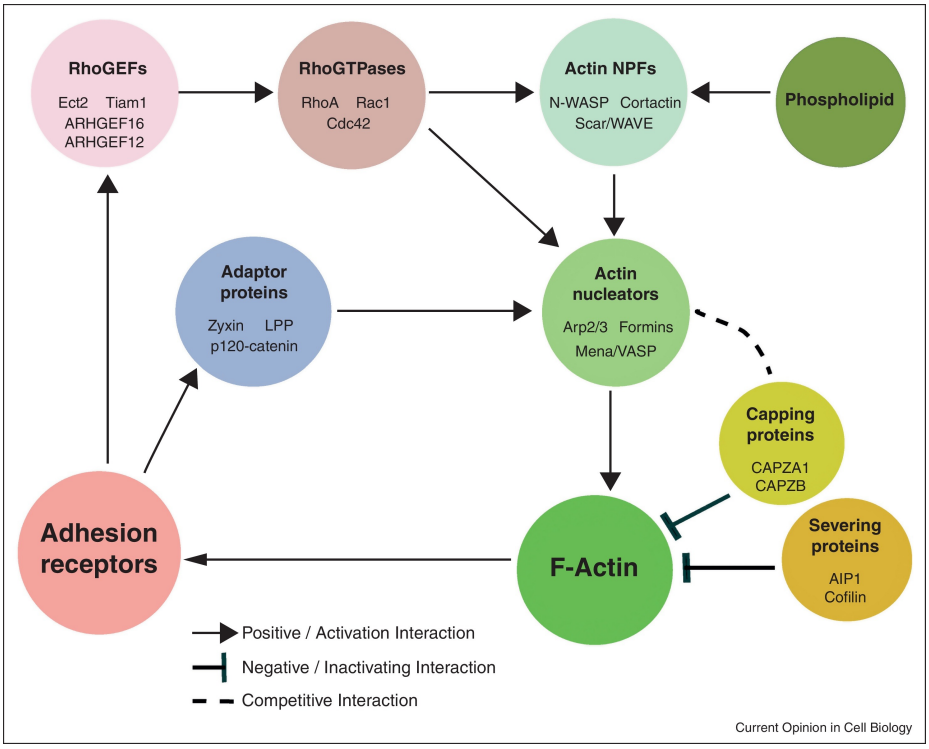

Figure 3.16: Summary of actin dynamics regulation modules between cell adhesion and actin dynamics. Figure from [281].

Maintenance of junction under mechanical tension

The adherens junction proteins form dimers in the extracellular space and connect to the cytoskeleton networks beneath the cytoplasm membrane. Therefore, junctions are under significant tension due to the external stretching stress within the tissues and the internal contractile forces generated by the cytoskeleton. How to maintain the stable architecture and the proper function of the junction is one important aspect for junction lengthening during morphogenesis.

In *C. elegans*, the cadherin-catenin complex component HMP-1/α-catenin connects actin filaments and E-cadherin. It modulates the F-actin-binding through some conserved C-terminal amino acids [282, 283, 284, 285]. Therefore, it becomes a key regulator of junction stability. Besides HMP-1/α-catenin itself, screening in a weak-mutated *hmp-1* background, identifies several junction-related proteins that can stabilize the structure of junctions and the interaction between junctions and the actin network under tension during morphogenesis. The first protein is *C. elegans* p120

catenin homologue, JAC-1, a cadherin-catenin complex component [170]. Knock-down of JAC-1 in a wild-type background does not significantly harm the embryogenesis process. But it increases the severity and penetrance of development defects in a *hmp-1* hypomorphic mutant, *fe4*, due to the detachment of actin bundles from the cadherin-catenin complex and the structure disruption of epidermal apical junctions. Another protein that stabilizes junctions is MAGI-1, which physically interacts with an actin regulator, AFD-1/afadin [221]. Like JAC-1, knock-down of MAGI-1 in a weak *hmp-1*-mutated background will increase the actin disorganization and lead to a complete morphogenetic failure. Loss of MAGI-1 results in the greater mobility of junction proteins and greater expansion of apical junctions because the spatial segregation of junction is lost.

Both JAC-1 and MAGI-1 are located at junctions and affect the maintenance during morphogenesis. Intriguingly, an actin capping protein, UNC-94/tropomodulin1, also functions in synergy with HMP-1/α-catenin to maintain junction stability [286]. Loss of UNC-94 leads to a discontinuity in HMP-1-dependent junctional actin network. In the *unc-94*/*hmp-1* double mutant, embryos present largely displaced junctions, which are modulated by the Rho-kinase pathway (Figure 3.17). These results imply that junctions must resist morphogenetic tension and that actin capping proteins such as UNC-94 must protect the α-catenin-recruited actin filaments from minus-end subunit loss.

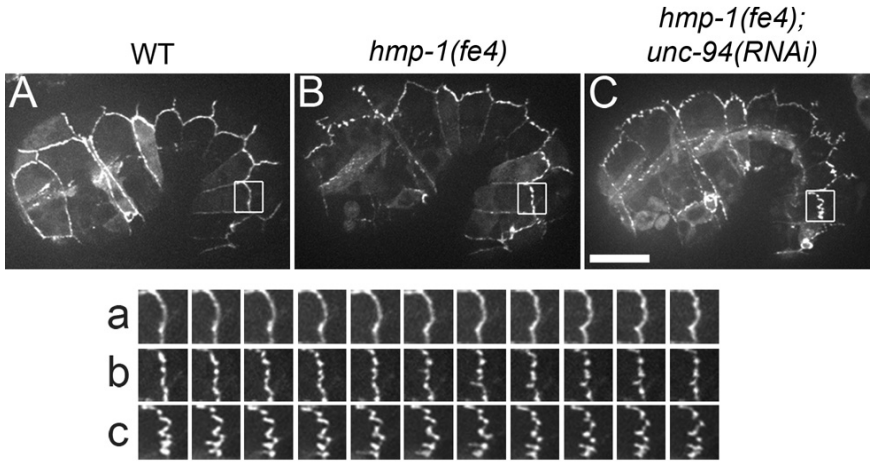

Figure 3.17: Junction discontinuity in *hmp-1* mutant and *hmp-1*/*unc-94* double mutant. Figure adapted from [286].

Although the junction component dynamics and the architecture maintenance are controlled by intracellular molecules, local polarized tissue-scale pulling forces can also orient junction polarized lengthening. Recent research in *Drosophila* germband extension showed that junction growth is driven by the local planar polarized stresses from the actomyosin contractions [128]. These tissue-scale forces function as an entire polarized fluid flow within the tissue to trigger the cell-cell displacement. This pattern has not yet been observed in *C. elegans* embryogenesis. However, considering the facts

that UNC-94 is mainly expressed in the lateral epidermis, and that the loss of UNC-94 induces a development defective phenotype mainly happening when HMP-1 is affected in dorsal and ventral cells, a similar tissue-scale tension flow may also exist in *C. elegans* embryo to help the junction growth and tissue extension.

Insertion of new junctional proteins through exocytosis

During junction lengthening, how do the junction components get delivered to the membrane and inserted into the junction area is crucial for this process. It has been proven that the remodeling of apical junctions, as well as tight junctions, are controlled by vesicle trafficking, where the endocytosis and exocytosis of junction proteins mediate the disassembly and assembly of the junction, respectively. As discussed in the previous part, non-muscle myosin-II induced endocytosis triggers the shrinking of junctions during cell-intercalation [28].

Although little is known yet about the mechanisms controlling junction exocytosis during development, researches in mammalian MDCK cells showed that SNARE-mediated membrane fusion is important for junction assembly. E-cadherin has been reported to be delivered by post-Golgi structure and co-accumulate with the basolateral membrane aquaporin AQP3 at the site of initial cell-cell adhesion [287]. Intriguingly, cell-cell adhesion or the co-localization of other junction components with E-cad will not be interrupted when individual components of a putative lateral targeting patch such as microtubules, SNAREs, or the exocyst are disrupted. This implies that the lateral targeting patches function as a complex to ensure the vesicle delivery for E-cadherin and other junctional proteins [287]. Moreover, SNARE family also affect the vesicle trafficking of junction components and the junction formation. Mis-located syntaxin-3 leads to the disturbance of tight junction formation [288]. Likewise, syntaxin-5 has been reported to contribute to apical junction formation during *C. elegans* embryogenesis (Figure 3.18) [19].

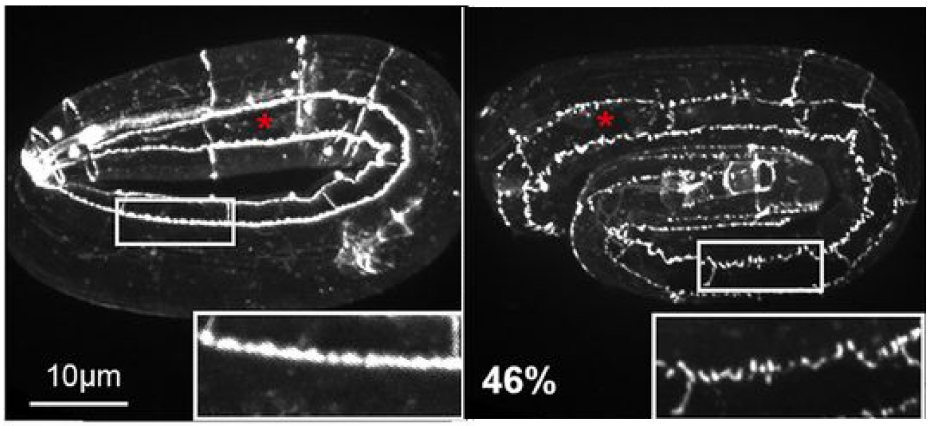

Figure 3.18: Left, wild-type embryo apical junction. Right, syntaxin-5 mutated embryo presenting a junction discontinuity. Figure adapted from [19].

Some recent researches in epithelial and neural cells have demonstrated the molecular details and modulatory mechanisms for SNARE-mediated vesicle trafficking of E-cadherin. In mammalian epithelial cells, a key regulator of exocytosis, soluble N-ethylmaleimide sensitive factor (NSF) attachment protein alpha (αSNAP), mediates the assembly of adherens and tight junctions. Knock-down of αSNAP also leads to a significant down-regulation of E-cadherin and p120-catenin. Like in kidney cells, this process is also associated with the Golgi-complex, and a Golgi-associated guanidine nucleotide exchange factor GBF1, suggesting that Golgi-involved trafficking controls the apical and tight junction formation in epithelial cells [289]. In *Drosophila* neuromusclular cells, SNAP-25 has been shown to play an essential role in neuroexocytosis. Mutated SNAP-25 leads to a reduction in spontaneous neurotransmitter release [290].

3.3 Planar polarity in development

Planar polarity is an essential feature of tissues. Unlike apical-basal polarity, planar polarity distinguishes the asymmetry of cellular components organization along the perpendicular axis within a plane of tissue sheet [291]. The most famous example for planar polarity is identified in *Drosophila*, where the external bristles and hairs are oriented coordinately into one direction (Figure 3.19). Planar polarity is mainly established during development, guided by multiple global factors, including the expression of specific molecular determinants, polarized intracellular trafficking, gradients of secreted WNT ligands, and anisotropic mechanical forces within the tissue. The establishment and maintenance of planar polarity are crucial for development because it executes the polarized cell shape changes during morphogenesis. Defects in planar polarity establishment result in problematic development even drivers pathologies [291].

3.3.1 Planar polarity in morphogenesis

The establishment of planar polarity is largely dependent on the core planar cell polarity signaling pathway. Within this pathway, transmembrane signaling components get enriched in different cell subsections through their complementary and exclusive distribution. This enrichment leads to an asymmetric tissue patterning, which in turn directly affect regulation of the subcellular structure and cellular behavior by modulating cytoskeleton and adhesion junctions.

Core planar polarity signaling components

The planar cell polarity (PCP) signaling components are most well-studied in *Drosophila*. It includes the transmembrane proteins Fmi/Stan/CELSR (Flamingo/Starry Night or CELSR in vertebrates), Fz/FZD (Frizzled), and Vang/Stbm/VANGL (Van Gogh/Strabismus or VANGL in vertebrates) and the cytoplasmic proteins Dsh (Dishevelled, DVL in vertebrates), Pk (Prickles) and Dgo (Diego, ANKRD6 in vertebrates). The transmembrane proteins allow the polarity information exchange between cells, whereas

the cytoplasmic proteins amplify the intracellular asymmetries and convert them into cellular behaviors [292, 293, 294, 295, 296].

To develop an asymmetric pattern within cells, PCP proteins form a distinct distribution that revolves in two complementary domains on the opposite sides of the cell. Fz, Dsh, and Dgo accumulate on one side of the cell whereas Vang and Pk accumulate at the other side of the cell (Figure 3.20) [292, 293, 294, 295, 296].

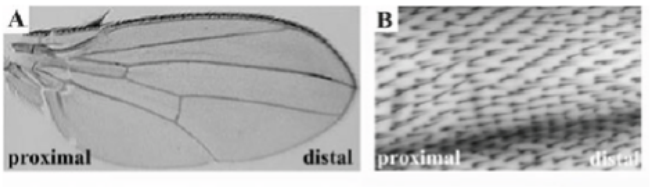

Figure 3.19: Planar polarity example in *Drosophila* wing (A) and the hair distribution (B). Figure adapted from [297].

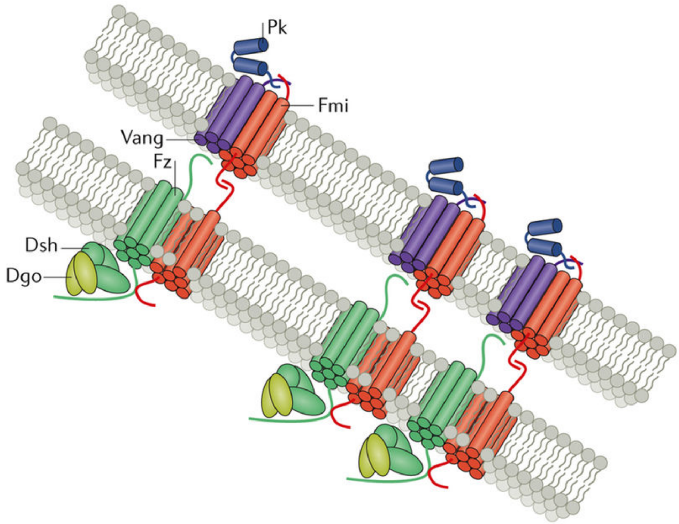

Figure 3.20: Asymmetric planar cell polarity signaling components distribution at cell junction. Details see text. Figure adapted from [291].

The specified locations of different groups of proteins are differentially controlled by the dynamic trafficking, signaling interactions and binding and unbinding of proteins. Through these processes, the asymmetric sorting and symmetry breaking are accomplished.

The propagation and the amplification of planar polarity signals

After being stably localized at the different domains of the cell, the physical interaction of PCP signaling proteins starts to facilitate the propagation of planar polarity between cells. First of all, Fmi forms homodimer across apical junction domains through its extracellular cadherin repeat domains. This homodimer ensures the stable structure of the whole core PCP machinery [298, 299, 300, 301], and therefore conveys a uniform pattern of polarity information transmission system within the tissue. Second, Fmi promotes the recruitment of other core PCP proteins such as Fz and Vang to the junction, stabilizing the PCP signaling components [298, 301, 302, 303, 304]. Genetic analysis have shown that to maintain planar polarity within the tissue, Fz must be present in at least one of the two adjacent polarized cells, whereas Vang does not need to be present for the initiation of the planar polarity.

However, after the initial establishment of PCP signaling pathway, the feedback amplification of asymmetry is mainly directed by the cytoplasmic proteins, Dsh, Dgo and Pk, which are also recruited to junction region through a Fmi-dependent manner as Fz [305]. These proteins cluster the transmembrane complexes into large stable domains to accumulate the intracellular polarity signals and amplify these signals among neighboring cells [301, 306]. Importantly, to amplify the PCP signals, all the signaling components, both transmembrane and cytoplasmic proteins are required. Loss of any PCP signaling component will lead to the disruption of asymmetric patterning and further affects the cellular structure and cell behaviors during development.

On the contrary, there are also negative feedbacks that exclude the complementary proteins from their location of the cell and diminish the PCP interactions. Pk and Dsh have been observed to compete to bind to the Fmi-Vang complex through the same binding domain of Vang [305, 307]. Meanwhile, Dgo has to compete with Pk to bind with Dsh to complete the large PCP domain at the one side of the cell [308].

Asymmetric sorting through trafficking

To avoid that the mislocated and unstable PCP components affect the PCP signaling domain, endosomal trafficking must be active to diminish the mistakes during PCP maintenance. Two proteins that have been shown to play a part in internalization of unstable PCP signaling components are Rab5 and dynamin [298, 309, 310]. When endocytosis is inhibited, over-accumulation of Fmi, Fz and Vang will happen at the plasma membrane [298, 301, 311]. Ubiquitination of Pk also promotes the internalization of Fmi-Vang-Pk complex [311].

Cytoplasmic PCP components can also mediate the internalization of other components to ensure the correct assembly of the large PCP domains. Since Dsh requires Fz to bind to Fmi, it has been observed in *X. laevis* that down regulation of the interaction between DVL2, the Dsh vertebrate homologue, and AP2 will directly impair FZD4 internalization and further lead to a PCP defective gastrulation [312, 313]. Likewise, another cytoplasmic protein Pk has been described to mediate the internalization of Fmi and Vang [311].

After the internalization of the mislocated proteins, several downstream processes including the recycling, degrading or trafficking to other membrane region continue to regulate the PCP proteins within the cell. For example, the internalized Fmi will be over accumulated in the cytoplasm when lysosomal maturation is inhibited, suggesting some Fmi undergo lysosomal degradation after removal from cell membranes [298, 301]. Otherwise, Fmi seems to be recycled back to the membrane under the control of Rab4, Rab5, Rab7 and Rab11 [298, 301, 310].

After the unstable components have been removed from the membrane, newly syntheses proteins can be added to the membrane through a Golgi-endosome dependent pathway. Loss of function of AP1 and trafficking GTPase ARF1 will lead to strong PCP defects [314]. Endocytosis and trafficking can further affect the dynamic cellular behavior during cell rearrangement and mitosis. For instance, synchronized with cell division, the CELSR phosphorylation promotes the internalization of CELSR1 and their association with FZD proteins [315].

PCP proteins anisotropy under polarized microtubules trafficking

Besides the Golgi-dependent trafficking, microtubules (MTs)-dependent transport also helps to break the cellular symmetry and the pre-existing axis of the cells [316, 317]. Planar polarized MT arrays have been reported to transport the PCP components such as Dsh, Fz, and Fmi preferentially in vesicles towards the plus end, assisting the PCP machinery establishment [318, 318, 319, 320]. Nevertheless, other potential mechanisms align the PCP asymmetry in cells, since the MT-plus end transporting is diminished in the distal region of *Drosophila* wings, though the hair alignment in this region remains planar polarized. The MT cytoskeleton also contributes to maintaining this pattern after they are generated [318, 321]. Together, the bias MT transporting suggests an intricate relationship between the cytoskeleton and the planar polarity patterning.

3.3.2 Planar polarity patterning alignment in tissue

After the establishment of molecular PCP pattern within one cell, this symmetry has to be distributed into the tissues and to direct the global tissue behaviors, according to the axis of the whole tissue. There are three major potential influences for the tissue-scale PCP pattern that overlap with each other to some extent.

Ft-Ds-Fj singling pathway

In this Fat/Dachsous(Ds)/Four-jointed(Fj) singling pathway, Ft and Ds are atypical protocadherins that comprise a subgroup of cadherins with various extracellular domains and form heterodimers across the plasma membrane. Fj modulates the interaction between Ds and Ft across the membrane as a transmembrane kinase.

To achieve the planar polarity within the tissues, gradient expression of these three proteins is the primary regulatory mechanism. In *Drosophila*, the opposite expression gradient of Ds and Fj has been observed along the axis of polarity in the tissue

[322, 323]. As a result, Ds and Fj are localized on the opposite of the cell similar to the localization of the core PCP components. However, the expression gradients of these two isoforms of Pk, the Prickle(Pk) and the Spiny legs (Sple) can alter the location of Fmi-Dsh and Vang-Pk complexes and determines the different PCP pattern within different tissues (Figure 3.21) [324, 325, 326]. Meanwhile, the direction of expression gradients of Ds and Fj are always fixed within the tissue [325, 326].

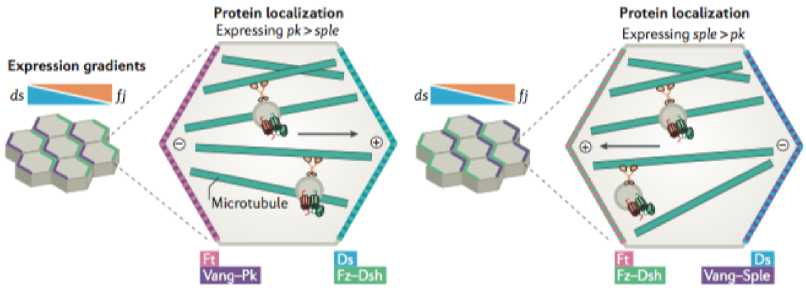

Figure 3.21: Graded expression of Ds and Fj controls the global planar polarity alignment in two different situations. Details see text. Figure adapted from [291].

The functional consequence of this altering PCP pattern within cells is that the orientation of MTs arrays are altered. The plus ends of MTs point to Ds in the Pk-dominating cells and to Fj in the Sple-dominating cells. Together with the different expression of the two isoforms of Pk, the global gradients of Ft-Ds-Fj conserve and regulate the polarity of tissue [327, 319].

Wnt ligand gradients

Besides the gradient expression of PCP pathway proteins, secreted ligands function along the planar polarity axis. Wnt proteins act as the Fz receptors and contribute to the global PCP pattern within the tissue. For example, in *Drosophila* wings, Wg and Wnt4 function redundantly to control the PCP complexes orientation. During early wing morphogenesis, the distal PCP components point towards the secreted Wnt proteins (Figure 3.22) [328, 329]. Likewise, Wnt5a, Wnt11, and Wnt11b can affect the orientation of Pk and Vang in *X. laevis* ectoderm [329].

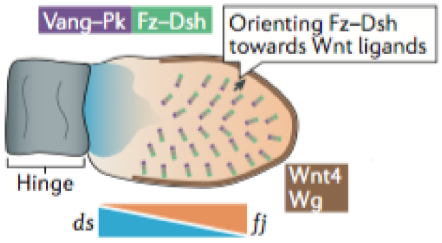

Figure 3.22: Distal PCP components point to Wnt4 and Wg proteins in early pupal wings. Figure adapted from [291].

Although the detailed mechanism through which Wnt proteins regulate the PCP pattern is not fully understood, one possibility found in *Drosophila* is that Wnt proteins locally compete with Vang for Fz binding [328]. In mice, it has been reported that WNT5A promotes the phosphorylation of VANGL2 and therefore upregulates the planar polarity in epithelia [330].

Anisotropic mechanical forces

Like in many morphogenesis processes, mechanical tension, especially the anisotropic tissue strains, can influence the development and maintenance of PCP pattern across the tissue. During the gastrulation of *X. laevis*, forces exerted on the epidermis affect the direction of MTs array, and therefore, affect the initial establishment of the polarised axis in the tissue. They also increase the core PCP proteins accumulate at the junction region of the cell through the up regulation of VANGL2 stability at the anterior/posterior junction (Figure 3.23) [242, 243].

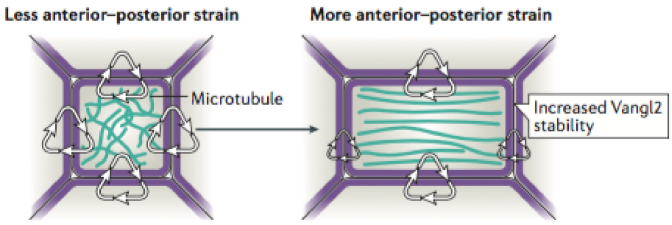

Figure 3.23: Anisotropic tissue strain during morphogenesis orienting the microtubules along the axis to promote the stability of planar cell polarity components. Figure adapted from [291].

Tissue PCP pattern has been reported to be associated with both embryo elongation and increased fluid flow under the directional mechanical forces events during morphogenesis. For the tissue within which planar polarity axis already exists, morphogenetic mechanical forces can shift the orientation or the location of the pre-existing polarity axis. For instance, the PCP components in *Drosophila* wings shift their direction from pointing toward the Wnt signaling to pointing toward the A/P direction while the wings go through shape change towards the anterior/posterior direction under the mechanical force from the hinge contractions (Figure 3.24) [39]. Similar events have been reported in mouse epidermis, that PCP complexes alignments change with the junction remodeling and tissue shape change [244]. Also, when actin regulators that mediate the cortical tension are disrupted, PCP patterning establishment will fail, so will the coordinating cell rearrangements [245, 246].

Although the PCP pattern location and orientation can be affected in a biased way by the anisotropic tension flow, the mechanisms behind this are still not clear. One possible player is Rab11, which controls vesicle trafficking and recycling of PCP proteins to the apicolateral junction and maintains cortical tension through actin regulators [301, 246].

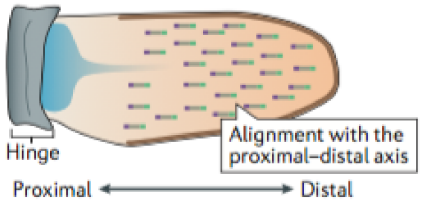

Figure 3.24: Distal PCP components aligning with the proximal-distal axis in the late pupal wing of *Drosophila*. Figure adapted from [291].

3.3.3 Effects of planar polarity during morphogenesis

PCP proteins instruct the morphogenetic process in multiple ways. In *Drosophila*, PCP patterns control both planar polarized cell organization and the asymmetric cell fate during morphogenesis [247]. This study was followed by the discovery in vertebrates such as *X. laevis* and zebrafish [248, 331, 332].

Convergent extension

In *Drosophila*, the convergent extension of cells along the polarity axis of the tissue is a major driving force for embryo elongation. During eye formation, for example, the PCP signaling directly controls the contraction of actomyosin through Rho GTPase and Rho kinase [333, 334]. They also regulate the activities of other actin modulators such as formin Daam1 and Rho GTPase Cdc42 [335]. PCP signaling triggers polarized junction shrinkage through actin contraction, suggesting a possible model in which PCP pattern induces collective cell movements.

Moreover, during the development of the *Drosophila* thorax, Ds can regulate the distribution of atypical myosin Dachs to induce asymmetric tension at the junction to promote the polarized cell rearrangement [31]. This PCP protein-induced myosin enrichment at the junction region can also be observed by light-microscopy in *X. laevis* gastrula mesenchyme and chick neural epithelia [168, 254]. Additionally, another vertebrate-specific core PCP complex regulator, PTK7 has been reported to regulate myosin activation through the Src-kinase [336, 337, 338]. The possible mediator of this process has been suggested to be septins [168, 339].

The difficulty in studying how PCP signaling affect the convergent extension is that cells constantly change their neighbors during this process and therefore the dynamic nature of PCP is hard to be clearly observed. Time-lapse imaging and probing localization with photo-bleaching and photo-converging have started to provide more insight of PCP signaling during convergent extension [301, 321, 242, 340].

Directional beating of motile cilia in epidermis

In many organs, motile cilia beat to drive fluid flow across the tissue and to move cells. PCP complexes have been shown to control the polarized beating of motile cilia in mammalian brains, air-duct and oviduct [316, 321, 341, 342].

The multi ciliated cells in both vertebrates and invertebrates present rotational polarity, the organization of cilia base bodies and tissue-level polarity [335, 343]. Disruption of DVL or PK in mammalian epithelial cells will lead to rotational polarity defects [340, 344, 345] and disruption of VANGL, FZD or CELSR will lead to tissue-level polarity defects [243, 340, 344, 346].

Intriguingly, PCP proteins from the same family may have distinct functions: in mouse ependymal cells, CELSR1 affects the tissue-level polarity through regulating the microtubules pattern, while CELSR 2 and CERSL3 are required for rotational polarity through actin control [346].

Although the exact mechanism through which PCP proteins control the motile cilia beating is not clear yet, the control of the cytoskeleton by PCP singling has been shown to be a key player. Both actin and microtubules have been reported to control the polarized beating of motile cilia [335, 343, 346]. Therefore, it is important that PCP complexes localize to the cell cortex, where they can regulate the polarization pattern of the cytoskeleton and at the basal body to control the basal body polarity [316, 246, 340, 344, 347].

In this project, instead of actomyosin cortical tension, we propose another mechanical tension, which is from muscle activity and embryo rotations, triggers the planar-polarized lengthening of the junction. This event has never been reported in other model systems before as the non-muscle myosin II contributes to the junction remodeling and cell rearrangement, possibly through the modulations of vesicle trafficking. Here we also propose that the muscle-induced anisotropic tension along the anterior/posterior direction triggers the junction components trafficking and their fusions into the junction. In this process, trafficking regulator such as AP1, Rab family may also mediate protein trafficking and fusion, contributing to the new material insertion to the junction and the junction polarized lengthening during morphogenesis.

3.4 Axes of the thesis

Contractility of non-muscle Myosin-II has been reported to be the mechanical force generator in many organisms. However, it seems that it does not contribute to the junction polarized lengthening during *C. elegans* tissue morphogenesis due to its non-polarized distribution. Instead, muscle activity is the key player for *C. elegans* morphogenesis during late elongation. How muscle activity promotes embryo elongation is not entirely understood yet.

This thesis revolves around four questions, addressed in the chapters 4 and 5.

I) How do muscles contribute to embryo movements and elongation? II) Does muscle activity fit any pattern? III) What is the source for planar polarized growth of *C. elegans* during late elongation? IV) How does muscle activity promote the polarized lengthening of junctions during late elongation?

The first two questions are organized in chapter 4, written in the form of a manuscript to be submitted. The last two questions are organized in chapter 5.

Part II

Results

Chapter 4

Manuscript:

Muscle activity and regional rigidity differences affect embryo movements during *C. elegans* morphogenesis

Muscle activity and regional rigidity differences affect embryo movements during *C. elegans* morphogenesis

X. Yang[1,2], T. Ferraro[1], J. Pontabry[2,¶], N. Maghelli[3], L. Royer[3], S. Grill[3,§], G. Myers[3] and M. Labouesse[1,2,*]

1. Laboratoire de Biologie du Développement - Institut de Biologie Paris Seine (LBD - IBPS), CNRS (UMR7622), INSERM (U1156), Sorbonne Universités, UPMC, 7-9 quai Saint Bernard 75005 Paris, France.

2. Development and stem cell program, IGBMC, CNRS (UMR7104), INSERM (U964), Universit de Strasbourg, 1 rue Laurent Fries, BP10142, 67400 Illkirch, France

3. Max Planck Institute of Molecular Cell Biology and Genetics, Dresden, Germany

¶. Current address: Institute of epigenetics and stem cells, HelmholtzZentrum München, Germany.

§. Current address: Technische Universität Dresden, Biotechnology Center, Tatzberg 47/49, 01307 Dresden, Germany

*. Corresponding author: michel.labouesse@upmc.fr

SUMMARY

Tissue morphogenesis relies largely on mechanical stimuli. Muscle activity is one of the two mechanical force inputs for *C. elegans* embryo elongation. How muscle activity affects global embryo movements and spreads along the anterior/posterior axis of the embryo during late elongation has not been described yet. Using fast 3D imaging, we discover that embryos rotate after muscle activation and we describe the global pattern of embryo rotation induced by muscle activity. Muscle activity also triggers epidermal cell deformation, which presents local characters, suggesting rigidity differences in different regions of the embryo. Calcium sensor activation imaging demonstrates the existence of pacemaker muscle cells, which initiate the muscle contraction, indicating a potential calcium center that regulates the muscle activation of the embryo.

INTRODUCTION

The idea that cells sense and respond to mechanical stimuli is widely accepted for tissue development, function, and diseases [1]. However, the mechanisms through which cells sense tension, and then respond to such mechanical stimuli remain poorly understood. Using the *C. elegans* embryo as a model, our goal is to better understand how mechanical forces contribute to embryo development and influence cellular behaviors during embryo development. Unlike *Drosophila* germband extension, during which the polarized distribution of non-muscle Myosin-II drives the planar polarized lengthening of the tissue [2, 3], the mechanical stimuli for *C. elegans* embryonic elongation mainly come from actomyosin contractility and muscle activity. Here, we mainly focus on the late elongation stage of *C. elegans* embryo development, during which muscle activity provides the mechanical stimuli for embryo elongation. We aim to describe the embryo movement after muscles become active and to discover if the embryo movements present any global or local patterns. We also intend to explore the relationship between muscle activation and epidermal cell movements.

The elongation of *C. elegans* embryos starts immediately after ventral epidermal cells enclose the embryo. This process lasts around 250 minutes, during which embryos elongate from a lima-bean shape to a characteristic worm shape within the egg shell, increasing their body length by four-fold and reducing their circumference by almost three-fold (figure 1A) [3, 4]. During the embryonic development of *C. elegans*, there are two major driving forces. The first one results from epidermal actomyosin

contractility, which squeezes the embryo circumferentially from the beginning of elongation until 2-fold [4, 5, 6]. The second results from muscle activity starting at the 1.7-fold stage. Losing any one of these two forces leads to embryonic elongation defects. The Rho-kinase mutants (LET-502), in which the phosphorylation of myosin-II regulatory light chain is reduced, arrest at the 2-fold stage or before (figure 1B) [6]. On the other hand, muscle defective mutants, in which muscle function is completely lost, fail to continue their elongation beyond 2-fold (they are called Pat mutants, which stands for paralyzed at two-fold) (figure 1C) [7].

Here, to study the embryo movements after muscle activation, we acquire high time-resolution 3D movies with embryos expressing fluorescence junction marker to image embryo movements during late elongation. By analyzing the fast 3D movies, we define the global movement pattern of embryos. We also describe the aspect changes in different lateral epidermal cells and how they present a local difference. In addition, we discover regional differences of muscle activation and unravel the material rigidity difference in embryos by combining the results of the local epidermis deformation with the results of regional muscle activation.

RESULTS

Acquisition of high-speed 3D movies and analysis strategy

During late elongation, muscles actively contract, which promotes embryonic elongation, since Pat mutants arrest at the two-fold stage. In our previous experience [8, 9], conventional confocal or spinning disc microscopy offers serious time and spatial resolution limitations, because in embryos beyond the 1.8-fold stage, muscle contractions will cause the embryo to very frequently change position. As a result, it becomes difficult to track any marker over time, and phototoxicity becomes a very serious issue.

To circumvent these limitations, we used Single Plane Illumination Microscopy (SPIM) [10-12] to record the elongation process in a wild-type strain, in the hypocontractile mutant *let-502 (sb118ts)* raised at the non-permissive temperature, and in muscle-defective *unc-112 (RNAi)* embryos expressing a functional GFP-labeled DLG-1 protein to track cell-cell junctions. The time-resolution for these SPIM movies was between 0.3 to 0.5 second per frame, depending on the number of focal planes. We limited the length of each movie to 500 seconds or less to avoid phototoxicity.

To analyze the SPIM movies and define the global and local movements of the embryo, we specifically tracked the positions of the vertices between lateral epidermal cells. Thereby we could compute the perimeter and the apical area of each lateral epidermis for each time point (figure 1D), as well as the total length of the lateral epidermis (figure 1E). Moreover, we could quantify and compare the local compression and extension of neighboring lateral epidermal cells (figure 1F). We limited our

imaging to the beginning of the muscle contraction period, as the pattern became too complex (in part because the tip of the cell starts wagging and overlay other areas) and too rapid beyond the 2-fold stage, even under SPIM microscopy.

Asymmetric rotations are crucial for embryo elongation

When tracking the position of the lateral epidermis, we noticed that after dorsal epidermal cells have fused (1.5-fold stage), the embryo displayed important twitching causing one side of the embryo to contract, presumably as a result of muscle contractions (figure 2A, movie 1). These occasional movements lasted until the embryo reached the 1.7-fold stage, at which point the contraction/relaxation movements became very regular. This second phase went on until hatching and was accompanied by constant rotation of the embryo along its long anterior-posterior (A/P) axis (figure 2B, movie 2).

To characterize the embryo rotation pattern, and determine whether rotations had a relationship with embryonic elongation, we measured embryo mid-body length along the nine lateral epidermal cells on one side (yellow line in figure 1E). We repeatedly observed that the total length of the lateral epidermis decreased when embryos rotated inward (e.g, when lateral cells get displaced to the fold) (figure 2C′), and increased when they rotated outward (figure 2C″). Moreover, we observed over time that the total length increased regularly with each rotation (see black line in figure 2C). To simplify the rotation pattern scoring, we normalized the total length of lateral epidermal cells by the elongation ratio over the period and set up the inward-rotation threshold and the outward rotation threshold (two yellow lines in figure 2D). From

there, we skeletonized the tracing (figure 2E). We found that the average total rotation time was 70%, based on eight wild-type embryos aged 1.7- to 1.9-fold. During this period, embryos spent on average 34% time rotating inward and 36% time outward (Table 1), showing that embryos rotate equally in both directions. There was no apparent rotation pattern, but instead, the rotation direction was random.

To test whether muscle activity triggered rotations, we examined the Rho-kinase/*let-502 (sb118ts)* mutant embryos reaching an age comparable to the wild-type 2-fold stage, based on the time elapsed since the time of dorsal cell fusion (n=12), scarcely rotated at all with an average of 1% total rotation time (figure 2F, Table 1). Previous studies showed that mutations affecting non-muscle myosin-II activity will reduce the rate of elongation prior to muscle contraction [9, 13]. As a consequence, *let-502 (sb118ts)* mutant embryos were barely 1.3-fold when wild-type embryos reach the 2-fold stage. Since they displayed frequent muscle activity during imaging (movie 3), we suggest that the embryo must reach a certain length to allow embryo rotations. We also examined the muscle-defective *unc-112 (RNAi)* embryos. These embryos also rotated on average only 1% of the time (n = 5), indicating that muscle contractions are probably responsible for embryo rotations (figure 2G, Table 1) (movie 4). Altogether, we conclude that rotations are caused by muscle activity and that active rotations are crucial for proper elongation of the embryo.

Rotations affect the aspect ratio of the epidermis

To further characterize the pattern of muscle-depended embryo elongation, we quantified the individual dimensions of lateral epidermal cells to define if they deformed

uniformly. As illustrated for wild-type head (H1), body (V1) and tail (V5) lateral epidermal cells (figure 1D), we observed that the cell apical area, cell perimeter, and cell length changed with embryo rotations (note that we are considering 2D projections of these factors) (figure 3A, first row) (figure S1). Valleys of the values corresponded to inward rotations and peaks to outward rotations (figure 3A′, A″). Within a given embryo, the 2D apical area projection perimeter and anterior-posterior cell length co-evolved (figure S1).

When we quantified these parameters in Rho-kinase defective and muscle-defective embryos (figure 3A, second and third row), we observed much smaller changes compared to wild-type embryos (figure 3B, C). Taking the change of cell length of H1, V1, and V5 cells as examples, the average maximum amplitude of cell length changes were 30%, 59% and 61%, respectively in wild-type embryos (n = 8; figure 3C, Table 2). By contrast, in *let-502* mutant embryos, the average maximum amplitude of cell length changes were 16%, 16% and 37% for H1, V1 and V5, respectively (figure 3C, Table 2). Although *let-502 (sb118ts)* muscles were still active, the changes were lower than in control embryos. This might originate from the abnormal organization of muscles and hemidesmosomes in these embryos, which become twice wider than in control embryos and more tilted to the dorsal-ventral axis [13]. The average maximum amplitude of cell length changes was 17%, 25%, and 11%, respectively, in *unc-112 (RNAi)* embryos (n = 5; figure 3C, table 2). While control scoring of the RNAi efficiency showed that these embryos failed to elongate beyond the 2-fold stage, we suspect that the residual twitching resulted from partial RNAi knocking-down of

the gene. Nevertheless, the results are consistent with the notion that muscle activity trigger lateral cell deformation. They also suggest that that muscle function was required throughout the anterior-posterior axis, although the head was comparatively less affected than the body and tail.

Altogether, our observations confirm that active muscle contractions were essential to deform lateral epidermal cells and promote embryo elongation.

Muscle-induced epidermal cell shape changes present a local difference

After characterizing the deformation pattern of individual lateral epidermal cells during embryo rotations, we examined to what extent neighboring cells changed together. Since the area, perimeter and length of cell deformation behave similarly within a given embryo, we compared the change of cell length using a cross correlation analysis. We noticed that on average neighboring lateral epidermal cells presented a similar deformation trend. However, the similarity decreased when the distance between two cells increased (figure 4A, B). Moreover, cross-correlation analysis of eight wild-type embryos suggested that lateral epidermal cells form different groups (figure 4C, first row). Indeed, taking as a cut-off value of cross-correlation changes above 60%, we could define three mechanically semi-independent groups of lateral epidermal cells. Therefore, based on the change of cell length, the embryo could be divided into a head group comprising H1, H2 and V1 cells, a body group comprising H2, V1, V2, V3 and V4 cells, and a tail group comprising V5, and V6 cells (figure 4D). Within these three groups, the change of apical area and perimeter of epidermis correlated as well (Data not shown). Intriguingly, these local characters were partially or totally lost

in different *let-502 (sb118ts)* (figure 4C, second row, figure 4E) and muscle-defective embryos, except partially for head cells in *unc-112 (RNAi)* embryos (figure 4C, third row, figure 4F). This is consistent with our previous observations on the effect of these mutants on body deformation.

The local body groups described above may reflect a local difference in cell rigidity in their response to muscle contractions, and/or the presence of distinct groups of head, body and tail muscles contracting independently. Indeed, before the embryo starts to rotate, muscle activity induces embryo to strong twitching jumps. When we compared the relative length changes of the H2, V1, and V2 lateral epidermal cells during these jumps, we noticed that the V1 cell underwent much stronger compression than its two neighbor H2 and V2 cells (figure 5A). Furthermore, H1 and H2 experienced on average 30% and 38% maximum cell compression, respectively, less than that of V2, which was 65% maximum cell compression, and other body lateral cells (Table 2). We thus suggest that the head might indeed be more rigid, which is consistent with the fact that it contains more cells.

Muscle activation is initiated by pace maker cells

The results described thus far have highlighted that these muscle contractions locally deform the lateral epidermal cells, and potentially delineate mechanically different regions. To complete the characterization of this initial phase of the muscle-dependent embryo elongation, we decided to characterize the pattern of muscle contractions. To address this issue, we expressed a GFP-marked chameleon Ca^{2+} sensor together with the fluorescent DLG-1::RFP junction marker in wild-type embryos (movie 5). We

selected five muscle cells in the head-body groups and defined their relative positions to the lateral epidermal cells (figure 5B), bearing in mind that muscle cells are beneath the dorsal and ventral epidermis instead of the lateral epidermis. We quantified 10 Ca^{2+} pulses per embryo in five embryos. We noticed that muscle cell number 2 (figure 5B) are closer to the lateral epidermal cells H2 and number 3 is between lateral epidermal cells H2 and V1, which made them perfect to compare their activity and lateral epidermis deformation. We first compared the Ca^{2+} pulse duration and intensity, which showed that muscle cells number 2 and 3 had a similar relative duration of pulses (figure 5C). The relative duration of each fluorescence pulse in muscle cells number 2 and 3 was slightly longer than in muscle cells number 1 by 30%, and muscle cells 4 and 5 by 10% (figure 5C). The relative intensity of muscle cell number 3 was 1.3 times stronger than that of muscle cell number 2, 1.6 times stronger than muscle cell number 1 and 2.5 times stronger than muscle cells 4 and 5 (figure 5D). When examining the time delay between the onset of the Ca^{2+} fluorescent signal in different muscles, we found that muscle cells 2 and 3 fired together in wild-type embryos (figure 5E). By contrast, muscle cells 1, 4 and 5 fired slightly later, with a delay from 0.5 seconds to 1.5 seconds (figure 5E). Altogether, this analysis suggests that the muscle cells number 2 and number 3 were activated stronger and earlier than the other muscle cells.

Altogether, our results suggest that the muscle cell 3, perhaps together with muscle cell 2, represents the pacemaker in the muscle contraction pattern since its contraction precedes that of other muscles. This indicates a potential Ca^{2+} center near the H2

and V1 lateral epidermal cells that regulate the activation of muscles. Intriguingly, the V1 region underwent the strongest cell compression during the switching jumps before embryo rotation. It formed a hinge between the two mechanically distinct regions, the head and the body parts, suggesting that the embryo body may also contains a neck part like in the more complex organisms to better connect the head and the body and let this two parts to communicate more coordinately.

DISCUSSION

Here, we have characterized how muscles contribute to embryo elongation by using fast 3D imaging. We show that during late elongation of *C. elegans* embryos, muscle activity triggers the global rotation of the embryo and local deformations of epidermal cells. Lateral epidermal cells could be divided into three semi-independent groups, the head, the body and the tail group, based on their cell deformation pattern. Also, stronger cell compressions induced by muscle activity in certain lateral epidermis suggest a difference of rigidity in different regions of the embryo. Our characterization of the muscle activity pattern suggests the existence of pace-maker muscles that initiate contraction, indicating a potential calcium enriched region in the embryo that regulates muscle activation.

After the embryo has reached the 1.7-fold stage, muscles beneath the dorsal and ventral epidermal cells start to contract. This muscle activity must be important for proper embryo elongation since the loss of muscle activity leads to a 2-fold arrest during elongation and a failure of embryonic development [7]. However, how do muscles contribute to embryo elongation was not completely understood. Our laboratory has recently discovered that muscle activity triggers the maturation of cell-extracellular matrix junctions through a tension-induced pathway, which in turn promotes late elongation [8]. However, other consequences of muscle activity during late elongation are left to be discovered.

Our data establish that muscle activity can drive the embryo to rotate beyond the 1.7-fold stage. Wild type embryos spend on average 70% of the time rotating,

and do not have any preference for rotation directions since they spend around 35% time rotating inward and 35% time rotating outward. Meanwhile, the distribution of inward or outward rotation is random overall, suggesting that embryos do not follow any rotation pattern. The characterization of muscle-defective and of Rho-kinase defective embryos indicates that embryo rotations are necessary for further elongation. Indeed, we failed to observe active rotation in muscle defective embryos, which arrest at the two-fold stage. Likewise, actomyosin hypocontractility Rho-kinase mutants, which arrest before the two-fold stage, also failed to rotate. In *unc112*-defective embryos, the assembly of muscle myofilaments is disrupted, resulting in muscle inefficiency and a failure to transmit mechanical tension to the epidermis. In *let-502* embryos, muscles start to contract when embryos reach the 1.2/1.4-fold stage since their elongation rate is reduced due to epidermal actomyosin hypocontractility. Yet, they also failed to rotate. There are two possibilities for this. First, the short length structure of the embryo could seriously hamper embryo rotations. Second, hemidesmosomes in *let-502* embryos are broadened with a different organization angle compared to wild-type, suggesting that muscle tension might not transmit with the same efficiency [14]. Therefore, the transmission of mechanical tension from muscle to the epidermis is slightly impaired as well, leading to less cell deformation (figure 4E, F) and a failure to the rotation.

Our analysis of SPIM movies also showed that muscle activity leads to deformations of lateral epidermal cells. The degree of cell deformation was greater in wild-type embryos than in *unc-112* and *let-502* defective embryos, suggesting that both of them

are linked and further suggests that embryo rotations are essential for elongation. We also noticed that at the beginning of late elongation, embryos undergo twitching jumps before they start to rotate. During these jumps, the V1 lateral epidermal cell experienced the strongest cell compression along the A/P axis, compared to its neighboring cells such H2 in the head and V2 and V3 in the body. This region-specific strong cell compression suggests a difference of embryo rigidity in different regions of the embryo. The head part from H0 to H2 lateral epidermal cells seemed to be more rigid than the body part and the tail part of the embryo. This difference in embryo rigidity may come from the inner structure of the head, which harbors the pharynx [15] and the bulk of the nervous system [16]. On the contrary, the body and tail parts contain less complex organs (the intestine), which may allow higher flexibility.

When we hunt for epidermal cells that became deformed at the same time, we observed that the head, body, and tail behaved mechanically as partially independent entities. This local deformation pattern suggests that the activation of muscles may be different underneath the epidermal cell, in other words, embryonic muscles along the body contract sequentially.

To understand how muscle activity triggers the epidermal cell shape change and to characterize the muscle contraction pattern, we use the Ca^{2+} sensor to indicate muscle activations. We analyzed five muscle cells from the head part to the body part of the embryo (figure 5B). We discovered that two muscle cells, localized near the lateral epidermal cell H2, undergo a longer and stronger activation pulse compared to their neighboring muscle cells that are near H1 and V1-V2 cells. Moreover, these two muscle

cells start activation earlier than their neighboring muscle cells too. Altogether, we determined that the muscle cells near H2 lateral epidermis are the pacemaker for embryo muscle activity. Hence it is likely that these cells are set aside through some local signaling event which could involve either a calcium signal, as observed during defecation [17] or oocyte ovulation [18], or a morphogen such as Notch and EGF which are required between the 1.3- and 1.5-fold stages to specify cell fates in the excretory system[19]. To test if any of these signals is important, both genetic methods and laser ablation experiments could be used in future studies.

MATERIALS AND METHODS

Animal strains, conditions of maintenance

C. elegans strains used in this study are listed in Table S1. Animals were maintained at 20°C on Nematode Growth Medium agar plates as described in [20]. N2 Bristol was used as the wild-type in this study.

RNAi feeding for SPIM microscopy

We used RNAi feeding to inactivate *unc-112* for muscle defective mutant during SPIM imaging. *unc-112* RNAi was from the Ahringer RNAi library [21, 22]. Wild-type L4 larvae were fed for 48 hours before transferring them to a fresh RNAi plate. 24 hours later, the embryos between 1.5-2 fold were selected to do the imaging. In parallel, the terminal phenotype of embryos was scored to ensure RNAi efficiency and found to generate 95% two-fold arrested embryos.

SPIM imaging

In this paper, the Single Plane Illustration Microscopy imaging was done using a homemade microscope built up by Dr. N. Maghelli and Dr. L. Royer in MPI-CBG, Dresden [12]. The objective used for imaging was 40×. To start the imaging, embryos younger than 1.5 fold were selected. The imaging began with a pre-acquisition time-lapse with 2-minute time interval until the embryos started to actively twitch or rotate, at which point the pre-acquisition was stopped and the acquisition started. During pre-acquisition and acquisition, the embryos whose lateral epidermal cells were parallel or nearly parallel to the camera were selected for imaging. Embryos were scanned from one side to the other side, with a focal plane depth of 0.5μm.

For one-colored movies, embryos carried the junction marker *mcIs46 [dlg-1::RFP, unc-119(+)]*; the exposure time for both pre-acquisition and acquisition was from 3000μs to 10000μs and the acquisition process was continuous imaging.

For two-colored movies, embryos carried the junction marker *mcIs46 [dlg-1::RFP, unc-119(+)]* and muscle nucleus marker *st10089 [hlh-1(3,3kb)::his24::mCherry+unc-119(+)]*; the exposure time for both pre-acquisition and acquisition was 5000μs and the acquisition was with 2 second time interval.

For both one-colored and two-colored movies, control movies were made overnight after acquisition with a 2-minute time interval and the same Z-step depth and exposure time to make sure the imaging protocol was not phototoxic for proper embryonic development process. All control embryos hatched after acquisition, suggesting the imaging protocol was not phototoxic for embryos to develop properly.

Points Of Interests (POI) tracking in SPIM movies

To calculate the changes of cell aspects, the vertices of lateral epidermal cells were tracked in Fiji after the SPIM movies were made. For wild type and *let-502* embryos, the tracking was finished manually and the original positions of vertices were saved.

For *unc-112* embryos, the tracking of POI was done by a Fiji plugin, CE Time lapse analysis of POI, created by Dr. Julien Pontabry. The surrounding background of the initial POI was compared in the following frames to find the potential point with exact or similar surrounding background to define the position of POI in the following frames.

After gathering the original positions of all POIs, we used shape inserter in MATLAB to circle the position of each POI back on the SPIM movies to check if the original tracking of the POI is correct.

Cell aspects and total lateral epidermal cell length calculation

After confirming the POI position tracking, we calculated the apical area and the perimeter of the cell by a pre-existing MATLAB function.

function[geom, iner, cpmo] = polygeom(x, y).

Function website:

https://fr.mathworks.com/matlabcentral/fileexchange/319-polygeom-m

The length of the cell was calculated as the total length from the mid-point of the two most anterior vertices passing the central position of all the cell vertices to the mid-point of the two most posterior vertices of the same lateral epidermal cells. The positions of these three points were calculated in MATLAB by using the original positions of the vertices of a lateral epidermis. The length was calculated by

$$dist = sqrt[(X_1\text{-}X_2)^2+(Y_1\text{-}Y_2)^2]+sqrt[(X_2\text{-}X_3)^2+(Y_2\text{-}Y_3)^2] \quad \text{(Equation 1)}$$

The total length of all lateral epidermis is the sum of the length of each lateral epidermal cells.

Calcium imaging and analyzing

Calcium sensor imaging to report on muscle activity was conducted by Spinning Disc microscopy, using a 100/N.A. 1.4 oil-immersion objective. Embryos expressing calcium sensor (*goeIs3 [pmyo-3::GCamP3.35::unc-54-3′utr, unc-119(+)]V*) [23] between 1.7- to 2-fold were selected for imaging. Half of the embryo was scanned with eleven

focal planes with a Z-step size of 1μm and a time interval of 0.89 seconds.

To analyse the images after imaging, time series were first corrected for bleaching by using the standard plugin of Fiji 'Bleach Correction' with the 'exponential fit' option. Starting from muscles located closer to the H1 epidermal cell, the first five cells from anterior to posterior were labeled as cells 1, 2, 3, 4 and 5 and they were selected for further analysis (see Figure 6a). Selected muscle cells were restricted to the first five cells because the posterior cells were not always visible and clear. The same logic of selection was applied both for the dorsal and the ventral sides of the embryo.

Along one line of muscles, the cells often touch each other and they change aspect and intensity across time. Therefore, by using a custom MATLAB graphical interface, cell contours were segmented manually in order to avoid segmentation artifacts. With the same MATLAB script, cell contours were used as a mask to measure the fluorescence intensity (I) of the segmented cells and to record the positions or their centers of mass in each frame. Finally, for each of the 5 cells, a temporal trace of the calcium content during one of more pulses was extracted. During a calcium pulse, more than one cells in a muscle row showed a progressive signal increase up to a peak and a subsequent decrease to a level close to the basal one. From the temporal traces, the following observables were extracted: 1) delay in pulsing; 2) relative pulse duration; 3) peak of intensity. The movies were acquired with a time interval between frames of 0.89 seconds; to have a more detailed sampling of the temporal behavior of the traces we interpolated them with a step of 0.05 seconds.

1). Delay in pulsing and pulse duration

In order to estimate the delay in pulsing and the duration of pulses, the following normalized intensity was introduced:

Normalized intensity = $(I_t - I_{initial})/\max(I_t - I_{initial})$ (Equation 2)

where I_t is the intensity in each frame and $I_{initial}$ is the intensity in the first frame. The time when the normalized intensity first reached 0.3 was considered as the beginning of a pulse. The time when the normalized intensity decreased to 0.3, after its maximum peak was considered as the termination time of the pulse. Time in-between theses two frames was the duration of a pulse. The delay in pulsing for each calcium pulse event was estimated as the difference in initiation time between the first pulsing cell and the remaining four cells. The relative duration was computed as the duration divided by the maximal duration among the five analyzed cells.

2). Peak of intensity

The frame in which the normalized intensity reached 1 was considered as the time of the peak of pulses. To compare the peak intensity of pulses with respect to the basal expression among all five muscle cells, the relative intensity of pulses of each frame was defined as follows:

Relative intensity of pulses = $(I_t - I_{min})/I_{min}$ (Equation 3)

where I_{min} was the minimum intensity of all five muscle cells along time.

Table S1. Strains used in this study

Strain	Genotype
N2	Wild type
ML1652	*mcIs46 [dlg-1::RFP, unc-119(ed3)]*
ML1840	*let-502(sb118ts) ; mcIs46*
HBR4	*goeIs3 [pmyo-3::GCamP3.35::unc-54C3utr, unc-119(+)]V*
ML2705	*mc103 X; goeIs3 V*

REFERENCE

1. Ingber, D.E., *Mechanobiology and diseases of mechanotransduction.* Ann Med, 2003. 35(8): p. 564-77.

2. Collinet, C., et al., *Local and tissue-scale forces drive oriented junction growth during tissue extension.* Nat Cell Biol, 2015. 17(10): p. 1247-58.

3. Levayer, R., A. Pelissier-Monier, and T. Lecuit, *Spatial regulation of Dia and Myosin-II by RhoGEF2 controls initiation of E-cadherin endocytosis during epithelial morphogenesis.* Nat Cell Biol, 2011. 13(5): p. 529-40.

4. Chisholm, A.D. and J. Hardin, *Epidermal morphogenesis.* WormBook, 2005: p. 1-22.

5. Diogon, M., et al., *The RhoGAP RGA-2 and LET-502/ROCK achieve a balance of actomyosin-dependent forces in C. elegans epidermis to control morphogenesis.* Development, 2007. 134(13): p. 2469-79.

6. Wissmann, A., et al., *Caenorhabditis elegans LET-502 is related to Rho-binding kinases and human myotonic dystrophy kinase and interacts genetically with a homolog of the regulatory subunit of smooth muscle myosin phosphatase to affect cell shape.* Genes Dev, 1997. 11(4): p. 409-22.

7. Lee, R.Y., et al., *Mutations in the alpha1 subunit of an L-type voltage-activated Ca2+ channel cause myotonia in Caenorhabditis elegans.* EMBO J, 1997. 16(20): p. 6066-76.

8. Zhang, H., et al., *A tension-induced mechanotransduction pathway promotes epithelial morphogenesis.* Nature, 2011. 471(7336): p. 99-103.

9. Vuong-Brender, T.T., et al., *The interplay of stiffness and force anisotropies drives embryo elongation.* Elife, 2017. 6.

10. Weber, M. and J. Huisken, *Light sheet microscopy for real-time developmental biology.* Curr Opin Genet Dev, 2011. 21(5): p. 566-72.

11. Hockendorf, B., T. Thumberger, and J. Wittbrodt, *Quantitative analysis of embryogenesis: a perspective for light sheet microscopy.* Dev Cell, 2012. 23(6): p. 1111-20.

12. Royer, L.A., et al., *ClearVolume: open-source live 3D visualization for light-sheet microscopy.* Nat Methods, 2015. 12(6): p. 480-1.

13. Norman, K.R. and D.G. Moerman, *Alpha spectrin is essential for morphogenesis and body wall muscle formation in Caenorhabditis elegans.* J Cell Biol, 2002.

157(4): p. 665-77.

14. Quintin, S., et al., *Non-centrosomal epidermal microtubules act in parallel to LET-502/ROCK to promote C. elegans elongation.* Development, 2016. 143(1): p. 160-73.

15. Mango, S.E., *The C. elegans pharynx: a model for organogenesis.* WormBook, 2007: p. 1-26.

16. White, J.G., et al., *The structure of the nervous system of the nematode Caenorhabditis elegans.* Philos Trans R Soc Lond B Biol Sci, 1986. 314(1165): p. 1-340.

17. Dal Santo, P., et al., *The inositol trisphosphate receptor regulates a 50-second behavioral rhythm in C. elegans.* Cell, 1999. 98(6): p. 757-67.

18. Samuel, A.D., V.N. Murthy, and M.O. Hengartner, *Calcium dynamics during fertilization in C. elegans.* BMC Dev Biol, 2001. 1: p. 8.

19. Abdus-Saboor, I., et al., *Notch and Ras promote sequential steps of excretory tube development in C. elegan*s. Development, 2011. 138(16): p. 3545-55.

20. Brenner, S., *The genetics of Caenorhabditis elegans.* Genetics, 1974. 77(1): p. 71-94.

21. Fire, A., et al., *Potent and specific genetic interference by double-stranded RNA in Caenorhabditis elegans.* Nature, 1998. 391(6669): p. 806-11.

22. Kamath, R.S. and J. Ahringer, *Genome-wide RNAi screening in Caenorhabditis elegans.* Methods, 2003. 30(4): p. 313-21.

23. Schwarz, J., J.P. Spies, and H. Bringmann, *Reduced muscle contraction and a relaxed posture during sleep-like Lethargus.* Worm, 2012. 1(1): p. 12-4.

Figure legends

Figure 1. Embryo elongation process and main parameters of measurement.

(A-C) Embryo elongation scheme of wild type (A), actomyosin hypocontraction mutants (*let-502*) (B) and muscle defective mutants (*unc-112*) (C). Blue cells, dorsal epidermal cells; pink cells, ventral epidermal cells; yellow cells, lateral epidermal cells. Black lines, apical junctions. (D) Color-coded lateral epidermis outlines. (E) Midline of the lateral epidermis. (F) Local cell deformation of certain lateral epidermal cells. Red star, H2 lateral epidermal cell; yellow star, V1 lateral epidermal cell; blue star, V2 lateral epidermal cell. Junctions are labeled with *dlg-1::RFP*. Scale bar = 10μm (D-F).

Figure 2. Active rotations are crucial for embryo elongation.

(A) One example of embryo twitching at the 1.7-fold. Yellow circle, embryo twitching at V1 lateral epidermal cell. (B) One example of rotation of embryo at 1.9-fold. Yellow line, extended lateral epidermal cells during a rotation. (C) Total length of the lateral epidermis along time for one particular wild-type embryo. Orange line indicates the growth of the embryo. (D) Corrected length of the lateral epidermis along time from (C). Yellow lines, upper and lower thresholds for outward and inward rotation, respectively. (E) Skeletonized rotation status of (C). Number "1" represents the outward rotation, as shown in (C′); number "-1" represents the inward rotation, as shown in (C″); number "0" represents the relaxed position. (F) Skeletonized rotation status of one *let-502* mutant. (G). Skeletonized rotation status of one muscle

defective embryo.

Figure 3. Muscle activity results in lateral epidermis deformations.

(A) Perimeter changes along time of H1, V1 and V5 lateral epidermal cells in wild-type, *let-502* and muscle-defective embryos. Red arrowhead, perimeter of extended V1 cell during outward rotation, as shown in (A′). Yellow arrowhead, perimeter of compressed V1 cell during inward rotation, as shown in (A″). (B) Cell anterior-posterior length change amplitude along time of H1, V1 and V5 lateral epidermal cells in wild-type, *let-502* and muscle-defective embryos. (C) Maximum cell anterior-posterior length change in absolute value of H1, V1 and V5 epidermal cells in wild-type, *let-502* and muscle-defective embryos. Scale bar = 10μm.

Figure 4. Local movements divide the embryo into semi-independent mechanical subgroups.

(A) Comparison of cell length between the V1 cell and other lateral epidermal cells. Orange curve, V1 epidermal cell anterior-posterior length. Blue curves, H1, V2 and V5 epidermal cell anterior-posterior length. (B) Cross correlation of the AP length comparison between nine lateral epidermal cells and H1, V1 and V5 epidermal cells, respectively in one embryo. (C) Summary of cross-correlation results of cell length between lateral epidermal cells and H1, V1, and V5 epidermal cells, in wild type, *let-502* mutants, and muscle defective mutants. Yellow line, thresholds at 0.6. (D) The three semi-independent groups of wild-type embryo. Blue circle, the head group; orange circle, the body group; green circle, the tail group. (E) The three

semi-independent groups are lost in *let-502* mutant (symbolized by a cross). (F) The three semi-independent groups are lost in muscle defective mutant (symbolized by a cross).

Figure 5. The pattern of muscle activation.

(A) One example of strong contraction of the V1 epidermal cell. Yellow arrowheads, V1 epidermal cells. (B) Embryo expressing the *pmyo-3::gcamp3.35::unc-54-3′utr* (green) and *dlg-1::RFP* (red) markers. Muscle cells numbered 1-5 and 1′-5′ were easier to track. (C) Relative duration of muscle activation pulses in five muscle cells in either dorsal or ventral side of embryos. (D) Relative intensity of muscle activation pulses in five muscle cells in either dorsal or ventral side of embryos. (E) Delay of the activation pulses among five muscle cells in either dorsal or ventral side of embryos.

Figure S1. Apical area, perimeter and cell length changes of lateral epidermal cell in a wild-type embryo.

(A) Apical area, perimeter and cell length changes along time of H1, V1 and V5 lateral epidermal cells in a wild-type embryo. Red arrowhead, apical area of an extended V1 lateral epidermal cell during outward rotation, as shown in (A′); yellow arrowhead, apical area of a compressed V1 cell during inward rotation, as shown in (A″). Scale bar = 10μm.

Movie legends

Movie 1. Wild-type embryo twitches at 1.7-fold.

Z-projection of four-dimensional time-lapse (xyzt) of a wild-type embryo expressing DLG-1::RFP. Images are average intensity projections of 36 z planes acquired in the RFP channel, separated by 0.5μm steps. 5 stacks were acquired every 2.2s during 220 sec (total movie time). Movie is played in 15 frames per second. Scale bar = 5μm. This movie is a typical example showing how wild-type embryos twitch between 1.5- to 1.7-fold.

Movie 2. Wild-type embryo rotates at 1.9-fold.

Z-projection of four-dimensional time-lapse (xyzt) of a wild-type embryo expressing DLG-1::RFP. Images are average intensity projections of 36 z planes acquired in the RFP channel, separated by 0.5μm steps. 5 stacks were acquired every 2.2s during 220 sec (total movie time). Movie is played in 15 frames per second. Scale bar = 5μm. This movie is a typical example showing how wild-type embryos rotate after 1.7-fold.

Movie 3. *let-502* embryo movements.

Z-projection of four-dimensional time-lapse (xyzt) of a *let-502* embryo expressing DLG-1::RFP. Images are average intensity projections of 36 z planes acquired in the RFP channel, separated by 0.5μm steps. 5 stacks were acquired every 2s during 400 sec (total movie time). Movie is played in 15 frames per second. Scale bar = 5μm.

This movie is a typical example showing the movements of 1.3-fold *let-502* embryos (equivalent to 2-fold wild-type embryo).

Movie 4. *unc-112* embryo movements.

Z-projection of four-dimensional time-lapse (xyzt) of *unc-112* embryo expressing DLG-1::RFP. Images are average intensity projections of 46 z planes acquired in the RFP channel, separated by 0.5μm steps. 5 stacks were acquired every 2.15s during 215 sec (total movie time). Movie is played in 15 frames per second. Scale bar = 5μm. This movie is a typical example showing the movements of 1.9-fold *unc-112* embryo.

Movie 5. Muscle activations underneath the epidermis of wild-type *C. elegans* embryo.

Z-projection of five-dimensional time-lapse (xyztc) of a wild-type embryo expressing DLG-1::RFP and the calcium sensor GCaMP3.35. Images are average intensity projections of 2 z planes acquired in the RFP and GFP channels, separated by 1 μm steps. Stacks were acquired every 13.3s during 119 sec (total movie time). Movie is played in 15 frames per second. Scale bar = 5μm. This movie is used to determine the positions of selected muscle cells relative to lateral epidermal cells.

Figure 1:

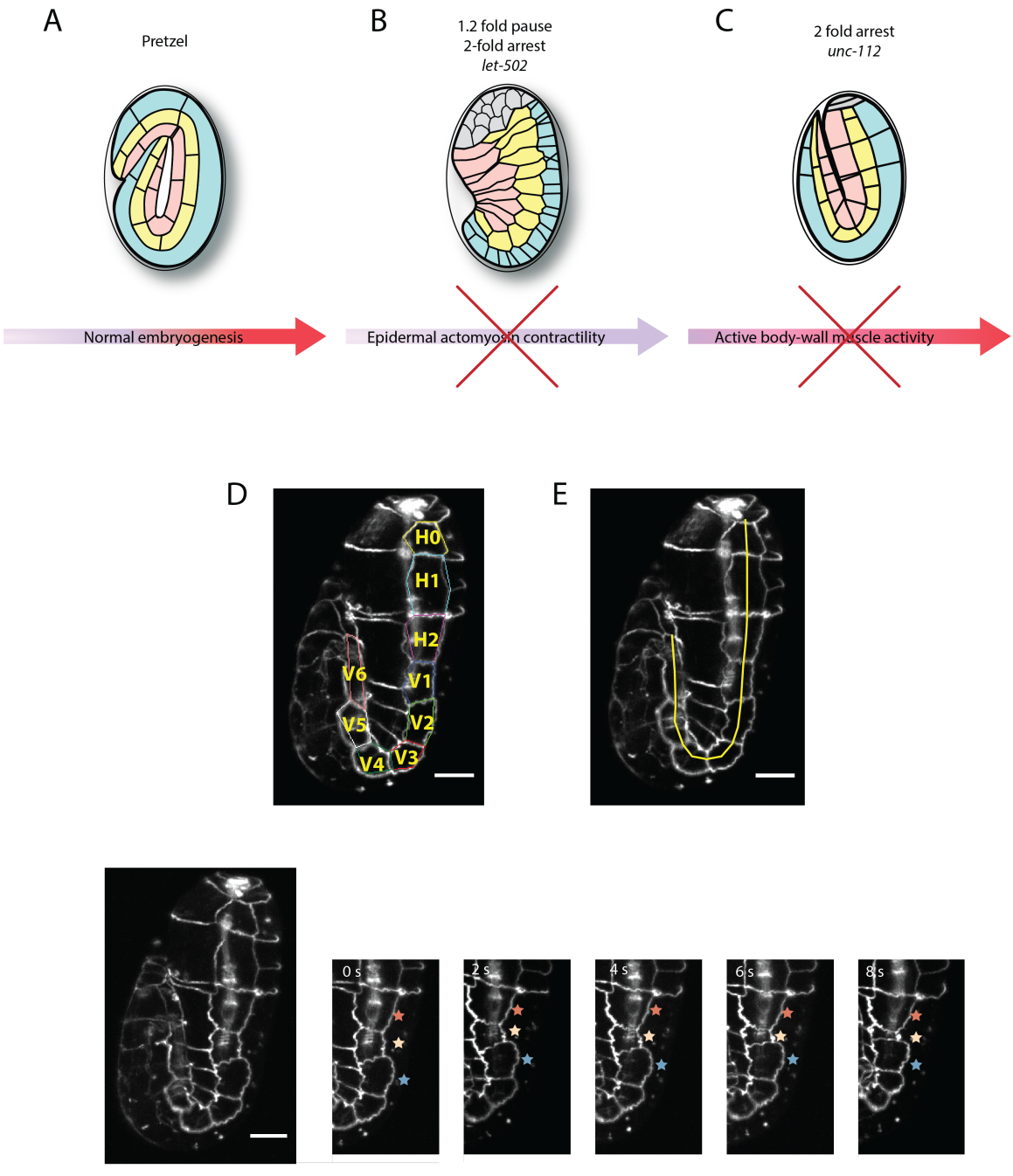
A
Pretzel
B
1.2 fold pause
2-fold arrest
let-502
C
2 fold arrest
unc-112
Normal embryogenesis
Epidermal actomyosin contractility
Active body-wall muscle activity
D
H0
H1
H2
V6
V1
V5
V2
V4
V3
E
0 s
2 s
4 s
6 s
8 s

Figure 2:

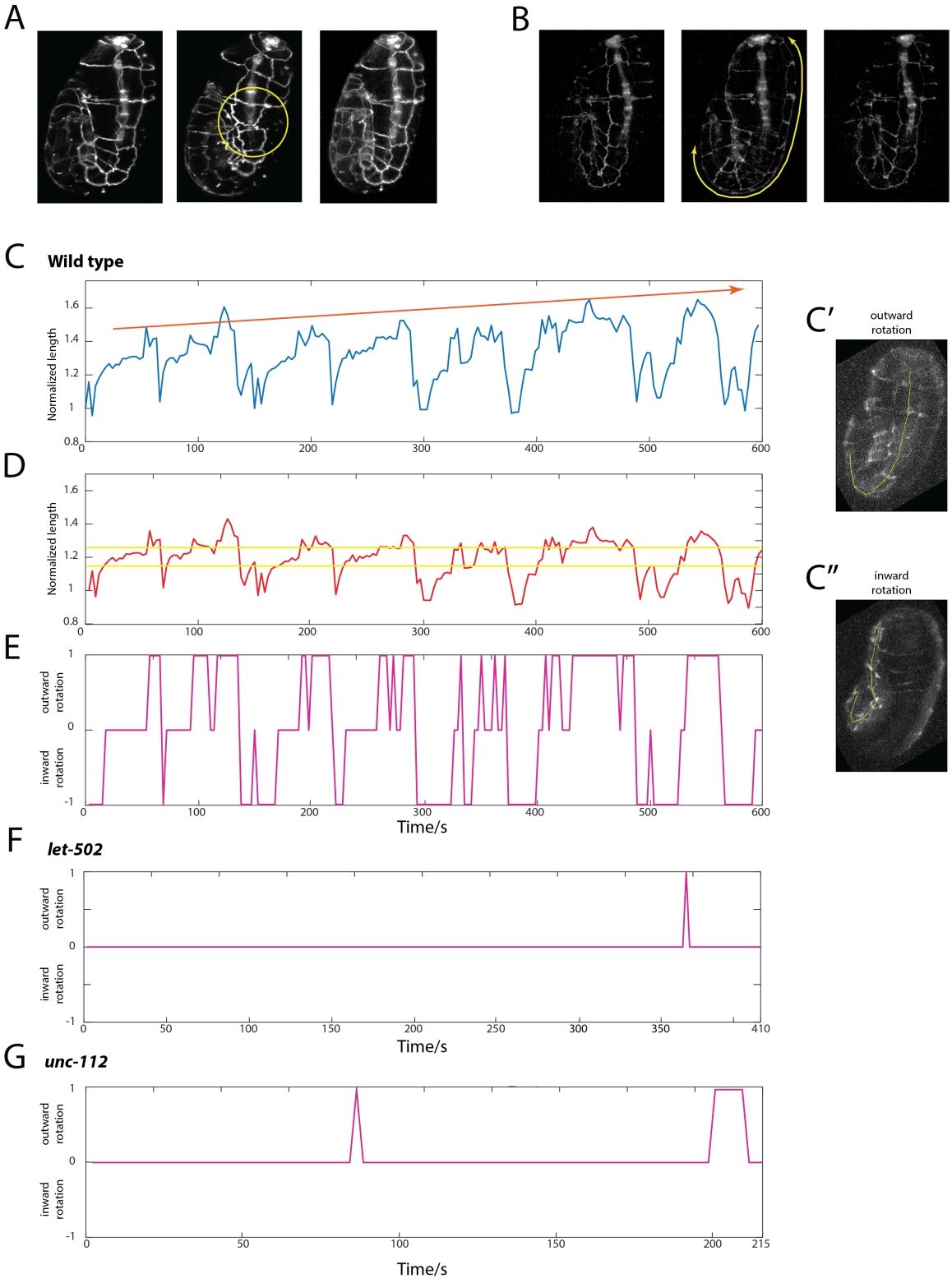
A
B
C
Wild type
Normalized length
C′
outward rotation
C″
inward rotation
D
Normalized length
E
outward rotation
inward rotation
Time/s
F
let-502
outward rotation
inward rotation
Time/s
G
unc-112
outward rotation
inward rotation
Time/s

Figure 3:

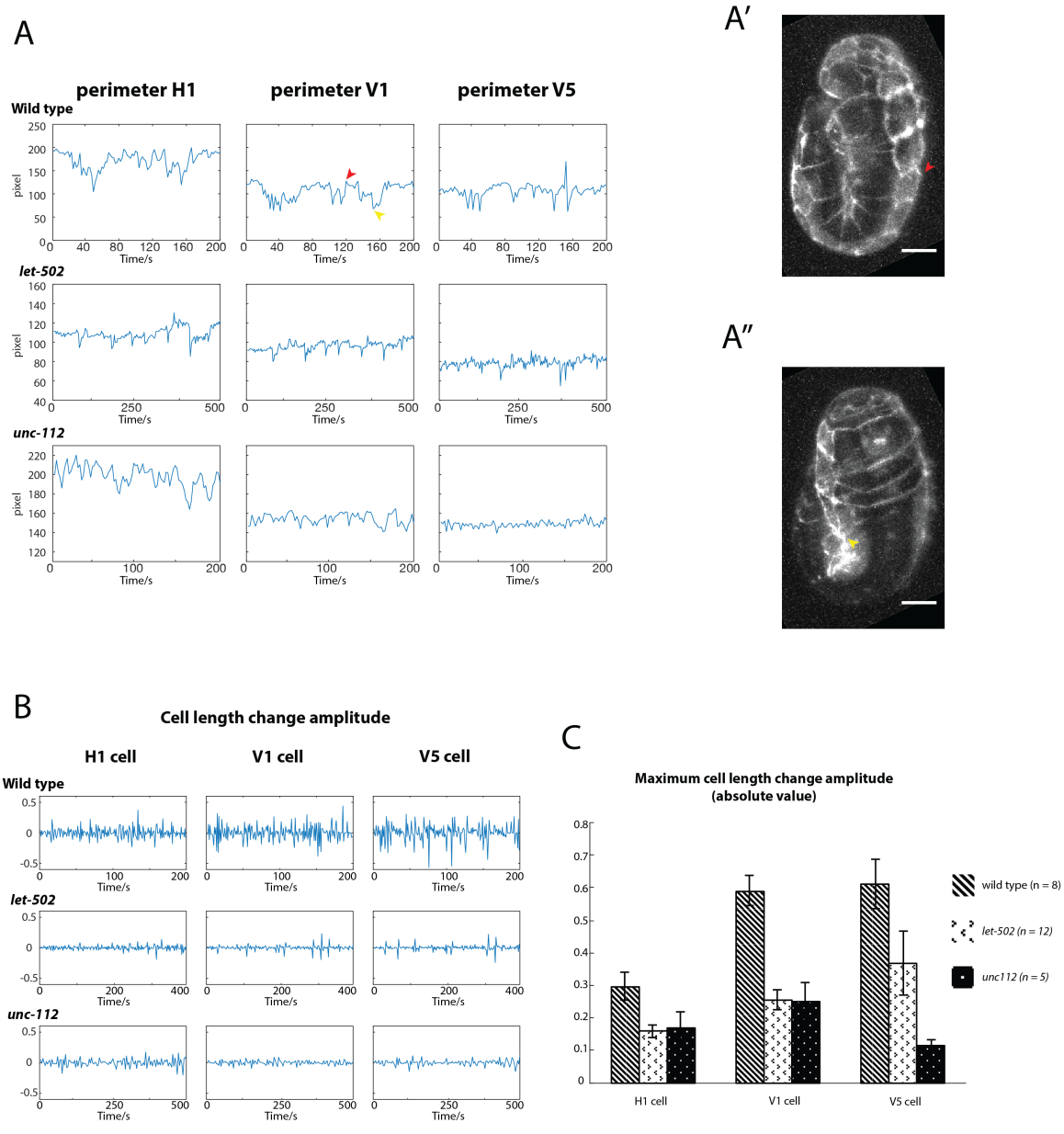
A
perimeter H1
perimeter V1
perimeter V5
Wild type
let-502
unc-112
pixel
Time/s
A′
A″
B
Cell length change amplitude
H1 cell
V1 cell
V5 cell
Wild type
let-502
unc-112
Time/s
C
Maximum cell length change amplitude
(absolute value)
wild type (n = 8)
let-502 (n = 12)
unc112 (n = 5)
H1 cell
V1 cell
V5 cell

Figure 4:

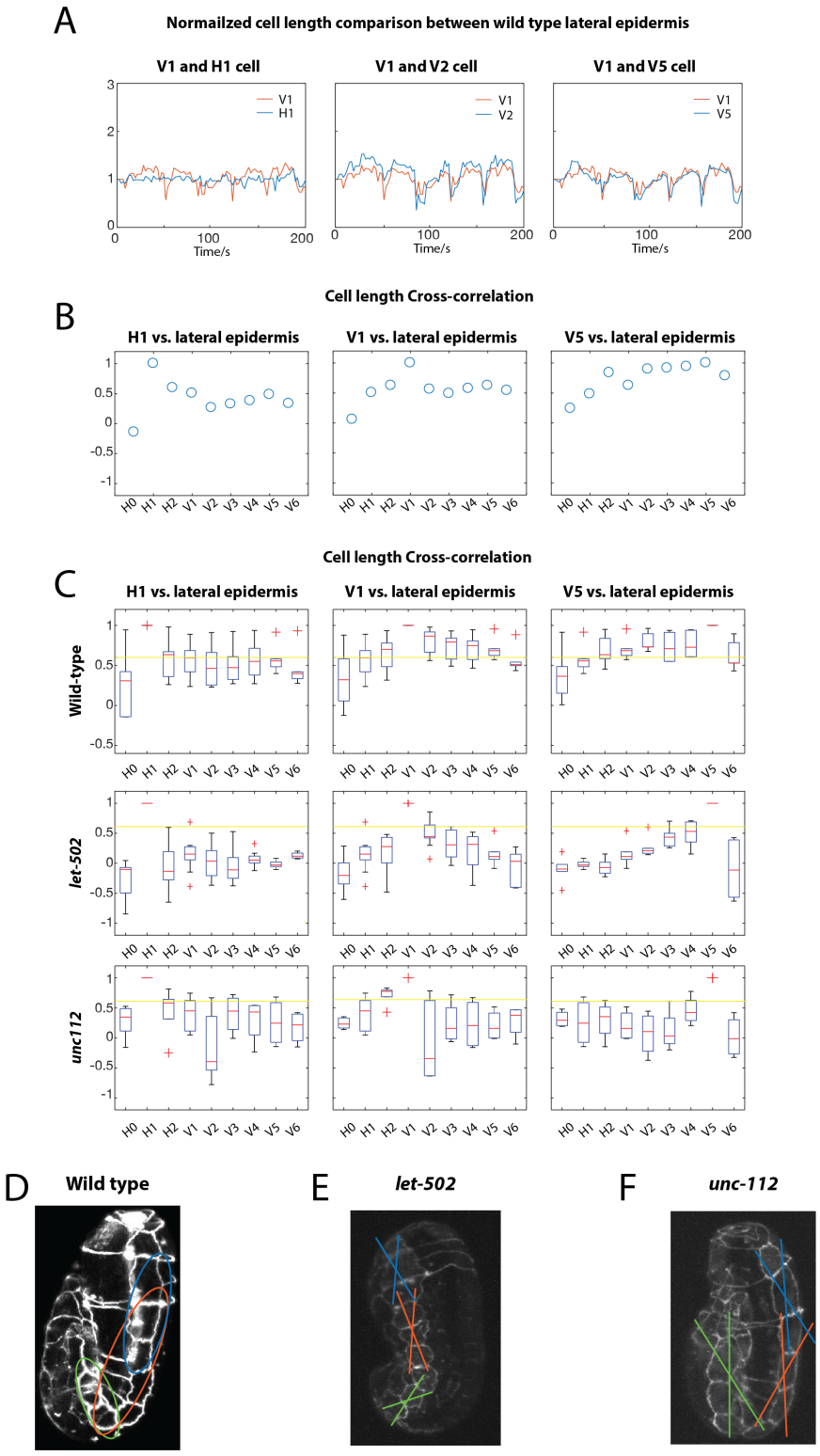
A
Normailzed cell length comparison between wild type lateral epidermis
V1 and H1 cell
V1 and V2 cell
V1 and V5 cell
V1
H1
V2
V5
Time/s
B
Cell length Cross-correlation
H1 vs. lateral epidermis
V1 vs. lateral epidermis
V5 vs. lateral epidermis
C
Cell length Cross-correlation
H1 vs. lateral epidermis
V1 vs. lateral epidermis
V5 vs. lateral epidermis
Wild-type
let-502
unc112
H0 H1 H2 V1 V2 V3 V4 V5 V6
D
Wild type
E
let-502
F
unc-112

Figure 5:

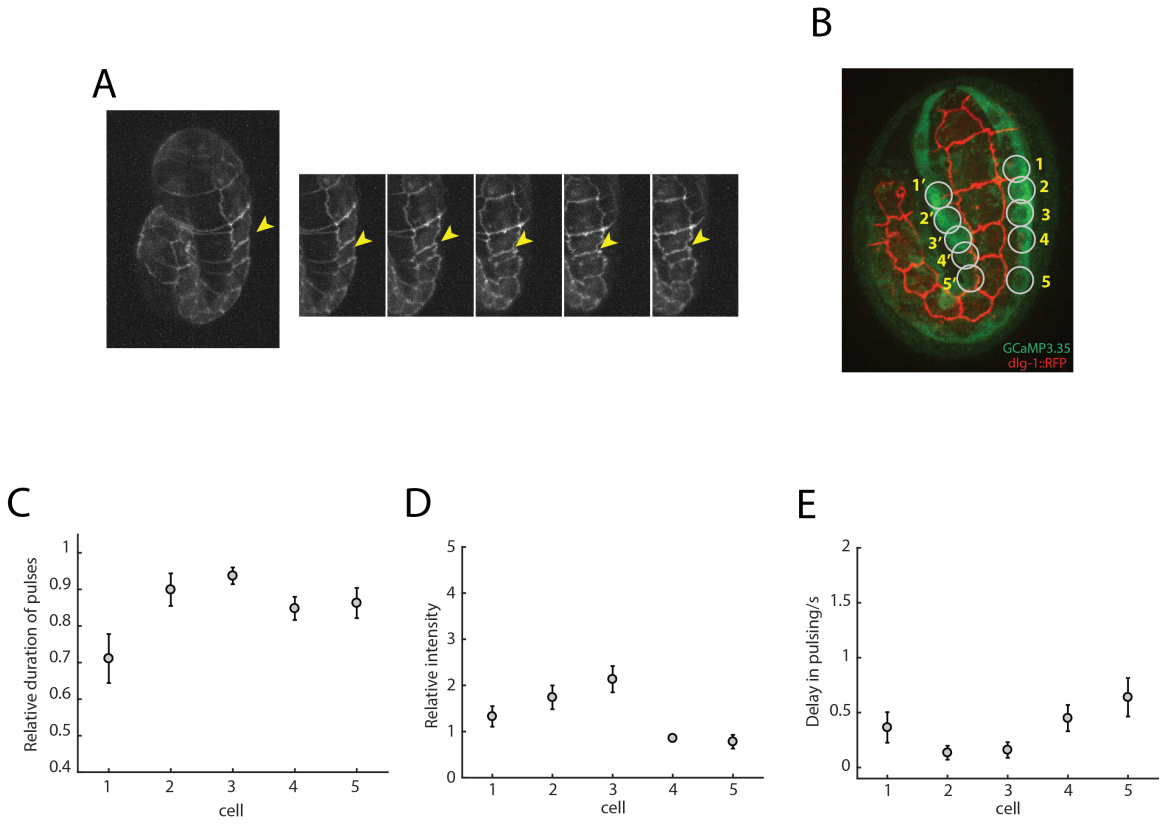
A
B
1′
2′
3′
4′
5′
1
2
3
4
5
GCaMP3.35
dlg-1::RFP
C
Relative duration of pulses
cell
D
Relative intensity
cell
E
Delay in pulsing/s
cell

Tables:

Table 1

Summary of total rotation time for three different phenotypes

Genotype	Developing status	Rotation time	Rotation description
Wild type	Elongate normally	70% (n = 8)	Strong rotations
let-502	Elongate slowly	1% (n = 5)	Scarcely any rotation
unc112	Elongation stops at 2-fold	3% (n = 12)	Scarcely any rotation

Table 2

Maximum cell length change amplitude (absolute value)

Genotype	H0	H1	H2	V1	V2	V3	V4	V5	V6	Head	Body	Tail
Wild type	0.3	0.3	0.38	0.59	0.65	0.73	0.79	0.61	0.54	0.33	0.66	0.65
let-502	0.32	0.16	0.15	0.26	0.25	0.33	0.36	0.37	0.33	0.21	0.29	0.35
unc112	0.22	0.17	0.17	0.25	0.2	0.16	0.12	0.11	0.17	0.19	0.20	0.13

Figure S1:

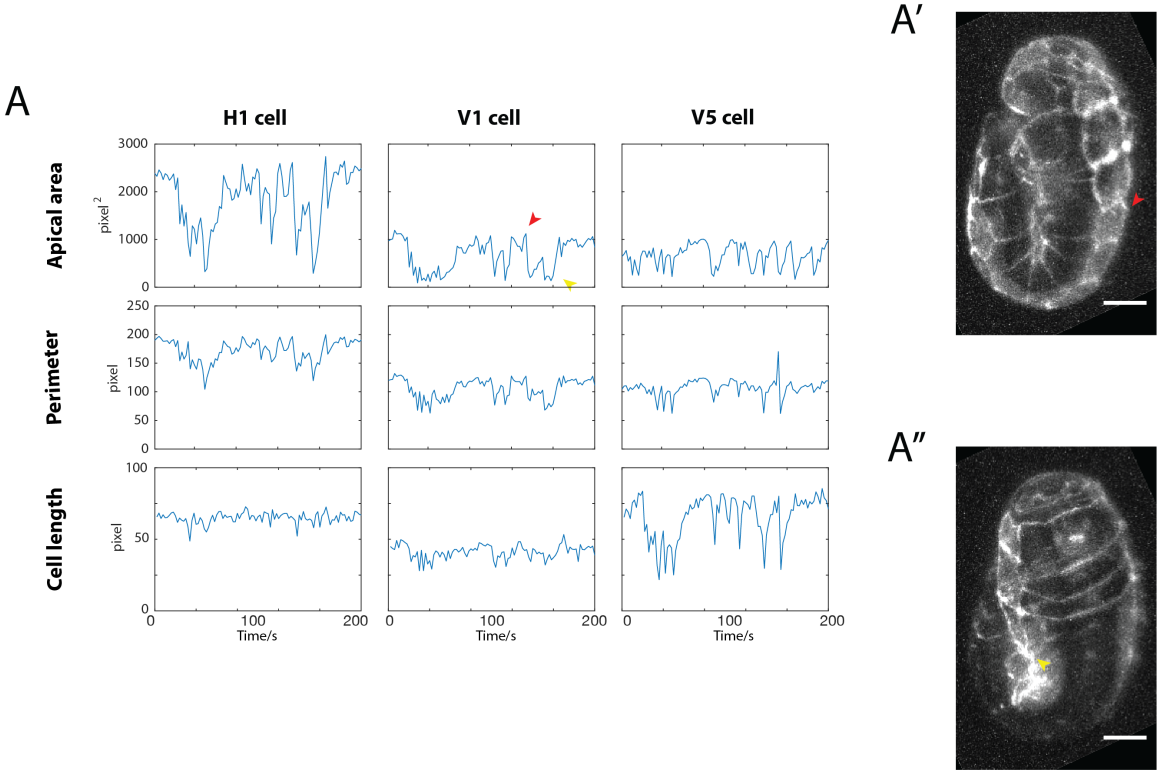
A
H1 cell
V1 cell
V5 cell
Apical area
Perimeter
Cell length
pixel 2
pixel
pixel
3000
2000
1000
0
250
200
150
100
50
0
100
50
0
0
100
200
Time/s
A′
A″

Chapter 5

Result Part II: Repeated muscle-induced mechanical stimuli polarize junction lengthening in a ratchet morphogenetic process

Repeated muscle-induced mechanical stimuli polarize junction lengthening in a ratchet morphogenetic process

X. Yang[1,2], T. Ferraro[1], J. Pontabry[2,¶], N. Maghelli[3], L. Royer[3], S. Grill[3,§], G. Myers[3] and M. Labouesse[1,2,*]

1. Laboratoire de Biologie du Développement - Institut de Biologie Paris Seine (LBD - IBPS), CNRS (UMR7622), INSERM (U1156), Sorbonne Universités, UPMC, 7-9 quai Saint Bernard 75005 Paris, France.

2. Development and stem cell program, IGBMC, CNRS (UMR7104), INSERM (U964), Universit de Strasbourg, 1 rue Laurent Fries, BP10142, 67400 Illkirch, France

3. Max Planck Institute of Molecular Cell Biology and Genetics, Dresden, Germany

¶. Current address: Institute of epigenetics and stem cells, HelmholtzZentrum München, Germany.

§. Current address: Technische Universität Dresden, Biotechnology Center, Tatzberg 47/49, 01307 Dresden, Germany

*. Corresponding author: michel.labouesse@upmc.fr

SUMMARY

Epithelial cell shape changes can orchestrate tissue morphogenetic processes. Forces driving this process can either originate from the intracellular non-muscle Myosin-II contractility or from the extracellular mechanical stimuli. For example, the late elongation of *C. elegans* embryos largely relies on muscle activity from underneath epidermal cells. However, the detailed molecular mechanisms through which muscle activity promotes the elongation process remains to be fully understood. Here, using fast-3D imaging we show that muscles located on opposite side of the embryo contract alternatively, triggering the embryo to bend and extend repeatedly. As a consequence, adherens junctions get stretched along the anterior/posterior (A/P) direction during embryo rotations. Laser ablation experiments showed that A/P oriented junctions are under higher tension when they are stretched due to muscle activity. We propose a model through which muscle activity repeatedly exerts tension on adherens junctions along A/P direction and stimulates the insertion of junction material into these junctions during late elongation. Our preliminary results from single molecule imaging showed that more junction material E-cadherin fuses with A/P oriented junctions when there is high tension on these junctions. Our findings suggest that muscle activity could be the key player for the junction remodeling in a ratchet mode during *C. elegans* later elongation, to ensure cell connections. Moreover, our discovery suggests a novel source of tissue asymmetry to establish planar polarity during tissue morphogenesis.

5.1 Introduction

During animal morphogenesis, the establishment of planar cell polarity (PCP) is a key process that organizes tissues across long distances. Loss of the proper orientation of subcellular structures and cell arrangement in tissues can lead to severe birth defects [1-3]. For example, failure of convergent extension in animal models will cause neural tube defects (NTDs). NTD is a common human birth defect and mutations in core PCP genes have been identified in NTDs patients [2, 3]. The establishment of core planar cell polarity relies on cell-cell communication, components of the Wnt and the Ft-Ds-Fj signaling pathways, and cytoskeleton-dependent transport [4]. More recently, it has become apparent that mechanical forces can influence the development of PCP asymmetry [4]. They can do so by stabilizing PCP signaling components, altering their recycling or modifying tension [4]. Although many of the PCP effectors seem to be context-specific, the mechanisms through which the planar polarity is established in multifaceted tissues consisting of multiple tissue layers and multiple cell types need to be further studied [4, 5].

One possible consequence of PCP during the development process is to promote the elongation of cells and tissues along a specific direction. During cell polarized elongation, for example, subcellular structures must also go through certain remodeling processes, corresponding to the polarized lengthening of the cells, to preserve the stable cell-cell contacts and maintain tissue integrity. One important cellular structure that undergoes such remodeling during tissue elongation is the adherens

junction.

The apicolateral cell-cell junction is a preserved subcellular structure that exists in both invertebrate and vertebrate animals. In *C. elegans*, apical junctions (known as the CeAJ) comprise two molecular complexes, the cadherin-catenin complex and the DLG-1/AJM-1 complex [5], which mediate cell-cell adhesion, anchor the cytoskeleton and helps establish epithelial polarity [5].

During *C. elegans* embryonic elongation, epithelial cells undergo shape changes and elongate along the anterior/posterior (A/P) direction. To maintain cell-cell adhesion, the CeAJs also have to undergo planar polarized remodeling, which includes the shrinkage along the dorsal/ventral (D/V) direction and lengthening along the A/P direction. However, the driving force for apical junction remodeling is not clear yet for *C. elegans* embryos. In *Drosophila* germband extension, it has been suggested that non-muscle myosin-II contractility contributes to both junction shrinkage along the D/V direction and the junction lengthening along the A/P direction during cell intercalation [6, 7]. However, the non-muscle myosin-II is not distributed in a polarized way along the apical junction [8], leaving the mechanism for apical junction remodeling during *C. elegans* morphogenesis unknown.

The elongation process of *C. elegans* embryo lasts about 4 hours, during which the embryo develops from a lima-bean shape to a characterized-worm shape, which is ready to hatch. This process can be divided into early and late elongation phases based on the main driving force. During early elongation (until the two-fold stage), embryos elongate due to the circumferential tension created by epidermal actomyosin.

During that stage, the lateral epidermal cells mainly shrink along the D/V axis and keep a constant perimeter. Beyond the 2-fold stage, muscles located beneath the dorsal and ventral epidermal cells become essential. During that stage, the lateral epidermal cells keep lengthening along the A/P direction (figure 1A).

In this project, I focused on the junction polarized lengthening after muscles become active. The main goal of this work was to discover the driving force that is responsible for the polarized lengthening of apical junctions in the lateral epidermis and to unravel the molecular mechanism through which new junction components are added to the lengthening junction. To accomplish this goal, I first used fast 3D imaging to study the growth pattern and muscle activation pattern of *C. elegans* embryos around 1.7-fold after muscle contraction. I discovered that embryos grow under repeated stimulations from muscle activity. Then I examined the status of the junction during the rotation of the embryo and then measured the tension on junction by using multi-photon laser ablation. The results showed that junctions were under higher tension when the embryo rotated outward. Based on a paper from Michael Sheetz, which suggests that higher membrane tension stimulates the exocytosis [9], we came up with the hypothesis that more junction components might be added to junctions that are under higher tension, due to the outward rotations induced by muscle activity. To prove this hypothesis, I created a knock-in strain, in which E-cadherin is linked to a modified GFP protein to monitors the fusion of E-cad into the junction. The last part of this project is still ongoing and I will present preliminary data here.

5.2 *C. elegans* embryo growth under repeated muscle-induced stimulations

During the second half of elongation, embryos start to twitch actively and to rotate quickly under the muscle activity. The movements of embryos are faster than the possible time resolution of traditional confocal microscopes such as spinning disk microscopes. To better study the pattern of junction lengthening during embryo elongation and to compare the difference in junction lengthening between embryos with normal muscles and with defective muscles, Dr. Labouesse and I acquired real-time 3D images recordings of *C. elegans* embryos by Single Plane Illumination Microscopy (SPIM) at the Max Planck Institute of Molecular Cell Biology and Genetics, Dresden [10]. We imaged embryos between 1.7- to 2-fold, which express the junctional marker DLG-1::RFP so that the movements of the epidermal cells during the beginning of late elongation can be tracked.

As described in chapter 4, the positions of lateral epidermal cell vertices were tracked. From the change of vertex positions, I computed the total length of the lateral epidermis as a proxy for the embryo length in the following analysis. The results showed that the length of the lateral epidermis grew along the time, but in a progressive mode (figure 1B, C, Movie 1). The total lateral epidermis length (yellow line in figure 1B) oscillated between valleys and peaks due to the embryo bending and extending induced by muscle activity. Between the 1.7- and 2-fold stages examined in these graphs, there are two driving forces for embryo elongation resulting from

epidermal actomyosin contractility and muscle contractions. The tension from actomyosin does not show a pulsatile behavior (T. Vuong and M Labouesse, unpublished observations) as during *Drosophila* germband extension [8]. Therefore, the progressive extension of the embryo is more likely to be the result of muscle activity. Indeed, the lateral epidermis length reflected the rotation situations of the embryo, as we discussed in chapter 4, result part 1. Also, the Ca^{2+} sensor results indicated that in different regions of the embryo muscle activity appeared in a pulsating form (see chapter 4, result part 1, figure 6).

5.3 Alternate muscle activity breaks the embryo symmetry

During the analysis of SPIM movies, I noticed that the lateral epidermal cell deformation happened in an asymmetric mode. More specifically, when the lateral epidermis on one side of the embryo bent, the epidermis on the other side of the embryo extended (figure 2A, right panel). For instance, kymographs tracking the distance between the vertices of selected junctions from the embryo left and the right sides suggest that changes were anti-correlated to each other (figure 2B). These cell deformations were the direct consequence of muscle activity (see chapter 4, figure 3A, B). Therefore, understanding what the muscle activity pattern is seemed important.

Intriguingly, though the lateral epidermal cell deformation presented an asymmetric pattern, the distribution of embryo muscles is symmetric. There are two stripes

of muscles localized under the dorsal epidermis and two other under the ventral epidermis, which are all oriented along the A/P axis with a small D/V tilt of 6 degrees (figure 2C). To determine the pattern of muscle movement, I tracked the distance between two muscle nuclei on each of the four muscles over time (figure 2D, movie 2, 3). More specifically, I compared the distance changes between the left vs. the right and the dorsal side vs. the ventral side, as well as the two opposite sides of the embryos, the ventral-left (VL) vs. the dorsal-right (DR) and the ventral-right (VR) vs. the dorsal-left (DL).

The results showed that the distance changes of two nuclei from the dorsal and ventral side of the embryo were either correlated or anti-correlated with each other (figure 2F, left column, standard error bar). Similar results were found in distance changes for the muscle nuclei from the left and right sides (figure 2F, middle column, standard error bar). This indicated that during late elongation, embryos bent and extended to both dorsal/ventral direction and left/right direction. This choice of bending/extending direction was random but distributed almost equally.

However, the distance changes between the nuclei from two muscles located in opposite sides, left-ventral versus right-dorsal, were always anti-correlated with each other (figure 2F, right column). This means that these muscles did not contract or relax together; instead, they contracted in a group of two: left/right group or dorsal/ventral group. The contractions of muscles on one side of the embryo were coupled with the extension of the muscles on the other side of the embryo.

Altogether, this analysis showed that the muscles on opposite sides of the body

generally contracted alternatively, accounting for the rotation movements. These alternative contractions on each side of the embryo broke their symmetry and could provide a source of polarity during embryonic morphogenesis.

5.4 Mechanical rotations exert tension on A/P oriented junctions

To test how the alternating muscle contraction pattern could alter planar polarity in the embryo, I first investigated whether the junctions go through a compressing/stretching status change during embryo rotations. During embryo rotations, the lateral epidermis looked more folded when embryos rotated inward (figure 3A). By contrast, the lateral epidermis looked more stretched when embryos rotated outward (figure 3B).

To study the junction compressing/stretching status, I first measured the apparent junction length of each A/P oriented junction between the lateral epidermal cells and dorsal epidermal cells during embryo rotation (figure 3C, yellow line). Then I computed the smoothened length of the junctions (figure 3C, blue dash line). The ratio between the apparent junction length and the smoothened one is defined as the junction roughness. Higher values of junction roughness are characteristic of compressed junctions and the lower values of junction roughness occur for stretched junctions.

To study the relationship between junction status and embryo rotations, I quantified the embryo rotation degree. I selected V1 lateral epidermal cell to track the

change of cell center position during embryo rotations. I set the V1 cell center position during the extreme inward rotation as the initial position 0 and normalized the farthest V1 cell center position to 1. Therefore, the V1 cell center position during embryo rotation was normalized between 0 and 1, indicated as embryo rotation index (figure 3D).

Measurements showed that for the V1 lateral epidermal cell in one embryo, when the embryo rotated inward, junction roughness was higher, indicating a compressed junction. On the contrary, when the embryos rotated outward, the junction roughness was lower, indicating a stretched junction (figure 3E). This trend was universal for all nine lateral epidermal cells in all five embryos, though the slope of junction roughness change with embryo rotation position might vary among different epidermal cells (figure 3F, G).

Since the junctions were more stretched when embryos rotated outward, they were more likely to be under tension at this time. To test whether this was the case, I used multi-photon microscopy to ablate A/P oriented junctions between the V3 lateral epidermal cell and the dorsal epidermis in 1.8- to 2-fold embryos (figure 3H). These embryos were aged enough to have strong muscle contractions and asymmetric rotations to generate local tension on junctions. I faced a great difficulty when I conducted this experiment because the embryo very actively rotated, making it quite difficult to ablate the selected junctions and further track them without having them fall out of the focal plane. Eventually, out of 89 ablations on the V3-dorsal/ventral

junctions, 20 showed that when the embryos rotated outward, the opening of junctions right after ablation was 0.7μm. By contrast, ablation of the same junction in 60 embryos rotating inward showed that the opening after ablation was 0.4μm (figure 3I). Moreover, junction roughness analysis of these junctions showed that junctions with lower roughness tended to recoil more than junctions with a higher roughness (figure 3J). This result confirmed that when the embryos rotated outward, the rotation stretched the junctions and generated local tension along the anterior-posterior direction on junctions.

5.5 Hypothesis for junction polarized lengthening under tension

After proving that the rotation-induced tension may be the source of junction lengthening, I needed to further investigate the molecular mechanism through which the new junction components could be added. Michael Sheetz proposed in 1996 that increased membrane tension could stimulate exocytosis. Therefore, we proposed that additional junctional material is being added preferentially to junctions along the A/P direction when they are under higher tension, to enable the polarized lengthening of junctions.

To prove this, I intended to observe at which position vesicles containing the junctional protein E-cadherin might get inserted and to compare the differences between embryos rotating outward and inward. According to the hypothesis outlined above, the insertion events should happen more often or at a faster rate on stretched

junctions when the embryos rotate outward compared to folded junctions when the embryos rotate inward.

The imaging was performed with Total Internal Reflection Fluorescence (TIRF) microscopy from our imaging platform with a young group leader who is an expert in TIRF imaging. In the beginning, I tried to observe fusion events with GFP labeled E-cadherin. However, the fusion events were hard to determine during imaging, as the disappearance of E-cadherin at the junction region could not be clearly defined as a fusion, since the vesicles containing E-cadherin could move out of the focal plane and bias results (data not shown). To solve this problem and precisely track E-cadherin fusion events, I created an pHluorin::E-cadherin construct, with a modified worm-specific super-ecliptic pHluorin inserted in the extracellular domain of E-cadherin, between exon 7 and exon 8 of E-cadherin coding gene (figure 4A). Super-ecliptic pHluorin is a modified GFP, which de-quenches when transported from an acidic environment, normally the inner side of the vesicles, to a pH-neutral environment, normally the extracellular domain of the cell [11]. It has been used to monitor exocytosis in mammalian immune cells and neurons, including by some *C. elegans* researchers (figure 4B) [12-15].

As the pHluorin was linked to the extracellular domain of E-cad, it should de-quench and give a signal similar to the normal GFP when fused into the plasma membrane. In this case, to successfully image the de-quenching of pHluorin::E-cadherin that newly arrived at the junction, I first bleached the embryo to decrease the signal

intensity at junctions and be able to capture the low-intensity signal of single vesicles containing E-cadherin molecules. We observed that pHluorin de-quenched along junctions (figure 4C, movie 4) and did not stay at junctions for a very long time, but disappeared within 80-160 ms (figure 4D).

To quantify the E-cadherin insertion at junctions, we measured the intensity of each pHluorin de-quenching event and the rate of pHluorin de-quenching. Preliminary analysis of one rotating embryo indicates that there were more E-cadherin de-quenching events when the distance between two vertices was larger than when the distance was smaller (figure 4E), initially suggesting that more fusion events happened when junctions were stretched. To further prove that we could trust the differences described above, we quantified events occurring at D/V oriented junctions between two lateral epidermal cells. We observed more de-quenching events at junctions along the A/P direction than along the D/V direction during outward rotations (figure 4F). This was probably because junctions along the D/V direction are parallel to the rotation direction and would be under no or little tension during any rotation. Likewise, we observed less de-quenching events at A/P oriented junctions in 1.5-fold embryos (before muscles become active) than in 2-fold embryos. Altogether, my preliminary data support the hypothesis that E-cadherin molecules get primarily inserted at the stretched junctions during outward rotations of the embryo.

To confirm my initial conclusion, I need to acquire more pHluorin::E-cadherin de-quenching events. Also, I shall compare the insertion of E-cad in wild-type embryos,

muscle defective mutants and exocytosis defective mutants in which vesicle trafficking is impaired. The two kinds of mutants should present a less efficient insertion compared to the wild type.

After three months of intense imaging, the numbers of useful movies are still limited. The reason of this awkward situation is because, like the laser ablation, embryos move very fast during their rotations. Therefore, the junction gets easily lost, especially when they rotate inward. In addition, we experienced air conditioning problems over the past two months. Overall, the study of a dynamic process is more difficult than the stable process. But I will continue the imaging before my defense, aiming at taking more inward rotation movies to confirm my conclusion.

5.6 Conclusion and discussion

Here, we have shown that *C. elegans* embryos grow under repeated stimulations from muscle activity. During embryo late elongation, muscle activity exerts tension on adherens junctions along anterior/posterior (A/P) direction, and hypothetically promotes the insertion of junction proteins into these junctions and triggers the polarized junction lengthening. We discover that the contractions of embryo muscles are alternate between muscle residing in opposite positions, resulting in an asymmetric bending and extension of the embryo. This in turn, exerts mechanical tension on the A/P oriented junctions. Consistent with this notion, we prove that lateral epidermal cells being stretched are under tension along A/P direction. Lastly, our preliminary results suggest that the insertion of more junction material is favored on stretched

junctions.

Altogether, we propose a model whereby mechanical tension breaks the symmetry of the embryo and favors a ratchet elongation through the progressive insertion of E-cadherin on stretched junctions.

How do muscle activity contribute to *C. elegans* embryonic elongation is not fully understood yet. Here with the fast 3D imaging, we manage to acquire detailed imaging recording of embryo elongation after muscle become active. Our data show that muscle activity stretches the embryo in a repeated manner. With an average period of 15 seconds, muscle activity drives the embryo to rotate from a contraction on one side to a full extension and then back to a full contraction on the same side. Unlike the contractility of actomyosin, which squeezes the embryo body circumferentially without any pulsatile flow as has been observed during *Drosophila* germband elongation [6-8], this pulsatile muscle activity exerts mechanical stimulations on epidermal cells periodically.

Based on muscle distribution, the *C. elegans* embryo body can be considered as symmetric. There are four rows of muscles beneath the dorsal and the ventral epidermis. However, we discover that this symmetry of *C. elegans* embryo is broken by the muscle activity. Our analysis of SPIM movies show that muscles on opposite sides of the embryo do not contract or extend together. Instead, the contraction of muscles on one side of the embryo is coupled with the extension on the other side of the embryo. This alternate contraction pattern of muscles leads to the rotations of the embryo.

We further observe that the junction status changes along with the embryo rotation status. Junctions along the A/P direction are stretched when the embryo extends during their rotations. When being stretched, most of the A/P oriented junctions are under mechanical tension from the muscle activity. In 1996, Michael Sheetz pointed out that increased membrane tension could promote exocytosis [9]. Therefore, we propose a model for junction lengthening predicting that more junction material, E-cadherin, will be added preferentially to the junctions when they are under higher tension to stimulate the polarized lengthening (figure 5).

Till now, our preliminary results to test this model suggest that when the embryo rotates outward to extend epidermal cells, there are more E-cadherin containing vesicles inserted into the A/P oriented junctions. Since junctions are under higher tension when epidermal cells are extended during rotations, this result initially supports our hypothesis. Moreover, we observe that more E-cadherin inserted to A/P oriented junction than in D/V oriented junction even when the epidermal cells are stretched. Since the D/V oriented junctions are parallel to the direction of mechanical forces, they are rarely under tension during embryo rotations. Therefore, this observation further confirms our hypothesis.

For now, we are still working on acquiring more movies to test our hypothesis of junction material insertion. We are facing some practical difficulties in imaging, that is, wild type embryo rotates very fast and changes the location and the focus of junction constantly. This makes it very difficult to acquire enough movies in which the junctions are stretched or folded during rotations with a sharp focus. In this case, we

are going to acquire more movies to further confirm our hypothesis. In addition, since the junction material insertion relies on muscle activity and the exocytosis process, we will examine the insertion of E-cadherin in muscle defective mutants and exocytosis defective mutants in order to compare with the results in wild-type embryos.

During tissue morphogenesis, the convergent extension has been reported to contribute to the establishment of planar polarity [16, 17]. Rho GTPase and Rho kinase-depend activation of non-muscle myosin-II has been reported to be the forces powering this process during *Drosophila* germband extension [6, 7]. Here, our results suggest muscle activity could be another source of tissue asymmetry during *C. elegans* embryonic elongation. Like non-muscle Myosin-II promotes endocytosis to shorten the junctions along one direction during *Drosophila* germband extension [6], we suggest that muscle activity breaks the symmetry of the embryo to promote the exocytosis of junction material to A/P orientated junctions by exerting polarized tension on these junctions. Similar mechanisms could promote the establishment of planar polarity during morphogenesis in other organisms.

The repeated and periodical addition of junction material is a pre-requisite to the subsequent lengthening of the embryo. Since muscle contractions occur every few seconds during approximately one hour, it suggests that embryo growth follows a ratchet mode. Altogether, our preliminary results could suggest that repeated mechanical input represents a source of planar polarized growth in a ratchet mode of morphogenesis.

References

1. Juriloff, D.M. and M.J. Harris, A consideration of the evidence that genetic defects in planar cell polarity contribute to the etiology of human neural tube defects. Birth Defects Res A Clin Mol Teratol, 2012. 94(10): p. 824-40.

2. De Marco, P., et al., Planar cell polarity gene mutations contribute to the etiology of human neural tube defects in our population. Birth Defects Res A Clin Mol Teratol, 2014. 100(8): p. 633-41.

3. Robinson, A., et al., Mutations in the planar cell polarity genes CELSR1 and SCRIB are associated with the severe neural tube defect craniorachischisis. Hum Mutat, 2012. 33(2): p. 440-7.

4. Butler, M.T. and J.B. Wallingford, Planar cell polarity in development and disease. Nat Rev Mol Cell Biol, 2017. 18(6): p. 375-388.

5. Labouesse, M., Epithelial junctions and attachments. WormBook, 2006: p. 1-21.

6. Levayer, R., A. Pelissier-Monier, and T. Lecuit, Spatial regulation of Dia and Myosin-II by RhoGEF2 controls initiation of E-cadherin endocytosis during epithelial morphogenesis. Nat Cell Biol, 2011. 13(5): p. 529-40.

7. Collinet, C., et al., Local and tissue-scale forces drive oriented junction growth during tissue extension. Nat Cell Biol, 2015. 17(10): p. 1247-58.

8. Vuong-Brender, T.T., et al., The interplay of stiffness and force anisotropies drives embryo elongation. Elife, 2017. 6.

9. Sheetz, M.P. and J. Dai, Modulation of membrane dynamics and cell motility by membrane tension. Trends Cell Biol, 1996. 6(3): p. 85-9.

10. Royer, L.A., et al., ClearVolume: open-source live 3D visualization for light-sheet microscopy. Nat Methods, 2015. 12(6): p. 480-1.

11. Miesenbock, G., D.A. De Angelis, and J.E. Rothman, Visualizing secretion and synaptic transmission with pH-sensitive green fluorescent proteins. Nature, 1998. 394(6689): p. 192-5.

12. Merrifield, C.J., D. Perrais, and D. Zenisek, Coupling between clathrin-coated-pit invagination, cortactin recruitment, and membrane scission observed in live cells. Cell, 2005. 121(4): p. 593-606.

13. Dittman, J.S. and J.M. Kaplan, Factors regulating the abundance and localization of synaptobrevin in the plasma membrane. Proc Natl Acad Sci U S A, 2006.

103(30): p. 11399-404.

14. Wilson, J.D., et al., Rab11 Regulates the Mast Cell Exocytic Response. Traffic, 2016. 17(9): p. 1027-41.

15. Nehrke, K., A reduction in intestinal cell pHi due to loss of the Caenorhabditis elegans Na+/H+ exchanger NHX-2 increases life span. J Biol Chem, 2003. 278(45): p. 44657-66.

16. Shih, J. and R. Keller, Cell motility driving mediolateral intercalation in explants of *X. laevis*. Development, 1992. 116(4): p. 901-14.

17. Shindo, A. and J.B. Wallingford, PCP and septins compartmentalize cortical actomyosin to direct collective cell movement. Science, 2014. 343(6171): p. 649-52.

Figure legends

Figure 1. Repeated mechanical stimuli during embryo elongation.

(A) Scheme of embryo elongation and junction remodeling. Blue cells, dorsal epidermis; pink cells, ventral epidermis; yellow cells, lateral epidermis. Black lines, apical junctions. (B) 1.7-fold embryo from SPIM movies. Yellow line, the midline of all lateral epidermal cells. Scale bar = 5μm. (C) The normalized total length of the lateral epidermis along time. The value of each time point indicates the length of the yellow line in (B). Orange line indicates the growing trend of the embryo. (D) Average time between two extensions of lateral epidermal cells. (E) Average embryo elongation rate between two extensions of lateral epidermal cells.

Figure 2. Alternate muscle activity breaks the symmetry of embryo.

(A) Left, wild-type embryo at a relaxed position. Image from one frame of a SPIM movie. Green lines indicate the relaxed epidermal cells at both left and right sides of the embryo. Right, wild-type embryo during a twitch. Image from another frame of the same SPIM movie. The blue line indicates the extending epidermis on the right side and orange lines indicate the contracting epidermis on the left side of the embryo. Scale bar = 5μm. (B) Kymograph of junction extension and contraction in the second embryo presented in (A). Green line, relaxed junctions at the initial time point. Yellow line, contracted junction on the right side of the embryo; blue line, extended junctions on the left side of the embryo. Red spots, vertices of the selected junctions. Time resolution = 0.46 second. (C) Up, the scheme of a 1.7-fold embryo. Color-code

as in Figure 1A. Below, scheme of *C. elegans* embryo cross-section (internal organs were omitted for clarity). Important components are labeled in the figure. (D) 2-color SPIM movie. Red, mCherry-labeled muscle nuclei. Green, GFP-labeled junction protein DLG-1. Yellow circles, two selected muscle nuclei on one side. Yellow line, the distance between the two selected nuclei. Scale bar = 5μm. (E) Normalized distance change between two selected muscle nuclei on dorsal left muscles (blue), dorsal right muscles (yellow) and ventral right muscles (pink). Time resolution, 2 seconds. (F) Average value of muscle nuclei distance change cross-correlation between dorsal and ventral nuclei, left and right nuclei and nuclei in the left-ventral and right-dorsal sides (or right-ventral and life-dorsal sides) of the embryo.

Figure 3. Membrane status during embryo rotations.

(A) Left, an inward rotating embryo from SPIM movie. Right, V1 lateral epidermal cell. Yellow line, folded V1 cell apical junction. (B) Left, an outward rotating embryo from the same SPIM movie. Right. V1 lateral epidermal cell, red line, extended V1 cell apical junction. (C) Yellow line, actual junction; blue dash line, smoothened junction. (D) Yellow cell, V1 lateral epidermal cell; yellow dot, cell center of the V1 cell. Black dash curve, V1 cell displacement range. (E-G) Junction roughness as a function of embryo rotation index. Yellow and red cells below the x-axis represent the folded and extended junction during inward and outward rotation, respectively. (E) Roughness change for the A/P orientated junction between V1 lateral epidermal cell and the dorsal epidermal cells. (F) Roughness change of the A/P orientated junction

between 6 lateral epidermal cells (H0 - V3) and the dorsal epidermal cells in the same embryo in (C). (G) Roughness changes of A/P orientated junctions between the V3 lateral epidermal cell and the dorsal epidermal cells in five embryos. (H) 1.8-fold embryo for laser ablation experiment. Green short line represents the laser ablation ROI (Region Of Interest); pink arrows indicate the directions of junction recoiling after laser ablation. (I) Junction recoil size in the first frame after laser ablation. Yellow and red cells below the plot represent the inward or outward embryos rotations during laser ablation, respectively. (J) Junction recoil size after laser ablation as a function of junction roughness.

Figure 4. pHluorin indicated E-cadherin fusion at stretched junctions.

(A) Construct of the pHluorin::E-cadherin. Modified worm-specific super-ecliptic pHluorin is inserted in the extracellular domain of E-cadherin, at S838. (B) Schematic drawing of pHluorin::E-cadherin vesicle trafficking. Left, pHluorin::E-cadherin inside a vesicle is exposed to an acidic environment. Dark green spots indicate that the super-ecliptic pHluorin is in a quenched state. Right, a vesicle containing pHluorin::E-cadherin fusing with the plasma membrane. Light green spots indicate that the super-ecliptic pHluorin is in a de-quenching state due to the neutral environment outside the cell. Vesicles, plasma membrane, and E-cadherin protein are as indicated in the drawing. (C) Fusion happened at junctions in an outward rotation. Green spots represent each fusion event. Yellow circle, one fusion event shown in kymograph in (D). (D) Kymograph of one fusion event. Yellow arrowhead indicates the fusion event

on the junction. (E) E-cadherin fusion level as a function of vertices distance of one selected junction during outward rotations. (F) Comparison of fusion levels between A/P oriented junctions and D/V oriented junctions in the same embryo. (G) Comparison of fusion levels in A/P oriented junctions between the 2-fold embryo and the 1.5-fold stage embryo.

Figure 5. Scheme for junction polarized lengthening.

Yellow cell, cells with less stretched A/P orientated junctions during inward rotations; red cell, cells with more stretched A/P orientated junctions during outward rotation. Green triangle, E-cadherin containing vesicles.

Movie legends

Movie 1. Lengthen change of lateral epidermis during embryo rotation during.

Z-projection of four-dimensional time-lapse (xyzt) of a wild-type embryo expressing DLG-1::RFP. Images are average intensity projections of 54 z planes acquired in the RFP channel, separated by 0.5μm steps. 5 stacks were acquired every 2s during 600 sec (total movie time). Movie is played in 15 frames per second. Scale bar = 5μm. Yellow line is the mid-line of all lateral epidermis. This movie illustrates how embryo rotates and how the total length of lateral epidermis changes during rotations.

Movie 2. 2-color movie of embryo movements.

Z-projection of five-dimensional time-lapse (xyztc) of a wild-type embryo expressing junction marker, DLG-1::GFP and muscle nuclei marker, HLH-1::HIS-24::mCherry. Images are average intensity projections of 42 z planes acquired in the GFP and RFP channels, separated by 0.5μm steps. Stacks were acquired every 2s during 600 sec (total movie time). Movie is played in 15 frames per second. Scale bar = 5μm. This movie illustrates how embryo twitches and how muscle nuclei move during embryo movements.

Movie 3. Muscle nuclei distance change during embryo movements.

Z-projection of five-dimensional time-lapse (xyztc) of the same wild-type embryo in movie 2. Images are average intensity projections of 31 z planes (from z plane 33

to 63). Z step size, time resolution, scale bar size and playing speed are the same as movie 2. Yellow circles are two muscle nuclei in the dorsal-right side of the embryo changing their positions along time. Yellow line is the projected distance between these two muscle nuclei. This movie illustrates how the distance of two muscle nuclei changes during embryo movements.

Movie 4. Single molecule imaging of E-cadherin fusion events.

Time-lapse movie of a 2-fold stage wild-type embryo expressing pHluorin::HMR-1. Embryo was pre-bleached before imaging (see Materials and Methods). Images were acquired every 80 ms during 3.28 sec (total movie time). Embryo in this movie is undergoing an outward rotation. Green blinks indicate fusion events happening at the junction.

Movie 5. Single molecule imaging of E-cadherin fusion events on one junction.

Zoom-in of the embryo in movie 4 at H1 lateral epidermal cell region. This movie is corresponding to figure 4C and figure 4D.

Figure 1:

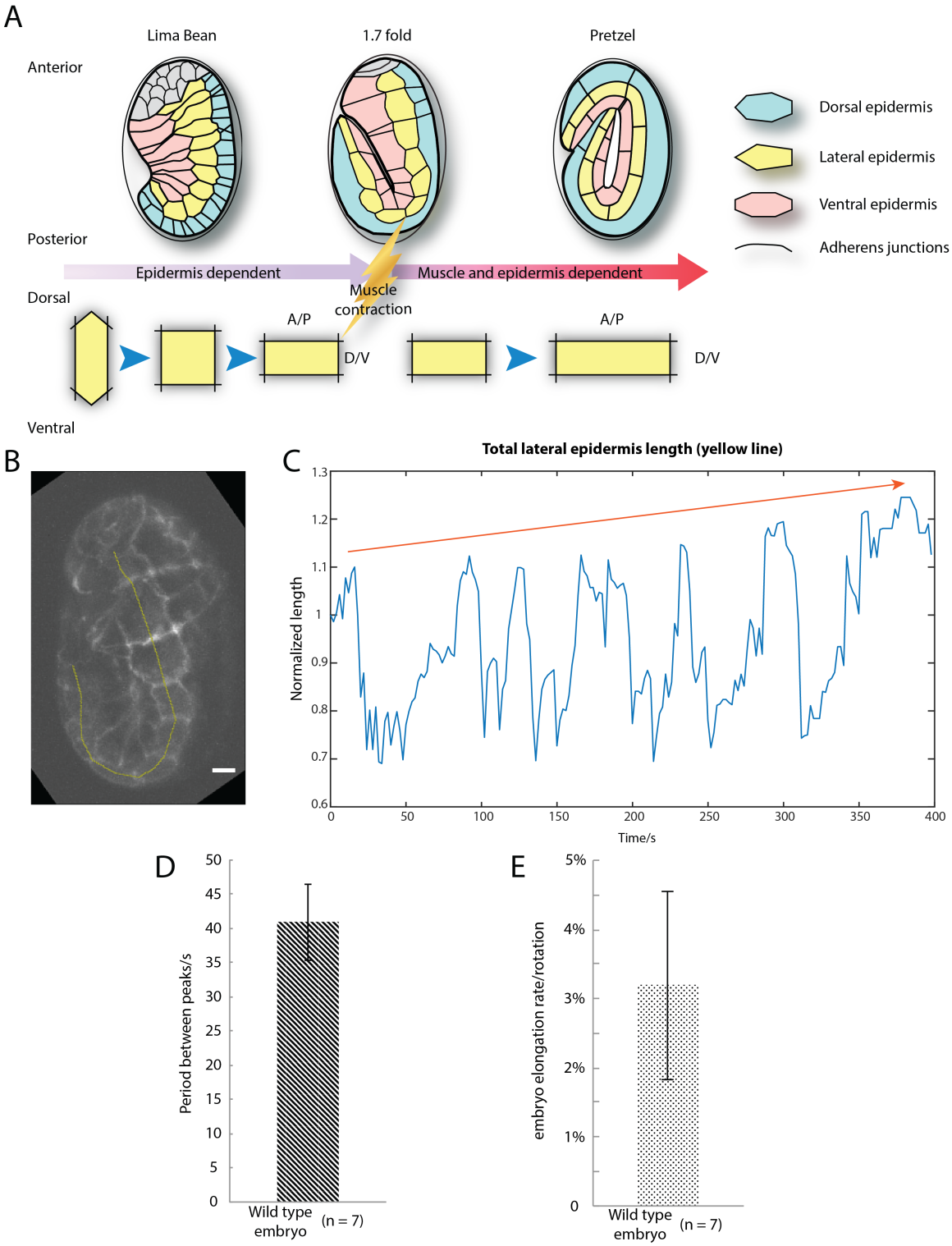
A
Lima Bean
1.7 fold
Pretzel
Anterior
Posterior
Dorsal
Ventral
Dorsal epidermis
Lateral epidermis
Ventral epidermis
Adherens junctions
Epidermis dependent
Muscle and epidermis dependent
Muscle contraction
A/P
D/V
A/P
D/V
B
C
Total lateral epidermis length (yellow line)
Normalized length
Time/s
D
Period between peaks/s
Wild type embryo (n = 7)
E
embryo elongation rate/rotation
Wild type embryo (n = 7)

Figure 2:

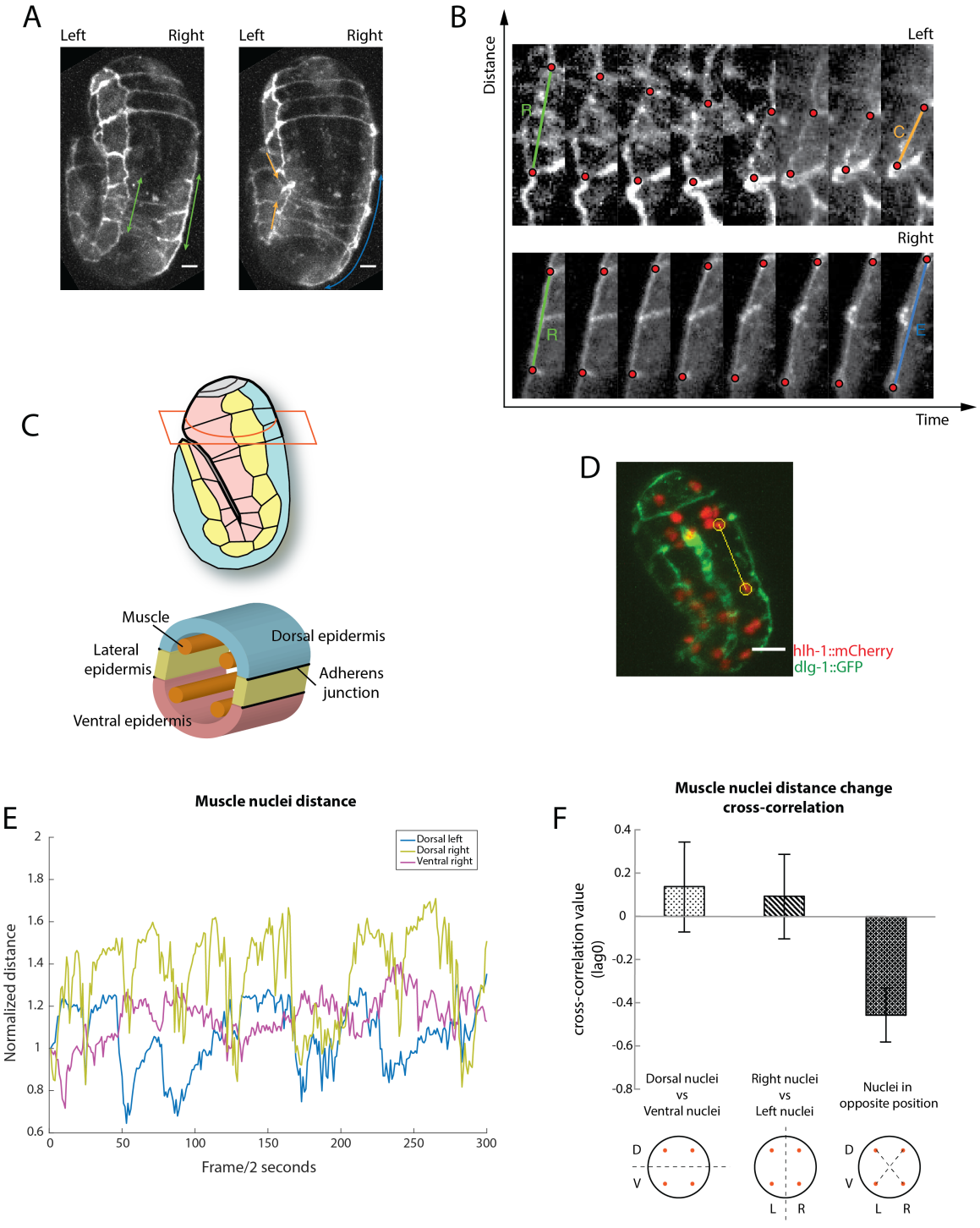
A
Left
Right
Left
Right
B
Distance
Left
R
C
Right
R
E
Time
C
Muscle
Lateral epidermis
Dorsal epidermis
Adherens junction
Ventral epidermis
D
hlh-1::mCherry
dlg-1::GFP
E
Muscle nuclei distance
Dorsal left
Dorsal right
Ventral right
Normalized distance
Frame/2 seconds
F
Muscle nuclei distance change cross-correlation
cross-correlation value (lag0)
Dorsal nuclei vs Ventral nuclei
Right nuclei vs Left nuclei
Nuclei in opposite position
D
V
L
R

Figure 3:

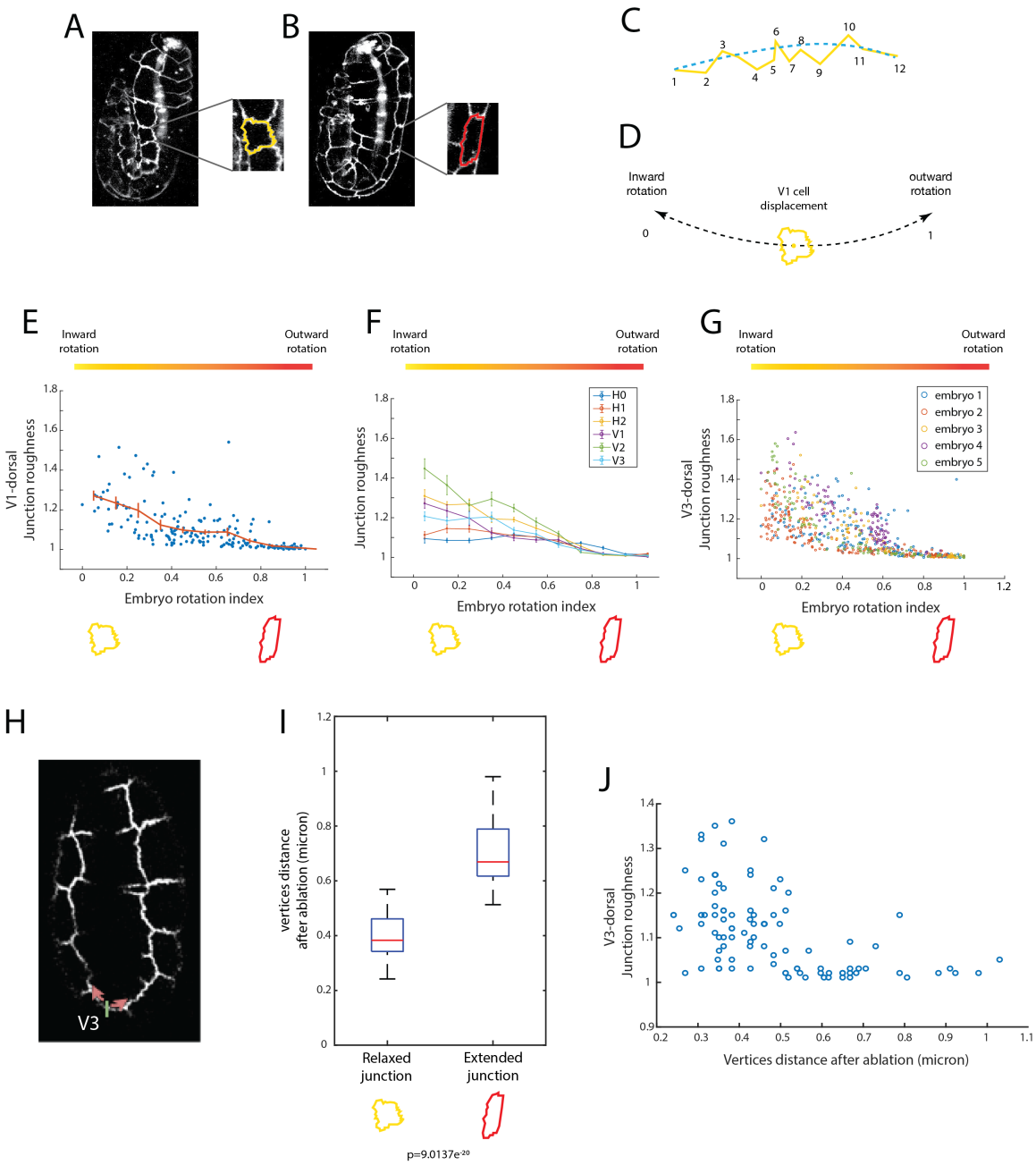
A
B
C
1
2
3
4
5
6
7
8
9
10
11
12
D
Inward rotation
V1 cell displacement
outward rotation
0
1
E
Inward rotation
Outward rotation
V1-dorsal Junction roughness
Embryo rotation index
F
Inward rotation
Outward rotation
Junction roughness
H0
H1
H2
V1
V2
V3
Embryo rotation index
G
Inward rotation
Outward rotation
V3-dorsal Junction roughness
embryo 1
embryo 2
embryo 3
embryo 4
embryo 5
Embryo rotation index
H
V3
I
vertices distance after ablation (micron)
Relaxed junction
Extended junction
p=9.0137e-20
J
V3-dorsal Junction roughness
Vertices distance after ablation (micron)

Figure 4:

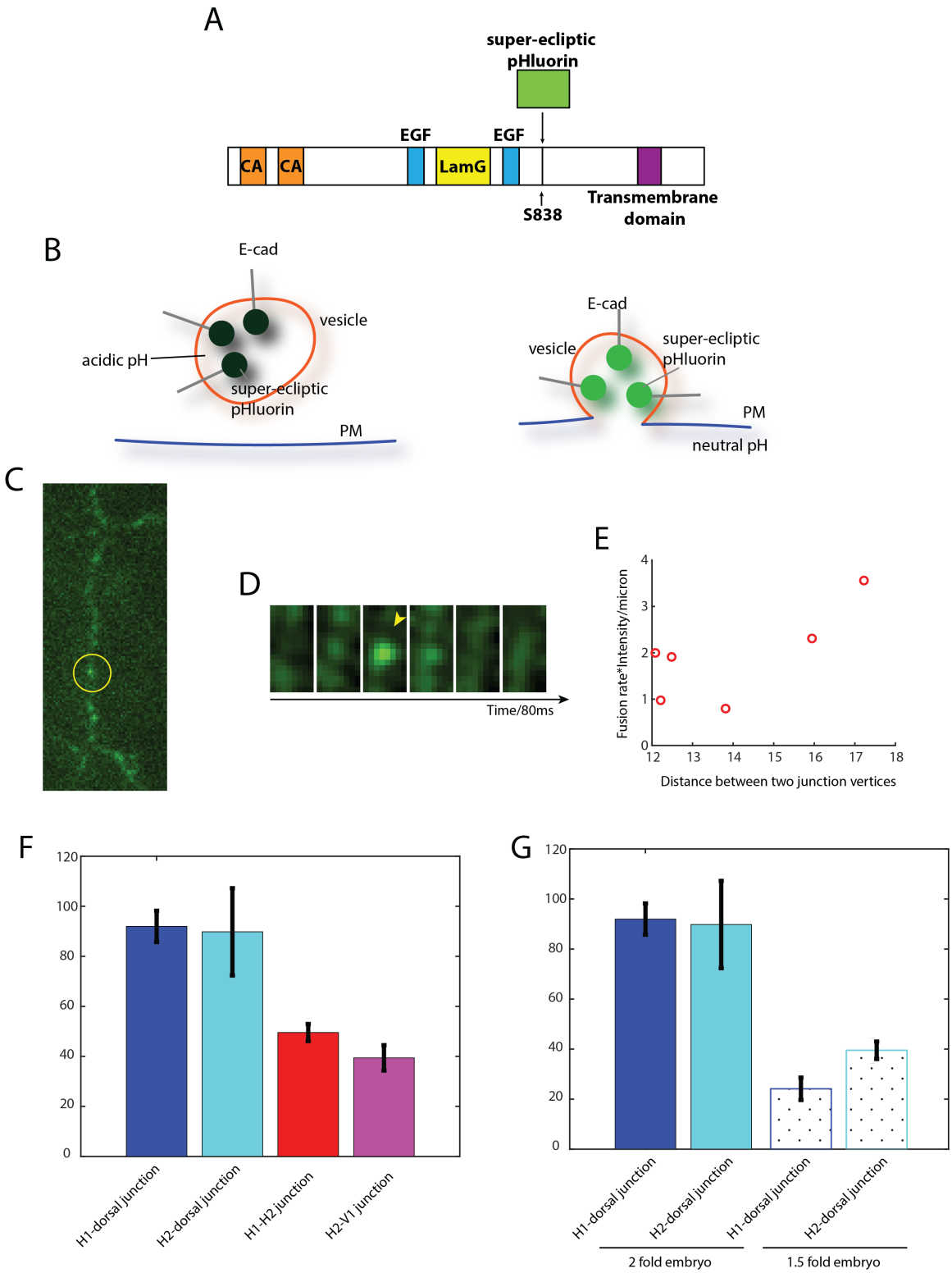
A
super-ecliptic
pHluorin
EGF
EGF
CA
CA
LamG
S838
Transmembrane
domain
B
E-cad
vesicle
acidic pH
super-ecliptic
pHluorin
PM
E-cad
vesicle
super-ecliptic
pHluorin
PM
neutral pH
C
D
Time/80ms
E
Fusion rate*Intensity/micron
Distance between two junction vertices
F
H1-dorsal junction
H2-dorsal junction
H1-H2 junction
H2-V1 junction
G
H1-dorsal junction
H2-dorsal junction
H1-dorsal junction
H2-dorsal junction
2 fold embryo
1.5 fold embryo

Figure 5:

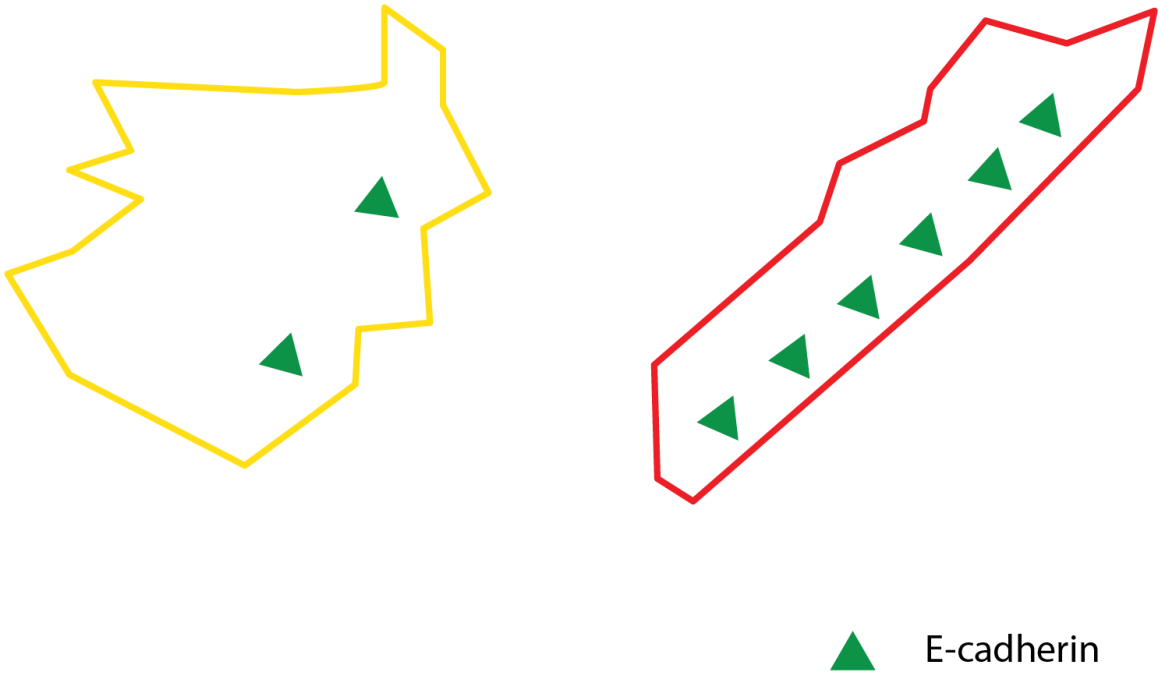

Part III

Materials and methods

Materials and methods

Strains and genetic methods

Animal strains, conditions of maintenance

C. elegans strains used in this study are listed in Table S1. Animals were maintained at 20°C on Nematode Growth Medium agar plates as described in [348]. N2 Bristol was used as the wild-type in this study.

Construction of ML2615 *[mc103]* by the Crispr/Cas9 method

A homozygous DLG-1::GFP strain was obtained by the method described in [349]. A repair template for Designing Homologous Repair (HDR) was constructed in the pJET1.2 vector (Thermo Fisher Scientific) by the Megawhop method [350]. The repair template included the new sequence (GFP) to be inserted and 1500 or 500 base pair of homologous sequence on either side of the insertion site. The Protospacer Adjacent Motif (PAM) was mutated (protein sequence was not changed) in the repair template to prevent the plasmid and the repaired genomic locus from being cleaved by Cas9. The small guide RNA (sgRNA) sequence specific to *dlg-1* was inserted in the pDD162 vector [349] that also encodes Cas9 under a germline promoter. The primer and SG sequences used in this study are described below.

The repair template and Cas9/sgRNA plasmids were co-injected into both gonads of adult hermaphrodites with the roller marker pRF4 and red pharynx marker pCFJ90. After injection, animals were kept at 20°C. Rollers or animals with red pharynx from the F1 progeny were picked and were checked by PCR to find positive hits after egg-laying. A positive hit was defined by the specific band amplified from GFP internal primer and the primer outside of the repair template. One successful knock-in was found in 40 F1 animals. After selecting the homozygote in the F2 progeny, this transgenic line was sequenced around the insertion site in order to make sure there was no mutation that occurred during the knock-in process. Both embryos and larvae were in a healthy condition, behaved like wild-type worm N2 and showed no lethality.

sgRNA sequence: CCAATTTCATCTAATGACG

Megawhop primer:

Forward: ACACATGGCATGGATGAACTATACAAACGTCATTAGATGAAATTG-GATA

Reverse: CCCCAAAAAGCAAAAGCAGGAAAATTAAAATGCAAGTATTTG-TAAGGTG

Construction of ML2773 *[mc118]* by Crispr/Cas9 method

A homozygous pHluorin::HMR-1 strain was obtained by the method described in [349]. A repair template for HDR was constructed in the pJET1.2 vector (Thermo Fisher Scientific) by the Megawhop method [350]. The repair template included the new sequence (worm-specific super-ecliptic pHluorin) to be inserted and 1500 or 500 base pair of homologous sequence on either side of the insertion site, the extracellular domain of HMR-1, at position S838. The modified worm-specific super-ecliptic pHluorin was amplified from plasmid pSJN788 [351] (a gift from Dr. Josh Kaplan). The PAM mutant was made as described above. The sgRNA sequence specific to *hmr-1* was inserted in pDD162 vector [349] that also encodes Cas9 under a germline promoter. The primer and SG sequences used in this study are described below.

The injection and following screening and sequencing steps were as described above. The new pHluorin::HMR-1 strain showed 60-70% lethality at 20°C, but could nevertheless be maintained in a homozygous state. Embryos that passed 2-fold stage could develop successfully until hatching.

sgRNA sequence: AAAAGGGTTGTAGGCTGTG

Megawhop primer:

Forward: TGTGGGAAGCCACGTGTGACAGTAACTCAAGTAAAGGAGAA-GAACTTTTCACTGG

Reverse: ATGCAATGATTCAACGAGTCGAC TTTGTATAGTTCATCCATGC-CATGTG

Construction of ML2616 *[mc103 X; st10089]* by crossing

To generate a homozygous strain expressing both green junction marker and red muscle nucleus marker, the ML2615 *[mc103]* strain was crossed with ML1616 *[mcIs50; st10089]*. Homozygous progeny with green junction and red muscle nuclei but no green actin bundles were selected for SPIM imaging.

RNAi feeding for SPIM microscopy

We used RNAi feeding to inactivate *unc-112* for muscle defective mutant during SPIM imaging. *unc-112* RNAi was from the Ahringer RNAi library [352, 353]. Wild-type L4 larvae were fed for 48 hours before transferring them to a fresh RNAi plate. 24 hours later, the embryos between 1.5-2 fold were selected to do the imaging. In parallel, the terminal phenotype of embryos was scored to ensure RNAi efficiency and found to generate 95% two-fold arrested embryos.

SPIM imaging

In this paper, the Single Plane Illustration Microscopy imaging was done using a home made microscope built up by Dr. N. Maghelli and Dr. L. Royer in MPI-CBG, Dresden [354]. The objective used for imaging was 40×. To start the imaging, embryos younger than 1.5 fold were selected. The imaging began with a pre-acquisition time-lapse with 2-minute time interval until the embryos started to actively twitch or rotate, at which point the pre-acquisition was stopped and the acquisition started. During pre-acquisition and acquisition, the embryos whose lateral epidermal cells were parallel or nearly parallel to the camera were selected for imaging. Embryos were scanned from one side to the other side, with a focal plane depth of 0.5μm.

For one-colored movies, embryos carried the junction marker *mcIs46 [dlg-1::RFP, unc-119(+)]*; the exposure time for both pre-acquisition and acquisition was from 3000μs to 10000μs and the acquisition process was continuous imaging.

For two-colored movies, embryos carried the junction marker *mcIs46 [dlg-1::RFP, unc-119(+)]* and muscle nucleus marker *st10089 [hlh-1(3,3kb)::his24::mCherry+unc-119(+)]*, the exposure time for both pre-acquisition and acquisition was 5000μs and the acquisition was with 2 second time interval.

For both one-colored and two-colored movies, control movies were made overnight after acquisition with a 2-minute time interval and the same Z-step depth and exposure time to make sure the imaging protocol was not phototoxic for proper embryonic development process. All control embryos hatched after acquisition, suggesting the imaging protocol was not phototoxic for embryos to develop properly.

Points Of Interests (POI) tracking in SPIM movies

To calculate the changes of cell aspects, the vertices of lateral epidermal cells were tracked in Fiji after the SPIM movies were made. For wild type and *let-502* embryos, the tracking was finished manually and the original positions of vertices were saved.

For *unc-112* embryos, the tracking of POI was done by a Fiji plugin, CE Time lapse analysis of POI, created by Dr. Julien Pontabry. The surrounding background of the initial POI was compared in the following frames to find the potential point with exact or similar surrounding background to define the position of POI in the following frames.

After gathering the original positions of all POIs, we used shape inserter in MATLAB to circle the position of each POI back on the SPIM movies to make sure that the original tracking of the POI is correct.

Cell aspects and total lateral epidermal cell length calculation

After confirming the POI position tracking, we calculated the apical area and the perimeter of the cell by a pre-existing MATLAB function.

function[geom, iner, cpmo] = polygeom(x, y).

Function website:

https://fr.mathworks.com/matlabcentral/fileexchange/319-polygeom-m

The length of the cell was calculated as the total length from the mid-point of the two most anterior vertices passing the central position of all the vertices to the mid-point of the two most posterior vertices of the same lateral epidermis. The positions of these three points were calculated in MATLAB by using the original positions of the vertices of a lateral epidermis. The length was calculated by

$\text{dist} = \text{sqrt}[(X_1\text{-}X_2)^2+(Y_1\text{-}Y_2)^2]+\text{sqrt}[(X_2\text{-}X_3)^2+(Y_2\text{-}Y_3)^2]$ (Equation 1)

The total length of all lateral epidermis is the sum of the length of all the lateral epidermal cells.

Nuclei distance calculation

The positions of two selected muscle nuclei from each row of muscles were tracked in Fiji at each time point. The distance between the two muscle nuclei were calculated in MATLAB by equation 1.

Measurement of junction roughness

To measure the roughness of junctions during embryo rotation, SPIM movies were loaded in MATLAB frame by frame. In each frame, the position of every vertex of each junction was recorded by the MATLAB function ginput (Graphical input from mouse or cursor). And the position of each vertex was smoothened by MATLAB function smooth with the exponential smooth option. Based on the actual position of the smoothened position of each point, the total length and the smoothened length of each junction were calculated by adding up the distance between each vertex.

Based on the tracking of junctions during rotation, a smoothened length of the junction was calculated by MATLAB automatically too, by

$\text{Junction roughness} = \text{Junction}_{totallength}/\text{Junction}_{smoothenedlength}$ (Equation 2)

Laser ablation experiment

Laser ablations of adherens junction were conducted on a Leica SP8 multi-photon microscope using a 63×/N.A. 1.4 oil-immersion objective. Embryos older than 1.7-fold were selected for ablation at the junction between V3 lateral epidermis and dorsal cells.

The laser ablation imaging was obtained in the following order: three frames of pre-ablation, laser ablation and 50 frames of post-ablation. Both the pre-ablation and post-ablation were imaged with a 488 nm laser. The ablation of junction was done by the multi-photon laser with a wavelength of 904 nm and an average laser power of 1700 mW. The size of the laser-ablated region was 5 nm x 0.08 nm, diagonal to junctions. The exposure time for pre- and post-ablation was 0.5 second and was 0.27 second for ablation.

Ablated embryos were numbered and their positions were recorded in order to check if they went through the proper elongation after ablation. Embryos who died after ablation or elongated abnormally were excluded.

Measurement of junction opening

As the laser ablation experiment was conducted on rotating embryos, the ablated junction in most situations did not remain in focus for long enough to make a typical kymograph. To circumvent this problem, we always measured the distance between the two vertices of the ablated junction in the first frame of post-ablation. Since it took 1.25 seconds for the microscope to change from a 904 nm ablation laser mode to the 448 nm laser imaging mode, the distance between the two vertices represented the junction recoiled size 1.25 seconds after laser ablation to indicate the tension level exerted on the junctions.

Calcium imaging and analyzing

Calcium sensor imaging to report on muscle activity was conducted by Spinning Disc microscopy, using a 100/N.A. 1.4 oil-immersion objective. Embryos expressing calcium sensor (*goeIs3 [pmyo-3::GCamP3.35::unc-54C3′utr, unc-119(+)]V*) between 1.7-2 fold were selected for imaging. Half of the embryo was scanned with eleven focal planes with a ZCstep size of 1μm and a time interval of 0.89 seconds.

To analyse the images after imaging, time series were first corrected for bleaching by using the standard plugin of Fiji 'Bleach Correction' with the 'exponential fit' option. Starting from muscles located closer to the H1 epidermal cell, the first five cells from anterior to posterior were labeled as cells 1, 2, 3, 4 and 5 and they were selected for further analysis (see Figure 6a). Selected muscle cells were restricted to the first five cells because the posterior cells were not always visible and clear. The same logic of selection was applied both for the dorsal and the ventral sides of the embryo.

Along one line of muscles, the cells often touch each other and they change aspect and intensity across time. Therefore, by using a custom MATLAB graphical interface, cell contours were segmented manually in order to avoid segmentation artifacts. With the same MATLAB script, cell contours were used as a mask to measure the fluorescence intensity (I) of the segmented cells and to record the positions or their centers of mass in each frame. Finally, for each of the 5 cells, a temporal trace of the calcium content during one of more pulses was extracted. During a calcium pulse, more than one cells in a muscle row showed a progressive signal increase up to a peak and a subsequent decrease to a level close to the basal one. From the temporal traces, the following observables were extracted: 1) delay in pulsing; 2) relative pulse duration; 3) peak of intensity. The movies were acquired with a time interval between frames of 0.89 seconds; to have a more detailed sampling of the temporal behavior of the traces we interpolated them with a step of 0.05 seconds.

1) Delay in pulsing and pulse duration

In order to estimate the delay in pulsing and the duration of pulses, the following normalized intensity was introduced

$$\text{Normalized intensity} = (I_t - I_{initial})/\max(I_t - I_{initial}) \quad \text{(Equation 3)}$$

where I_t is the intensity in each frame and $I_{initial}$ is the intensity in the first frame. The time when the normalized intensity first reached 0.3 was considered as the beginning of a pulse. The time when the normalized intensity decreased to 0.3,

after its maximum peak, was considered as the termination time of the pulse. Time in-between theses two frames was the duration of a pulse. The delay in pulsing for each calcium pulse event was estimated as the difference in initiation time between the first pulsing cell and the remaining 4. The relative duration was computed as the duration divided by the maximal duration among the five analyzed cells.

2) Peak of intensity

The frame in which the normalized intensity reached 1 was considered as the time of the peak of pulses. To compare the peak intensity of pulses with respect to the basal expression among all five muscle cells, the relative intensity of pulses of each frame was defined as follows:

Relative intensity of pulses = $(I_t\text{-}I_{min})/I_{min}$ (Equation 4)

where I_{min} was the minimum intensity of all five muscle cells along time.

Single molecule imaging

Single molecule imaging was conducted on a Nikon Total Internal Reflection Fluorescence (TIRF) Microscope. Embryos older than 1.7-fold were selected for imaging. To image pHluorin::HMR-1 construct (allele *mc118*), a 488 nm laser was used. The initial laser power was set up as 100 mW. The exposure time was 80 ms with continuous imaging. Before imaging, embryos were bleached for three rounds until the histogram showed that the peak of imaging intensity decreased to between 7,500 and 10,000. Each round lasted for 30 seconds, with 80% laser power. The incident laser was set up at 0 to bleach through the whole embryo. Between each round of bleaching, the embryo rested for 45 seconds without any imaging to avoid high photo-toxicity. After bleaching, the rotations of the embryos were imaged with the incident light set up at the optimal degree, usually between 64° and 67.5°.

Fusion events determination and analysis

After imaging, one or more sub-portions of a movie were selected for analysis. These sub-portions presenting A/P and D/V junctions that were in sharp focus and in a stretch position during rotation. The length of these short movies was normally around 4-10 seconds (40-130 frames 80 ms/frame). By using a MATLAB interface, a region surrounding the selected junction was masked. From each time series, the difference in intensity between two frames D(t) was calculated to extract potential fusion events. D(t) was defined as follows:

D(t) = I(t) - I(t-1) (Equation 5)

where I(t) is the frame at time t and I (t-1) is the frame at the previous time. D(t) was filtered by a gaussian filter with sigma=1 to average out noise. Then a threshold was set up for all the sub-portion of a movie, based on a representative frame. The threshold was the same for all the sub-movies belonging to the same movie and was estimated with respect to the background of a region outside the junction as follows:

Threshold = bkg + $4*\sigma_{bkg}$ (Equation 6)

where bkg was the average value of the background and σ_{bkg} was its standard

deviation. After thresholding, fusion events were automatically registered and analyzed. A fusion event was identified as a super-threshold spot with a size bigger than 4 pixels. For each fusion event the integral fluorescence intensity and the position of the spots were recorded. Moreover, the distance between the two vertices of the selected junction in each frame was measured.

The normalized E-cadherin fusion rate in one sub-portion of movies was defined as follows:

Normalized fusion rate = total event number $*$ average (integral intensity) / (junction vertices distance $*$ number of frames)

Table S1. Strains used in this study

Strain	Genotype
N2	Wild type
ML1652	*mcIs46 [dlg-1::RFP, unc-119(ed3)]*
ML1616	*mcIs50 [ABD::GFP, myo-2::GFP]; st10089 [hlh-1(3,3kb)::his24::mCherry+unc-119(+)]*
ML1840	*let-502(sb118ts); mcIs46*
ML2615	*mc103 [dlg-1::GFP] X*
ML2616	*mc103 X; st10089*
HBR4	*goeIs3 [pmyo-3::GCamP3.35::unc-54C3utr, unc-119(+)]V*
ML2705	*mc103 X; goeIs3 V*
ML2773	*mc118 [pHluorin::hmr-1]*

Part IV

Conclusion and Perspective

Conclusion and Perspective

In this thesis, I determine how muscle activity contributes to *C. elegans* embryo elongation in two different aspects. My results make breakthroughs in understanding *C. elegans* morphogenesis process in both technology and scientific ways.

Technologically speaking, I used two different advanced microscopies to achieve my goals in my project.

First, using Single Plane Illustrating Microscopy (SPIM), I recorded the embryo movements during late elongation with great details in real-time 3D movies for the first time. SPIM has been used to study the neural development [355] and the early embryo cell development (4-6 cell stage) [356] in *C. elegans*, but not used in the study of epidermis morphogenesis. A very common difficulty to study the late elongation process of *C. elegans* embryo is that after the muscle activation, embryos start to move very fast. Normal confocal or spinning disc microscopy are not fast enough to multi-focal-plane live imaging. For the first time, we used SPIM, which can scan the whole embryo in 60-100 focal planes within half a second. As we expected, these movies provided massive information of embryo and cell behaviors during late elongation and therefore solved the difficulty that has long been disturbing us.

Second, by fusing the pHluorin protein with junctional protein E-cadherin, plus the single molecule microcopy, total internal reflection fluorescent (TIRF) microscope, we made it possible to examine directly the insertion of junctional material into the junctions through exocytosis process. Unlike endocytosis, the accumulation of trafficking vesicle at the junction region does not necessarily mean the increase of fusion events. Super-ecliptic pHluorin, which de-quenches when transported from an acidic environment to a neutral environment, has been widely used to indicate fusion events in mammalian cells in the past decade [357, 358]. With TIRF microscope, whose thickness of the excitation depth can be less than 100 nm [359], we were able to capture the fusion of E-cadherin into junction during worm morphogenetic process.

Scientifically speaking, I discovered how muscles contribute to embryo elongation by driving embryos to move, both globally and locally. More importantly, I propose a model through which repeated mechanical stimuli from muscle activity break the symmetry of the embryo and trigger the ratchet growing of the embryo.

First, by analyzing the SPIM movies, I discovered that muscle activity after 1.7-fold stage drives the embryo to rotate. These rotations are crucial for proper embryo elongation. I also discovered that muscle activity deforms epidermal cells with

local pattern. Lateral epidermal cells can be divided into three partially independent groups based on their deformation pattern. All of these global and local movement patterns of embryo are lost in the muscle defective mutants and the actomyosin hypocontractility mutants. In addition, we characterized muscle activation pattern to understand how these activations are triggered. We determined the "pacemaker" muscle cells that are potentially involved in local signaling events.

Second, my results in chapter 5 suggested that muscle activity can be a novel source of asymmetry during morphogenesis other than non-muscle Myosin-II, to establish the planar polarity of the tissue. Even though the contractile actomyosin machinery has been reported to provide mechanical forces for tissue polarized lengthening [360, 361], it is not polarized distributed in *C. elegans* embryo [144]. My discovery answered the question about what the source of planar polarity is in *C. elegans* embryo late elongation. My results revealed that, practically, muscle activity exerted tension on junction along A/P directions and trigger the insertion of junctional material, E-cadherin. Since this tension was exerted on junctions in a repeated manner, the insertion of junctional material would be periodically too. Altogether, my results suggest a new ratchet mode of *C. elegans* embryo growing.

Of course, during my four-year study, I encountered many difficulties. For that, I still am trying to overcome. For example, during the single molecule imaging, the embryos rotate too fast so that the junctions change their positions and lose their focus very fast. This made me abandon the majority of my movies. Therefore, I need to collect more movies to finish the fusion event analysis in wild type embryos. Furthermore, if our hypothesis of tension triggering the E-cadherin insertion into junction would be proven in wild type embryo, I will continue to examine the fusion event in muscle defective and exocytosis defective mutants.

Besides, for the first part of my result, I need to confirm the muscle activation pattern by increasing the sample number. To confirm the potential calcium enriched region in the embryo, genetic methods or laser killing experiments or both of them could be used in the coming three months.

Overall, after four-year Ph.D. study, I discovered how muscles contribute to *C. elegans* embryo elongation, defined muscle activity as a novel source for planar polarity and proposed a ratchet growing of *C. elegans* embryo.

Bibliography

[1] C. Guillot and T. Lecuit. Mechanics of epithelial tissue homeostasis and morphogenesis. *Science*, 340(6137):1185–9, 2013.

[2] John Shaw-Dunn. Essentials of human anatomy and physiology. *J anatomy*, 179:206, 1991.

[3] R.S. Weinstein F.B. Merk and J. Alroy. The structure and function of intercellular junctions in cancer. *Adv Cancer Res*, 23:23–89, 1976.

[4] J. Sullivan-Brown and B. Goldstein. Neural tube closure: the curious case of shrinking junctions. *Current Biology*, 22(14):R574–R576, 2012.

[5] J.M. Diamond. Twenty-first bowditch lecture. the epithelial junction: bridge, gate, and fence. *Physiologist*, 20(1):10–8, 1977.

[6] M. Labouesse. Epithelial junctions and attachments. *WormBook*, pages 1–21, 2006.

[7] Y. Yu and R.C. Elble. Homeostatic signaling by cell-cell junctions and its dysregulation during cancer progression. *J Clin Med*, 5(2):427–430, 2016.

[8] E.A. Bornslaeger C.M. Corcoran and et al. Breaking the connection: displacement of the desmosomal plaque protein desmoplakin from cell-cell interfaces disrupts anchorage of intermediate filament bundles and alters intercellular junction assembly. *J Cell Biol*, 134(4):985–1001, 1996.

[9] G. Walko M.J. Castanon and G. Wiche. Molecular architecture and function of the hemidesmosome. *Cell Tissue Res*, 360(2):363–78, 2015.

[10] D.P. Kelsell J. Dunlop and M.B. Hodgins. Human diseases: clues to cracking the connexin code? *Trends Cell Biol*, 11(1):2–6, 2001.

[11] K. Willecke J. Eiberger and et al. Structural and functional diversity of connexin genes in the mouse and human genome. *Biol Chem*, 383(5):725–737, 2002.

[12] R.S. Fischer and V.M. Fowler. Thematic minireview series: The state of the cytoskeleton in 2015. *J Biol Chem*, 290(28):17133–6, 2015.

[13] J. Kolega. Effects of mechanical tension on protrusive activity and microfilament and intermediate filament organization in an epidermal epithelium moving in culture. *J Cell Biol*, 102(4):1400–11, 1986.

[14] T.J. Mitchison. Evolution of a dynamic cytoskeleton. *Philos Trans R Soc Lond B Biol Sci*, 349(1329):299–304, 1995.

[15] E. Sackmann. How actin/myosin crosstalks guide the adhesion, locomotion and polarization of cells. *Biochim Biophys Acta*, 1853(11 Pt B):3132–42, 2015.

[16] M. Pilhofer M.S. Ladinsky and et al. Microtubules in bacteria: ancient tubulins build a five-protofilament homolog of the eukaryotic cytoskeleton. *PLoS Biol*, 9(12):e1001213, 2011.

[17] R.C. Weisenberg. Microtubule formation in vitro in solutions containing low calcium concentrations. *Science*, 177(4054):1104–5, 1972.

[18] R.C. Weisenberg W.J. Deery and P.J. Dickinson. Tubulin-nucleotide interactions during the polymerization and depolymerization of microtubules. *Biochemistry*, 15(19):4248–4254, 1976.

[19] S. Quintin S. Wang, et al., and M Labouesse. Non-centrosomal epidermal microtubules act in parallel to let-502/rock to promote c. elegans elongation. *Development*, 143(1):160–173, 2016.

[20] Masatoshi Takeichi. Dynamic contacts: rearranging adherens junctions to drive epithelial remodelling. *Nature reviews. Molecular cell biology*, 15(6):397, 2014.

[21] J.B. Bard and A.S. Ross. The morphogenesis of the ciliary body of the avian eye: I. lateral cell detachment facilitates epithelial folding. *Developmental biology*, 92(1):73–86, 1982.

[22] G.C. Schoenwolf and M.V. Franks. Quantitative analyses of changes in cell shapes during bending of the avian neural plate. *Developmental biology*, 105(2):257–272, 1984.

[23] B.E. Kerman A.M. Cheshire and D.J. Andrew. From fate to function: the drosophila trachea and salivary gland as models for tubulogenesis. *Differentiation*, 74(7):326–348, 2006.

[24] A.R. Fischer H. Elliot C. Waterman and G. Danuser. Myosin II controls cellular branching morphogenesis and migration in 3d by minimizing plasma membrane curvature. *Biophysical Journal*, 106(2):13a, 2014.

[25] Akankshi Munjal, Jean-Marc Philippe, Edwin Munro, and Thomas Lecuit. A self-organized biomechanical network drives shape changes during tissue morphogenesis. *Nature*, 524(7565):351, 2015.

[26] Guangliang Wang, M Lisa Manning, and Jeffrey D Amack. Regional cell shape changes control form and function of kupffer's vesicle in the zebrafish embryo. *Developmental biology*, 370(1):52–62, 2012.

[27] A.C. Martin M. Gelbart and et al. Integration of contractile forces during tissue invagination. *The Journal of cell biology*, pages jcb–200910099, 2010.

[28] Romain Levayer, Anne Pelissier-Monier, and Thomas Lecuit. Spatial regulation of dia and myosin-ii by rhogef2 controls initiation of e-cadherin endocytosis during epithelial morphogenesis. *Nature cell biology*, 13(5):529, 2011.

[29] M. Roh-Johnson G. Shemer and et al. Triggering a cell shape change by exploiting pre-existing actomyosin contractions. *Science (New York, NY)*, 335(6073):1232, 2012.

[30] Carl-Philipp Heisenberg and Yohanns Bellaïche. Forces in tissue morphogenesis and patterning. *Cell*, 153(5):948–962, 2013.

[31] F. Bosveld I. Bonnet and et al. Mechanical control of morphogenesis by fat/dachsous/four-jointed planar cell polarity pathway. *Science*, 336(6082):724–727, 2012.

[32] Amy Brittle, Chloe Thomas, and David Strutt. Planar polarity specification through asymmetric subcellular localization of fat and dachsous. *Current biology*, 22(10):907–914, 2012.

[33] Abhijit A Ambegaonkar, Guohui Pan, Madhav Mani, Yongqiang Feng, and Kenneth D Irvine. Propagation of dachsous-fat planar cell polarity. *Current Biology*, 22(14):1302–1308, 2012.

[34] Yaopan Mao, Cordelia Rauskolb, Eunjoo Cho, Wei-Li Hu, Heather Hayter, Ginny Minihan, Flora N Katz, and Kenneth D Irvine. Dachs: an unconventional myosin that functions downstream of fat to regulate growth, affinity and gene expression in drosophila. *Development*, 133(13):2539–2551, 2006.

[35] Cordelia Rauskolb, Guohui Pan, BVVG Reddy, Hyangyee Oh, and Kenneth D Irvine. Zyxin links fat signaling to the hippo pathway. *PLoS biology*, 9(6):e1000624, 2011.

[36] Huimin Zhang, Frédéric Landmann, Hala Zahreddine, David Rodriguez, Marc Koch, and Michel Labouesse. A tension-induced mechanotransduction pathway promotes epithelial morphogenesis. *Nature*, 471(7336):99, 2011.

[37] J Todd Blankenship, Stephanie T Backovic, Justina SP Sanny, Ori Weitz, and Jennifer A Zallen. Multicellular rosette formation links planar cell polarity to tissue morphogenesis. *Developmental cell*, 11(4):459–470, 2006.

[38] Rodrigo Fernandez-Gonzalez, Sérgio de Matos Simoes, Jens-Christian Röper, Suzanne Eaton, and Jennifer A Zallen. Myosin ii dynamics are regulated by tension in intercalating cells. *Developmental cell*, 17(5):736–743, 2009.

[39] Benoît Aigouy, Reza Farhadifar, Douglas B Staple, Andreas Sagner, Jens-Christian Röper, Frank Jülicher, and Suzanne Eaton. Cell flow reorients the axis of planar polarity in the wing epithelium of drosophila. *Cell*, 142(5):773–786, 2010.

[40] Andreas Sagner, Matthias Merkel, Benoit Aigouy, Julia Gaebel, Marko Brankatschk, Frank Jülicher, and Suzanne Eaton. Establishment of global patterns of planar polarity during growth of the drosophila wing epithelium. *Current Biology*, 22(14):1296–1301, 2012.

[41] Olivier Hamant, Marcus G Heisler, Henrik Jönsson, Pawel Krupinski, Magalie Uyttewaal, Plamen Bokov, Francis Corson, Patrik Sahlin, Arezki Boudaoud, Elliot M Meyerowitz, et al. Developmental patterning by mechanical signals in arabidopsis. *science*, 322(5908):1650–1655, 2008.

[42] Erika E Kuchen, Samantha Fox, Pierre Barbier de Reuille, Richard Kennaway, Sandra Bensmihen, Jerome Avondo, Grant M Calder, Paul Southam, Sarah Robinson, Andrew Bangham, et al. Generation of leaf shape through early patterns of growth and tissue polarity. *Science*, 335(6072):1092–1096, 2012.

[43] Sevan Hopyan, James Sharpe, and Yingzi Yang. Budding behaviors: Growth of the limb as a model of morphogenesis. *Developmental Dynamics*, 240(5):1054–1062, 2011.

[44] Caroline McKeown, Vida Praitis, and Judith Austin. sma-1 encodes a betah-spectrin homolog required for caenorhabditis elegans morphogenesis. *Development*, 125(11):2087–2098, 1998.

[45] John E Sulston, E Schierenberg, John G White, and JN Thomson. The embryonic cell lineage of the nematode caenorhabditis elegans. *Developmental biology*, 100(1):64–119, 1983.

[46] Bernd Junkersdorf and Einhard Schierenberg. Embryogenesis in c. elegans after elimination of individual blastomeres or induced alteration of the cell division order. *Development Genes and Evolution*, 202(1):17–22, 1992.

[47] James R Priess and David I Hirsh. Caenorhabditis elegans morphogenesis: the role of the cytoskeleton in elongation of the embryo. *Developmental biology*, 117(1):156–173, 1986.

[48] Michalina Smolarkiewicz and Pankaj Dhonukshe. Formative cell divisions: principal determinants of plant morphogenesis. *Plant and Cell Physiology*, 54(3):333–342, 2012.

[49] Joao Firmino, Didier Rocancourt, Mehdi Saadaoui, Chloe Moreau, and Jerome Gros. Cell division drives epithelial cell rearrangements during gastrulation in chick. *Developmental cell*, 36(3):249–261, 2016.

[50] Amata Hornbruch and L Wolpert. Cell division in the early growth and morphogenesis of the chick limb. *Nature*, 226(5247):764–766, 1970.

[51] Cristina I Llavata Peris, Eike H Rademacher, and Dolf Weijers. Chapter one-green beginnings–pattern formation in the early plant embryo. *Current topics in developmental biology*, 91:1–27, 2010.

[52] Sangho Jeong, Martin Bayer, and Wolfgang Lukowitz. Taking the very first steps: from polarity to axial domains in the early arabidopsis embryo. *Journal of experimental botany*, 62(5):1687–1697, 2010.

[53] G Jurgens, U Mayer, M Busch, W Lukowitz, and T Laux. Pattern formation in the arabidopsis embryo: a genetic perspective. *Philosophical Transactions of the Royal Society of London B: Biological Sciences*, 350(1331):19–25, 1995.

[54] Ive De Smet and Tom Beeckman. Asymmetric cell division in land plants and algae: the driving force for differentiation. *Nature reviews. Molecular cell biology*, 12(3):177, 2011.

[55] Gerd Jürgens, Markus Grebe, and Thomas Steinmann. Establishment of cell polarity during early plant development. *Current opinion in cell biology*, 9(6):849–852, 1997.

[56] Thomas Berleth and G Jurgens. The role of the monopteros gene in organising the basal body region of the arabidopsis embryo. *Development*, 118(2):575–587, 1993.

[57] Ramón A Torres-Ruiz and G Jurgens. Mutations in the fass gene uncouple pattern formation and morphogenesis in arabidopsis development. *Development*, 120(10):2967–2978, 1994.

[58] Jan Traas, Catherine Bellini, Philippe Nacry, Jocelyne Kronenberger, David Bouchez, and Michel Caboche. Normal differentiation patterns in plants lacking microtubular preprophase bands. *Nature*, 375(6533):676–677, 1995.

[59] Christine Camilleri, Juliette Azimzadeh, Martine Pastuglia, Catherine Bellini, Olivier Grandjean, and David Bouchez. The arabidopsis tonneau2 gene encodes a putative novel protein phosphatase 2a regulatory subunit essential for the control of the cortical cytoskeleton. *The Plant Cell Online*, 14(4):833–845, 2002.

[60] Gerd Jürgens, Ulrike Mayer, Thomas Berleth, Simon Miséra, et al. Genetic analysis of pattern formation in the arabidopsis embryo. *Development*, 113(Supplement 1):27–38, 1991.

[61] Didier Reinhardt, Therese Mandel, and Cris Kuhlemeier. Auxin regulates the initiation and radial position of plant lateral organs. *The Plant Cell*, 12(4):507–518, 2000.

[62] Jirí Friml, Anne Vieten, Michael Sauer, Dolf Weijers, et al. Efflux-dependent auxin gradients establish the apical-basal axis of arabidopsis. *Nature*, 426(6963):147, 2003.

[63] M. Furutani T. Vernoux and et al. Pin-formed1 and pinoid regulate boundary formation and cotyledon development in arabidopsis embryogenesis. *Development*, 131(20):5021–5030, 2004.

[64] N. Dharmasiri S. Dharmasiri and et al. Plant development is regulated by a family of auxin receptor f box proteins. *Developmental cell*, 9(1):109–119, 2005.

[65] Christian S Hardtke and Thomas Berleth. The arabidopsis gene monopteros encodes a transcription factor mediating embryo axis formation and vascular development. *The EMBO journal*, 17(5):1405–1411, 1998.

[66] Thorsten Hamann, Ulrike Mayer, and G Jurgens. The auxin-insensitive bodenlos mutation affects primary root formation and apical-basal patterning in the arabidopsis embryo. *Development*, 126(7):1387–1395, 1999.

[67] T. Hamann, E. Benkova, and et al. The arabidopsis bodenlos gene encodes an auxin response protein inhibiting monopteros-mediated embryo patterning. *Genes & Development*, 16(13):1610–1615, 2002.

[68] D. Weijers, A. Schlereth, and et al. Auxin triggers transient local signaling for cell specification in arabidopsis embryogenesis. *Developmental cell*, 10(2):265–270, 2006.

[69] S.K. Song and S.E. Clark. Pol and related phosphatases are dosage-sensitive regulators of meristem and organ development in arabidopsis. *Developmental biology*, 285(1):272–284, 2005.

[70] J.M. Gagne S.K. Song and S.E. Clark. Poltergeist and pll1 are required for stem cell function with potential roles in cell asymmetry and auxin signaling. *Communicative & integrative biology*, 1(1):53–55, 2008.

[71] J.M. Gagne and S.E. Clark. The arabidopsis stem cell factor poltergeist is membrane localized and phospholipid stimulated. *The Plant Cell*, 22(3):729–743, 2010.

[72] R. Bodmer and Y.N. Jan. Morphological differentiation of the embryonic peripheral neurons in drosophila. *Development genes and evolution*, 196(2):69–77, 1987.

[73] E. Rozbicki M. Chuai and et al. Myosin ii-mediated cell shape changes and cell intercalation contribute to primitive streak formation. *Nature cell biology*, 17(4):397, 2015.

[74] O. Voiculescu F. Bertocchini and et al. The amniote primitive streak is defined by epithelial cell intercalation before gastrulation. *Nature*, 449(7165):1049, 2007.

[75] O. Voiculescu L. Bodenstein and et al. Local cell interactions and self-amplifying individual cell ingression drive amniote gastrulation. *Elife*, 3:e01817, 2014.

[76] P. Friedl and D. Gilmour. Collective cell migration in morphogenesis, regeneration and cancer. *Nature reviews Molecular cell biology*, 10(7):445–457, 2009.

[77] Denise J Montell. Morphogenetic cell movements: diversity from modular mechanical properties. *Science*, 322(5907):1502–1505, 2008.

[78] Erika R Geisbrecht and Denise J Montell. Myosin vi is required for e-cadherin-mediated border cell migration. *Nature cell biology*, 4(8):616, 2002.

[79] Pernille Rørth. Collective guidance of collective cell migration. *Trends in cell biology*, 17(12):575–579, 2007.

[80] Anne Marie Murphy and Denise J Montell. Cell type-specific roles for cdc42, rac, and rhol in drosophila oogenesis. *The Journal of cell biology*, 133(3):617–630, 1996.

[81] Tudor A Fulga and Pernille Rørth. Invasive cell migration is initiated by guided growth of long cellular extensions. *Nature cell biology*, 4(9):715, 2002.

[82] P. Niewiadomska D. Godt and U. Tepass. De-cadherin is required for intercellular motility during drosophila oogenesis. *The Journal of cell biology*, 144(3):533–547, 1999.

[83] Anne Pacquelet and Pernille Rørth. Regulatory mechanisms required for de-cadherin function in cell migration and other types of adhesion. *J Cell Biol*, 170(5):803–812, 2005.

[84] Kevin A Edwards and Daniel P Kiehart. Drosophila nonmuscle myosin ii has multiple essential roles in imaginal disc and egg chamber morphogenesis. *Development*, 122(5):1499–1511, 1996.

[85] A. Bianco M. Poukkula and et al. Two distinct modes of guidance signalling during collective migration of border cells. *Nature*, 448(7151):362–365, 2007.

[86] P. Duchek K. Somogyi and et al. Guidance of cell migration by the drosophila pdgf/vegf receptor. *Cell*, 107(1):17–26, 2001.

[87] C. Ribeiro A. Ebner and M. Affolter. In vivo imaging reveals different cellular functions for fgf and dpp signaling in tracheal branching morphogenesis. *Developmental cell*, 2(5):677–683, 2002.

[88] E. Caussinus J. Colombelli and M. Affolter. Tip-cell migration controls stalk-cell intercalation during drosophila tracheal tube elongation. *Current biology*, 18(22):1727–1734, 2008.

[89] M. Llimargas. The notch pathway helps to pattern the tips of the drosophila tracheal branches by selecting cell fates. *Development*, 126(11):2355–2364, 1999.

[90] A.S. Ghabrial and M.A. Krasnow. Social interactions among epithelial cells during tracheal branching morphogenesis. *Nature*, 441(7094):746, 2006.

[91] Alain Ghysen and Christine Dambly-Chaudière. The lateral line microcosmos. *Genes & development*, 21(17):2118–2130, 2007.

[92] Nicolas B David, Dora Sapède, Laure Saint-Etienne, Christine Thisse, Bernard Thisse, Christine Dambly-Chaudière, Frédéric M Rosa, and Alain Ghysen. Molecular basis of cell migration in the fish lateral line: role of the chemokine receptor cxcr4 and of its ligand, sdf1. *Proceedings of the National Academy of Sciences*, 99(25):16297–16302, 2002.

[93] Petra Haas and Darren Gilmour. Chemokine signaling mediates self-organizing tissue migration in the zebrafish lateral line. *Developmental cell*, 10(5):673–680, 2006.

[94] Virginie Lecaudey, Gulcin Cakan-Akdogan, William HJ Norton, and Darren Gilmour. Dynamic fgf signaling couples morphogenesis and migration in the zebrafish lateral line primordium. *Development*, 135(16):2695–2705, 2008.

[95] Alex Nechiporuk and David W Raible. Fgf-dependent mechanosensory organ patterning in zebrafish. *Science*, 320(5884):1774–1777, 2008.

[96] Guillaume Valentin, Petra Haas, and Darren Gilmour. The chemokine sdf1a coordinates tissue migration through the spatially restricted activation of cxcr7 and cxcr4b. *Current Biology*, 17(12):1026–1031, 2007.

[97] Christine Dambly-Chaudière, Nicolas Cubedo, and Alain Ghysen. Control of cell migration in the development of the posterior lateral line: antagonistic interactions between the chemokine receptors cxcr4 and cxcr7/rdc1. *BMC developmental biology*, 7(1):23, 2007.

[98] Bijan Boldajipour, Harsha Mahabaleshwar, Elena Kardash, Michal Reichman-Fried, Heiko Blaser, Sofia Minina, Duncan Wilson, Qiling Xu, and Erez Raz. Control of chemokine-guided cell migration by ligand sequestration. *Cell*, 132(3):463–473, 2008.

[99] Yelena Y Bernadskaya, Andre Wallace, Jillian Nguyen, William A Mohler, and Martha C Soto. Unc-40/dcc, sax-3/robo, and vab-1/eph polarize f-actin during embryonic morphogenesis by regulating the wave/scar actin nucleation complex. *PLoS genetics*, 8(8):e1002863, 2012.

[100] Falshruti B Patel, Yelena Y Bernadskaya, Esteban Chen, Aesha Jobanputra, Zahra Pooladi, Kristy L Freeman, Christelle Gally, William A Mohler, and Martha C Soto. The wave/scar complex promotes polarized cell movements and actin enrichment in epithelia during c. elegans embryogenesis. *Developmental biology*, 324(2):297–309, 2008.

[101] Mariko Sawa, Shiro Suetsugu, Asako Sugimoto, Hiroaki Miki, Masayuki Yamamoto, and Tadaomi Takenawa. Essential role of the c. elegans arp2/3 complex in cell migration during ventral enclosure. *Journal of cell science*, 116(8):1505–1518, 2003.

[102] Martha C Soto, Hiroshi Qadota, Katsuhisa Kasuya, Makiko Inoue, Daisuke Tsuboi, Craig C Mello, and Kozo Kaibuchi. The gex-2 and gex-3 proteins are required for tissue morphogenesis and cell migrations in c. elegans. *Genes & development*, 16(5):620–632, 2002.

[103] Svitlana Havrylenko, Philippe Noguera, Majdouline Abou-Ghali, John Manzi, Fahima Faqir, Audrey Lamora, Christophe Guérin, Laurent Blanchoin, and Julie Plastino. Wave binds ena/vasp for enhanced arp2/3 complex–based actin assembly. *Molecular biology of the cell*, 26(1):55–65, 2015.

[104] Rajat Rohatgi, Le Ma, Hiroaki Miki, Marco Lopez, Tomas Kirchhausen, Tadaomi Takenawa, and Marc W Kirschner. The interaction between n-wasp and the arp2/3 complex links cdc42-dependent signals to actin assembly. *Cell*, 97(2):221–231, 1999.

[105] Jim Withee, Barbara Galligan, Nancy Hawkins, and Gian Garriga. Caenorhabditis elegans wasp and ena/vasp proteins play compensatory roles in morphogenesis and neuronal cell migration. *Genetics*, 167(3):1165–1176, 2004.

[106] Thanh TK Vuong-Brender, Xinyi Yang, and Michel Labouesse. Chapter thirty-five-c. elegans embryonic morphogenesis. *Current topics in developmental biology*, 116:597–616, 2016.

[107] MARIA Leptin and BARBARA Grunewald. Cell shape changes during gastrulation in drosophila. *Development*, 110(1):73–84, 1990.

[108] DARI Sweeton, SUKI Parks, MICHAEL Costa, and ERIC Wieschaus. Gastrulation in drosophila: the formation of the ventral furrow and posterior midgut invaginations. *Development*, 112(3):775–789, 1991.

[109] Matteo Rauzi, Uros Krzic, Timothy E Saunders, Matej Krajnc, Primož Ziherl, Lars Hufnagel, and Maria Leptin. Embryo-scale tissue mechanics during drosophila gastrulation movements. *Nature communications*, 6, 2015.

[110] Maria Leptin. Gastrulation movements: the logic and the nuts and bolts. *Developmental cell*, 8(3):305–320, 2005.

[111] Maria Leptin. Gastrulation in drosophila: the logic and the cellular mechanisms. *The EMBO journal*, 18(12):3187–3192, 1999.

[112] MICHAEL Costa, DARI Sweeton, and ERIC Wieschaus. Gastrulation in drosophila: cellular mechanisms of morphogenetic movements. *The development of Drosophila melanogaster*, 1:425–465, 1993.

[113] Vito Conte, Florian Ulrich, Buzz Baum, Jose Muñoz, Jim Veldhuis, Wayne Brodland, and Mark Miodownik. A biomechanical analysis of ventral furrow formation in the drosophila melanogaster embryo. *PLoS One*, 7(4):e34473, 2012.

[114] Akankshi Munjal and Thomas Lecuit. Actomyosin networks and tissue morphogenesis. *Development*, 141(9):1789–1793, 2014.

[115] Bernard Moussian and Siegfried Roth. Dorsoventral axis formation in the drosophila embryoshaping and transducing a morphogen gradient. *Current biology*, 15(21):R887–R899, 2005.

[116] David S Stein and Leslie M Stevens. Maternal control of the drosophila dorsal–ventral body axis. *Wiley Interdisciplinary Reviews: Developmental Biology*, 3(5):301–330, 2014.

[117] David Kosman, Y Tony Ip, Michael Levine, and Kavita Arora. Establishment of the mesoderm-neuroectoderm boundary in the drosophila embryo. *Science*, pages 118–122, 1991.

[118] Alyssa J Manning, Kimberly A Peters, Mark Peifer, and Stephen L Rogers. Regulation of epithelial morphogenesis by the g-protein coupled receptor mist and its ligand fog. *Science signaling*, 6(301):ra98, 2013.

[119] Stephen Kerridge, Akankshi Munjal, Jean-Marc Philippe, Ankita Jha, Alain Garcia De Las Bayonas, Andrew j Saurin, and Thomas Lecuit. Modular activation of rho1 by gpcr signalling imparts polarized myosin ii activation during morphogenesis. *Nature cell biology*, 18(3):261, 2016.

[120] Sam J Mathew, Stephen Kerridge, and Maria Leptin. A small genomic region containing several loci required for gastrulation in drosophila. *PLoS One*, 4(10):e7437, 2009.

[121] Alyssa J Manning and Stephen L Rogers. The fog signaling pathway: insights into signaling in morphogenesis. *Developmental biology*, 394(1):6–14, 2014.

[122] Elise Walck-Shannon and Jeff Hardin. Cell intercalation from top to bottom. *Nature reviews. Molecular cell biology*, 15(1):34, 2014.

[123] Kenneth D Irvine and Eric Wieschaus. Cell intercalation during drosophila germband extension and its regulation by pair-rule segmentation genes. *Development*, 120(4):827–841, 1994.

[124] Claire Bertet, Lawrence Sulak, and Thomas Lecuit. Myosin-dependent junction remodelling controls planar cell intercalation and axis elongation. *Nature*, 429(6992):667, 2004.

[125] Jennifer A Zallen and Eric Wieschaus. Patterned gene expression directs bipolar planar polarity in drosophila. *Developmental cell*, 6(3):343–355, 2004.

[126] Matteo Rauzi, Pascale Verant, Thomas Lecuit, and Pierre-Francois Lenne. Nature and anisotropy of cortical forces orienting drosophila tissue morphogenesis. *Nature cell biology*, 10(12):1401, 2008.

[127] Thomas Lecuit and Pierre-Francois Lenne. Cell surface mechanics and the control of cell shape, tissue patterns and morphogenesis. *Nature reviews. Molecular cell biology*, 8(8):633, 2007.

[128] Claudio Collinet, Matteo Rauzi, Pierre-Francois Lenne, and Thomas Lecuit. Local and tissue-scale forces drive oriented junction growth during tissue extension. *Nature cell biology*, 17(10):1247, 2015.

[129] Mayuko Nishimura, Yoshiko Inoue, and Shigeo Hayashi. A wave of egfr signaling determines cell alignment and intercalation in the drosophila tracheal placode. *Development*, 134(23):4273–4282, 2007.

[130] Benjamin D Williams and Robert H Waterston. Genes critical for muscle development and function in caenorhabditis elegans identified through lethal mutations. *The Journal of cell biology*, 124(4):475–490, 1994.

[131] Heidi N Fridolfsson and Daniel A Starr. Kinesin-1 and dynein at the nuclear envelope mediate the bidirectional migrations of nuclei. *The Journal of cell biology*, 191(1):115–128, 2010.

[132] Elise Walck-Shannon, David Reiner, and Jeff Hardin. Polarized rac-dependent protrusions drive epithelial intercalation in the embryonic epidermis of c. elegans. *Development*, 142(20):3549–3560, 2015.

[133] Daniel A Starr, Greg J Hermann, Christian J Malone, William Fixsen, James R Priess, H Robert Horvitz, and Min Han. unc-83 encodes a novel component of the nuclear envelope and is essential for proper nuclear migration. *Development*, 128(24):5039–5050, 2001.

[134] Paul J Heid, William B Raich, Ryan Smith, William A Mohler, Kristin Simokat, Steven B Gendreau, Joel H Rothman, and Jeff Hardin. The zinc finger protein die-1 is required for late events during epithelial cell rearrangement in c. elegans. *Developmental biology*, 236(1):165–180, 2001.

[135] Xin Li, Isabelle Roszko, Diane S Sepich, Mingwei Ni, Heidi E Hamm, Florence L Marlow, and Lilianna Solnica-Krezel. Gpr125 modulates dishevelled distribution and planar cell polarity signaling. *Development*, 140(14):3028–3039, 2013.

[136] Lance A Davidson, Mungo Marsden, Raymond Keller, and Douglas W DeSimone. Integrin α 5 β 1 and fibronectin regulate polarized cell protrusions required for xenopus convergence and extension. *Current biology*, 16(9):833–844, 2006.

[137] Ivan BN Clark, Villö Muha, Anna Klingseisen, Maria Leptin, and Hans-Arno J Müller. Fibroblast growth factor signalling controls successive cell behaviours during mesoderm layer formation in drosophila. *Development*, 138(13):2705–2715, 2011.

[138] Takashi Shimizu, Taijiro Yabe, Osamu Muraoka, Shigenobu Yonemura, Shinsuke Aramaki, Kohei Hatta, Young-Ki Bae, Hideaki Nojima, and Masahiko Hibi. E-cadherin is required for gastrulation cell movements in zebrafish. *Mechanisms of development*, 122(6):747–763, 2005.

[139] Robert Bensch, Sungmin Song, Olaf Ronneberger, and Wolfgang Driever. Non-directional radial intercalation dominates deep cell behavior during zebrafish epiboly. *Biology open*, page BIO20134614, 2013.

[140] Dianne Fristrom. The cellular basis of epithelial morphogenesis. a review. *Tissue and Cell*, 20(5):645–690, 1988.

[141] Michael Costa, Bruce W Draper, and James R Priess. The role of actin filaments in patterning thecaenorhabditis eleganscuticle. *Developmental biology*, 184(2):373–384, 1997.

[142] Michael Costa, William Raich, Cristina Agbunag, Ben Leung, Jeff Hardin, and James R Priess. A putative catenin–cadherin system mediates morphogenesis of the caenorhabditis elegans embryo. *The Journal of cell biology*, 141(1):297–308, 1998.

[143] Marie Diogon, Frédéric Wissler, Sophie Quintin, Yasuko Nagamatsu, Satis Sookhareea, Frédéric Landmann, Harald Hutter, Nicolas Vitale, and Michel Labouesse. The rhogap rga-2 and let-502/rock achieve a balance of actomyosin-dependent forces in c. elegans epidermis to control morphogenesis. *Development*, 134(13):2469–2479, 2007.

[144] Thanh Thi Kim Vuong-Brender, Martine Ben Amar, Julien Pontabry, and Michel Labouesse. The interplay of stiffness and force anisotropies drives embryo elongation. *Elife*, 6, 2017.

[145] James R Sellers. Myosins: a diverse superfamily. *Biochimica et Biophysica Acta (BBA)-Molecular Cell Research*, 1496(1):3–22, 2000.

[146] Andrew D Chisholm and Jeff Hardin. Epidermal morphogenesis. *WormBook*, 2005.

[147] Christelle Gally, Frédéric Wissler, Hala Zahreddine, Sophie Quintin, Frédéric Landmann, and Michel Labouesse. Myosin ii regulation during c. elegans embryonic elongation: Let-502/rock, mrck-1 and pak-1, three kinases with different roles. *Development*, 136(18):3109–3119, 2009.

[148] Christine Ruff, Marcus Furch, Bernhard Brenner, Dietmar J Manstein, and Edgar Meyhöfer. Single-molecule tracking of myosins with genetically engineered amplifier domains. *Nature Structural & Molecular Biology*, 8(3):226, 2001.

[149] Ivan Rayment, Hazel M Holden, Michael Whittaker, Christopher B Yohn, Michael Lorenz, Kenneth C Holmes, and Ronald A Milligan. Structure of the actin-myosin complex and its implications for muscle contraction. *SCIENCE-NEW YORK THEN WASHINGTON-*, 261:58–58, 1993.

[150] Jeffrey T Finer, Robert M Simmons, and James A Spudich. Single myosin molecule mechanics: piconewton forces and nanometre steps. *Nature*, 368(6467):113–119, 1994.

[151] Richard Niederman and Thomas D Pollard. Human platelet myosin. ii. in vitro assembly and structure of myosin filaments. *The Journal of Cell Biology*, 67(1):72–92, 1975.

[152] ML Gardel, F Nakamura, JH Hartwig, JC Crocker, TP Stossel, and DA Weitz. Prestressed f-actin networks cross-linked by hinged filamins replicate mechanical properties of cells. *Proceedings of the National Academy of Sciences of the United States of America*, 103(6):1762–1767, 2006.

[153] Masahiko Sato, William H Schwarz, and Thomas D Pollard. Dependence of the mechanical properties of actin/α-actinin gels on deformation rate. *Nature*, 325(6107):828–830, 1987.

[154] D Humphrey, C Duggan, D Saha, D Smith, and J Käs. Active fluidization of polymer networks through molecular motors. *Nature*, 416(6879):413–416, 2002.

[155] Romain Levayer and Thomas Lecuit. Biomechanical regulation of contractility: spatial control and dynamics. *Trends in cell biology*, 22(2):61–81, 2012.

[156] Anne-Cecile Reymann, Fabio Staniscia, Anna Erzberger, Guillaume Salbreux, and Stephan W Grill. Cortical flow aligns actin filaments to form a furrow. *eLife*, 5:e17807, 2016.

[157] Mirjam Mayer, Martin Depken, Justin S Bois, Frank Jülicher, and Stephan W Grill. Anisotropies in cortical tension reveal the physical basis of polarizing cortical flows. *Nature*, 467(7315):617, 2010.

[158] Mirjam Mayer, Martin Depken, Justin S Bois, Frank Jülicher, and Stephan W Grill. Anisotropies in cortical tension reveal the physical basis of polarizing cortical flows. *Nature*, 467(7315):617, 2010.

[159] Anne-Cecile Reymann, Fabio Staniscia, Anna Erzberger, Guillaume Salbreux, and Stephan W Grill. Cortical flow aligns actin filaments to form a furrow. *eLife*, 5:e17807, 2016.

[160] Akankshi Munjal, Jean-Marc Philippe, Edwin Munro, and Thomas Lecuit. A self-organized biomechanical network drives shape changes during tissue morphogenesis. *Nature*, 524(7565):351, 2015.

[161] Andreas Wissmann, Julia Ingles, James D McGhee, and Paul E Mains. Caenorhabditis elegans let-502 is related to rho-binding kinases and human myotonic dystrophy kinase and interacts genetically with a homolog of the regulatory subunit of smooth muscle myosin phosphatase to affect cell shape. *Genes & Development*, 11(4):409–422, 1997.

[162] Andreas Wissmann, Julia Ingles, and Paul E Mains. Thecaenorhabditis elegans mel-11myosin phosphatase regulatory subunit affects tissue contraction in the somatic gonad and the embryonic epidermis and genetically interacts with the rac signaling pathway. *Developmental biology*, 209(1):111–127, 1999.

[163] Benjamin G Chan, Simon K Rocheleau, Ryan B Smit, and Paul E Mains. The rho guanine exchange factor rhgf-2 acts through the rho-binding kinase let-502 to mediate embryonic elongation in c. elegans. *Developmental biology*, 405(2):250–259, 2015.

[164] Alisa J Piekny, Jacque-Lynne F Johnson, Gwendolyn D Cham, and Paul E Mains. The caenorhabditis elegans nonmuscle myosin genes nmy-1 and nmy-2 function as redundant components of the let-502/rho-binding kinase and mel-11/myosin phosphatase pathway during embryonic morphogenesis. *Development*, 130(23):5695–5704, 2003.

[165] Christopher A Shelton, J Clayton Carter, Gregory C Ellis, and Bruce Bowerman. The nonmuscle myosin regulatory light chain gene mlc-4 is required for cytokinesis, anterior-posterior polarity, and body morphology during caenorhabditis elegans embryogenesis. *The Journal of cell biology*, 146(2):439–451, 1999.

[166] Emmanuel Martin, Sharon Harel, Bernard Nkengfac, Karim Hamiche, Mathieu Neault, and Sarah Jenna. pix-1 controls early elongation in parallel with mel-11 and let-502 in caenorhabditis elegans. *PloS one*, 9(4):e94684, 2014.

[167] Chrisotpher A Vanneste, David Pruyne, and Paul E Mains. The role of the formin gene fhod-1 in c. elegans embryonic morphogenesis. In *Worm*, page e25040. Taylor & Francis, 2013.

[168] Asako Shindo and John B Wallingford. Pcp and septins compartmentalize cortical actomyosin to direct collective cell movement. *Science*, 343(6171):649–652, 2014.

[169] Jeffrey S Simske, Mathias Köppen, Paul Sims, Jonathan Hodgkin, Alicia Yonkof, and Jeff Hardin. The cell junction protein vab-9 regulates adhesion and epidermal morphology in c. elegans. *Nature cell biology*, 5(7):619, 2003.

[170] Jonathan Pettitt, Elisabeth A Cox, Ian D Broadbent, Aileen Flett, and Jeff Hardin. The caenorhabditis elegans p120 catenin homologue, jac-1, modulates cadherin–catenin function during epidermal morphogenesis. *The Journal of cell biology*, 162(1):15–22, 2003.

[171] Renaud Legouis, Anne Gansmuller, Satis Sookhareea, Julia M Bosher, David L Baillie, and Michel Labouesse. Let-413 is a basolateral protein required for the assembly of adherens junctions in caenorhabditis elegans. *Nature Cell Biology*, 2(7):415, 2000.

[172] Jonathan S Coravos and Adam C Martin. Apical sarcomere-like actomyosin contracts nonmuscle drosophila epithelial cells. *Developmental cell*, 39(3):346–358, 2016.

[173] Tobias I Baskin. Anisotropic expansion of the plant cell wall. *Annu. Rev. Cell Dev. Biol.*, 21:203–222, 2005.

[174] Christina Lockwood, Ronen Zaidel-Bar, and Jeff Hardin. The c. elegans zonula occludens ortholog cooperates with the cadherin complex to recruit actin during morphogenesis. *Current Biology*, 18(17):1333–1337, 2008.

[175] Robert H Waterston. The minor myosin heavy chain, mhca, of caenorhabditis elegans is necessary for the initiation of thick filament assembly. *The EMBO Journal*, 8(11):3429, 1989.

[176] Robert J Barstead, Lawrence Kleiman, and Robert H Waterston. Cloning, sequencing, and mapping of an α-actinin gene from the nematode caenorhabditis elegans. *Cytoskeleton*, 20(1):69–78, 1991.

[177] G Ross Francis and Robert H Waterston. Muscle organization in caenorhabditis elegans: localization of proteins implicated in thin filament attachment and i-band organization. *The Journal of cell biology*, 101(4):1532–1549, 1985.

[178] Raymond YN Lee, Leslie Lobel, Michael Hengartner, H Robert Horvitz, and Leon Avery. Mutations in the α1 subunit of an l-type voltage-activated ca 2+ channel cause myotonia in caenorhabditis elegans. *The EMBO journal*, 16(20):6066–6076, 1997.

[179] Teresa M Rogalski, Gregory P Mullen, Mary M Gilbert, Benjamin D Williams, and Donald G Moerman. The unc-112 gene in caenorhabditis elegansencodes a novel component of cell–matrix adhesion structures required for integrin localization in the muscle cell membrane. *J Cell Biol*, 150(1):253–264, 2000.

[180] Ross Francis and Robert H Waterston. Muscle cell attachment in caenorhabditis elegans. *The Journal of cell biology*, 114(3):465–479, 1991.

[181] Huimin Zhang and Michel Labouesse. The making of hemidesmosome structures in vivo. *Developmental Dynamics*, 239(5):1465–1476, 2010.

[182] Julia M Bosher, Bum-Soo Hahn, Renaud Legouis, Satis Sookhareea, Robby M Weimer, Anne Gansmuller, Andrew D Chisholm, Ann M Rose, Jean-Louis Bessereau, and Michel Labouesse. The caenorhabditis elegans vab-10 spectraplakin isoforms protect the epidermis against internal and external forces. *The Journal of cell biology*, 161(4):757–768, 2003.

[183] Arnoud Sonnenberg and Ronald KH Liem. Plakins in development and disease. *Experimental cell research*, 313(10):2189–2203, 2007.

[184] Bum-Soo Hahn and Michel Labouesse. Tissue integrity: hemidesmosomes and resistance to stress. *Current biology*, 11(21):R858–R861, 2001.

[185] Mark Bercher, Jim Wahl, Bruce E Vogel, Charles Lu, Edward M Hedgecock, David H Hall, and John D Plenefisch. mua-3, a gene required for mechanical tissue integrity in caenorhabditis elegans, encodes a novel transmembrane protein of epithelial attachment complexes. *J Cell Biol*, 154(2):415–426, 2001.

[186] Leexan Hong, Tricia Elbl, James Ward, Clara Franzini-Armstrong, Krystyna K Rybicka, Beth K Gatewood, David L Baillie, and Elizabeth A Bucher. Mup-4 is a novel transmembrane protein with functions in epithelial cell adhesion in caenorhabditis elegans. *J Cell Biol*, 154(2):403–414, 2001.

[187] Michelle Coutu Hresko, Lawrence A Schriefer, Paresh Shrimankar, and Robert H Waterston. Myotactin, a novel hypodermal protein involved in muscle–cell adhesion incaenorhabditis elegans. *The Journal of cell biology*, 146(3):659–672, 1999.

[188] Beth K Gatewood and Elizabeth A Bucher. The mup-4 locus in caenorhabditis elegans is essential for hypodermal integrity, organismal morphogenesis and embryonic body wall muscle position. *Genetics*, 146(1):165–183, 1997.

[189] Sonya N Gettner, Cynthia Kenyon, and Louis F Reichardt. Characterization of beta pat-3 heterodimers, a family of essential integrin receptors in c. elegans. *The Journal of cell biology*, 129(4):1127–1141, 1995.

[190] Gary L Moulder, MING MING Huang, Robert H Waterston, and Robert J Barstead. Talin requires beta-integrin, but not vinculin, for its assembly into focal adhesion-like structures in the nematode caenorhabditis elegans. *Molecular Biology of the Cell*, 7(8):1181–1193, 1996.

[191] Oliver Hobert, Donald G Moerman, Kathleen A Clark, Mary C Beckerle, and Gary Ruvkun. A conserved lim protein that affects muscular adherens junction integrity and mechanosensory function in caenorhabditis elegans. *The Journal of cell biology*, 144(1):45–57, 1999.

[192] A Craig Mackinnon, Hiroshi Qadota, Kenneth R Norman, Donald G Moerman, and Benjamin D Williams. C. elegans pat-4/ilk functions as an adaptor protein within integrin adhesion complexes. *Current Biology*, 12(10):787–797, 2002.

[193] Xinyi Lin, Hiroshi Qadota, Donald G Moerman, and Benjamin D Williams. C. elegans pat-6/actopaxin plays a critical role in the assembly of integrin adhesion complexes in vivo. *Current Biology*, 13(11):922–932, 2003.

[194] Guy M Benian, Tina L Tinley, Xuexin Tang, and Mark Borodovsky. The caenorhabditis elegans gene unc-89, required fpr muscle m-line assembly, encodes a giant modular protein composed of ig and signal transduction domains. *The Journal of Cell Biology*, 132(5):835–848, 1996.

[195] Jiang He, Ruobo Zhou, Zhuhao Wu, Monica A Carrasco, Peri T Kurshan, Jonathan E Farley, David J Simon, Guiping Wang, Boran Han, Junjie Hao, et al. Prevalent presence of periodic actin–spectrin-based membrane skeleton in a broad range of neuronal cell types and animal species. *Proceedings of the National Academy of Sciences*, 113(21):6029–6034, 2016.

[196] Kenneth Kin Lam Wong, Wenyang Li, Yanru An, Yangyang Duan, Zhuoheng Li, Yibin Kang, and Yan Yan. β-spectrin regulates the hippo signaling pathway and modulates the basal actin network. *Journal of Biological Chemistry*, 290(10):6397–6407, 2015.

[197] Xin-Tong Wu, Lian-Wen Sun, Xiao Yang, Dong Ding, Dong Han, and Yu-Bo Fan. The potential role of spectrin network in the mechanotransduction of mlo-y4 osteocytes. *Scientific reports*, 7, 2017.

[198] Marc Aristaeus de Asis, Manuel Pires, Kevin Lyon, and A Wayne Vogl. A network of spectrin and plectin surrounds the actin cuffs of apical tubulobulbar complexes in the rat. *Spermatogenesis*, 3(3):e25733, 2013.

[199] Kenneth R Norman and Donald G Moerman. α spectrin is essential for morphogenesis and body wall muscle formation in caenorhabditis elegans. *J Cell Biol*, 157(4):665–677, 2002.

[200] Suraj Moorthy, Lihsia Chen, and Vann Bennett. Caenorhabditis elegans β-g spectrin is dispensable for establishment of epithelial polarity, but essential for muscular and neuronal function. *The Journal of cell biology*, 149(4):915–930, 2000.

[201] Marc Hammarlund, Warren S Davis, and Erik M Jorgensen. Mutations in β-spectrin disrupt axon outgrowth and sarcomere structure. *The Journal of cell biology*, 149(4):931–942, 2000.

[202] Vida Praitis, Emily Ciccone, and Judith Austin. Sma-1 spectrin has essential roles in epithelial cell sheet morphogenesis in c. elegans. *Developmental biology*, 283(1):157–170, 2005.

[203] Wahyu Hendrati Raharjo, Vikas Ghai, Aidan Dineen, Michael Bastiani, and Jeb Gaudet. Cell architecture: surrounding muscle cells shape gland cell morphology in the caenorhabditis elegans pharynx. *Genetics*, 189(3):885–897, 2011.

[204] Pasquale Ciarletta, M Ben Amar, and Michel Labouesse. Continuum model of epithelial morphogenesis during caenorhabditis elegans embryonic elongation. *Philosophical Transactions of the Royal Society of London A: Mathematical, Physical and Engineering Sciences*, 367(1902):3379–3400, 2009.

[205] Douglas Corrigall, Rhian F Walther, Lilia Rodriguez, Pierre Fichelson, and Franck Pichaud. Hedgehog signaling is a principal inducer of myosin-ii-driven cell ingression in drosophila epithelia. *Developmental cell*, 13(5):730–742, 2007.

[206] Jen-Yi Lee and Richard M Harland. Actomyosin contractility and microtubules drive apical constriction in xenopus bottle cells. *Developmental biology*, 311(1):40–52, 2007.

[207] Chanjae Lee, Heather M Scherr, and John B Wallingford. Shroom family proteins regulate γ-tubulin distribution and microtubule architecture during epithelial cell shape change. *Development*, 134(7):1431–1441, 2007.

[208] Akif Uzman. Molecular biology of the cell: Alberts, b., johnson, a., lewis, j., raff, m., roberts, k., and walter, p., 2003.

[209] Robert P Ray, Alexis Matamoro-Vidal, Paulo S Ribeiro, Nic Tapon, David Houle, Isaac Salazar-Ciudad, and Barry J Thompson. Patterned anchorage to the apical extracellular matrix defines tissue shape in the developing appendages of drosophila. *Developmental cell*, 34(3):310–322, 2015.

[210] Bo Dong, Edouard Hannezo, and Shigeo Hayashi. Balance between apical membrane growth and luminal matrix resistance determines epithelial tubule shape. *Cell Reports*, 7(4):941–950, 2014.

[211] Isabelle Fernandes, Hélène Chanut-Delalande, Pierre Ferrer, Yvan Latapie, Lucas Waltzer, Markus Affolter, François Payre, and Serge Plaza. Zona pellucida domain proteins remodel the apical compartment for localized cell shape changes. *Developmental cell*, 18(1):64–76, 2010.

[212] Vincent P Mancuso, Jean M Parry, Luke Storer, Corey Poggioli, Ken CQ Nguyen, David H Hall, and Meera V Sundaram. Extracellular leucine-rich repeat proteins are required to organize the apical extracellular matrix and maintain epithelial junction integrity in c. elegans. *Development*, 139(5):979–990, 2012.

[213] Thanh Thi Kim Vuong-Brender, Shashi Kumar Suman, and Michel Labouesse. The apical ecm preserves embryonic integrity and distributes mechanical stress during morphogenesis. *Development*, pages dev–150383, 2017.

[214] Elisabeth Knust and Olaf Bossinger. Composition and formation of intercellular junctions in epithelial cells. *Science*, 298(5600):1955–1959, 2002.

[215] Mathias Köppen, Jeffrey S Simske, Paul A Sims, Bonnie L Firestein, David H Hall, Anthony D Radice, Christopher Rongo, and Jeffrey D Hardin. Cooperative regulation of ajm-1 controls junctional integrity in caenorhabditis elegans epithelia. *Nature cell biology*, 3(11):983–991, 2001.

[216] Laura McMahon, Renaud Legouis, Jean-Luc Vonesch, and Michel Labouesse. Assembly of c. elegans apical junctions involves positioning and compaction by let-413 and protein aggregation by the maguk protein dlg-1. *Journal of cell science*, 114(12):2265–2277, 2001.

[217] Olaf Bossinger, Ansgar Klebes, Christoph Segbert, Carin Theres, and Elisabeth Knust. Zonula adherens formation in caenorhabditis elegans requires dlg-1, the homologue of the drosophila gene discs large. *Developmental biology*, 230(1):29–42, 2001.

[218] Bonnie L Firestein and Christopher Rongo. Dlg-1 is a maguk similar to sap97 and is required for adherens junction formation. *Molecular biology of the cell*, 12(11):3465–3475, 2001.

[219] Christoph Segbert, Kevin Johnson, Carin Theres, Daniela van Fürden, and Olaf Bossinger. Molecular and functional analysis of apical junction formation in the gut epithelium of caenorhabditis elegans. *Developmental biology*, 266(1):17–26, 2004.

[220] Akira Asano, Kimiko Asano, Hiroyuki Sasaki, Mikio Furuse, and Shoichiro Tsukita. Claudins in caenorhabditis elegans: their distribution and barrier function in the epithelium. *Current biology*, 13(12):1042–1046, 2003.

[221] Allison M Lynch, Theresa Grana, Elisabeth Cox-Paulson, Annabelle Couthier, Michel Cameron, Ian Chin-Sang, Jonathan Pettitt, and Jeff Hardin. A genome-wide functional screen shows magi-1 is an l1cam-dependent stabilizer of apical junctions in c. elegans. *Current Biology*, 22(20):1891–1899, 2012.

[222] Patrick Humbert, Sarah Russell, and Helena Richardson. Dlg, scribble and lgl in cell polarity, cell proliferation and cancer. *Bioessays*, 25(6):542–553, 2003.

[223] Ronald Totong, Annita Achilleos, and Jeremy Nance. Par-6 is required for junction formation but not apicobasal polarization in c. elegans embryonic epithelial cells. *Development*, 134(7):1259–1268, 2007.

[224] Zita Balklava, Saumya Pant, Hanna Fares, and Barth D Grant. Genome-wide analysis identifies a general requirement for polarity proteins in endocytic traffic. *Nature cell biology*, 9(9):1066, 2007.

[225] Kathryn P Harris and Ulrich Tepass. Cdc42 and par proteins stabilize dynamic adherens junctions in the drosophila neuroectoderm through regulation of apical endocytosis. *J Cell Biol*, 183(6):1129–1143, 2008.

[226] Ben Leung, Greg J Hermann, and James R Priess. Organogenesis of the caenorhabditis elegans intestine. *Developmental biology*, 216(1):114–134, 1999.

[227] Annita Achilleos, Ann M Wehman, and Jeremy Nance. Par-3 mediates the initial clustering and apical localization of junction and polarity proteins during c. elegans intestinal epithelial cell polarization. *Development*, 137(11):1833–1842, 2010.

[228] Renaud Legouis, Fanny Jaulin-Bastard, Sonia Schott, Christel Navarro, Jean-Paul Borg, and Michel Labouesse. Basolateral targeting by leucine-rich repeat domains in epithelial cells. *EMBO reports*, 4(11):1096–1100, 2003.

[229] Jennifer Pilipiuk, Christophe Lefebvre, Tobias Wiesenfahrt, Renaud Legouis, and Olaf Bossinger. Increased ip 3/ca 2+ signaling compensates depletion of let-413/dlg-1 in c. elegans epithelial junction assembly. *Developmental biology*, 327(1):34–47, 2009.

[230] Denise S Walker, Sung Ly, Katherine C Lockwood, and Howard A Baylis. A direct interaction between ip 3 receptors and myosin ii regulates ip 3 signaling in c. elegans. *Current Biology*, 12(11):951–956, 2002.

[231] Christina L Thomas-Virnig, Paul A Sims, Jeffrey S Simske, and Jeff Hardin. The inositol 1, 4, 5-trisphosphate receptor regulates epidermal cell migration in caenorhabditis elegans. *Current biology*, 14(20):1882–1887, 2004.

[232] William B Raich, Cristina Agbunag, and Jeff Hardin. Rapid epithelial-sheet sealing in the caenorhabditis elegans embryo requires cadherin-dependent filopodial priming. *Current biology*, 9(20):1139–S1, 1999.

[233] Lihsia Chen, Bryan Ong, and Vann Bennett. Lad-1, the caenorhabditis elegans l1cam homologue, participates in embryonic and gonadal morphogenesis and is a substrate for fibroblast growth factor receptor pathway-dependent phosphotyrosine-based signaling. *J Cell Biol*, 154(4):841–856, 2001.

[234] Xuelin Wang, Junghun Kweon, Stephanie Larson, and Lihsia Chen. A role for the c. elegans l1cam homologue lad-1/sax-7 in maintaining tissue attachment. *Developmental biology*, 284(2):273–291, 2005.

[235] Mei Ding, Alexandr Goncharov, Yishi Jin, and Andrew D Chisholm. C. elegans ankyrin repeat protein vab-19 is a component of epidermal attachment structures and is essential for epidermal morphogenesis. *Development*, 130(23):5791–5801, 2003.

[236] Benjamin Podbilewicz and John G White. Cell fusions in the developing epithelia of c. elegans. *Developmental biology*, 161(2):408–424, 1994.

[237] Ranjana Sharma-Kishore, John G White, Eileen Southgate, and Benjamin Podbilewicz. Formation of the vulva in caenorhabditis elegans: a paradigm for organogenesis. *Development*, 126(4):691–699, 1999.

[238] Bruce B Wang, Michael M Müller-Immergluck, Judith Austin, Naomi Tamar Robinson, Andrew Chisholm, and Cynthia Kenyon. A homeotic gene cluster patterns the anteroposterior body axis of c. elegans. *Cell*, 74(1):29–42, 1993.

[239] William A Mohler, Jeffrey S Simske, Ellen M Williams-Masson, Jeffrey D Hardin, and John G White. Dynamics and ultrastructure of developmental cell fusions in the caenorhabditis elegans hypodermis. *Current biology*, 8(19):1087–1091, 1998.

[240] Gidi Shemer, Meital Suissa, Irina Kolotuev, Ken CQ Nguyen, David H Hall, and Benjamin Podbilewicz. Eff-1 is sufficient to initiate and execute tissue-specific cell fusion in c. elegans. *Current Biology*, 14(17):1587–1591, 2004.

[241] William A Mohler, Gidi Shemer, Jacob J del Campo, Clari Valansi, Eugene Opoku-Serebuoh, Victoria Scranton, Nirit Assaf, John G White, and Benjamin Podbilewicz. The type i membrane protein eff-1 is essential for developmental cell fusion. *Developmental cell*, 2(3):355–362, 2002.

[242] Yuan-Hung Chien, Ray Keller, Chris Kintner, and David R Shook. Mechanical strain determines the axis of planar polarity in ciliated epithelia. *Current Biology*, 25(21):2774–2784, 2015.

[243] Brian Mitchell, Jennifer L Stubbs, Fawn Huisman, Peter Taborek, Clare Yu, and Chris Kintner. The pcp pathway instructs the planar orientation of ciliated cells in the xenopus larval skin. *Current Biology*, 19(11):924–929, 2009.

[244] Wen Yih Aw, Bryan W Heck, Bradley Joyce, and Danelle Devenport. Transient tissue-scale deformation coordinates alignment of planar cell polarity junctions in the mammalian skin. *Current Biology*, 26(16):2090–2100, 2016.

[245] James P Mahaffey, Joaquim Grego-Bessa, Karel F Liem, and Kathryn V Anderson. Cofilin and vangl2 cooperate in the initiation of planar cell polarity in the mouse embryo. *Development*, 140(6):1262–1271, 2013.

[246] Chen Luxenburg, Evan Heller, H Amalia Pasolli, Sophia Chai, Maria Nikolova, Nicole Stokes, and Elaine Fuchs. Wdr1-mediated cell shape dynamics and cortical tension are essential for epidermal planar cell polarity. *Nature cell biology*, 17(5):592, 2015.

[247] Andreas Jenny. Planar cell polarity signaling in the drosophila eye. *Current topics in developmental biology*, 93:189, 2010.

[248] Masazumi Tada and JC Smith. Xwnt11 is a target of xenopus brachyury: regulation of gastrulation movements via dishevelled, but not through the canonical wnt pathway. *Development*, 127(10):2227–2238, 2000.

[249] George T Eisenhoffer, Patrick D Loftus, Masaaki Yoshigi, Hideo Otsuna, Chi-Bin Chien, Paul A Morcos, and Jody Rosenblatt. Crowding induces live cell extrusion to maintain homeostatic cell numbers in epithelia. *Nature*, 484(7395):546, 2012.

[250] Eliana Marinari, Aida Mehonic, Scott Curran, Jonathan Gale, Thomas Duke, and Buzz Baum. Live-cell delamination counterbalances epithelial growth to limit tissue overcrowding. *Nature*, 484(7395):542, 2012.

[251] Charlène Guillot and Thomas Lecuit. Mechanics of epithelial tissue homeostasis and morphogenesis. *Science*, 340(6137):1185–1189, 2013.

[252] Kevin J Sonnemann and William M Bement. Wound repair: toward understanding and integration of single-cell and multicellular wound responses. *Annual review of cell and developmental biology*, 27:237–263, 2011.

[253] Georgios Trichas, Aaron M Smith, Natalia White, Vivienne Wilkins, Tomoko Watanabe, Abigail Moore, Bradley Joyce, Jacintha Sugnaseelan, Tristan A Rodriguez, David Kay, et al. Multi-cellular rosettes in the mouse visceral endoderm facilitate the ordered migration of anterior visceral endoderm cells. *PLoS biology*, 10(2):e1001256, 2012.

[254] Tamako Nishimura, Hisao Honda, and Masatoshi Takeichi. Planar cell polarity links axes of spatial dynamics in neural-tube closure. *Cell*, 149(5):1084–1097, 2012.

[255] LA Davidson and RE Keller. Neural tube closure in xenopus laevis involves medial migration, directed protrusive activity, cell intercalation and convergent extension. *Development*, 126(20):4547–4556, 1999.

[256] Tamako Nishimura and Masatoshi Takeichi. Shroom3-mediated recruitment of rho kinases to the apical cell junctions regulates epithelial and neuroepithelial planar remodeling. *Development*, 135(8):1493–1502, 2008.

[257] Sérgio de Matos Simões, J Todd Blankenship, Ori Weitz, Dene L Farrell, Masako Tamada, Rodrigo Fernandez-Gonzalez, and Jennifer A Zallen. Rho-kinase directs bazooka/par-3 planar polarity during drosophila axis elongation. *Developmental cell*, 19(3):377–388, 2010.

[258] Matteo Rauzi, Pierre-François Lenne, and Thomas Lecuit. Planar polarized actomyosin contractile flows control epithelial junction remodelling. *Nature*, 468(7327):1110, 2010.

[259] Nicolas Olivier, Miguel A Luengo-Oroz, Louise Duloquin, Emmanuel Faure, Thierry Savy, Israël Veilleux, Xavier Solinas, Delphine Débarre, Paul Bourgine, Andrés Santos, et al. Cell lineage reconstruction of early zebrafish embryos using label-free nonlinear microscopy. *Science*, 329(5994):967–971, 2010.

[260] Andrea L Knox and Nicholas H Brown. Rap1 gtpase regulation of adherens junction positioning and cell adhesion. *Science*, 295(5558):1285–1288, 2002.

[261] Nabila Founounou, Nicolas Loyer, and Roland Le Borgne. Septins regulate the contractility of the actomyosin ring to enable adherens junction remodeling during cytokinesis of epithelial cells. *Developmental cell*, 24(3):242–255, 2013.

[262] Sophie Herszterg, Andrea Leibfried, Floris Bosveld, Charlotte Martin, and Yohanns Bellaiche. Interplay between the dividing cell and its neighbors regulates adherens junction formation during cytokinesis in epithelial tissue. *Developmental cell*, 24(3):256–270, 2013.

[263] Charlène Guillot and Thomas Lecuit. Adhesion disengagement uncouples intrinsic and extrinsic forces to drive cytokinesis in epithelial tissues. *Developmental cell*, 24(3):227–241, 2013.

[264] Mark Sheffield, Timothy Loveless, Jeff Hardin, and Jonathan Pettitt. C. elegans enabled exhibits novel interactions with n-wasp, abl, and cell-cell junctions. *Current Biology*, 17(20):1791–1796, 2007.

[265] Tinya Fleming, Shih-Chieh Chien, Pamela J Vanderzalm, Megan Dell, Megan K Gavin, Wayne C Forrester, and Gian Garriga. The role of c. elegans ena/vasp homolog unc-34 in neuronal polarity and motility. *Developmental biology*, 344(1):94–106, 2010.

[266] Yao Wu, Pakorn Kanchanawong, and Ronen Zaidel-Bar. Actin-delimited adhesion-independent clustering of e-cadherin forms the nanoscale building blocks of adherens junctions. *Developmental cell*, 32(2):139–154, 2015.

[267] Elise Houssin, Ulrich Tepass, and Patrick Laprise. Girdin-mediated interactions between cadherin and the actin cytoskeleton are required for epithelial morphogenesis in drosophila. *Development*, 142(10):1777–1784, 2015.

[268] Kristin M Sherrard and Richard G Fehon. The transmembrane protein crumbs displays complex dynamics during follicular morphogenesis and is regulated competitively by moesin and apkc. *Development*, 142(10):1869–1878, 2015.

[269] Soonjin Hong, Regina B Troyanovsky, and Sergey M Troyanovsky. Binding to f-actin guides cadherin cluster assembly, stability, and movement. *J Cell Biol*, 201(1):131–143, 2013.

[270] Haibo Bai, Qingfeng Zhu, Alexandra Surcel, Tianzhi Luo, Yixin Ren, Bin Guan, Ying Liu, Nan Wu, Nora Eve Joseph, Tian-Li Wang, et al. Yes-associated protein impacts adherens junction assembly through regulating actin cytoskeleton organization. *American Journal of Physiology-Gastrointestinal and Liver Physiology*, 311(3):G396–G411, 2016.

[271] Kris A DeMali, Christy A Barlow, and Keith Burridge. Recruitment of the arp2/3 complex to vinculin. *J Cell Biol*, 159(5):881–891, 2002.

[272] Dror S Chorev, Oren Moscovitz, Benjamin Geiger, and Michal Sharon. Regulation of focal adhesion formation by a vinculin-arp2/3 hybrid complex. *Nature communications*, 5:3758, 2014.

[273] Charu Rajput, Vidisha Kini, Monica Smith, Pascal Yazbeck, Alejandra Chavez, Tracy Schmidt, Wei Zhang, Nebojsa Knezevic, Yulia Komarova, and Dolly Mehta. Neural wiskott-aldrich syndrome protein (n-wasp)-mediated p120-catenin interaction with arp2-actin complex stabilizes endothelial adherens junctions. *Journal of Biological Chemistry*, 288(6):4241–4250, 2013.

[274] Jae Ryun Ryu, Asier Echarri, Ran Li, and Ann Marie Pendergast. Regulation of cell-cell adhesion by abi/diaphanous complexes. *Molecular and cellular biology*, 29(7):1735–1748, 2009.

[275] Rebecca Bakkevig Sperry, Nicholas H Bishop, Jeremy J Bramwell, Michael N Brodeur, Matthew J Carter, Brent T Fowler, Zachery B Lewis, Steve D Maxfield, Davis M Staley, Ryan M Vellinga, et al. Zyxin controls migration in

epithelial–mesenchymal transition by mediating actin-membrane linkages at cell–cell junctions. *Journal of cellular physiology*, 222(3):612–624, 2010.

[276] Marc DH Hansen and Mary C Beckerle. Opposing roles of zyxin/lpp acta repeats and the lim domain region in cell-cell adhesion. *Journal of Biological Chemistry*, 281(23):16178–16188, 2006.

[277] Robert J Cain, Bart Vanhaesebroeck, and Anne J Ridley. The pi3k p110α isoform regulates endothelial adherens junctions via pyk2 and rac1. *The Journal of cell biology*, 188(6):863–876, 2010.

[278] Angeliki Malliri, Saskia van Es, Stephan Huveneers, and John G Collard. The rac exchange factor tiam1 is required for the establishment and maintenance of cadherin-based adhesions. *Journal of Biological Chemistry*, 279(29):30092–30098, 2004.

[279] Aparna Ratheesh, Guillermo A Gomez, Rashmi Priya, Suzie Verma, Eva M Kovacs, Kai Jiang, Nicholas H Brown, Anna Akhmanova, Samantha J Stehbens, et al. Centralspindlin and [alpha]-catenin regulate rho signalling at the epithelial zonula adherens. *Nature cell biology*, 14(8):818–828, 2012.

[280] Zhenhuan Guo, Lisa J Neilson, Hang Zhong, Paul S Murray, Megha Vaman Rao, Sara Zanivan, and Ronen Zaidel-Bar. E-cadherin interactome complexity and robustness resolved by quantitative proteomics. *Science signaling*, 7(354):rs7, 2014.

[281] Anup Padmanabhan, Megha Vaman Rao, Yao Wu, and Ronen Zaidel-Bar. Jack of all trades: functional modularity in the adherens junction. *Current opinion in cell biology*, 36:32–40, 2015.

[282] Stephanie L Maiden, Neale Harrison, Jack Keegan, Brian Cain, Allison M Lynch, Jonathan Pettitt, and Jeff Hardin. Specific conserved c-terminal amino acids of caenorhabditis elegans hmp-1/α-catenin modulate f-actin binding independently of vinculin. *Journal of Biological Chemistry*, 288(8):5694–5706, 2013.

[283] Yuzo Imamura, Masahiko Itoh, Yoshito Maeno, Shoichiro Tsukita, and Akira Nagafuchi. Functional domains of α-catenin required for the strong state of cadherin-based cell adhesion. *The Journal of cell biology*, 144(6):1311–1322, 1999.

[284] Akira Nagafuchi, Satoru Ishihara, and Shoichiro Tsukita. The roles of catenins in the cadherin-mediated cell adhesion: functional analysis of e-cadherin-alpha catenin fusion molecules. *The Journal of Cell Biology*, 127(1):235–245, 1994.

[285] Sabine Pokutta, Frauke Drees, Yoshimi Takai, W James Nelson, and William I Weis. Biochemical and structural definition of the l-afadin-and actin-binding sites of α-catenin. *Journal of Biological Chemistry*, 277(21):18868–18874, 2002.

[286] Elisabeth A Cox-Paulson, Elise Walck-Shannon, Allison M Lynch, Sawako Yamashiro, Ronen Zaidel-Bar, Celeste C Eno, Shoichiro Ono, and Jeff Hardin. Tropomodulin protects α-catenin-dependent junctional-actin networks under stress during epithelial morphogenesis. *Current Biology*, 22(16):1500–1505, 2012.

[287] Lene N Nejsum and W James Nelson. A molecular mechanism directly linking e-cadherin adhesion to initiation of epithelial cell surface polarity. *The Journal of cell biology*, 178(2):323–335, 2007.

[288] Nikunj Sharma, Seng Hui Low, Saurav Misra, Bhattaram Pallavi, and Thomas Weimbs. Apical targeting of syntaxin 3 is essential for epithelial cell polarity. *The Journal of cell biology*, 173(6):937–948, 2006.

[289] Nayden G Naydenov, Bryan Brown, Gianni Harris, Michael R Dohn, Victor M Morales, Somesh Baranwal, Albert B Reynolds, and Andrei I Ivanov. A membrane fusion protein αsnap is a novel regulator of epithelial apical junctions. *PloS one*, 7(4):e34320, 2012.

[290] Aram Megighian, Michele Scorzeto, Damiano Zanini, Sergio Pantano, Michela Rigoni, Clara Benna, Ornella Rossetto, Cesare Montecucco, and Mauro Zordan. Arg206 of snap-25 is essential for neuroexocytosis at the drosophila melanogaster neuromuscular junction. *J Cell Sci*, 123(19):3276–3283, 2010.

[291] Mitchell T Butler and John B Wallingford. Planar cell polarity in development and disease. *Nature reviews molecular cell biology*, 2017.

[292] Lisa V Goodrich and David Strutt. Principles of planar polarity in animal development. *Development*, 138(10):1877–1892, 2011.

[293] Paul N Adler. The frizzled/stan pathway and planar cell polarity in the drosophila wing. *Current topics in developmental biology*, 101:1, 2012.

[294] Ying Peng and Jeffrey D Axelrod. Asymmetric protein localization in planar cell polarity: mechanisms, puzzles and challenges. *Current topics in developmental biology*, 101:33, 2012.

[295] Peter A Lawrence and José Casal. The mechanisms of planar cell polarity, growth and the hippo pathway: some known unknowns. *Developmental biology*, 377(1):1–8, 2013.

[296] Yingzi Yang and Marek Mlodzik. Wnt-frizzled/planar cell polarity signaling: cellular orientation by facing the wind (wnt). *Annual review of cell and developmental biology*, 31:623–646, 2015.

[297] Chonnettia Jones and Ping Chen. Planar cell polarity signaling in vertebrates. *Bioessays*, 29(2):120–132, 2007.

[298] Helen Strutt and David Strutt. Differential stability of flamingo protein complexes underlies the establishment of planar polarity. *Current Biology*, 18(20):1555–1564, 2008.

[299] Wei-Shen Chen, Dragana Antic, Maja Matis, Catriona Y Logan, Michael Povelones, Graham A Anderson, Roel Nusse, and Jeffrey D Axelrod. Asymmetric homotypic interactions of the atypical cadherin flamingo mediate intercellular polarity signaling. *Cell*, 133(6):1093–1105, 2008.

[300] Jun Wu and Marek Mlodzik. The frizzled extracellular domain is a ligand for van gogh/stbm during nonautonomous planar cell polarity signaling. *Developmental cell*, 15(3):462–469, 2008.

[301] Helen Strutt, Samantha J Warrington, and David Strutt. Dynamics of core planar polarity protein turnover and stable assembly into discrete membrane subdomains. *Developmental cell*, 20(4):511–525, 2011.

[302] Tadao Usui, Yasuyuki Shima, Yuko Shimada, Shinji Hirano, Robert W Burgess, Thomas L Schwarz, Masatoshi Takeichi, and Tadashi Uemura. Flamingo, a seven-pass transmembrane cadherin, regulates planar cell polarity under the control of frizzled. *Cell*, 98(5):585–595, 1999.

[303] David I Strutt. Asymmetric localization of frizzled and the establishment of cell polarity in the drosophila wing. *Molecular cell*, 7(2):367–375, 2001.

[304] Rebecca Bastock, Helen Strutt, and David Strutt. Strabismus is asymmetrically localised and binds to prickle and dishevelled during drosophila planar polarity patterning. *Development*, 130(13):3007–3014, 2003.

[305] Andreas Jenny, Jessica Reynolds-Kenneally, Gishnu Das, Micheal Burnett, and Marek Mlodzik. Diego and prickle regulate frizzled planar cell polarity signalling by competing for dishevelled binding. *Nature cell biology*, 7(7):691, 2005.

[306] David Strutt and Helen Strutt. Differential activities of the core planar polarity proteins during drosophila wing patterning. *Developmental biology*, 302(1):181–194, 2007.

[307] Andreas Jenny, Rachel S Darken, Paul A Wilson, and Marek Mlodzik. Prickle and strabismus form a functional complex to generate a correct axis during planar cell polarity signaling. *The EMBO journal*, 22(17):4409–4420, 2003.

[308] Gishnu Das, Andreas Jenny, Thomas J Klein, Suzanne Eaton, and Marek Mlodzik. Diego interacts with prickle and strabismus/van gogh to localize planar cell polarity complexes. *Development*, 131(18):4467–4476, 2004.

[309] Giovanna Mottola, Anne-Kathrin Classen, Marcos González-Gaitán, Suzanne Eaton, and Marino Zerial. A novel function for the rab5 effector rabenosyn-5 in planar cell polarity. *Development*, 137(14):2353–2364, 2010.

[310] Anne-Kathrin Classen, Kurt I Anderson, Eric Marois, and Suzanne Eaton. Hexagonal packing of drosophila wing epithelial cells by the planar cell polarity pathway. *Developmental cell*, 9(6):805–817, 2005.

[311] Bomsoo Cho, Gandhy Pierre-Louis, Andreas Sagner, Suzanne Eaton, and Jeffrey D Axelrod. Clustering and negative feedback by endocytosis in planar cell polarity signaling is modulated by ubiquitinylation of prickle. *PLoS genetics*, 11(5):e1005259, 2015.

[312] Hing-C Wong, Audrey Bourdelas, Anke Krauss, Ho-Jin Lee, Youming Shao, Dianqing Wu, Marek Mlodzik, De-Li Shi, and Jie Zheng. Direct binding of the pdz domain of dishevelled to a conserved internal sequence in the c-terminal region of frizzled. *Molecular cell*, 12(5):1251–1260, 2003.

[313] Anan Yu, Jean-François Rual, Keiko Tamai, Yuko Harada, Marc Vidal, Xi He, and Tomas Kirchhausen. Association of dishevelled with the clathrin ap-2 adaptor is required for frizzled endocytosis and planar cell polarity signaling. *Developmental cell*, 12(1):129–141, 2007.

[314] Jose Maria Carvajal-Gonzalez, Sophie Balmer, Meg Mendoza, Aurore Dussert, Giovanna Collu, Angel-Carlos Roman, Ursula Weber, Brian Ciruna, and Marek Mlodzik. The clathrin adaptor ap-1 complex and arf1 regulate planar cell polarity in vivo. *Nature communications*, 6:6751, 2015.

[315] Rezma Shrestha, Katherine A Little, Joel V Tamayo, Wenyang Li, David H Perlman, and Danelle Devenport. Mitotic control of planar cell polarity by polo-like kinase 1. *Developmental cell*, 33(5):522–534, 2015.

[316] Eszter K Vladar, Roy D Bayly, Ashvin M Sangoram, Matthew P Scott, and Jeffrey D Axelrod. Microtubules enable the planar cell polarity of airway cilia. *Current Biology*, 22(23):2203–2212, 2012.

[317] Suzanne Eaton, Roger Wepf, and Kai Simons. Roles for rac1 and cdc42 in planar polarization and hair outgrowth in the wing of drosophila. *The Journal of Cell Biology*, 135(5):1277–1289, 1996.

[318] Diane S Sepich, Mohsinah Usmani, Staci Pawlicki, and Lila Solnica-Krezel. Wnt/pcp signaling controls intracellular position of mtocs during gastrulation convergence and extension movements. *Development*, 138(3):543–552, 2011.

[319] Jessica Olofsson, Katherine A Sharp, Maja Matis, Bomsoo Cho, and Jeffrey D Axelrod. Prickle/spiny-legs isoforms control the polarity of the apical microtubule network in planar cell polarity. *Development*, 141(14):2866–2874, 2014.

[320] Maja Matis, David A Russler-Germain, Qie Hu, Claire J Tomlin, and Jeffrey D Axelrod. Microtubules provide directional information for core pcp function. *Elife*, 3:e02893, 2014.

[321] Dongbo Shi, Fumiko Usami, Kouji Komatsu, Sanae Oka, Takaya Abe, Tadashi Uemura, and Toshihiko Fujimori. Dynamics of planar cell polarity protein vangl2 in the mouse oviduct epithelium. *Mechanisms of development*, 141:78–89, 2016.

[322] Chung-hui Yang, Jeffrey D Axelrod, and Michael A Simon. Regulation of frizzled by fat-like cadherins during planar polarity signaling in the drosophila compound eye. *Cell*, 108(5):675–688, 2002.

[323] Dali Ma, Yang Chung-Hui, Helen McNeill, Michael A Simon, and Jeffrey D Axelrod. Fidelity in planar cell polarity signalling. *Nature*, 421(6922):543, 2003.

[324] David Gubb, Clare Green, David Huen, Darin Coulson, Glynnis Johnson, David Tree, Simon Collier, and John Roote. The balance between isoforms of the prickle lim domain protein is critical for planar polarity in drosophila imaginal discs. *Genes & development*, 13(17):2315–2327, 1999.

[325] Tomonori Ayukawa, Masakazu Akiyama, Jennifer L Mummery-Widmer, Thomas Stoeger, Junko Sasaki, Juergen A Knoblich, Haruki Senoo, Takehiko Sasaki, and Masakazu Yamazaki. Dachsous-dependent asymmetric localization of spiny-legs determines planar cell polarity orientation in drosophila. *Cell Reports*, 8(2):610–621, 2014.

[326] Abhijit A Ambegaonkar and Kenneth D Irvine. Coordination of planar cell polarity pathways through spiny-legs. *Elife*, 4:e09946, 2015.

[327] Yuko Shimada, Shigenobu Yonemura, Hiroyuki Ohkura, David Strutt, and Tadashi Uemura. Polarized transport of frizzled along the planar microtubule arrays in drosophila wing epithelium. *Developmental cell*, 10(2):209–222, 2006.

[328] Jun Wu, Angel-Carlos Roman, Jose Maria Carvajal-Gonzalez, and Marek Mlodzik. Wg and wnt4 provide long-range directional input to planar cell polarity orientation in drosophila. *Nature cell biology*, 15(9):1045, 2013.

[329] Chih-Wen Chu and Sergei Y Sokol. Wnt proteins can direct planar cell polarity in vertebrate ectoderm. *Elife*, 5:e16463, 2016.

[330] Bo Gao, Hai Song, Kevin Bishop, Gene Elliot, Lisa Garrett, Milton A English, Philipp Andre, James Robinson, Raman Sood, Yasuhiro Minami, et al. Wnt signaling gradients establish planar cell polarity by inducing vangl2 phosphorylation through ror2. *Developmental cell*, 20(2):163–176, 2011.

[331] Carl-Philipp Heisenberg, Masazumi Tada, Gerd-Jorg Rauch, et al. Silberblick/wnt11 mediates convergent extension movements during zebrafish gastrulation. *Nature*, 405(6782):76, 2000.

[332] John B Wallingford, Brian A Rowning, Kevin M Vogeli, Ute Rothbacher, et al. Dishevelled controls cell polarity during xenopus gastrulation. *Nature*, 405(6782):81, 2000.

[333] U Weber and M Mlodzik. The role of rhoa in tissue polarity and frizzled signaling. *Nature*, 387(6630):292–5, 1997.

[334] Christopher G Winter, Bruce Wang, Anna Ballew, Anne Royou, Roger Karess, Jeffrey D Axelrod, and Liqun Luo. Drosophila rho-associated kinase (drok) links frizzled-mediated planar cell polarity signaling to the actin cytoskeleton. *Cell*, 105(1):81–91, 2001.

[335] John B Wallingford. Planar cell polarity and the developmental control of cell behavior in vertebrate embryos. *Annual review of cell and developmental biology*, 28:627–653, 2012.

[336] Xiaowei Lu, Annette GM Borchers, Christine Jolicoeur, Helen Rayburn, et al. Ptk7/cck-4 is a novel regulator of planar cell polarity in vertebrates. *Nature*, 430(6995):93, 2004.

[337] Jianyi Lee, Anna Andreeva, Conor W Sipe, Lixia Liu, Amy Cheng, and Xiaowei Lu. Ptk7 regulates myosin ii activity to orient planar polarity in the mammalian auditory epithelium. *Current Biology*, 22(11):956–966, 2012.

[338] Anna Andreeva, Jianyi Lee, Madhura Lohia, Xiaoji Wu, Ian G Macara, and Xiaowei Lu. Ptk7-src signaling at epithelial cell contacts mediates spatial organization of actomyosin and planar cell polarity. *Developmental cell*, 29(1):20–33, 2014.

[339] Su Kyoung Kim, Asako Shindo, Tae Joo Park, Edwin C Oh, Srimoyee Ghosh, Ryan S Gray, Richard A Lewis, Colin A Johnson, Tania Attie-Bittach, Nicholas Katsanis, et al. Planar cell polarity acts through septins to control collective cell movement and ciliogenesis. *Science*, 329(5997):1337–1340, 2010.

[340] Mitchell T Butler and John B Wallingford. Control of vertebrate core planar cell polarity protein localization and dynamics by prickle 2. *Development*, 142(19):3429–3439, 2015.

[341] Boris Guirao, Alice Meunier, Stéphane Mortaud, Andrea Aguilar, Jean-Marc Corsi, Laetitia Strehl, Yuki Hirota, Angélique Desoeuvre, Camille Boutin, Young-Goo Han, et al. Coupling between hydrodynamic forces and planar cell polarity orients mammalian motile cilia. *Nature cell biology*, 12(4):341, 2010.

[342] Peter S Hegan, Eric Ostertag, Aron M Geurts, and Mark S Mooseker. Myosin id is required for planar cell polarity in ciliated tracheal and ependymal epithelial cells. *Cytoskeleton*, 72(10):503–516, 2015.

[343] Danelle Devenport. Tissue morphodynamics: translating planar polarity cues into polarized cell behaviors. In *Seminars in cell & developmental biology*, volume 55, pages 99–110. Elsevier, 2016.

[344] Tae Joo Park, Brian J Mitchell, Philip B Abitua, Chris Kintner, and John B Wallingford. Dishevelled controls apical docking and planar polarization of basal bodies in ciliated epithelial cells. *Nature genetics*, 40(7):871–879, 2008.

[345] John Shih and Ray Keller. Cell motility driving mediolateral intercalation in explants of xenopus laevis. *Development*, 116(4):901–914, 1992.

[346] Camille Boutin, Paul Labedan, Jordane Dimidschstein, Fabrice Richard, Harold Cremer, Philipp André, Yingzi Yang, Mireille Montcouquiol, Andre M Goffinet, and Fadel Tissir. A dual role for planar cell polarity genes in ciliated cells. *Proceedings of the National Academy of Sciences*, 111(30):E3129–E3138, 2014.

[347] Shinya Ohata, Jin Nakatani, Vicente Herranz-Pérez, JrGang Cheng, Haim Belinson, Toshiro Inubushi, William D Snider, Jose Manuel García-Verdugo, Anthony Wynshaw-Boris, and Arturo Álvarez-Buylla. Loss of dishevelleds disrupts planar polarity in ependymal motile cilia and results in hydrocephalus. *Neuron*, 83(3):558–571, 2014.

[348] S. Brenner. The genetics of caenorhabditis elegans. *Genetics*, 77(1):71–94, 1974.

[349] D.J. Dickinson D.J. Ward D.J. Reiner and B. Goldstein. Engineering the caenorhabditis elegans genome using cas9-triggered homologous recombination. *Nature methods*, 10(10):1028–1034, 2013.

[350] K. Miyazaki and M. Takenouchi. Creating random mutagenesis libraries using megaprimer pcr of whole plasmid. *Biotechniques*, 33(5):1033–4, 2002.

[351] J.S. Dittman and J.M. Kaplan. Factors regulating the abundance and localization of synaptobrevin in the plasma membrane. *Proceedings of the National Academy of Sciences*, 103(30):11399–11404, 2006.

[352] A Fire S.Q. Xu M.K. Montgomery et al. Potent and specific genetic interference by double-stranded rna in caenorhabditis elegans. *nature*, 391(6669):806, 1998.

[353] R.S. Kamath and J. Ahringer. Genome-wide rnai screening in caenorhabditis elegans. *Methods*, 30(4):313–321, 2003.

[354] L.A. Royer M. Weigert et al. Clearvolume: open-source live 3d visualization for light-sheet microscopy. *Nature methods*, 12(6):480–481, 2015.

[355] Y.C. Wu A. Ghitani et al. Inverted selective plane illumination microscopy (ispim) enables coupled cell identity lineaging and neurodevelopmental imaging in caenorhabditis elegans. *Proceedings of the National Academy of Sciences*, 108(43):17708–17713, 2011.

[356] Q.Y. Fu, B.L. Martin, D.Q. Matus, and L. Gao. Imaging multicellular specimens with real-time optimized tiling light-sheet selective plane illumination microscopy. *Nature communications*, 7:11088–11088, 2016.

[357] C.J. Merrifield D. Perrais and D. Zenisek. Coupling between clathrin-coated-pit invagination, cortactin recruitment, and membrane scission observed in live cells. *Cell*, 121(4):593–606, 2005.

[358] J.D. Wilson, S.A. Shelby D. Holowka, and B. Baird. Rab11 regulates the mast cell exocytic response. *Traffic*, 17(9):1027–1041, 2016.

[359] K.N. Fish. Total internal reflection fluorescence (tirf) microscopy. *Current protocols in cytometry*, pages 12–18, 2009.

[360] T. Nishimura H. Honda and M. Takeichi. Planar cell polarity links axes of spatial dynamics in neural-tube closure. *Cell*, 149(5):1084–1097, 2012.

[361] A. Shindo and J.B. Wallingford. Pcp and septins compartmentalize cortical actomyosin to direct collective cell movement. *Science*, 343(6171):649–652, 2014.

[362] T.K. Vuong-Brender M.B. Amar J. Pontabry and M. Labouesse. The interplay of stiffness and force anisotropies drives embryo elongation. *Elife*, 6, 2017.

APPENDIX: *C. elegans* Embryonic Morphogenesis - Book chapter

C. elegans Embryonic Morphogenesis

Thanh T.K. Vuong-Brender, Xinyi Yang and Michel Labouesse

Current Topics in Developmental Biology, Volume 116, 2016

By the end of my second year, I participated in writing a book chapter, *C.elegans* Embryonic Morphogenesis in *Current Topics in Developmental Biology*, Volume 116. In this chapter, I mainly wrote the section 3, Elongation Beyond the Twofold Stage, pp 608-612. The whole chapter is included in this appendix.

CHAPTER THIRTY-FIVE

C. elegans Embryonic Morphogenesis

Thanh T.K. Vuong-Brender[1], Xinyi Yang, Michel Labouesse[1]
Laboratoire de Biologie du Développement, CNRS-UMR7622, Institut de Biologie Paris-Seine, Université Pierre et Marie Curie, Sorbonne Universités, Paris, France
[1]Corresponding authors: e-mail address: thanh.vuong@upmc.fr; michel.labouesse@upmc.fr

Contents

Abstract

Morphogenesis is a four-dimensional process which involves the crucial interplay between signaling, mechanical forces, and spatial changes. *Caenorhabditis elegans* presents a simple yet versatile model to study morphogenesis. Here, we review recent progress on cellular and molecular drivers of morphological changes during *C. elegans* epiboly and embryonic elongation: actin dynamics and actomyosin contractility, migration guidance cues and junction remodeling. In addition, we discuss how mechanical forces contribute to the process.

The free-living nematode *Caenorhabditis elegans* is well known for its simplicity as a model organism (Ankeny, 2001; Antoshechkin & Sternberg, 2007). In particular, its tube-like shape represents one of the most basic forms in the animal kingdom. How the animal acquires its shape results from the morphogenesis of the epidermal sheet, which spreads out to enclose the embryo and undergoes striking shape changes to become cylindrical over a period of less than 3 h. Analysis of these processes (called ventral enclosure and embryonic elongation, respectively) has shown the importance of precise regulation of signaling and mechanical forces at the cellular scale. Here, we review these processes and discuss what recent findings bring to our understanding of cell migration through actin-based protrusions in response to guidance cues, cell shape changes based on actomyosin contractility, and junction remodeling.

Current Topics in Developmental Biology, Volume 116
ISSN 0070-2153
http://dx.doi.org/10.1016/bs.ctdb.2015.11.012

1. VENTRAL ENCLOSURE

Epidermal cells are born at the end of gastrulation as a group of cells on the posterior and dorsal surface of the embryo. They form six rows of cells: two dorsal, two lateral, and two ventral rows (Heid, Raich, et al., 2001; Sulston, Schierenberg, et al., 1983). The first morphogenetic event to occur in the epidermis corresponds to the intercalation of dorsal epidermal cells which we will not discuss (for review, see Bone, Tapley, et al., 2014; Chisholm & Hardin, 2005; Fridolfsson, Ly, et al., 2010; Meyerzon, Fridolfsson, et al., 2009; Walck-Shannon, Reiner, et al., 2015). Dorsal intercalation leads to a lengthening of the epithelial epidermal cell sheet and to the establishment of correct circumferentially oriented actin bundles, which are essential for the elongation phase (Chisholm & Hardin, 2005; Heid et al., 2001). Very soon after completion of dorsal intercalation, the ventral epidermal cells on each side of the embryo migrate toward the ventral midline and seal up to enclose the embryo.

Ventral enclosure takes place in two steps (Raich, Agbunag, et al., 1999; Williams-Masson, Malik, et al., 1997; Fig. 1). First, the two most anterior epidermal cells on each side, called the "leading cells," initiate the migration by extending long protrusions toward the ventral midline (Fig. 1A). They eventually meet and establish contacts. In the second step, the posterior cells form a continuous actin-rich border around the "ventral pocket" (Fig. 1B). The pocket cells become wedge-shaped and initiate a coordinated

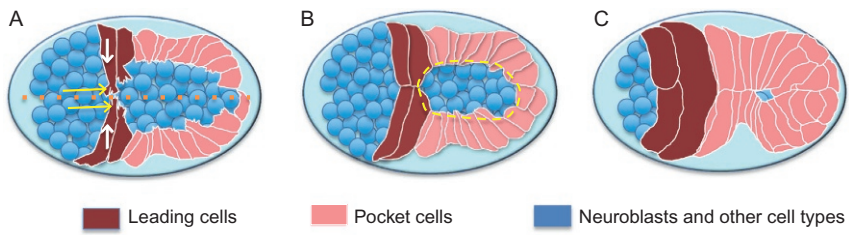

Figure 1 The two steps of epidermal ventral enclosure. (A) Schematic ventral view of an embryo (anterior to the left). First, the leading cells (dark red) extend long protrusions (yellow arrows), migrate (white arrows show the direction of migration) toward the ventral midline (dotted line), meet and establish adherens junctions. (B) The pocket cells (pink) exert coordinated contraction to close the open pouch (dashed line). (C) End of ventral closure; the head is not totally enclosed (some head epidermal cells anterior to the leading cells are not illustrated). Neuroblasts and other cell types are depicted in blue.

contraction to fully enclose the posterior part through a purse-string mechanism reminiscent of *D. melanogaster* dorsal closure (Fig. 1B; Gorfinkiel, Schamberg, et al., 2011). The anterior part of the embryo is finally enclosed by head epidermal cells (Fig. 1C; Chisholm & Hardin, 2005). In the next paragraphs, we discuss how imaging and drug assays helped uncover the cytoskeletal proteins and the cells required for enclosure. We also review the results of genetic screens that identified mutants that either fail to migrate, or that do not seal properly.

Laser inactivation experiments, in which epidermal cells are not completely killed but lose their capacity to migrate, have confirmed the role of leading cells in migration initiation and the cooperative action of more posterior cells in pocket closure (Williams-Masson et al., 1997). In particular, inactivation of leading cells on both sides of the ventral midline induces a retraction of the whole epidermis dorsally. Likewise, inactivation of the ventral pocket cells even on one side of the ventral midline leads to pocket cell retraction and their inability to reinitiate enclosure (Williams-Masson et al., 1997).

Mechanistically, pharmacological experiments have established the primary role of actin dynamics during ventral enclosure, while genetic studies helped identify conserved actin remodeling factors. Inhibition of actin polymerization with cytochalasin-D immediately blocks migration and causes the leading cells to regress dorsally (Williams-Masson et al., 1997). Affecting actin dynamics by mutations in the WAVE/SCAR and ARP2/3 complex, which act downstream of CED-10/Rac1 (Fig. 2A), strongly reduces actin at the leading edge, resulting in fewer and smaller protrusions in epidermal cells, and in severe ventral enclosure phenotypes (Bernadskaya, Wallace, et al., 2012; Patel, Bernadskaya, et al., 2008; Sawa, Suetsugu, et al., 2003; Soto, Qadota, et al., 2002). The WAVE/SCAR complex is known to activate the Arp2/3 complex, which in turn promotes actin filament branching to enable cell migration (Blanchoin, Boujemaa-Paterski, et al., 2014). In *C. elegans*, the dynamics of actin assembly is enhanced by the protein UNC-34/VASP, which can bind the proline-rich domain of WAVE to increase cell motility (Havrylenko, Noguera, et al., 2015). In addition, the *C. elegans* WASP homologue WSP-1, acting probably downstream of CDC-42, works redundantly with UNC-34 and WAVE to activate ARP2/3 and promote F-actin nucleation (Rohatgi, Ma, et al., 1999; Sawa et al., 2003; Withee, Galligan, et al., 2004; Fig. 2A). Although initially identified and characterized in *Dictyostelium discoideum* and mammals (Blanchoin et al., 2014), work in *C. elegans* has been instrumental in establishing the role of the WAVE/SCAR, UNC-34/VASP, and ARP2/3 pathway in an *in vivo* morphogenetic process.

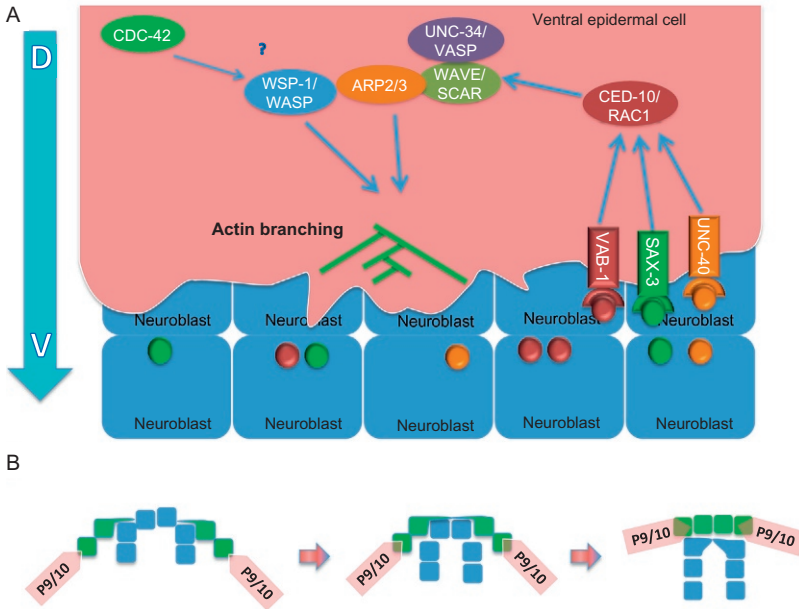

Figure 2 Neuroblasts guide ventral epidermis migration during ventral enclosure. (A) Signaling from neuroblasts promotes actin dynamics in the ventral epidermis. CED-10/Rac1, which acts probably downstream of VAB-1/EphR, SAX-3/Robo, and UNC-40/DCC, activates the WAVE/SCAR complex, and in turn the ARP2/3 complex. UNC-34/VASP binds WAVE/SCAR to promote actin polymerization. WSP-1, probably activated by CDC-42, contributes to a redundant pathway with WAVE/SCAR and UNC-34/VASP, which has not yet been fully investigated. Expression of guidance cues is discussed in the text. Big blue arrow: direction of migration; D, dorsal side; V, ventral side. Small ovals: guidance cues secreted by neuroblasts. (B) Schematic ventral view of the ventral midline, depicting how epidermal ventral cells (P9/10) migrate over a bridge made by neuroblasts. Some neuroblasts (green squares; only key neuroblasts are represented) extend protrusions and translocate over their neighbors (blue squares) to establish a bridge (Ikegami et al., 2012).

The outcome of ventral epidermal enclosure depends on an earlier event, the closure of the ventral cleft which is a depression on the ventral surface created by cell ingression during gastrulation. Neuroblasts migrate to fill in the cleft about 1 h before epidermal cell migration (Chisholm & Hardin, 2005). Semiautomated nuclear tracking has shown that neuroblast movements are not stochastic but follow a pattern that correlates with that of ventral epidermal cells before and during ventral enclosure (Giurumescu, Kang, et al., 2012). Thus, neuroblasts play a key role, in particular, to guide pocket cell movements. Precise imaging has revealed that some neuroblasts under

the ventral pocket extend protrusions and translocate themselves toward the ventral midline (Fig. 2B). Thereby, they queue up in a row spanning the ventral pocket and form a "bridge" over which the epidermal pocket cells can "walk" before joining together from the two edges of the pocket (Ikegami, Simokat, et al., 2012).

The characterization of partially penetrant ventral enclosure mutants identified the Ephrin, Semaphorin, Robo/Slit, and Netrin guidance proteins, which also mediate neuronal migration and axon pathfinding (Bernadskaya et al., 2012; Chin-Sang, George, et al., 1999; Chin-Sang, Moseley, et al., 2002; George, Simokat, et al., 1998; Ghenea, Boudreau, et al., 2005; Ikegami et al., 2012; Miller & Chin-Sang, 2012; Nakao, Hudson, et al., 2007; Roy, Zheng, et al., 2000; Wang, Roy, et al., 1999). Their study established that ventral enclosure depends on the completion of ventral cleft closure and on signaling between neuroblasts and ventral epidermal cells. Indeed, mutants in these genes often cause a larger, deeper, and more persistent ventral cleft, which subsequently affects the final steps of epidermal cell migration during ventral closure. It suggests that signaling provided by these pathways guides the movement of neuroblasts (Chin-Sang et al., 1999, 2002; George et al., 1998; Ghenea et al., 2005; Ikegami et al., 2012; Nakao et al., 2007; Roy et al., 2000; Wang et al., 1999). In addition, genetic analysis strongly suggests that neuroblasts represent a signaling center for ventral epidermal cell migration. Many of these guidance proteins, such as VAB-1/EphR, EFN-2/Ephrin, SAX-3/Robo, PLX-2/Plexin, MAB-20/Semaphorin-2a, are expressed both in neuroblasts and in the epidermis (George et al., 1998; Ghenea et al., 2005; Ikegami et al., 2012; Nakao et al., 2007; Roy et al., 2000; Wang et al., 1999). In particular, SAX-3 is expressed in the leading cells (Ghenea et al., 2005), and UNC-40 is expected to act cell autonomously (Chan, Zheng, et al., 1996). Finally, rescue experiments show that expression of VAB-1/EphR in P9/10 or in a subset of neuroblasts can rescue mutant lethality, showing a close communication between both cell types (Ikegami et al., 2012). Other proteins, like EFN-1/Ephrin, work nonautonomously in the developing neurons to regulate epidermal morphogenesis (Chin-Sang et al., 1999).

There is a high level of redundancy between these guidance pathways, such that embryos lacking two of them often exhibit more severe enclosure defects. Specifically, the unique *C. elegans* Ephrin receptor VAB-1 can form a coreceptor with SAX-3/Robo to guide cell migration (Ghenea et al., 2005). Interestingly, EFN-4/Ephrin does not interact with VAB-1/EphR but acts instead in a redundant pathway involving the *C. elegans* Semaphorin-2a MAB-20 (Chin-Sang et al., 2002; Wang et al.,

1999). The VAB-1/EphR and SAX-3/Robo pathways are also redundant with the Netrin pathway (Bernadskaya et al., 2012). Given the complexity of the guidance cue system, how these pathways affect precisely neuronal and epidermal cell movements requires further investigation.

How the guidance cues are translated to changes in the orientation and motility of epidermal cells is starting to be revealed. VAB-1/EphR, SAX-3/Robo, and UNC-40/DCC Netrin receptor mutants affect the correct accumulation of CED-10/Rac1 and WVE-1/WAVE at the basolateral membrane of the epidermis (Bernadskaya et al., 2012; Fig. 2A). They display reduced level of actin polarization along the dorsoventral axis of migrating epidermal cells. Although not as pronounced even in double mutants, it is similar to what is observed in WAVE/SCAR mutants, consistent with the fact that the ventral enclosure phenotype of *vab-1/ephR, sax-3/robo*, and *unc-40/DCC* mutants is less severe than those of *wave/scar* and *arp2/3* mutants. It is unclear yet whether there is another redundant pathway to be identified, or whether removing all three guidance pathways (which would certainly be embryonic lethal) would abrogate cell migration.

Once the contralateral ventral cells have met at the ventral midline, they assemble stable junctions through the cadherin–catenin complex, which become capable of resisting mechanical tension. Depletion of zygotic HMR-1/E-cadherin or maternal and zygotic HMP-1/α-catenin leads to unenclosed embryos, which extrude their pharynx and intestine anteriorly (Costa, Raich, et al., 1998). During the sealing process, HMP-1/α-catenin quickly localizes to the point of contact between the filopodia-like extensions of contralateral leading cells, while concomitantly disappearing from the cytoplasm (Raich et al., 1999). This process requires HMR-1/E-cadherin function, as in *hmr-1* mutants, the accumulation of HMP-1 at the cell contact region and the drop in the concentration of HMP-1 cytoplasmic pool are not observed. In these mutants, the leading cells still extend filopodia and meet at the ventral midline like in wild type. However, after failing to make contact at the ventral midline, the leading cells cease their protrusive activity and retract dorsally (Raich et al., 1999). Thus, stable contacts require both cell–cell adhesion via E-cadherin and junction "reinforcement" by connection with the cytoskeleton through α- and β-catenin. In contrast, the sealing of ventral pocket cells does not have a stringent requirement for the cadherin–catenin complex. In *hmr-1/E-cadherin* and *hmp-1/α-catenin* mutant, ventral pocket cells still close albeit incompletely (Raich et al., 1999). These results suggest that the ventral pocket cells may use a cadherin-independent adhesion system or redundant

adhesion signals. The building of new junctions and the feedback loop with the leading cell cytoskeleton remain poorly understood.

Many of the guidance cue mutant embryos (*vab-1*, *sax-3*, *mab-20*, *efn-1*, *efn-4)* undergo apparently normal ventral enclosure, yet they rupture during elongation (Chin-Sang et al., 1999, 2002; George et al., 1998; Ghenea et al., 2005; Nakao et al., 2007). Although this phenomenon is also observed when the ventral epidermal cells are inactivated by laser during enclosure (Williams-Masson et al., 1997), it is not clear if the rupture phenotype results solely from improper epidermal sealing, or if the guidance cues have some impact on the integrity of epidermis at a later stage. Since these mutants affect the correct actin distribution (Bernadskaya et al., 2012), one possibility could be that junction reinforcement through actin-dependent processes becomes defective as tension increases during elongation.

Although superficially similar, the closure of *C. elegans* ventral epidermis differs from dorsal closure of *Drosophila* in several aspects. In *Drosophila*, the dorsal closure is aided mechanically by the amnioserosa (Gorfinkiel et al., 2011; Harden, 2002). It is not known if in *C. elegans*, the neuroblasts or other embryonic tissues exert repeated pulsatile contractions like the amnioserosa cells (Solon, Kaya-Copur, et al., 2009). Although myosin II is enriched at the ventral border of pocket cells in *C. elegans*, it is unclear to what extent the cable akin to that observed at the *Drosophila* dorsal leading edge plays a role in ventral enclosure. In *C. elegans*, mutations in the upstream regulators of myosin II, like *rho-1/rhoA*, *let-502/Rock*, and *mel-11/Mypt*, induce a small proportion of ventral enclosure defective or early ruptured embryos (Fotopoulos, Wernike, et al., 2013). However, the defects are not penetrant enough to conclude that myosin is essential. Precise force measurements will be necessary to elucidate the contribution of neuroblasts, the epidermis, and the supracontractile ring around the pocket during *C. elegans* ventral enclosure.

2. ELONGATION FROM THE LIMA-BEAN TO THE TWOFOLD STAGE

Once ventral enclosure has finished, the embryo elongates from a lima-bean (equivalent to onefold stage) shape to the characteristic worm shape, resulting in a fourfold increase in length and a twofold decrease in diameter approximately since the volume remains constant (Priess & Hirsh, 1986). The whole process takes place with neither cell division nor change in the relative positions of epidermal cells (Sulston et al.,

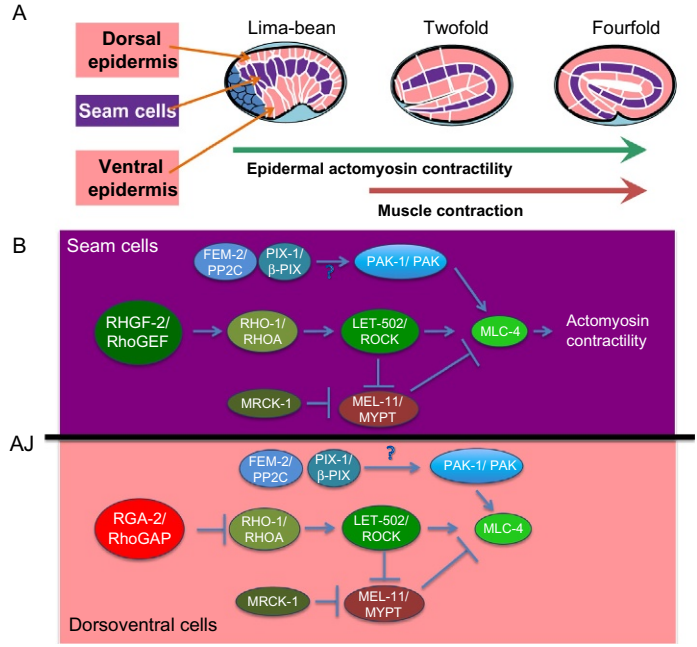

Figure 3 Overview of *C. elegans* embryonic elongation. (A) Schematic drawings of embryos along elongation. Note the change in shape of the seam cells (lateral epidermis; violet) where the junctions shorten in the dorsoventral (DV, circumferential) direction and lengthen in the anteroposterior (AP) direction. Embryos are staged according to their length (lima-bean or onefold to fourfold). Anterior to the left, dorsal up. (B) Molecular pathways mediating activation of nonmuscle myosin II contractility through phosphorylation of the myosin regulatory light chain MLC-4 during elongation.

1983). Instead, epidermal cells modify their shapes, as can be most easily observed among seam cells (Fig. 3A). About midway through the process, muscles start to contract; this is essential, since muscle-defective embryos are paralyzed and arrest their elongation at the twofold stage. This phenotype is called Pat, for paralyzed at twofold (Waterston, 1989; Williams & Waterston, 1994). Elongation can be divided in an early and a late phase with respect to the beginning of muscle contractions, each stage being mediated by distinct molecular pathways. In the following paragraphs, we discuss how actomyosin contractility drives elongation as well as how junctions and the cytoskeleton get remodeled during this process.

Genetic and pharmacological studies have shown that actomyosin contractility is essential for early elongation. Actin filaments form circumferential bundles in the dorsal and ventral epidermis but a rather disorganized pattern in seam cells characterized by thinner, shorter, and less-oriented

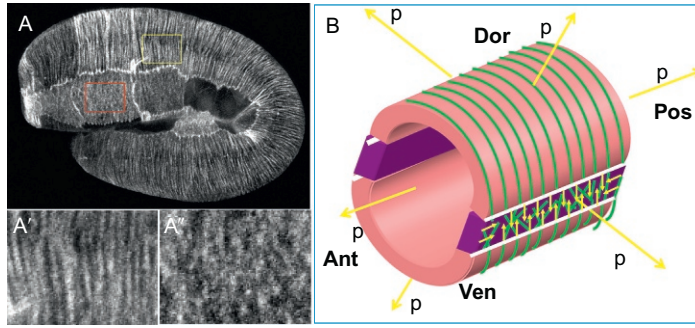

Figure 4 Actin organization and possible role during elongation. (A) Actin filaments in nearly twofold stage embryo are organized in parallel bundles in DV cells (yellow rectangle—dorsal cell hyp7, A′) and in thinner and less circumferentially oriented filaments in lateral seam cells (red rectangle, A″). (B) Hypothetical model for *C. elegans* elongation where the seam cells (violet) pull to increase the hydrostatic pressure and the DV cells (pink) orient the elongation in the direction perpendicular to actin bundle alignment (green lines), p, hydrostatic pressure; Ant, anterior; Pos, posterior; Dor, dorsal; Ven, ventral; arrows, force exerted. *Panel (A–A″) adapted with permission from Gally et al. (2009).*

filaments (Fig. 4A; Gally et al., 2009; Priess & Hirsh, 1986). The mechanism that controls the polarized organization of actin filaments in the circumferential direction is not known. Inhibition of actin polymerization with cytochalasin-D either blocks elongation if it is applied prior to the 1.5-fold stage or causes embryos to retract to their preelongation state later on (Priess & Hirsh, 1986). Actomyosin forces are thought to squeeze the embryo radially to decrease their diameter, inducing most likely anterior–posterior (AP) lengthening by an increase in hydrostatic pressure. Indeed, embryos burst if the epidermis is punctured with a laser (Priess & Hirsh, 1986). Nonmuscle myosin II motors are regulated through phosphorylation and dephosphorylation of the regulatory light chain MLC-4 by the LET-502/Rho-binding kinase and MEL-11/Myosin binding subunit of myosin phosphatase, respectively (Gally et al., 2009; Wissmann, Ingles, et al., 1997, 1999; Fig. 3B). LET-502 is the effector of the Rho GTPase RHO-1, which can be activated and inactivated by the *C. elegans* RhoGEF (Rho-Guanine nucleotide Exchange Factor) RHGF-2, and RhoGAP (Rho-GTPase-Activating Protein) RGA-2, respectively (Chan, Rocheleau, et al., 2015; Diogon, Wissler, et al., 2007). Mutations affecting positive regulators of contractility, such as RHGF-2/RhoGEF, LET-502/ROCK, MLC-4, and NMY-1/Myosin II heavy chain, lead to hypoelongation, whereby embryos arrest earlier than or at the twofold stage (Chan et al., 2015;

Gally et al., 2009; Piekny, Johnson, et al., 2003; Shelton, Carter, et al., 1999; Wissmann et al., 1997). By contrast, hypercontractility mutants like *mel-11* or *rga-2* cause embryos to burst during elongation due to increased tension exerted on adherens junctions (Diogon et al., 2007; Wissmann et al., 1999). Activation of myosin II is achieved mainly through the LET-502/Rho kinase, but two additional kinases can contribute to maintain myosin II active. Specifically, the p21-activated kinase PAK-1 and the CDC-42-activated kinase MRCK-1 act in parallel to LET-502, since their loss enhances the *let-502* mutant severity (Gally et al., 2009). Genetic analysis suggests that PAK-1 acts downstream of the phosphatase FEM-2/PP2C and the CDC-42/RAC-specific GEF (Guanine nucleotide Exchange Factor) PIX-1/β-PIX (Martin, Harel, et al., 2014; Vanneste, Pruyne, et al., 2013), whereas MRCK-1 acts upstream of MEL-11 (Gally et al., 2009). How FEM-2 regulates PAK-1 in this scheme is actually unclear (Vanneste et al., 2013). In addition, PIX-1 may more specifically promote head constriction (Martin et al., 2014).

Genetic and molecular data suggest that seam cells concentrate actomyosin forces, while the dorsoventral (DV) cells may remain passive. Indeed, several lines of evidence support this hypothesis. First, the activity of the nonmuscle myosin regulatory light chain MLC-4 is mainly required in seam cells (Gally et al., 2009). Second, MLC-4, MLC-5/myosin essential light chain, and NMY-1 are enriched in seam cells (Gally et al., 2009; Piekny et al., 2003; Shelton et al., 1999). Third, rescue experiments have shown that the positive regulator of contractility RHGF-2/RhoGEF acts specifically in seam cells, whereas the negative regulator RGA-2/RhoGAP is required only in DV cells (Chan et al., 2015; Diogon et al., 2007). Thus, all the players of actomyosin regulation pathway act in a way to keep contractility high in seam cells and low in DV cells (Fig. 3B).

During *Drosophila* gastrulation and germband extension, myosin II shows a pulsatile behavior which is essential for cell shape changes (Martin, Kaschube, et al., 2009; Rauzi, Lenne, et al., 2010). In particular during germband extension, myosin II is planar polarized with higher accumulation in vertical junctions (along DV direction) (Bertet, Sulak, et al., 2004; Blankenship, Backovic, et al., 2006; Rauzi et al., 2010). A planar polarity-dependent junctional shortening and actomyosin pulses are also observed during the convergence–extension of *Xenopus* mesoderm (Shindo & Wallingford, 2014). By contrast, myosin II distribution is not planar polarized (Gally et al., 2009; Piekny et al., 2003) and flows have so far not been reported during *C. elegans* elongation, although myosin II pulses and flows

have been described in *C. elegans* zygotes and at gastrulation (Mayer, Depken, et al., 2010; Munro, Nance, et al., 2004; Roh-Johnson, Shemer, et al., 2012). Similarly, the *C. elegans* cadherin–catenin complex is apparently not planar polarized in contrast to what is observed in *Drosophila* germband extension (Blankenship et al., 2006; Costa et al., 1998). Mechanistically, it is not clear how myosin II and adherens junctions are remodeled during early elongation; *C. elegans* may rely on different processes compared to other species.

The preferential extension of a material in one direction can come from higher forces in that direction (anisotropy of forces), or from an anisotropy of its response to isotropic forces. The extension of *Drosophila* germband is induced by anisotropic forces generated by planar-polarized actomyosin network (Bertet et al., 2004), whereas the oriented growth of plants is due to the anisotropic response of the cell wall to the isotropic force generated by turgor pressure (Baskin, 2005). As we argue below, because the myosin network does not seem to be planar polarized up to the twofold stage (Gally et al., 2009; Piekny et al., 2003; Shelton et al., 1999), the growth of plants provides a more relevant comparison with the elongation of *C. elegans* embryos than *Drosophila*. It has been proposed that the alignment of microfibrils in plants around the circumferential direction restricts radial expansion and orients the growth in the longitudinal direction (Baskin, 2005). The *C. elegans* actin filament organization in DV cells is reminiscent of the microfibril arrangement. Moreover, since myosin II activity is downregulated in DV cells, it supports the hypothesis that the DV cells create a passive anisotropic response to the hydrostatic pressure that is similar to the response of microfibrils to turgor pressure (Fig. 4B). While in plants the turgor pressure increase is due to osmosis across semipermeable cell membranes (Pritchard, 2001), in *C. elegans* embryo the increased hydrostatic pressure is likely to originate from actomyosin contractility in seam cells (Fig. 4B). The phenotypes of several mutants affecting junctional proteins thought to anchor actin bundles (Priess & Hirsh, 1986) support the role of actin bundles during elongation. In particular, zygotic *hmp-1/α-catenin* mutants, in which actin bundles detach from the junctional belt, display bulges and cannot elongate. Likewise, loss of ZOO-1/ZO-1 and VAB-9/Claudin homologues affects actin bundle organization in DV cells, leading to deformities and an incomplete elongation (Lockwood, Zaidel-Bar, et al., 2008; Simske, Koppen, et al., 2003). Although it has been proposed that the circumferentially oriented microtubules in DV cells could also provide a passive force to help elongation (Ciarletta, Ben Amar, et al., 2009; Priess & Hirsh, 1986), our

more recent data favor the notion that they act by enabling the transport of junctional proteins necessary for elongation (Quintin, Wang, et al., 2016). Perturbation of actin bundle organization in DV cells and computer modeling could help to shed light on their role during elongation.

3. ELONGATION BEYOND THE TWOFOLD STAGE

When the *C. elegans* embryo reaches the 1.7-fold stage, muscle cells located under the dorsal and ventral epidermal cells start to contract. During this period, muscles play a central role, whereas actomyosin contractility in the epidermis is thought to be less important. Indeed, time-shift experiments with a thermosensitive mutant of the LET-502/Rho kinase have suggested that it is only required until the twofold stage (Diogon et al., 2007). Moreover, our laboratory recently unraveled a possible mechanism for how muscles could promote elongation (Zhang, Landmann, et al., 2011), which features a prominent role for mechanical stimulation of the epidermis by muscles through hemidesmosome-like junctions. Below, we discuss how the tension exerted by muscles can help remodel epidermal cell–cell and cell–extracellular matrix junctions.

Muscles attach to the exoskeleton cuticle through transepithelial attachment structures, known as fibrous organelles (FOs), which span the thickness of the dorsal and ventral epidermis in areas of contact; in effect, they act as tendons transmitting the forces exerted by muscle contraction to the cuticle exoskeleton (Francis & Waterston, 1985, 1991). For this reason, muscles are tightly connected to dorsal and ventral epidermal cells. FOs correspond to two hemidesmosome-like junctions (known as CeHDs), one apical and the other basal, connected by intermediate filaments (Zhang & Labouesse, 2010; Fig. 5A). The only evolutionary conserved protein between vertebrate hemidesmosomes and CeHDs is VAB-10A, the homologue of vertebrate Plectin and BPAG1e. VAB-10A is thought to anchor intermediate filaments to membrane plaques on both the apical and basal sides of the epidermis (Bosher, Hahn, et al., 2003), and to interact with nematode-specific transmembrane extracellular matrix receptors, LET-805/Myotactin basally, MUP-4 and MUA-3 apically (Fig. 5A; Bercher, Wahl, et al., 2001; Hahn & Labouesse, 2001; Hong, Elbl, et al., 2001). Animals with defective hemidesmosomes have strong epidermal integrity defects and muscle anchoring defects; furthermore, in their absence, embryos arrest between the 1.7-fold and 2-fold stages of elongation (Bercher et al., 2001; Bosher et al., 2003; Ding, Goncharov, et al., 2003; Ding, King, et al., 2008;

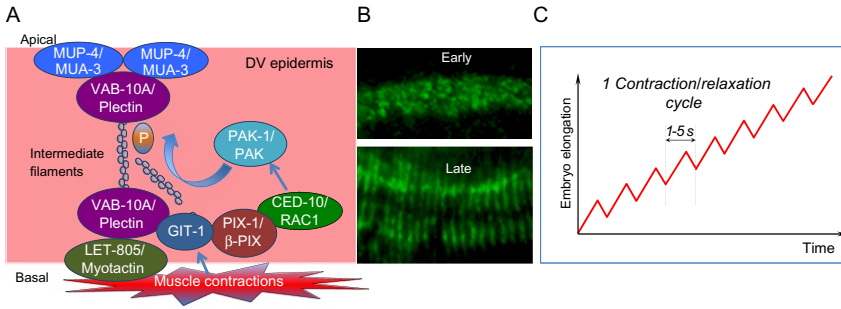

Figure 5 Muscle activity through CeHDs may promote elongation via a ratchet system. (A) CeHD remodeling under muscle contractile tension. Muscle contractions lead to GIT-1 recruitment, which subsequently activates PIX-1, CED-10/Rac1, and PAK-1. In turn, PAK-1 phosphorylates intermediate filaments leading to CeHD maturation (see panel B). (B) Images of a small portion of CeHD (marked with an antibody against the CeHD protein VAB-10A) when muscles start to contract (top) and at the end of elongation (bottom). (C) Elongation after the twofold stage as a ratchet-like process.

Hetherington, Gally, et al., 2011; Hong et al., 2001; Woo, Goncharov, et al., 2004; Zahreddine, Zhang, et al., 2010).

Due to the tight connection between muscles and the epidermis and their overall anterior–posterior orientation, muscle contractions create a longitudinal tension that is transmitted to the epidermis; thereby, the dorsal and ventral cells become locally compressed and stretched longitudinally (Zhang et al., 2011). These lateral cyclic stretches could promote elongation beyond the twofold stage. First, our laboratory showed that the tension originating from muscle contractions is felt at CeHDs and induces a mechanotransduction pathway in the epidermis (Fig. 5A). It ultimately activates the CeHD-associated p21-activated kinase homologue PAK-1, through a signaling cascade involving the Git1 homologue GIT-1 (an adaptor protein), its partner the β-Pix homologue PIX-1, and the Rac GTPase CED-10, resulting in the phosphorylation of intermediate filaments and their further recruitment to CeHDs (Zhang et al., 2011). In the absence of muscle contractions, the GIT-1 protein diffuses away from CeHDs; to account for this observation, we suggested that a CeHD component (which remains to be identified) might undergo a conformational change upon tension, triggering its interaction with GIT-1 to unleash the signaling. Prior to muscle contractions, CeHDs form puncta, which progressively evolve into short parallel circumferentially oriented stripes above the muscles, which are likely to provide stronger attachments as the force exerted by muscles increases (Fig. 5B). Since in the absence of muscle contractions, or when

GIT-1, PIX-1, or PAK-1 are knocked down together with a weak mutation in VAB-10A, CeHDs fall apart and do not mature, we proposed that the mechanotransduction pathway promotes CeHD maturation (Zhang et al., 2011).

Imaging the effect of muscle contractions on the epidermis revealed that muscles contract every few seconds (1–5 s), and do not all contract at the same time. Hence, the mechanical stimuli powered by muscles are oscillatory. Although cell shape changes during *C. elegans*, elongation do not appear to involve pulsatile flows of myosin II like in many *Drosophila* cell shape changes, it is nevertheless likely to involve a ratchet process (Fig. 5C).

Taking into consideration that *git-1*, *pix-1*, or *pak-1* mutants do not have an elongation phenotype as severe as that of muscle-defective *pat* mutants, it is conceivable that the muscle tensional input impinges on other processes in addition to CeHD maturation. In particular, since *pat* mutants fail to elongate beyond the twofold stage, tension might promote the shortening of the circumferential actin bundles present in dorsal and ventral cells (shortening is necessary since the embryonic diameter diminishes), and the lengthening of seam-dorsal and seam-ventral adherens junctions. In recent genetic screens, we have identified several genes whose downregulation in a *git-1* mutant results in a twofold arrest (C. Gally & M. Labouesse, unpublished). We anticipate that their characterization will further elucidate how muscles stimulate elongation.

How mechanical tension originating from muscles could stimulate adherens junction remodeling is not known. Lessons from other experimental systems are pointing to several potential directions. In both *Drosophila* embryonic epithelial cells and mammalian cells, endocytosis and the subsequent recycling of E-cadherin (E-cad) contribute to junction remodeling (Lecuit & Yap, 2015; Levayer & Lecuit, 2012). In particular, the nonmuscle myosin II (Myo-II) regulates E-cadherin trafficking by promoting E-cad endocytosis and by facilitating the formation of recycling endosomes containing E-cad and their targeting to adherens junctions (Lecuit & Yap, 2015; Levayer & Lecuit, 2012). Such pathways could be important during the first phase of elongation when junctions oriented along the circumference get shorter (Fig. 3A). Other studies suggest that the neosynthesis of junctional proteins and their lateral diffusion after reaching junctions by exocytosis is required to promote junction elongation (Goldenberg & Harris, 2013). Thus, one possibility for junction lengthening during *C. elegans* elongation could be that muscle contractions somehow trigger the expression of specific genes that promote E-cad synthesis, posttranslational modifications

or transport. In particular, sumoylation and phosphorylation of HMR-1/E-cadherin cytoplasmic tail mediate its binding to HMP-2/β-catenin, affecting HMR-1 accumulation at the apical junctions and the formation of a functional adherens junction (Callaci, Morrison, et al., 2015; Choi, Loveless, et al., 2015; Tsur, Bening Abu-Shach, et al., 2015). The dependence of HMR-1 maintenance on clathrin-mediated transport only seen after twofold stage may also be somehow promoted by muscle contractions (Gillard, Shafaq-Zadah, et al., 2015). Finally, recent studies in cell culture have established that adherens junctions are mechanosensitive, and stiffen in response to applied forces by recruiting vinculin and more actin (Chen, Hong, et al., 2015; le Duc, Shi, et al., 2010; Yonemura, Wada, et al., 2010). Moreover, the E-cadherin turnover rate appears to increase with increasing mechanical stress applied to a junction (de Beco, Perney, et al., 2015), suggesting that the trafficking machinery for junctional proteins may be mechanosensitive.

In *C. elegans*, the actin filaments anchored to adherens junctions might somehow transmit the tensional input originating from muscle contraction during elongation (Fig. 6A). Indeed, adherens junctions are likely to be under tension since mutants such as *mel-11* and *rga-2* that hyperactivate non-muscle myosin II cause the embryo to rupture (Diogon et al., 2007; Wissmann et al., 1999). Although vinculin is not expressed in the *C. elegans* epidermis, other proteins might serve a similar function as vinculin (without necessarily direct binding to α-catenin). In particular, several

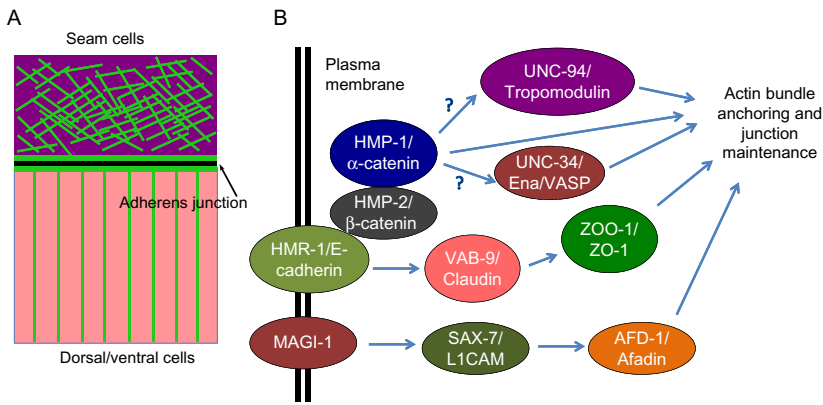

Figure 6 Role of cell junctions during elongation. (A) Junctional proteins are thought to anchor actin bundles in DV cells, green lines represent actin filaments and bundles. (B) Different junction-associated proteins may contribute to actin bundle anchoring and junction maintenance during elongation.

actin-binding proteins, such as AFD-1/Afadin (through binding with SAX-7/L1CAM and MAGI-1), UNC-94/Tropomodulin, and UNC-34/Ena, localize to *C. elegans* adherens junctions where they reinforce the attachment between cells and the connection with the actin cytoskeleton (Fig. 6B; Cox-Paulson, Walck-Shannon, et al., 2012; Lynch, Grana, et al., 2012; Sheffield, Loveless, et al., 2007). Their loss does not always induce a strong phenotype but enhances the defects of weak mutants of the cadherin–catenin complex (Cox-Paulson et al., 2012; Lynch et al., 2012; Sheffield et al., 2007). Force measurement on junctions to assess their distribution and evolution during elongation, and further characterization of E-cadherin transport pathways should help define how muscles might stimulate junction lengthening and embryo elongation.

In summary, research on *C. elegans* embryo morphogenesis has not only shown that many pathways found in vertebrates are conserved, but it has also opened perspectives on new mechanisms regulating morphogenetic processes. The next challenge will be to measure the properties of mechanical forces (magnitude, direction, point of application) at the cellular scale, and to understand how different proteins as well as feedback mechanisms regulate those properties. Biophysical methods and computer modeling will also be instrumental to clarify how the cooperation of signaling and mechanical forces shapes the organism.

ACKNOWLEDGMENTS

We thank Martha Soto, François Robin, Flora Llense, Christelle Gally, and Sophie Quintin for comments on the manuscript and for discussions. Our work is supported by a grant from the European Research Council to ML, and by institutional funds from the CNRS and University Pierre et Marie Curie (UPMC) to the IBPS and UMR7622. In addition, M.L. thanks the CNRS and the UPMC for a relocation package.

REFERENCES

Ankeny, R. A. (2001). The natural history of Caenorhabditis elegans research. *Nature Reviews Genetics*, *2*(6), 474–479.

Antoshechkin, I., & Sternberg, P. W. (2007). The versatile worm: Genetic and genomic resources for Caenorhabditis elegans research. *Nature Reviews Genetics*, *8*(7), 518–532.

Baskin, T. I. (2005). Anisotropic expansion of the plant cell wall. *Annual Review of Cell and Developmental Biology*, *21*, 203–222.

Bercher, M., Wahl, J., et al. (2001). mua-3, a gene required for mechanical tissue integrity in Caenorhabditis elegans, encodes a novel transmembrane protein of epithelial attachment complexes. *The Journal of Cell Biology*, *154*(2), 415–426.

Bernadskaya, Y. Y., Wallace, A., et al. (2012). UNC-40/DCC, SAX-3/Robo, and VAB-1/Eph polarize F-actin during embryonic morphogenesis by regulating the WAVE/SCAR actin nucleation complex. *PLoS Genetics*, *8*(8), e1002863.

Bertet, C., Sulak, L., et al. (2004). Myosin-dependent junction remodelling controls planar cell intercalation and axis elongation. *Nature*, *429*(6992), 667–671.
Blanchoin, L., Boujemaa-Paterski, R., et al. (2014). Actin dynamics, architecture, and mechanics in cell motility. *Physiological Reviews*, *94*(1), 235–263.
Blankenship, J. T., Backovic, S. T., et al. (2006). Multicellular rosette formation links planar cell polarity to tissue morphogenesis. *Developmental Cell*, *11*(4), 459–470.
Bone, C. R., Tapley, E. C., et al. (2014). The Caenorhabditis elegans SUN protein UNC-84 interacts with lamin to transfer forces from the cytoplasm to the nucleoskeleton during nuclear migration. *Molecular Biology of the Cell*, *25*(18), 2853–2865.
Bosher, J. M., Hahn, B. S., et al. (2003). The *Caenorhabditis elegans vab-10* spectraplakin isoforms protect the epidermis against internal and external forces. *The Journal of Cell Biology*, *161*(4), 757–768.
Callaci, S., Morrison, K., et al. (2015). Phosphoregulation of the C. elegans cadherin-catenin complex. *The Biochemical Journal*, *472*(3), 339–352.
Chan, B. G., Rocheleau, S. K., et al. (2015). The Rho guanine exchange factor RHGF-2 acts through the Rho-binding kinase LET-502 to mediate embryonic elongation in C. elegans. *The Biochemical Journal*, *405*(2), 250–259.
Chan, S. S., Zheng, H., et al. (1996). UNC-40, a C. elegans homolog of DCC (deleted in colorectal cancer), is required in motile cells responding to UNC-6 netrin cues. *Cell*, *87*(2), 187–195.
Chen, C. S., Hong, S., et al. (2015). alpha-Catenin-mediated cadherin clustering couples cadherin and actin dynamics. *The Journal of Cell Biology*, *210*(4), 647–661.
Chin-Sang, I. D., George, S. E., et al. (1999). The ephrin VAB-2/EFN-1 functions in neuronal signaling to regulate epidermal morphogenesis in C. elegans. *Cell*, *99*(7), 781–790.
Chin-Sang, I. D., Moseley, S. L., et al. (2002). The divergent C. elegans ephrin EFN-4 functions in embryonic morphogenesis in a pathway independent of the VAB-1 Eph receptor. *Development*, *129*(23), 5499–5510.
Chisholm, A. D., & Hardin, J. (2005). Epidermal morphogenesis. *WormBook*, 1–22. http://dx.doi.org/10.1895/wormbook.1.7.1.. http://www.wormbook.org.
Choi, H. J., Loveless, T., et al. (2015). A conserved phosphorylation switch controls the interaction between cadherin and beta-catenin in vitro and in vivo. *Developmental Cell*, *33*(1), 82–93.
Ciarletta, P., Ben Amar, M., et al. (2009). Continuum model of epithelial morphogenesis during Caenorhabditis elegans embryonic elongation. *Philosophical Transactions Series A, Mathematical, Physical, and Engineering Sciences*, *367*(1902), 3379–3400.
Costa, M., Raich, W., et al. (1998). A putative catenin-cadherin system mediates morphogenesis of the Caenorhabditis elegans embryo. *The Journal of Cell Biology*, *141*(1), 297–308.
Cox-Paulson, E. A., Walck-Shannon, E., et al. (2012). Tropomodulin protects alpha-catenin-dependent junctional-actin networks under stress during epithelial morphogenesis. *Current Biology*, *22*(16), 1500–1505.
de Beco, S., Perney, J. B., et al. (2015). Mechanosensitive Adaptation of E-Cadherin Turnover across adherens Junctions. *PLoS One*, *10*(6), e0128281.
Ding, M., Goncharov, A., et al. (2003). C. elegans ankyrin repeat protein VAB-19 is a component of epidermal attachment structures and is essential for epidermal morphogenesis. *Development*, *130*(23), 5791–5801.
Ding, M., King, R. S., et al. (2008). The cell signaling adaptor protein EPS-8 is essential for C. elegans epidermal elongation and interacts with the ankyrin repeat protein VAB-19. *PLoS One*, *3*(10), e3346.
Diogon, M., Wissler, F., et al. (2007). The RhoGAP RGA-2 and LET-502/ROCK achieve a balance of actomyosin-dependent forces in C. elegans epidermis to control morphogenesis. *Development*, *134*(13), 2469–2479.

Fotopoulos, N., Wernike, D., et al. (2013). Caenorhabditis elegans anillin (ani-1) regulates neuroblast cytokinesis and epidermal morphogenesis during embryonic development. *Developmental Biology*, *383*(1), 61–74.
Francis, G. R., & Waterston, R. H. (1985). Muscle organization in Caenorhabditis elegans: Localization of proteins implicated in thin filament attachment and I-band organization. *The Journal of Cell Biology*, *101*(4), 1532–1549.
Francis, R., & Waterston, R. H. (1991). Muscle cell attachment in Caenorhabditis elegans. *The Journal of Cell Biology*, *114*(3), 465–479.
Fridolfsson, H. N., Ly, N., et al. (2010). UNC-83 coordinates kinesin-1 and dynein activities at the nuclear envelope during nuclear migration. *Developmental Biology*, *338*(2), 237–250.
Gally, C., Wissler, F., et al. (2009). Myosin II regulation during C. elegans embryonic elongation: LET-502/ROCK, MRCK-1 and PAK-1, three kinases with different roles. *Development*, *136*(18), 3109–3119.
George, S. E., Simokat, K., et al. (1998). The VAB-1 Eph receptor tyrosine kinase functions in neural and epithelial morphogenesis in C. elegans. *Cell*, *92*(5), 633–643.
Ghenea, S., Boudreau, J. R., et al. (2005). The VAB-1 Eph receptor tyrosine kinase and SAX-3/Robo neuronal receptors function together during C. elegans embryonic morphogenesis. *Development*, *132*(16), 3679–3690.
Gillard, G., Shafaq-Zadah, M., et al. (2015). Control of E-cadherin apical localisation and morphogenesis by a SOAP-1/AP-1/clathrin pathway in C. elegans epidermal cells. *Development*, *142*(9), 1684–1694.
Giurumescu, C. A., Kang, S., et al. (2012). Quantitative semi-automated analysis of morphogenesis with single-cell resolution in complex embryos. *Development*, *139*(22), 4271–4279.
Goldenberg, G., & Harris, T. J. (2013). Adherens junction distribution mechanisms during cell-cell contact elongation in Drosophila. *PLoS One*, *8*(11), e79613.
Gorfinkiel, N., Schamberg, S., et al. (2011). Integrative approaches to morphogenesis: Lessons from dorsal closure. *Genesis*, *49*(7), 522–533.
Hahn, B. S., & Labouesse, M. (2001). Tissue integrity: Hemidesmosomes and resistance to stress. *Current Biology*, *11*(21), R858–R861.
Harden, N. (2002). Signaling pathways directing the movement and fusion of epithelial sheets: Lessons from dorsal closure in Drosophila. *Differentiation*, *70*(4–5), 181–203.
Havrylenko, S., Noguera, P., et al. (2015). WAVE binds Ena/VASP for enhanced Arp2/3 complex-based actin assembly. *Molecular Biology of the Cell*, *26*(1), 55–65.
Heid, P. J., Raich, W. B., et al. (2001). The zinc finger protein DIE-1 is required for late events during epithelial cell rearrangement in C. elegans. *Developmental Biology*, *236*(1), 165–180.
Hetherington, S., Gally, C., et al. (2011). PAT-12, a potential anti-nematode target, is a new spectraplakin partner essential for Caenorhabditis elegans hemidesmosome integrity and embryonic morphogenesis. *Developmental Biology*, *350*(2), 267–278.
Hong, L., Elbl, T., et al. (2001). MUP-4 is a novel transmembrane protein with functions in epithelial cell adhesion in *Caenorhabditis elegans*. *The Journal of Cell Biology*, *154*(2), 403–414.
Ikegami, R., Simokat, K., et al. (2012). Semaphorin and Eph receptor signaling guide a series of cell movements for ventral enclosure in C. elegans. *Current Biology*, *22*(1), 1–11.
le Duc, Q., Shi, Q., et al. (2010). Vinculin potentiates E-cadherin mechanosensing and is recruited to actin-anchored sites within adherens junctions in a myosin II-dependent manner. *The Journal of Cell Biology*, *189*(7), 1107–1115.
Lecuit, T., & Yap, A. S. (2015). E-cadherin junctions as active mechanical integrators in tissue dynamics. *Nature Cell Biology*, *17*(5), 533–539.
Levayer, R., & Lecuit, T. (2012). Biomechanical regulation of contractility: Spatial control and dynamics. *Trends in Cell Biology*, *22*(2), 61–81.

Résumé de these

Xinyi YANG

2017-05-04

I. Progrès scientifique:

Remodelage de jonction sous stress

Contexte du projet L'idée que les cellules peuvent répondre aux forces mécaniques et les convertir en signaux chimiques à travers un processus appelé mécanotransduction a été largement acceptée et considérée comme critique dans l'étude du développement, de la fonction et de la maladie des organes[1-4]. Cependant, les mécanismes par lesquels les cellules détectent une tension ou une rigidité, puis répondent à de tels stimuli mécaniques sont encore mal compris. En utilisant les embryons de *C. elegans* comme modèle, l'objectif principal de ma thèse de doctorat sera de mieux définir comment les forces mécaniques influent sur les comportements cellulaires.

Les embryons de *C. elegans*, dont l'allongement suit un schéma stéréotypé, augmentent leur longueur par un facteur de quatre fois le long de leur axe antérieur-postérieur et réduisent leurs circonférences d'un facteur trois en moins de trois heures[5]. Ces caractéristiques font de *C. elegans* un système très puissant pour répondre à cette question.

Les jonctions adventices sont des complexes protéiques qui se produisent dans les jonctions cellule-cellule dans les cellules épithéliales. La jonction apicale de *C. elegans* peut maintenir l'adhésion cellulaire[6, 7], fonctionner comme une porte paracellulaire[8, 9] et établir une polarité des cellules épithéliales[10-12]. Au début de l'allongement embryonnaire de *C. elegans*, la jonction d'adhérence peut transmettre la force contractile générée dans les cellules de couture latérales dans les cellules dorsales et ventrales, dans lesquelles les jonctions adhérentes ancrent les faisceaux circonférentiels de filaments d'actine[6] qui contribuent à répartir uniformément la force de contraction des coutures Dans toutes les cellules épidermiques[13]. À mesure que les cellules épidermiques s'allongent pendant l'allongement de l'embryon, la jonction apicale de l'épiderme doit s'allonger le long de l'axe antérieur-postérieur pour assurer l'allongement embryonnaire. Cependant, le mécanisme cellulaire de la façon dont les jonctions adhésives s'allongent sous ce stress mécanique n'est pas encore clair. Chez les cellules épithéliales de *Drosophila* et les cellules de mammifères, plusieurs découvertes récentes ont montré que l'endocytose et le recyclage ultérieur de l'E-cadhérine sont impliqués dans le remodelage de la jonction[14-16]. D'autres études suggèrent que les protéines de jonction nouvellement synthétisées et leur fusion latérale après leur transport vers la région de la jonction par exocytose sont également nécessaires pour favoriser l'allongement de la jonction[17]. Mais la façon dont les jonctions s'allongent pendant l'allongement embryonnaire est encore inconnue.

Le but de mon projet est de comprendre les mécanismes cellulaires par lesquels la contraction musculaire aide à allonger les jonctions adhérentes et à établir un modèle de réponse cellulaire à la tension mécanique pendant le développement embryonnaire de *C. elegans*.

Approche Les objectifs spécifiques du projet sont divisés en quatre tâches:

1. Acquérir des films à grande vitesse à 3 dimensions du processus d'allongement embryonnaire de *C. elegans* en utilisant la microscopie d'illumination à un seul plan (SPIM) pour fournir des informations détaillées sur l'allongement des jonctions et les mouvements nucléaires musculaires pour une analyse plus approfondie.

2. Analyser les films de SPIM pour comprendre l'établissement d'une polarité plane dans les épithéliums pendant l'allongement de l'embryon et définir le mouvement local et mondial de la torsion et de la rotation des embryons.

3. Mesurer la tension pour les jonctions adhérentes in vivo pendant l'élongation embryonnaire à l'aide d'un laser multi-photons pour explorer les mécanismes cellulaires qui stimulent l'allongement de la jonction avec les données d'analyse de l'imagerie.

4. Définir comment de nouveaux composants de jonction s'insèrent pendant l'allongement de la jonction pendant les rotations d'embryons en utilisant un microscope à une seule molécule et en étudiant la façon dont ce processus peut être modulé, en comparant cet événement à des mutants défectueux et comment cela peut affecter le processus d'allongement de jonction Et l'allongement embryonnaire.

Après une thèse de quatre ans, j'ai accompli les quatre tâches et je me prépare maintenant à publier mes résultats dans 2 documents de recherche scientifique. Les résultats sont résumés dans la session suivante.

Résultats

1. **Nouvelle accumulation de contraintes** Dans cette partie, je vais d'abord expliquer les nouvelles contraintes que j'ai faites lors de ma thèse, qui ont été utilisées pour accomplir différentes tâches dans mon projet et présenter le contexte de la nouvelle souche, afin de faciliter la compréhension des résultats suivants.

Dans ma deuxième année, pour apprendre la nature et la répartition des forces qui conduisent le remodelage de la jonction et étudier les micro-contractions musculaires partielles jouent dans ce processus, j'ai déterminé comment la tension change le long des jonctions dans la direction antéro-postérieure et l'orthogonal Direction après la contraction musculaire a commencé in vivo. J'ai conduit une nano-ablation par un laser multi-photons à haute énergie pour perturber localement la stabilité de la jonction de la cellule de couture sans détruire l'intégrité de la cellule. J'ai mené l'expérience d'ablation au laser en utilisant une souche DLG-1 :: RFP over-expression. Les résultats ont montré qu'après l'ablation, la force le long de la direction antéro-postérieure peut entraîner la jonction pour reculer après la coupe dans la tête et la partie du corps de l'embryon à 1,5 fois. Cependant, ce phénomène ne s'est pas produit à 100% dans tous les cas, mais cela s'est produit dans environ 40% des cas. Ce résultat peut être dû au fait que l'expression excessive de la protéine de jonction DLG-1 rend la jonction rigide de la jonction. Pour éviter cette situation et pour mieux examiner le recul de la jonction après l'ablation, j'ai créé une souche knock-in GFP (DLG-1 :: GFP). En utilisant la méthode Cas-9 / CRISPR, j'ai inséré la protéine GFP au C-terminal de la protéine DLG-1. Cette nouvelle souche s'appelle ML2615. Dans cette nouvelle souche, le niveau d'expression de DLG-1 est le même que les vers de type sauvage, fournissant un niveau de type sauvage d'expression de DLG-1 et reflétant le recul de jonction. La souche ML2615 a montré que les embryons et les vers se trouvaient dans un état très sain, comme le ver de forme sauvage N2 et n'avaient aucune létalité.

Au début de ma première année de doctorat, le Dr. Labouesse et moi avons pris des films SPIM à une couleur pour enregistrer le processus d'allongement embryonnaire. Pourtant, nous devons encore comprendre comment les activités musculaires déclenchent

l'allongement de jonction et l'établissement de polarité planaire. Au début de la 3ème année de mon projet, nous avons appris de notre collaborateur à Max Plank Institute (MPI), à Dresde, que leur microscopie SPIM avait été améliorée et pouvait prendre des films multicolores. Cette amélioration nous a permis d'acquérir des films pour capturer simultanément les activités de jonction et de muscle. J'ai donc fait de nouvelles souches qui expriment à la fois une jonction marquée par fluorescence et des noyaux musculaires pour d'autres acquisitions. Par conséquent, j'ai franchi ML2615 avec ML2113, une souche exprimant les noyaux musculaires marqués de la protéine fluorescente rouge (RFP). La nouvelle souche s'appelle ML2616, qui exprime la jonction marquée par GFP et les noyaux musculaires marqués par RFP en même temps. J'ai encore franchi ML2616 avec ML1688, mutant pak-1 (tm403) et OD761, mutant Rho-kinase (sb118t). Les nouvelles souches générées sont nommées ML2630 et ML2631, respectivement. Ces trois nouvelles souches sont en bonne santé et ne présentent aucune létalité. Avec la nouvelle souche ML2616, j'ai acquis environ 60 films SPIM pour analyser les activités de la jonction et des noyaux pendant le développement embryonnaire.

Au cours de ma dernière année, pour étudier l'insertion de la protéine de jonction, j'ai créé une souche de pH-fluorin (E-cadherin :: pHluorin) super-eclipse, nommée ML2773, par la méthode Cas-9 / CRISPR. Le plasmide qui code pour la protéine de pHluorine exprimée par le ver modifié a été un cadeau du Prof. Joshua M. Kaplan. La séquence de pHfluorine a été insérée entre l'exon 7 et l'exon 8 du génome E-cadhérine. Après l'expression, le pHluorine serait dans le domaine extracellulaire de l'E-cadhérine. La nouvelle souche ML2773 a une létale de 60 à 70% à 20 ° C, mais elle est maintenable. Ces embryons sont morts à différents stades avant les neuroblastes ventral jusqu'à 2 fois. Ils ont souffert d'une explosion dans la région de la tête et n'ont pas pu survivre. Cela peut être causé par un excès de clivage extracellulaire de l'E-cadhérine, mais le mécanisme détaillé est encore inconnu. Cependant, les embryons qui passent 2 fois peuvent se développer avec succès jusqu'à l'éclosion. Au cours de l'imagerie TIRF, l'embryon sain serait soigneusement sélectionné pour la fabrication de films et les embryons malades / morts seraient éliminés.

2. **Analyses d'images SPIM** Pour mieux étudier le schéma d'allongement de la jonction pendant l'allongement de l'embryon et pour comparer la différence dans l'allongement de la jonction entre les vers avec la capacité de contraction du muscle normal et les vers avec la capacité de contraction du muscle altérée, le Dr. Labouesse a acquis des images en 3D en temps réel enregistrant le processus de *C. elegans* Morphogenèse sur microscopie d'illumination à un seul avion (SPIM) dans l'Institut Max Planck de biologie cellulaire moléculaire et de génétique à Dresde. Le microscope SPIM est basé sur un modèle conçu par Eric Betzig qui nous permet d'acquérir des images en 3-D en temps réel de forme d'embryon qui changent pendant l'allongement en capturant près de centaines de plans focaux au 10ème de seconde. Ces images enregistrent le processus des cellules épidermiques, en particulier l'allongement des cellules de couture latérale lorsque les embryons en développement atteignent 1,7 fois, commençant à se tordre et à tourner sous la force motrice de la micro-contraction musculaire. Les vers expriment la protéine de fusion du marqueur de jonction dlg-1 :: RFP ou hmr-1 :: GFP afin que les mouvements de la jonction cellulaire épithéliale puissent être suivis pendant l'imagerie.

Pour étudier le schéma de l'allongement polarisé de la jonction épithéliale sous tension, les informations quantitatives sur les mouvements relatifs des cellules doivent être extraites des images. Dans ma première année, j'ai effectué un suivi manuel des sommets de l'épiderme latéral. Du changement de position des sommets, les informations principales et les propriétés dérivées de l'épiderme latéral, y compris les changements de la longueur de la cellule, des zones, des périmètres et des orientations, ont pu être calculées dans l'analyse secondaire, ainsi que l'accélération des mouvements de cellules épidermiques. Au cours de ma deuxième et troisième année, j'ai développé plusieurs programmes MATLAB pour mener une analyse secondaire du suivi primaire depuis les deux premières années de mon doctorat en interagissant avec le nouvel analyste de données Dr. Teresa FERRARO et un nouvel ami. Dr. François ROBIN. Les nouveaux codes MATLAB m'ont permis de mener une analyse approfondie de la nature du développement embryonnaire et du mouvement des mouvements embryonnaires, des rotations et de la torsion. De plus, j'ai terminé mon analyse de mutants défectueux musculaires de type sauvage et de mutants Rho-kinase à six génotypes différents, ajouté deux mutants spectrin différents et des mutants spectrin / kinase à mon groupe de résultats, à un nombre d'échantillons statistique significatif.

En effectuant l'analyse secondaire avec les programmes MATLAB nouvellement développés, j'ai étudié la compression et l'extension globales de l'embryon généré par les rotations et le modèle de changement local dans les aspects de l'épiderme et la correction entre différentes cellules épidermiques latérales.

Tout d'abord, j'ai étudié la tendance de la rotation dans huit embryons de type sauvage, assez âgés pour effectuer des rotations actives. J'ai constaté que les embryons ont commencé à tourner fortement peu de temps après que les muscles sont devenus actifs, en passant 65% du temps au cours des films et la fréquence des rotations vers l'intérieur et l'extérieur des embryons était égale. Après cela, j'ai essayé de rechercher un certain modèle de rotations, mais l'analyse a montré que l'embryon tournait vers différentes directions, à l'intérieur ou à l'extérieur, de façon aléatoire, ce qui suggère qu'il n'existe pas de modèle certain pour la rotation de l'embryon. Ensuite, j'ai analysé les différents mutants pour les comparer avec les embryons de type sauvage et les résultats sont intrigants. Dans les mutants musculaires défectueux, qui, en raison de la perte de la fonction musculaire, s'arrêtent à deux fois et ne survivent pas, les embryons (n = 5) tournent à peine et le temps de rotation moyen est d'environ 1%. Dans les deux mutants spectrin différents (n = 4 pour les deux mutants); De même, les mutants spectrin / kinase (n = 2), dans lesquels les mécanismes de récupération des contractions musculaires sont altérés, ont affiché un temps de rotation plus court par rapport aux embryons de type sauvage. Le temps de rotation pour chaque mutant est devenu plus court à mesure que les pertes deviennent plus sévères. Un autre résultat intéressant provient du mutant Rho-kinase, dans lequel l'actomyosine est altérée dans l'embryon, ne fournissant pas de tension pour que l'embryon s'allonge avant les activités musculaires et conduisant les embryons à s'arrêter à 1,2 fois jusqu'à ce que les muscles deviennent actifs. Les films ont montré que les embryons (n = 12) avaient une forte torsion après que le muscle est devenu actif mais pas de rotation du tout. L'analyse statistique a confirmé que le taux de rotation des mutants Rho-kinase était de 1%, aussi faible que les embryons défectifs musculaires. Étant donné que l'embryon de Rho-kinase peut éventuellement atteindre 2 fois après que le muscle est devenu actif pendant le développement, ces résultats peuvent nous fournir une nouvelle vue de la façon dont les torsions forts permettent d'allonger la jonction pendant l'allongement. Tous ensemble, l'analyse de type sauvage et les mutants ont montré que les rotations mondiales provoquées par les activités musculaires sont cruciales pour l'allongement de l'embryon et l'allongement de la jonction.

Deuxièmement, j'ai étudié comment les aspects cellulaires de différents épidermes latéraux ont changé pendant l'allongement embryonnaire. Pour commencer, j'ai calculé la zone apicale, le périmètre et la longueur de cellule de chaque cellule de couture pour tous les génotypes. Ensuite, à chaque génotype, j'ai utilisé une analyse de corrélation croisée pour comparer les changements d'aspect cellulaire entre chaque cellule de couture. J'ai observé que dans les embryons de type sauvage, la tête avec le corps et la queue se comportaient comme des entités mécaniques partiellement indépendantes. Ce modèle local a été totalement ou partiellement perdu dans tous les génotypes mutés. En outre, je voulais comprendre s'il y a un point de départ des activités musculaires et à quelle distance des tensions s'étendent du point initial. Pour atteindre cet objectif, j'ai comparé le changement de longueur de cellule de chaque cellule

de couture voisine. J'ai constaté que dans le type sauvage (n = 8), dans la partie tête de l'embryon, le changement de longueur de cellule de chaque cellule de couture était très indépendant l'un de l'autre. Mais dans le groupe du corps et les groupes de queue de l'embryon, la cellule de couture V1 et les cellules de couture V5, respectivement, ont changé leur longueur avant leurs cellules voisines. Ce résultat implique que les muscles sous les cellules V1 et V5 sont plus actifs que les muscles sous l'autre épiderme de l'embryon, ce qui entraîne la contraction de ces deux cellules. À l'intrigue, j'ai observé que lorsque la longueur de cellule de V1 diminuait, la longueur de cellule de sa cellule voisine H2 augmentait. Cette anti-corrélation de la longueur de cellule entre ces deux cellules n'a pas duré longtemps (~ 1,5s) ou est apparue souvent pendant les films. Cependant, cette observation impliquait que les activités musculaires pourraient fournir une tension locale exerçant sur l'épiderme pour l'allongement de la jonction.

Après avoir étudié les mouvements globaux et locaux des embryons, j'ai examiné comment les mouvements mondiaux et locaux peuvent contribuer à l'établissement d'une polarité planaire. J'ai donc analysé les mouvements de noyaux dans les films à deux couleurs avec ML2616, qui exprime en même temps la jonction marquée par GFP et les noyaux musculaires RFP. Les noyaux étiquetés par RFP m'ont permis d'étudier les mouvements de deux côtés opposés des embryons, de la gauche vers la droite et du côté dorsal par rapport au côté ventral, ainsi que les deux angles diagonaux des embryons, le ventral gauche (VL) par rapport à la droite dorsale (DR) et à la droite ventrale (VR) par rapport à la dorsale gauche (DL). J'ai choisi deux noyaux musculaires de chacun des quatre muscles et mesuré la distance entre les deux noyaux. Après avoir analysé quatre embryons de type sauvage, j'ai découvert que le changement de distance entre deux noyaux de deux muscles diagonaux était anti-corrélés les uns avec les autres. Pendant ce temps, le changement de distance de deux noyaux des côtés opposés des embryons présentait un schéma mixte à la fois corrélée et anti-corrélée. Ce résultat a signifié que les muscles ont contracté dans un groupe de deux: groupe gauche / droit ou groupe dorsal / ventral, ce qui explique pourquoi le changement de distance des noyaux du côté opposé a présenté un modèle corrélatif. En outre, ce résultat a révélé que ces deux mouvements de groupe musculaire ne sont pas réparés. Les embryons ont contracté dans le groupe gauche / droit et le groupe dorsal / ventral alternativement, prouvé par le fait que le changement de distance des noyaux du côté opposé présente parfois un modèle anti-corrélé. Au cours de toutes ces contractions alternatives, les muscles des angles diagonaux (VL vs DR et DL vs VR) n'ont jamais pu se contracter ensemble, ce qui a entraîné un modèle anti-corrélé des changements de distance des noyaux des muscles diagonaux. Dans l'ensemble, cette analyse a montré que les muscles des côtés opposés du corps se contraignaient alternativement, ce qui représentait les mouvements de rotation. Ces contractions alternatives de chaque côté des embryons brisent la symétrie des embryons et fournissent la source de polarité pendant le développement embryonnaire.

Après l'étude des mouvements globaux et locaux des embryons, nous avons posé notre hypothèse selon laquelle les rotations et les torsions brisent la symétrie de l'embryon et génèrent des tensions exercées sur les jonctions, étirant les jonctions et stimulant l'allongement de la jonction polarisée le long de la direction antéro-postérieure (figure 1).

3. **Étude de l'état de la membrane cellulaire** Après avoir abordé l'hypothèse, j'ai d'abord besoin d'étudier si les jonctions passent par un changement conformationnel pendant les rotations d'embryons. En utilisant le programme MATLAB développé par le Dr Teresa FERRARO, j'ai étudié le changement de jonction rectiligne le long de la direction antérieure / postérieure (direction de la liaison A / P). Après avoir étudié cinq embryons de type sauvage, neuf embranchements A / P chaque embryon, j'ai découvert que lorsque l'embryon a tourné vers l'intérieur, la rectitude de la jonction A / P a diminué, ce qui signifie que les jonctions étaient plus pliées. Au contraire, lorsque les embryons ont tourné vers l'extérieur, la rectitude de la jonction A / P a augmenté, ce qui signifie que les jonctions étaient plus étirées. Lorsque les embryons se trouvaient dans une position relaxante, la rectitude de la jonction était entre les deux premiers. Cette observation était universelle pour les neuf cellules épidermiques latérales dans les cinq embryons, bien que la pente du changement de rectitude de la jonction avec la position de rotation des embryons puisse varier selon les différentes cellules épidermiques.

Étant donné que les jonctions étaient plus étirées lorsque les embryons ont tourné vers l'extérieur, ils étaient plus susceptibles d'être sous tension à ce moment-là. Pour vérifier si les jonctions sont sous tension élevée après la rotation vers l'extérieur, j'ai utilisé un microscope à photométries multiples pour appliquer une ablation au laser sur les jonctions A / P dans les embryons de 1,8 fois à 2 fois. Ces embryons assez âgés pour avoir de fortes contractions musculaires et des rotations asymétriques pour générer des tensions locales lors de la jonction. J'ai fait face à une grande difficulté lorsque j'ai conduit cette expérience parce que l'embryon a tourné très activement et a rendu très difficile l'ablation des jonctions sélectionnées, en raison du changement rapide de la position de jonction dans le champ du microscope et de la chute du plan focal droit. Finalement, sur 89 ablations sur les jonctions V3-dorsales / ventrales, 20 ablations ont montré que lorsque les embryons ont tourné vers l'extérieur, l'ouverture de la jonction juste après l'ablation est de 0,7 μm et 60 ablations ont montré que les embryons tournaient vers l'intérieur, l'ouverture de la jonction Après l'ablation est de 0,4 μm. Ce résultat a confirmé que lorsque les embryons ont tourné vers l'extérieur, la rotation a généré une tension locale seule à la direction antéro-postérieure sur les jonctions.

Cette tension peut être la source de l'allongement de la jonction, mais le mécanisme doit être étudié plus avant. Pour atteindre cet objectif, nous avons commencé à imaginer avec un microscope à une seule molécule pour analyser la fusion des vésicules de matériaux de jonction dans différentes situations (voir ci-dessous).

4. **Microscopie à une seule molécule** Comme je l'ai décrit dans la dernière partie, j'ai vérifié que des tensions plus élevées sont exercées sur les jonctions lorsque les embryons ont tourné vers l'extérieur. Ensuite, j'ai voulu observer à quel point les vésicules contenant la protéine de jonction E-cadhérine sont insérées et comparer les différences entre les embryons tournés vers l'extérieur et vers l'intérieur / détendus. Selon mon hypothèse, les événements d'insertion se produiront plus souvent ou avec un taux plus rapide lors de la jonction étirée lorsque les embryons tournent vers l'extérieur se comparent à la jonction rétractable ou décontractée lorsque les embryons tournent vers l'intérieur ou restent détendus. De plus, je compare l'insertion de E-cad dans des embryons de type sauvage et des mutants défectifs d'exocytose dans lesquels le trafic de vésicules est altéré. Les deux mutants devraient présenter une insertion moins efficace par rapport au type sauvage. J'ai effectué la microscopie Total Internal Reflection Fluorescence (TIRF) de notre plate-forme d'imagerie avec un jeune chef de groupe qui est un expert en imagerie TIRF.

Après un essai rapide avec une souche E-cad :: GFP crispr knock-in (LP172, un cadeau du professeur Bob Goldstein), j'ai réalisé qu'il était difficile d'observer les événements de fusion avec cette souche. J'ai donc créé la souche ML2773, E-cad :: pHluorin (voir Résultat 1) et la désamorçage du pHluorine a montré un grand potentiel pour indiquer les événements de fusion, qui représentent l'insertion de protéines de jonction. L'analyse de type sauvage et de mutants sera terminée fin juillet, deux mois avant ma défense.

Conclusion Après quatre ans d'étude, le projet a progressé comme prévu, et la tâche principale du projet est presque terminée. L'analyse des films SPIM a fourni des informations massives et complètes sur la rotation des embryons et le modèle de mouvement

mondial et local, ainsi que le processus d'allongement embryonnaire à cliquet. Il a également découvert la source d'asymétrie à l'intérieur d'une structure biologique symétrique de l'embryon de *C. elegans* pour la première fois en révélant le mouvement du mouvement musculaire. Cette nouvelle découverte va compléter notre compréhension de l'établissement de la polarité plane lors de la morphogenèse embryonnaire. Ensemble avec l'analyse des films de SPIM, les expériences d'ablation par laser ont donné lieu à une explication très possible pour l'allongement de la jonction polarisée le long de la direction A / P. Les films à une seule molécule prêts à finir vont démêler le mécanisme moléculaire de l'allongement de la jonction sous tension et fermer tout le projet. Dans l'ensemble, mon hypothèse de la façon dont la polarité planaire pourrait être établie et de la façon dont la jonction allongée selon A / P pendant la morphogenèse a déjà été vérifiée dans un seul aspect.

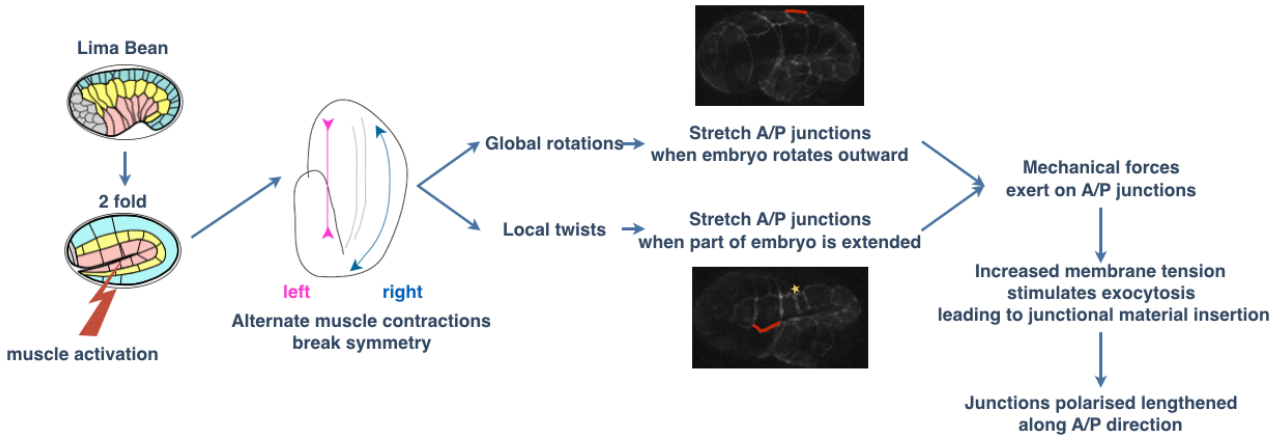

Figure 1. Model for junction polarized lengthening during *C. elegans* morphogenesis

II. Progrès avec les cours / conférences / publications

La liste d'articles publiés

1. *C. elegans Embryonic Morphogenesis.* Vuong-Brender TT, **Yang X**, Labouesse M. Curr Top Dev Biol. 2016;116:597-616. doi: 10.1016/bs.ctdb.2015.11.012. Epub 2016 Feb 1.

2. *Junction lengthening and planar polarity establishment in a ratchet format during C. elegans morphogenesis. (en cours de redaction)* **Xinyi YANG**, Teresa FERRARO, Julien PONTABRY, Nicola MAGHELLI, Loïc ROYER, Stephan GRILL, Gene Myers, Michel Labouesse.

La liste des communications orales et par affiches

1. Communications orales: *Rotating and elongating embryos: SPIM microscopy reveals how planar polarity could be established during morphogenesis.* **Xinyi YANG**, Teresa FERRARO, Julien PONTABRY, Nicola MAGHELLI, Loïc ROYER, Stephan GRILL, Gene Myers, Michel Labouesse. **The Allied Genetics Conference 2016 (TAGC),** July 13-17, 2016, Orlando, Florida, US

2. Communications orales: *Rotating and elongating embryos: SPIM microscopy reveals how C. elegans embryos extend through a ratchet mode.* **Xinyi YANG**, Teresa FERRARO, Julien PONTABRY, Nicola MAGHELLI, Loïc ROYER, Stephan GRILL, Gene Myers, Michel Labouesse. **VerMidi 20th,** 20 January 2017, École Normale Supérieure de Lyon, Lyon, France.

3. Communications orales: *A closer look at the dance of C. elegans embryos by SPIM microscopy.* **Xinyi YANG**, Teresa FERRARO, Julien PONTABRY, Nicola MAGHELLI, Loïc ROYER, Stephan GRILL, Gene Myers, Michel Labouesse. **Vers in Paris (VIP),** École Normale Supérieure (FRANCE), 18 Mar. 2016, Paris, France

4. Communications orales**:** *A closer look at the dance of C. elegans embryos by SPIM microscopy.* **Xinyi YANG,** Teresa FERRARO, Julien PONTABRY, Nicola MAGHELLI, Loïc ROYER, Stephan GRILL, Gene Myers, Michel Labouesse. **Journée scientifique**, 14 Mar. 2016**,** Institut de Biologie Paris-Seine**,** Paris, France

References:

1. Katsumi, K., et al.,Skeletal Radiol, 2003. **32**(12): p. 719-23.
2. Tavernarakis, N. and M. Driscoll, Annu Rev Physiol, 1997. **59**: p. 659-89.
3. Hackney, C.M. and D.N. Furness, Am J Physiol, 1995. **268**(1 Pt 1): p. C1-13.
4. Grigg, P., J Appl Physiol (1985), 1986. **60**(4): p. 1107-15.
5. Sulston, J.E., et al., Dev Biol, 1983. **100**(1): p. 64-119.
6. Costa, M., et al., J Cell Biol, 1998. **141**(1): p. 297-308.
7. Raich, W.B., C. Agbunag, and J. Hardin, Curr Biol, 1999. **9**(20): p. 1139-46.
8. Koppen, M., et al., Nat Cell Biol, 2001. **3**(11): p. 983-91.
9. Asano, A., et al., Curr Biol, 2003. **13**(12): p. 1042-6.
10. Knust, E. and O. Bossinger,. Science, 2002. **298**(5600): p. 1955-9.
11. Muller, H.A. and O. Bossinger, Mech Dev, 2003. **120**(11): p. 1231-56.
12. Nelson, W.J., Nature, 2003. **422**(6933): p. 766-74.
13. Chin-Sang, I.D. and A.D. Chisholm, Trends Genet, 2000. **16**(12): p. 544-51.
14. Levayer, R., A. Pelissier-Monier, and T. Lecuit, Nat Cell Biol, 2011. **13**(5): p. 529-40.
15. Yashiro, H., et al., Mol Biol Cell, 2014. **25**(19): p. 2956-69.
16. de Beco, S., et al., Plos One, 2015. **10**(6).
17. Goldenberg, G. and T.J. Harris, PLoS One, 2013. **8**(11): p. e79613.

Xinyi YANG

Remodelage des jonctions sous stress mécanique

Résumé:

Les changements de forme des cellules épithéliales sont cruciaux pour la morphogenèse embryonnaire. Chez les embryons de *C. elegans*, l'activité musculaire sous les cellules épidermiques est l'une des deux forces mécaniques qui dirigent ce processus. Cependant, les mécanismes moléculaires détaillés à travers lesquels l'activité musculaire favorise l'allongement polarisé le long de l'axe antérieur / postérieur (A / P) restent à être totalement compris. Ici, en utilisant l'imagerie rapide-3D, on découvre que les embryons tournent après l'activation musculaire et on décrit le schéma local et global de la rotation de l'embryon induite par activité musculaire. En outre, on a observé que les muscles des côtés opposés de l'embryon se contractent alternativement, expliquant les rotations de l'embryon. Par conséquent, les jonctions adhérentes sont étirées le long de la direction A / P pendant les rotations de l'embryon et sont donc sous une tension plus élevée. Nos résultats préliminaires d'imagerie en molécule unique ont montré que plus de E-cadhérine, matériau de jonction, fusionne avec des jonctions orientées A / P quand il y a une tension élevée sur ces jonctions.

Mots clés : *C. elegans,* morphogenèse, l'allongement polarisé, jonctions adhérentes, l'activation musculaire, stimuli mécaniques

Abstract:

Epithelial cell shape changes is essential for embryonic morphogenesis. In *C. elegans* embryos, muscle activity from underneath epidermal cells is one of the two mechanical force inputs driving this process. However, the detailed molecular mechanisms through which muscle activity promotes the polarized elongation along the anterior/posterior (A/P) axis remains to be fully understood. Here, using fast-3D imaging, we discover that embryos rotate after muscle activation and we describe the local and global pattern of embryo rotation induced by muscle activity. Furthermore, we observed that muscles located on opposite sides of the embryo mostly contract alternatively, accounting for embryo rotations. As a consequence, adherens junctions get stretched along the A/P direction during embryo rotations and therefore are under higher tension. Our preliminary results from single molecule imaging showed that more junction material E-cadherin fuses with A/P oriented junctions when there is high tension on these junctions.

Key word: *C. elegans,* morphogenesis, polarized elongation, adherens junctions, muscle activity, mechanical stimuli